

**BIOBASED LIPOPHILIC CHELATING AGENTS
AND THEIR APPLICATIONS IN METALS
RECOVERY**

KAANA ASEMAVE

PhD

UNIVERSITY OF YORK

CHEMISTRY

JUNE, 2016

Abstract

A bioderived lipophilic β -diketone (14,16-hentriacontanedione, Htd) was isolated from wheat straw wax. Keto-enol tautomerisation studies revealed that Htd was readily enolised in cyclohexane- D_{12} , toluene- D_8 and $CDCl_3$, thus demonstrating its suitability as a metal chelator when dissolved in nonpolar solvents. This work demonstrated for the first time that Htd in liquid-liquid biphasic condition was effective in the removal of Ni(II), Co(II), Cu(II), Pb(II), Cr(III) and Fe(III) comparable to dibenzoylmethane. Htd exhibited an excellent capacity for the rapid extraction of metal ions from aqueous solutions especially Ni(II) better than dibenzoylmethane.

Htd was modified with methyl acrylate and itaconate using a KF/alumina mediated Michael addition reaction followed by further hydrolysis, with hope of enhancing its metal chelating ability. The resulting modified Htd were characterised and tested in metal extraction. The carboxylate acids of the modified Htd were found to be more effective in the extraction of Cu(II) and Pb(II) than the unmodified Htd. It was found that the counter ion of the metal being chelated had a profound effect on the efficiency of extraction. These biobased compounds extracted metals ions from Cl^- and OAc^- media better than from SO_4^{2-} and NO_3^- . The unmodified Htd and carboxylate esters of modified Htd were efficiently recycled and re-used for metals extraction.

Attempts were made to make the purification of the Htd from wheat straw wax a greener process, as this was initially conducted with petroleum ether and cuprous acetate, in yields of 18.00wt%. Alternative solvents to petroleum ether with better environmental and safety credentials; cyclohexane, cyclopentyl methyl ether, *p*-cymene and 2,2,5,5-tetramethylTHF were tested for this purpose. The resulting isolated yields of the Htd were 6.00wt%, 7.80wt%, 8.20wt% and 21.40wt% for the cyclohexane, cyclopentyl methyl ether, *p*-cymene and 2,2,5,5-tetramethylTHF respectively. In order to avoid the use of both organic solvents and cuprous acetate, supercritical carbon dioxide ($scCO_2$) fractionation of the wheat straw wax for Htd were performed. The $scCO_2$ fractionation of the wheat straw wax using silica gel adsorbent at 300 bar, 313 K was found to give somewhat better selectivity for Htd than alumina and celite adsorbents. Although this method demonstrated some promise it was not as effective as the system utilising 2,2,5,5-tetramethylTHF and cuprous acetate, in which both the solvent and copper could be recovered for reuse.

List of Content

Abstract	3
List of Content	4
List of Tables	12
List of Figures	15
List of Equations and Schemes	22
Acknowledgements	25
Declaration	26
1 Chapter 1.....	28
1.1 Introduction	28
1.2 Aims/objectives.....	29
1.3 Green chemistry.....	29
1.4 The principles of Green Chemistry	30
1.5 Metal sustainability.....	31
1.6 Chelating agents.....	36
1.6.1 Traditional chelating agents.....	38
1.6.2 Challenges of traditional chelating agents.....	42
1.6.3 Alternatives Greener chelating agents	44
1.6.3.1 Glutamic diacetic acid (L-GLDA)	45
1.6.3.2 Polyaspartic acid (PASA)	46
1.6.3.3 Ethylenediamine dissunic acid ([S, S]-EDDS)	46
1.7 Brief review on β -diketones.....	51
1.7.1 Synthesis of lipophilic β -diketones	53
1.7.2 β -diketones as metal chelating agents	55

1.8	Solvent extraction of metals	57
1.9	Equilibrium slope analysis	62
1.10	Metal ligand (M-L) interaction	63
1.11	Wheat straw wax.....	65
1.12	Use of supercritical carbon dioxide (scCO ₂) for extraction/ fractionation ...	70
1.13	KF/alumina base catalyst	74
1.14	Michael addition reaction	76
1.15	Introduction to work in thesis.....	80
2	Chapter 2: Purification of lipophilic β-diketone from wheat straw wax using petroleum ether	84
2.1	Introduction.....	84
2.2	Results and discussion on isolation of the lipophilic β-diketone using cuprous acetate -Cu(OAc) ₂	85
2.2.1	GC characterisation of the Htd.....	88
2.2.2	Electrospray ionisation mass spectrum (ESI-MS) of the Htd	91
2.2.3	FTIR spectrum and UV absorption of the Htd	92
2.2.4	¹ H-NMR and ¹³ C-NMR spectra of the Htd	95
2.2.5	Thermal gravimetric analysis (TGA) of the Htd	98
2.2.6	Differential scanning calorimetric measurement (DSC) of the Htd	99
2.2.7	Solubility study of the Htd.....	100
2.2.8	Keto- enol tautomerisation studies of the Htd in comparison to Hacac and Hdbm	106
2.3	Conclusion	119
3	Chapter 3: Purification of the lipophilic β-diketone with greener solvents ...	122
3.1	Introduction.....	122
3.2	Results and discussion on alternative solvents used in the purification of Htd	123

3.2.1	The scCO ₂ extraction/fractionation of the wheat straw wax for the Htd	128
3.2.2	Simultaneous scCO ₂ extraction/fractionation of the wheat straw wax for Htd using celite adsorbent	130
3.2.3	Sequential scCO ₂ extraction of the wheat straw wax for Htd using celite adsorbent	134
3.2.4	Sequential scCO ₂ extraction of the wheat straw wax for Htd using silica adsorbent	136
3.2.5	Sequential scCO ₂ extraction of the wheat straw wax for Htd using alumina adsorbent	138
3.2.6	Simultaneous thermal analysis (STA) of some fractional extracts from the fractionation of wheat straw wax	142
3.3	Conclusion	148
4	Chapter 4: Modification of the biodrived lipophilic β-diketone	150
4.1	Introduction	150
4.2	Results and discussion of modification of the β -diketone	151
4.2.1	The modification of the Htd	153
4.2.2	Electrospray ionisation mass spectroscopy (ESI (+)-MS) of the carboxylate esters of modified bioderived β -diketone	157
4.2.3	GC-FIDs chromatogram of the modified Htd	161
4.2.4	Effect of Michael acceptors on the modification of the Htd	162
4.2.5	Effect of temperature on the modification of the Htd	163
4.2.6	Effect of time on the modification of the Htd	165
4.2.7	Effect of amount of KF/alumina on the modification of the Htd	167
4.2.8	Separation/purification of the modified Htd	168
4.2.9	NMR spectra of modified Htd	172
4.2.10	FTIR of the modified Htd	174
4.2.11	DSC of the modified Htd	175

4.2.12	Preparation of the carboxylate acid of the modified Htd	176
4.2.13	NMR spectra of the carboxylate acid of the modified β -diketones.....	177
4.2.14	ESI-MS of the carboxylate acids of modified Htd.....	178
4.2.15	FTIR of the MaH and ItaH	183
4.3	Conclusion	185
5	Chapter 5: Metals extraction with the unmodified and modified bioderived β-diketone	188
5.1	Introduction.....	188
5.2	Results and discussion on the extraction of metals with the unmodified and modified Htd	189
5.2.1	Influence of contact time on the removal of Cu(II) from Cu(OAc) ₂ solution	190
5.2.2	Effect of Htd concentration on removal of Cu(II) from Cu(OAc) ₂ solution	192
5.2.3	Slope analysis for Cu(II) extraction from Cu(OAc) ₂ solution with Htd ..	194
5.2.4	Effect of pH on the extraction of Cu(II) from Cu(OAc) ₂ with Htd.....	197
5.2.5	Effect of solvent on the extraction of Cu(II) from CuCl ₂ solution with Htd	199
5.2.6	Temperature effect on extraction of Cu(II) from CuCl ₂ solution with Htd	201
5.2.7	Effect of ionic strength on extraction of Cu(II) from CuCl ₂ solution	202
5.2.8	Removal of metal ions with Htd in comparison to Hdbm and Hacac ...	203
5.2.9	Extraction of the different metal ions with unmodified and modified Htd	207
5.2.10	Effect of initial metal ion concentration on Cu(II) extraction with the Htd, Hdbm, Ma, Ita, MaH and ItaH	208
5.2.11	UV/Visible spectrophotometric determination of Cu(II) extraction	209
5.2.12	Extraction of Co(II) from CoCl ₂ and Co(NO ₃) ₂ solutions.....	213
5.2.13	Removal of Ni(II) from NiCl ₂ solution	215

5.2.14	Removal of Fe(III) and Cr(III) from FeCl ₃ and CrCl ₃ solutions	218
5.2.15	Comparative summary of the extracted metal ions	221
5.2.16	Changes in pH during the extraction with these bioderived materials	225
5.2.17	Competitive extraction of Cu(II) and Co(II) from mixture of CoCl ₂ and CuCl ₂ solution (0.015 M each).....	229
5.2.18	Effect of pH on extraction of Cu(II) from CuCl ₂ solution with the bioderived materials and Hdbm	230
5.2.19	Determination of metal ions extracted with ICP-MS.....	232
5.2.20	ICP-MS determination of removed Pb(II) and Ga(III) with Htd and MaH	234
5.2.21	UV/visible spectra of some of the metal extracts with Htd and Hdbm	236
5.2.22	¹ H-NMR spectrum of Co and Cu- extracts with Htd.....	239
5.2.23	FTIR evidence for the Co- and Cu-extracts with the Htd	240
5.3	Conclusion.....	242
6	Chapter 6: Experimental	244
6.1	Materials and reagents	244
6.2	Equipment.....	244
6.3	Experimental procedures.....	245
6.3.1	Purification of Htd using petroleum ether with cuprous acetate	245
6.3.2	Solubility test of the Htd in different solvents.....	246
6.3.3	Keto-enol tautomeric studies of the Htd in comparison to Hdbm and Hacac	247
6.3.4	The scCO ₂ fractionation of wheat straw wax for Htd	247
6.3.5	Preparation of potassium <i>tert</i> -butoxide (<i>t</i> -BuOK)	249
6.3.6	Preparation of 2,4-hexanedione by Claisen condensation of methyl ethyl ketone (MEK) and ethyl acetate	249
6.3.7	Preparation of methyl ketone using Dakin-West reaction	250

6.3.8	Preparation of trimethyl aconitate	250
6.3.9	Preparation of the KF/alumina catalyst	251
6.3.10	Modification of Hacac with methyl acrylate by Michael addition	251
6.3.11	Modification of the Htd using carboxylate esters by Michael addition	251
6.3.12	Preparation of cinnamic acid by hydrolysis of methyl cinnamate	253
6.3.13	Preparation of palmitic acid by hydrolysis of methyl palmitate	254
6.3.14	Preparation of carboxylate acids of the Ma and Ita by hydrolysis	254
6.3.15	UV/Visible spectrophotometric analysis of some of the metal-diketonates	255
6.3.16	Calibration of some metals salts solutions by UV/Visible spectrophotometric technique	255
6.3.16.1	Calibration procedure of $\text{Cu}(\text{OAc})_2$	255
6.3.16.2	Calibration procedure for NiCl_2 and $\text{Co}(\text{NO}_3)_2 \cdot 6\text{H}_2\text{O}$	256
6.3.16.3	Calibration procedure for FeCl_3	258
6.3.16.4	Calibration procedure for CuCl_2 , $\text{CrCl}_3 \cdot 6\text{H}_2\text{O}$ and CoCl_2	258
6.3.16.5	Calibration procedure of $\text{CuSO}_4 \cdot 5\text{H}_2\text{O}$	260
6.3.16.6	Calibration procedure of $\text{Cu}(\text{NO}_3)_2 \cdot 3\text{H}_2\text{O}$	261
6.3.17	Preparation of the synthetic metal aqueous solutions (0.03 M each)	263
6.3.18	Preparation of the mixture of CuCl_2 and CoCl_2 (0.015 M each)	263
6.3.19	Preparation of the chelators standard solutions (3 mM)	265
6.3.20	Procedure of the solvent extraction of the metal ions	266
6.3.21	Determination of the metal ions extraction with ICP-MS	269
6.4	Instrumental analyses	269
6.4.1	FTIR analysis	269
6.4.2	NMR analysis	269

6.4.3	Thin layer chromatography (TLC) analysis	270
6.4.4	Purification of the Ita mixture by Kugelrohr distillation	270
6.4.5	Flash chromatographic separation of the Ma and Ita	270
6.4.6	GC-FID analysis	271
6.4.7	GC-MS analysis	271
6.4.8	Differential scanning calorimetric (DSC) analysis	272
6.4.9	ESI-MS analysis	272
6.4.10	GC-FID calibration procedure for Htd quantification	273
7	Chapter 7: Thesis conclusion and future work	276
7.1	Concluding remarks	276
7.2	Future work	277
7.2.1	Derivation of methyl ketone from lauric acid using Dakin-West reaction	277
7.2.2	Preparation of β -diketone using Claisen Condensation	279
7.2.3	Silica adsorbent support for the $scCO_2$ fractionation wheat straw wax for Htd	280
7.2.4	Amine functionalisation of the Ma_d	281
7.2.5	Preparation of polyfunctional molecules	281
7.2.6	Preparation of the carboxylate acids of Ma and Ita by acid hydrolysis	281
7.2.7	Precious metals extraction studies	282
7.2.8	Competitive metals extraction studies	282
7.2.9	Use as surfactants	282
	Appendices	283
	Appendix 1	284
	Appendix 2	290
	List of abbreviations	293

8	Reference.....	298
----------	-----------------------	------------

List of Tables

Table 1-1: Major uses of critical elements of global importance ²³	32
Table 1-2: Some representatives of conventional chelating agents ⁶⁷	39
Table 1-3: Commonly used bioderived and green chelating agents for recovery of metals from wastes.....	49
Table 1-4: Equilibrium constants for tautomerisation of acetylacetone in various solvents at 0.1 mole fraction solute	52
Table 1-5: M-L classification based on electronic structure, nature, ionic radii and hardness/softness of metal ions ¹⁰	65
Table 1-6: Abundance of the main constituent in wheat straw ^{164,165}	67
Table 1-7: Representative of common components of wheat straw wax	69
Table 1-8: Order of density, viscosity and diffusivity of gases, liquids and supercritical fluids ^{171,173}	71
Table 1-9: Critical temperatures and pressures of some fluids ¹⁷³	71
Table 2-1: ESI-MS(+) interpretation of the Htd.....	92
Table 2-2: FTIR assignments of the Htd	93
Table 2-3: GSK quick solvent guide ²¹⁷	102
Table 2-4: The results of the solubility studies of Htd at 293 K and the Kamlet-Taft parameters ²³²⁻²³⁴ of the selected solvents	105
Table 2-5: ¹ H-NMR chemical shifts (δ , ppm) for Htd in comparison to Hacac and Hdbm in different deuterated solvents	107
Table 2-6: Keto-enol content, equilibrium constant (K_{eq}) and ΔG° of Htd in comparison to Hacac and Hdbm in five different solvents at 295 K	115
Table 2-7: % enol and equilibrium constant in different solvents determined with FTIR ¹³⁶	118
Table 3-1: Comparison of the isolated β -diketone's yield and benefits of the alternative solvents to petroleum ether	124
Table 3-2: Properties of the alternative solvents used in the purification of Htd from wheat straw wax in comparison to petroleum ether and hexane. ²¹⁷	126

Table 3-3: Masses of the fractional extracts for the simultaneous scCO ₂ extraction/fractionation using 155 g wax: 165 g celite	130
Table 3-4: The various quantities of fractions from simultaneous scCO ₂ extraction/fractionation of the wax (A = 1 g wax: 200 g celite & B= 10 g wax: 200 g celite) for 4 h	132
Table 3-5: Materials collected from sequential scCO ₂ extraction with 1 g wax: 200 g celite adsorbent at 313 K and 40 min	135
Table 3-6: Masses collected from sequential extraction of wax using 1 g wax: 200 g silica adsorbent at 40 min at 313 K.....	137
Table 3-7: Masses collected from sequential extraction of wax using alumina adsorbent at 40 min.....	139
Table 3-8: Amount of lipophilic β-diketone (Htd) determined from the scCO ₂ fractions obtained from wheat straw wax	140
Table 3-9: Masses and melting point ranges of the fraction obtained from simultaneous scCO ₂ fractionation with 10 g wax: 200 g celite adsorbent	142
Table 3-10: Potential applications of different wheat straw wax components ¹⁶⁶	147
Table 4-1: The Michael acceptors that were tested for the modification of Htd	156
Table 4-2: ESI-MS peaks and interpretation for the Ma and Ita	160
Table 4-3: The <i>r_f</i> of the Htd, Ma _s , Ma _d , and Ita using 80% cyclohexane and 20% ethyl acetate.....	171
Table 4-4: Determination of the molar composition of the modified Htd	172
Table 4-5: Characteristic carbonyl peaks of the unmodified Htd and modified Htd ..	175
Table 4-6: Determination of melting points of the Ma and Ita by DSC	175
Table 4-7: Proposed assignment of the ESI (+)-MS peaks of the ItaH	179
Table 4-8: Proposed assignment of the ESI (-)-MS of the ItaH	180
Table 4-9: Proposed assignment of the major ESI (+)-MS peaks of the MaH.....	180
Table 4-10: FTIR of the carboxylate acid of the modified Htd	184
Table 5-1: Dependence of distribution of Cu(II) on concentration of the Htd	194
Table 5-2: Effect of adding various amount of KCl on removal of Cu(II) from CuCl ₂ solution with the Htd at M: L (5:1).....	203

Table 5-3: Distribution constant of Hacac, Hdbm and Htd at 298 K in cyclohexane..	205
Table 5-4: Distribution constants of β -diketones at 298 K in aqueous-organic phase ³²⁵	205
Table 5-5: Distribution constants of Hacac, $\log K_{D(HA)}$ between water and various organic solvents, 298 K ³²⁶	206
Table 5-6: The unmodified and modified Htd tested as metals chelators in comparison to Hdbm	207
Table 5-7: Effect of initial Cu(II) ion concentration on Cu(II) extraction with the these bioderived chelators and Hdbm	209
Table 5-8: Extracted Cu(II) from CuCl ₂ , Cu(OAc) ₂ and CuSO ₄ .5H ₂ O solutions with Htd determined with ICP-MS and UV/visible spectrophotometric methods.....	213
Table 5-9: Summary of metal ions extracted (mg/L) (10:1; M: L) with the unmodified and modified Htd at pH range 4 – 7 (Cu(II), Ni(II), Co(II)) and 1.5 – 2.6 (Fe(III) and Cr(III))	222
Table 5-10: pH variation following the removal of metal ions with the modified and unmodified Htd M: L (10:1).....	226
Table 5-11: pH variation following the extraction of Cu(II) in OAc ⁻ , Cl ⁻ , SO ₄ ²⁻ and NO ₃ ⁻ media with modified and unmodified Htd M: L (10:1)	227
Table 5-12: Effect of pH on extraction of Cu(II) from CuCl ₂ solution (M: L; 2:1)	232
Table 5-13: UV/visible spectra of Htd and Hdbm and their metal complexes in chloroform (1.0 X 10 ⁻⁵ M)	238
Table 5-14: FTIR (cm ⁻¹) of the metal-Htd complexes and the free Htd	241
Table 6-1: The UV/visible spectrophotometric calibration curves' features of the metals solutions	263

List of Figures

Figure 1-1: Time remaining of rare and precious metal reserves based on present consumption and disposal rate ¹	34
Figure 1-2: Uneven distribution of rare and precious metal reserves across the globe ^{1,33}	34
Figure 1-3: Current rate of recycling of different metals ¹	35
Figure 1-4: Percentages of applications of commonly used chelating agents, APCs (aminopolycarboxylates) ⁸	38
Figure 1-5: Some carboxylic and organophosphorus acid metals chelating extractants	41
Figure 1-6: Dimers of carboxylic and phosphorus acids metals chelating extractants.	41
Figure 1-7: Identified degradation products and pathways of the EDTA ⁸⁶	43
Figure 1-8: L-Glutamic diacetic acid (L-GLDA).....	45
Figure 1-9: Some schemes of β -diketone derivatives	53
Figure 1-10: Scheme biosynthesis of β -diketone ¹⁴⁵	54
Figure 1-11: common β -diketones used in metals extraction	56
Figure 1-12: fluorinated and other nonfluorinated β -diketones used in metals extraction	57
Figure 1-13: A typical traditional extracting vessel (mixer-settler) for solvent separation of metals.....	59
Figure 1-14: Incorporation of solvent extraction to achieve metal separation and concentration in a hydrometallurgical circuit which involves recycling of all reagents ⁸⁹	59
Figure 1-15: Description of a wheat straw	66
Figure 1-16: Breakdown of GB straw production (tonnes) by region in 2007.....	67
Figure 1-17: Major cyclic compounds in plant waxes	70
Figure 1-18: Phase diagram (P, V) for a pure compound in a close system. The triple point indicates the critical pressure of CO ₂	72
Figure 1-19: Cooperative basicity of F ⁻ and alumina.....	75

Figure 2-1: Isolation of Htd from wheat straw wax dissolved in petroleum ether with Cu(OAc) ₂	86
Figure 2-2: GC-FID chromatogram of the Htd.....	88
Figure 2-3: GC-MS of Htd	88
Figure 2-4: A Proposed fragmentation scheme of the bioderived β-diketone	90
Figure 2-5: ESI-MS(+) for the Htd	92
Figure 2-6: FTIR spectrum of the Htd.....	93
Figure 2-7: ¹ H-NMR spectrum of the Htd in CDCl ₃	96
Figure 2-8: ¹³ C-NMR spectrum of the Htd in CDCl ₃	97
Figure 2-9: TGA thermogram of bioderived β-diketone (Htd).....	98
Figure 2-10: DSC thermogram of wheat straw wax and the Htd.....	100
Figure 2-11: Keto-enol Integrated ¹ H-NMR spectrum of Htd	110
Figure 2-12: % enol of Htd, Hacac and Hdbm versus solvents polarizability.....	113
Figure 2-13: % enol of Htd, Hacac and Hdbm versus solvents hydrogen bond acceptor	114
Figure 2-14: % enol of Htd, Hacac and Hdbm versus solvents dipole moment	117
Figure 3-1: GC-FID chromatogram of the wheat straw wax before fractionation	130
Figure 3-2: Fractions from the simultaneous scCO ₂ extraction/fractionation using 155 g wax: 165 g celite adsorbent	131
Figure 3-3: GC-FID chromatograms of the simultaneous scCO ₂ extraction/fractionation of wheat straw wax for Htd from 10 g wax: 200 g clay	133
Figure 3-4: GC-FID chromatograms of the simultaneous scCO ₂ extraction/fractionation of wheat straw wax for Htd from 1 g wax: 200 g celite adsorbent	133
Figure 3-5: Fractional extracts from sequential scCO ₂ extraction of the wax from 1 g wax: 200 g celite adsorbent at 313 K and 40 min.....	134
Figure 3-6: GC-FIDs chromatogram of the fractions from the sequential scCO ₂ extraction using 1 g wax: 200 g celite adsorbent at 313 K and 40 min	136
Figure 3-7: GC-FIDs chromatogram of the fractions from the sequential scCO ₂ extraction using 1 g wax: 200 g silica adsorbent at 313 K and 40 min	137

Figure 3-8: GC-FIDs chromatogram of the fractions from the sequential scCO ₂ extraction using 1 g wax: 400 g alumina adsorbent at 313 K and 40 min	138
Figure 3-9: STA of the fraction at 250 bar and 323 K for the simultaneous scCO ₂ fractionation of wax using 10 g wax: 200 g celite adsorbent	143
Figure 3-10: STA of the fraction at 150 bar and 323 K for the simultaneous scCO ₂ fractionation of wax using 10 g wax: 200 g celite adsorbent	144
Figure 3-11: STA of the fraction at 75 bar and 308 K for the simultaneous scCO ₂ fractionation of wax using 10 g wax: 200 g celite adsorbent	145
Figure 3-12: STA of the fraction at 1 bar 308 K for the simultaneous scCO ₂ fractionation of wax using 10 g wax: 200 g celite adsorbent	146
Figure 4-1: GC-MS of the trimethyl aconitate.....	153
Figure 4-2: ESI (+)-MS of the Ma	159
Figure 4-3: ESI(+)-MS of Ita.....	159
Figure 4-4: GC-FID chromatogram of the Htd.....	161
Figure 4-5: GC-FID chromatogram of the Ita	161
Figure 4-6: GC-FID chromatogram for the Ma (single and double addition of methyl acrylate).....	162
Figure 4-7: % conversions of the modification of the Htd for 5 min at 423 K using conventional heating (Mma = methyl methacrylate product, Ita = itaconate product and Ma = methyl acrylate product.....	162
Figure 4-8: % conversions of the modification of the Htd for 5 min at 423 K using microwave heating (Mma = methyl methacrylate product, Ita = itaconate product and Ma = methyl acrylate product.....	163
Figure 4-9: % conversions of the modification of the Htd with methyl acrylate and dimethyl itaconate for 5 min at different temperatures.....	164
Figure 4-10: % conversion of the modification of Htd with dimethyl itaconate at 423 K at varying time (between 1-15 min) under conventional heating.....	165
Figure 4-11: % conversion of the modification of Htd with dimethyl itaconate at 423 K at varying time (between 1-15 min) under microwave heating.....	166
Figure 4-12: % conversions of the modification of the Htd with methyl acrylate at 393 K at different time under conventional heating	166

Figure 4-13: % conversions of the modification of the Htd with methyl acrylate at 393 K at different time under microwave heating	167
Figure 4-14: Effect of amount of catalyst (KF/alumina) on the modification of Htd with dimethyl itaconate and methyl acrylate	168
Figure 4-15: TLC for Ma using 80% cyclohexane and 20% ethyl acetate (M = Htd; and N, O = products, Ma _s and Ma _d respectively).....	169
Figure 4-16: TLC for Ita using 80% cyclohexane and 20% ethyl acetate (The spot marked A= excess dimethyl itaconate and B= Ita)	169
Figure 4-17: UV chromatogram for the separation Ma	170
Figure 4-18: UV chromatogram for the separation Ita	170
Figure 4-19: Fractions collected from the purification of Ma.....	171
Figure 4-20: Sample of purified Ita	171
Figure 4-21: ¹ H-NMR spectrum of Ita	173
Figure 4-22: ¹ H-NMR spectrum of Ma	174
Figure 4-23: DSC thermograms of Ma and Ita	176
Figure 4-24: ESI (+)-MS of the ItaH.....	179
Figure 4-25: ESI (-)-MS of the ItaH	179
Figure 4-26: ESI (+)-MS of the MaH	180
Figure 4-27: Proposed dissociation (fragmentation) of Htd derivatives as found in ESI-MS(+).....	182
Figure 4-28: Fragmentation of long chain 2,4-diketone silyl ether derivatives.....	182
Figure 5-1: Effect of contact time on the removal of Cu(II) from Cu(OAc) ₂ solution using Htd and Hdbm (in limonene; M: L; 10:1)	191
Figure 5-2: Cu(II) extraction from Cu(OAc) ₂ solution with different amount of the Htd	193
Figure 5-3: Cu(II) extracted (i.e. from 0.02 M Cu(OAc) ₂) versus % free Htd (initial concentration of Htd = 4.31 – 0.34 mM)	193
Figure 5-4: Plot of the log D vs log [Htd] for the extraction of Cu(II) from Cu(OAc) ₂ solution	195

Figure 5-5: Plot of log D vs ΔpH for the extraction of Cu(II) from Cu(OAc) ₂ solution with the Htd.....	195
Figure 5-6: Effect of pH on extraction of Cu(II) from Cu(OAc) ₂ solution using the Htd	198
Figure 5-7: Extraction of Cu(II) from CuCl ₂ solution with Htd in toluene, limonene, cyclohexane and cyclopentylmethyl ether (CPME)	201
Figure 5-8: Effect of temperature on extraction of Cu(II) from CuCl ₂ solution with Htd	202
Figure 5-9: Extraction of the metal ions using Htd, Hdbm and Hacac.....	204
Figure 5-10: Removal of Cu(II) with the bioderived chelators and Hdbm	211
Figure 5-11: Removal of Co(II) from CoCl ₂ solutions with the different biochelators	214
Figure 5-12: The extraction of Ni(II) from NiCl ₂ solution	216
Figure 5-13: Extraction of Ni(II) with Htd and Hdbm as function of contact time.....	217
Figure 5-14: Removal of Fe(III) and Cr(III) from FeCl ₃ and CrCl ₃ solutions with Htd and Hdbm	219
Figure 5-15: Cr(III) extraction from CrCl ₃ solution with Htd, Hdbm, Ma and Ita at pH 5-6 using M: L of 10:1	220
Figure 5-16: Single metal extraction of Co(II) and Cu(II) in Cl ⁻ medium.....	230
Figure 5-17: Competitive metal removal from mixture of Co(II) and Cu(II) in Cl ⁻ medium	230
Figure 5-18: ICP-MS determination of extracted Cu(II), Pb(II) and Mn(II) using Htd..	234
Figure 5-19: ICP-MS determination of extracted of Cu(II) from CuCl ₂ , Cu(OAc) ₂ and CuSO ₄ solutions with Htd (M: L, 1: 1).....	234
Figure 5-20: ICP-MS determination of recovered Ga(III) and Pb(II) with the Htd and MaH	236
Figure 5-21: UV/visible spectra of the metal extracts with the Htd in chloroform (1.0 x 10 ⁻⁵ M)	237
Figure 5-22: UV/visible- spectra of Hdbm and its metals complexes in chloroform- 1.0 x 10 ⁻⁵ M.....	238
Figure 5-23: ¹ H-NMR spectrum of Co and Cu- complexes after extraction with Htd.	239

Figure 5-24: Co- and Cu- 14,16-hentriacontanedionate with the marked vinyl protons	240
Figure 5-25: FTIR spectra of the free and metal-Htd chelate	241
Figure 6-1: The stages for the isolation of the Htd from wheat straw wax using petroleum ether with Cu(OAc) ₂	246
Figure 6-2: Schematic illustration of the scCO ₂ extractor's basic components.....	248
Figure 6-3: The scCO ₂ extractor used in the fractionation of the wax	249
Figure 6-4: Traditional stirrer hot plate and SP discoverer microwave (CEM) heating sources used for the modification of the Htd	253
Figure 6-5 Calibration curve for Cu(OAc) ₂	256
Figure 6-6: Calibration curve of NiCl ₂	257
Figure 6-7: Calibration curve of Co(NO ₃) ₂ .9H ₂ O	257
Figure 6-8: Calibration curve for FeCl ₃	258
Figure 6-9: Calibration curve of CuCl ₂ at 812 nm.....	259
Figure 6-10: Calibration curve of CrCl ₃ . 6H ₂ O	259
Figure 6-11: Calibration curve for CoCl ₂ at 511 nm	260
Figure 6-12: Calibration curve of CuSO ₄ .5H ₂ O	261
Figure 6-13: Calibration curve of Cu(NO ₃) ₂ .3H ₂ O	262
Figure 6-14: Calibration curve for CuCl ₂ at 511 nm	265
Figure 6-15: Calibration curve for CoCl ₂ at 811.5 nm	265
Figure 6-16: The Purification concept of the Htd from wheat straw and its application for metals recovery	267
Figure 6-17: Some samples during the biphasic extraction of the metal ions using the unmodified and modified Htd (0.03 M metals solution and 0.003 M chelants in each case)	268
Figure 6-18: Some samples of the biphasic extraction of the metals with Hacac (M: L; 10: 1)	268
Figure 6-19: GC-FID calibration curve for Htd quantification using tetradecane standard	274

Figure A-1: ^{13}C -NMR spectrum of the Ma	284
Figure A-2: ^{13}C -NMR spectrum of the Ita (similar assignment as in Fig. A-1)	284
Figure A-3: FTIR spectrum of Ita	285
Figure A-4: FTIR spectrum of Ma (similar assignments as in Fig. A-3)	285
Figure A-5: ^1H -NMR spectrum of the MaH	286
Figure A-6: ^1H -NMR spectrum of the ItaH	286
Figure A-7: ^{13}C -NMR spectrum of the ItaH	287
Figure A-8: ^{13}C -NMR spectrum of the MaH (similar assignment as in Fig. A-7)	287
Figure A-9: FTIR spectrum of the MaH	288
Figure A-10: FTIR spectrum of ItaH	288
Figure A-11: MS of the methyl ketone (2-Tridecanone)	289
Figure A-12: GC-MS of 2,4-hexanedione	289

List of Equations and Schemes

Equation 1-1: Formation of metal complex with carboxylic acid dimers.....	41
Equation 1-2: Synthesis of poly aspartate	46
Equation 1-3: Synthesis of [<i>S, S</i>] EDDS.....	47
Equation 1-4: keto-enol equilibrium of β -diketone	51
Equation 1-5: Synthesis of the 14, 16-hentriacontanedone.....	54
Equation 1-6: synthesis of decan-2,4-dione using Claisen condensation reaction	54
Equation 1-7: Synthesis of long chain β -diketone	55
Equation 1-8: Equation for extraction of metals using β -diketones as chelating extractant.....	56
Equation 1-9: An equilibrium reaction.....	57
Equation 1-10: Distribution constant of solute (distribuend) A	58
Equation 1-11: Metal/ligand equilibrium	62
Equation 1-12: An equation for equilibrium or extraction constant	62
Equation 1-13: Equilibrium distribution constant	63
Equation 1-14: linearize equation for determination of stoichiometry and extraction constant	63
Equation 1-15: Reactions of KF with alumina	75
Equation 1-16: General scheme of Michael Addition Reaction.....	77
Equation 1-17: Scheme of double and single Michael addition	78
Equation 1-18: Selective double Michael addition	78
Equation 1-19: Selective single Michael addition.....	78
Equation 1-20: The use of silica in Michael addition reaction of open chain amine....	79
Equation 1-21: Michael addition reaction with silica gel involving aromatic amine....	79
Equation 1-22: Addition of amine to methyl crotonate, acrylate and methyl methacrylate	79

Equation 2-1: Formation of Cu(II) β -diketone complex and subsequent recovery of the Htd	86
Equation 2-2: keto, chelated enol and non-chelated enol of acetyl acetone.....	94
Equation 2-3: Conjugated enol tautomer	95
Equation 2-4: Keto-enol tautomers of the Htd	97
Equation 2-5: Keto-enol tautomerism of β -diketone	107
Equation 2-6: Keto-enol equilibrium constant.....	111
Equation 2-7: Gibbs free energy	111
Equation 2-8: Influence of acetone on the keto- enol equilibrium	113
Equation 3-1: Synthesis of <i>p</i> -cymene from limonene ²³⁴	125
Equation 4-1: Preparation of trimethyl aconitate in acidified methanol medium	152
Scheme 4-2: A proposed fragmentation pattern for the trimethyl aconitate.....	153
Equation 4-3: Modification of the Htd using Michael addition reaction	154
Scheme 4-4: Detail scheme of Michael addition modification reaction.....	154
Equation 4-5: Renewable routes to acrylic acid ²⁷⁶	157
Equation 4-6: Isomerisation of dimethyl itaconate in the presence of KF/alumina at temperature of 363 K and above	164
Equation 4-7: Preparation of the carboxylate acid of the methyl acrylate modified bioderived β -diketone (MaH).....	177
Equation 4-8: Preparation of the carboxylate acid of the dimethyl itaconate modified bioderived β -diketone (ItaH).....	177
Equation 4-9: Retro-Claisen pathway for β -diketone ¹⁶⁶	183
Scheme 4-10: Scheme for the formation of the carboxylate acid of the modified Htd via direct hydrolysis	185
Scheme 4-11: Scheme for the formation of the carboxylate acid of the modified Htd via alcoholysis	185
Scheme 5-1: Equilibria for Cu(II) extraction with Cyanex 272 at low (a), medium (b) and high OAc ⁻ concentrations	196

Equation 5-2: The equilibrium equation for extraction of Cu(II) with Htd	197
Equation 5-3: Extraction equation with involvement of Cl ⁻ counter ion	215
Equation 5-4: Liberation of H ⁺ from water by high density +3 charge metal ions	218
Equation 5-5: Release of H ⁺ from the chelating chelators after extraction	228
Equation 5-6: Replacement of water in the aqua ion by ligand	229
Equation 6-1 (a and b): Beer-Lambert equations for the mixture of CuCl ₂ and CoCl ₂ solution	264
Equation 6-2: Mass and Area response ratios for the GC-FID calibration	273
Equation 7-1: Dakin West conversion of lauric acid into methyl ketone	278
Equation 7-2: Claisen Condensation of ethyl acetate and butan-2-one to form 2, 4-hexanedione.....	279
Scheme A-1: proposed mechanism for the Dakin-West formation of methyl ketone from lauric acid	290
Scheme A-2: Fragmentation pattern of 2-Tridecanone	291
Scheme A-3: Detail scheme for the formation of 2,4-hexanedione	291
Scheme A-4: Proposed fragmentation pattern of 2,4-hexanedione	292

Acknowledgements

I am deeply and most sincerely thankful to my supervisors, Professor James H. Clark; Dr. Andrew J. Hunt and Dr. Thomas J. Farmer for their support and effort in my training. Your input and advice are invaluable to completing my PhD programme. I will ever remain indebted for the positive difference you made in my life. In addition, I wish to express my profound gratitude to Hannah Briers, Charlotte Brannigan, Paul Elliot for laboratory training and guidance. I wish to thank all the staff in the graduate office and Chemistry Department, University of York, UK for the opportunity you given me to learn numerous skills and courses that you taught me. These courses and skills have really been crucial during my research work. I am so much grateful to Thomas Attard for proofreading the thesis constructively. I wish to express my thanks to Fergal Bryne for his numerous contribution towards my PhD in the areas of samples analysis, flash chromatographic separation, cross fertilization of ideas and writing of papers together. Thank you Dr. Con Robert McElroy and Dr. Vitaliy Budarin for the invaluable contribution in the area of scCO₂ fractionation and data analysis. Thanks Karl Heaton for the rigorous ESI-MS and other mass spectroscopic analyses. My heartfelt thanks goes to Alison Edmonds and Katy Brooke for all your help throughout my PhD training years especially in facilitating my settling down at the start of the programme, arranging meetings, arranging poster printing and travels. I am again indebted to TETFund, Nigeria and Benue State University Makurdi, Nigeria for sponsoring and letting me come to UK for my PhD. Finally, I am grateful to my wife (Mrs Asemave Tabitha) and children (Kamo and Kator) for their unfathomable support throughout my research studies.

Declaration

All these results are the work of the author. Some fraction of the results of this thesis were obtained from previous researchers who are fully acknowledged in the text as references. Details as follows;

Table 2-7: N. A. Abood and A. F. Ajam, *J. Chem. Soc. Pak.*, 1985, **7**, 1 – 6.

Figure 3-1: E. H. K. Sin, University of York, PhD thesis, 2012.

Table 5-4: T. Sekine, M. Katori, R. Murai, and T. Saitou, *Bunseki Kagaku (The Japan Soc. Anal. Chem.)*, 1984, **33**, E351–E358

Table 5-5: J. Stary and J. O. Liljenzin, *Pure Appl. Chem.*, 1982, **54**, 2557–2592.

References of some aspects of this research that have been published or presented as posters:

Asemave Kaana. Alternative bio-derived chelating agents. A talk presented at the conference titled: *Building sustainability into your business: The Case for bio-based chemicals*; Green Chemistry Centre Excellence, University of York, Heslington, UK. Oct. 6th, 2014

Jennifer Ruth Dodson, Helen L Parker, Andrea Muñoz García, Alexandra Hicken, **Kaana Asemave**, Thomas James Farmer, He He, James H. Clark, Andrew J Hunt. Bio-derived materials as a green route for precious & critical metal recovery and re-use; *Green Chemistry*; 46(23), 2015

Kaana Asemave, Fergal Byrne, Andrew J. Hunt, Thomas J. Farmer and James H. Clark. Bioderived alternative chelating agent for metal recovery. Being a poster presentation at the RSC conference, titled: *Renewable chemicals from waste- securing the molecular value from waste streams*; London, UK. Nov. 20th, 2015

Kaana Asemave. Bioderived alternative chelating agents for metals extractions. Being a talk presented at Northern Sustainable chemistry (NORSC), 5th PG symposium; King's Manor, York, UK. Sept. 23rd, 2015

Kaana Asemave, Andrew J. Hunt, Thomas J. Farmer, James H. Clark and Fergal Byrne. Alternative bioderived chelating agent (chelant) for metal recovery. Being a poster abstract for 2nd international conference on Past and Present Research Systems of Green Chemistry; Orlando, USA. Sept. 14-16, 2015

This work has not been previously presented for any award here or any other university.

Chapter 1

Introduction

Aspects of the work described in this chapter have been presented or published as:

Asemave Kaana. Alternative bio-derived chelating agents. A talk presented at the conference titled: *Building sustainability into your business: The Case for bio-based chemicals*; Green Chemistry Centre Excellence, University of York, Heslington, UK. Oct. 6th, 2014

Jennifer Ruth Dodson, Helen L Parker, Andrea Muñoz García, Alexandra Hicken, **Kaana Asemave**, Thomas James Farmer, He He, James H. Clark, Andrew J Hunt. Bio-derived materials as a green route for precious & critical metal recovery and re-use; *Green Chemistry*; 46(23), 2015

1 Chapter 1

1.1 Introduction

Heavy metals are utilised extensively in modern technologies, which has led to a high demand for this resource. The supply of heavy metals is mainly from their natural deposits; and their continuous depletion could eventually lead to scarcity.¹ These metals are often dispersed in the environment after use in the form of electronic and industrial wastes. This practice has been observed especially in the developing world. The large abundance of electronic and industrial metal waste has renewed interest in metal recovery from the environment to enhance sustainability. It is forecasted that the global e-waste only will increase to 50 metric tonnes (Mt) in 2018.² The metal value is dominated by gold and copper.² Most of the global e-waste are generated from Asia, Europe and America.² Essentially, wastes with substantial amount of heavy metals, are being considered as artificial or synthetic ores,^{3,4} i.e. potential points of recovery of these metals. In addition, trace amounts of iron, copper, manganese, calcium and other metals are usually found naturally in many raw materials which brings about scaling and undesirable metal-catalysed reactions while using these feedstocks. The presence of heavy metals in the environment could be hazardous even at low concentrations.^{5,6}

Chelating agents could be used to remove/extract metal ions from the environment by coordinating them via N, O, S or P atoms.^{7,8} The commonly used chelating agents are traditional ones, such as ethylenediaminetetraacetic acid-EDTA, nitrilotriacetic acid-NTA, phosphonates and phosphates etc. However their persistence in the environment⁸⁻¹¹ has generated concern due to their hazardous nature.^{8,9,12} In some instances they are toxic to both human and aquatic lives.^{13,14}

Therefore, the negative effects of traditional chelating agents have led to the search for environmentally benign (green) chelating agents. These are expected to experience fast growth, at about 10% annually,¹⁵ because of their low toxicological and biodegradability profile. Furthermore, there is renewed interest in utilising resources from biomass rather than petroleum feedstocks¹⁶ for sustainability.

1.2 Aims/objectives

The overall objectives of the project were:

- a. To isolate a known lipophilic β -diketone from wheat straw wax (referred to as bioderived β -diketone) using organic solvents and supercritical carbon dioxide (scCO₂).
- b. To modify this bioderived lipophilic β -diketone with appropriate pendants such as methyl acrylate, methyl methacrylate, dimethyl itaconate and trimethyl aconitate using the Michael addition reaction
- c. To test and compare the metal extraction ability of the unmodified and modified lipophilic bioderived β -diketone

1.3 Green chemistry

Green chemistry deals with the application of a set principles in order to reduce or eradicate the use of hazardous substances in design, manufacture and application of chemical products.¹⁷⁻²⁰ It is born out of the desire to practice chemistry in a sustainable manner. Its goals are to meet the present need without compromising the future generation meeting theirs. Green chemistry is not a new discipline in science but a philosophical approach towards tackling toxicity, renewability, human health and environmental threat by the judicious application of a set principles.^{17,18} The “Twelve

Principles of Green Chemistry” was established by Paul Anastas and John Warner in 1998 to help chemists to achieve sustainable chemical practices.²⁰ Green Chemistry principles were integrated into this work as much as possible.

1.4 The principles of Green Chemistry

1. **Prevention:** It is better to prevent waste than to treat or clean up waste after it is formed.
2. **Atom economy:** Synthetic methods should be designed to maximise the incorporation of all materials used in the process into final product.
3. **Less hazardous chemical synthesis:** Wherever practicable, synthetic methodologies should be designed to use and generate substances that possess little or no toxicity to human health and the environment.
4. **Designing safer chemicals:** Chemical products should be designed to preserve efficacy of function whilst reducing toxicity.
5. **Safer solvents and auxiliaries:** The use of auxiliary substances (e. g solvent, separation agents etc.) should be made unnecessary wherever possible and, innocuous when used.
6. **Design for energy efficiency:** Energy requirements should be recognised for their environmental and economic impacts and should be minimised. Synthetic methods should be conducted at ambient temperature and pressure.
7. **Use of renewable feed stocks:** A raw material or feedstock should be renewable rather than depleting wherever technically and economically practicable.
8. **Reduce derivatives:** Unnecessary derivatisation (blocking group, protection/deprotection and temporary modification of physical/chemical processes) should be avoided whenever possible.

9. **Catalysis:** Catalytic reagents (as selective as possible) are superior to stoichiometric reagents.
10. **Design for degradation:** Chemical products should be designed so that at the end of their function they do not persist in the environment and break down into innocuous degradation products.
11. **Real-time analysis for pollution prevention:** Analytical methodologies need to be further developed to allow for real-time, in-process monitoring and control prior to the formation of hazardous substances.
12. **Inherently safer chemistry for accident prevention:** Substances and the form of a substance used in a chemical process should be chosen so as to minimise the potential for chemical accidents, including releases, explosions and fires.

1.5 Metal sustainability

Metals are extensively used by industries in various applications such as electronics, materials, catalysts, chemicals, modern low-carbon energy technologies²¹ (nuclear, solar, wind, bioenergy, carbon capture and storage (CCS)) and electricity grids.^{21,22} Greater pressure has been placed on metal utilisation because of population growth coupled with a higher standard of living. Furthermore, industrialisation has led to the increasing demand for critical metals, as many of these are required in modern technologies. This is causing concern over the supply of critical metals for future generations. Therefore, according to Hunt *et al.*,²³ the sustainable use of metals is vital so that both the current and future generations have access to them without hitches. Industries or nations classify metals as critical depending on the purpose and need of assessment.²⁴ Some metals have been identified as critical metals because of their significance.²³ However, elements with significant supply restriction issues (geopolitical

issues, conflicts, international monopolies and mining as a by-product of other elements) and those which would have a dramatic impact on business or economy if limited are considered critical.²⁵ The top 14 metals, in order of decreasing demand, are tellurium, indium, tin, hafnium, silver, dysprosium, gallium, neodymium, cadmium, nickel, molybdenum, vanadium, niobium and selenium are commonly needed in these emergent low carbon energy technologies.^{21,26} The major uses of critical elements of global importance are described in Table 1-1 as follows,

Table 1-1: Major uses of critical elements of global importance²³

Element	Symbol	Major uses
Antimony	Sb	Flame retardant, semiconductors, alloys, pharmaceuticals, catalyst, flame and PET catalysts
Beryllium	Be	Electronics
Cobalt	Co	Super alloys, catalysts and batteries
Gallium	Ga	Semiconductors, solar cells, electronics (integrated circuits) and solar cells
Germanium	Ge	Semiconductors, solar cells, catalyst, infrared optics, PET catalysts, solar cells
Indium	In	Flat-panel displays, alloys, photocells and touch screens
Lithium	Li	Batteries, ceramics and glass
Molybdenum	Mo	High performance stainless steel
Niobium	Nb	HLA steel (high strength low alloy steels)
Palladium	Pd	Alloying agent, industrial catalyst, fuel cells and catalytic convertors for automobiles
Platinum	Pt	Alloying agent, industrial catalyst, fuel cells and catalytic convertors for automobiles
Rare Earth	REE	Magnets, batteries, ceramics and catalysts
Rhodium	Rh	Alloying agent, industrial catalyst, fuel cells and catalytic convertors for automobiles
Ruthenium	Ru	Hard disk drives, catalysts and electrochemistry

Selenium	Se	Glass, photovoltaics and infrared optics
Tantalum	Ta	Capacitors for electronics
Tellurium	Te	Steel additive, solar cells and thermoelectronics
Tungsten	W	High strength cutting tools
Vanadium	V	HLA steel (high strength low alloy steels)

Although the reserves of high-grade natural ores are depleting,²⁷ the metals are not lost but are dispersed throughout the environment in low concentrations as waste streams, mostly arising from end-of-life consumer and industrial products.²⁴ Major industrial waste includes electronic scraps, medical waste, metal finishing industry waste, spent petroleum catalysts, battery wastes, fly ash etc. These wastes contain different ranges of metals such as Au(I), Ag(I), In(III), Ni(II), Co(II), Cu(II), Pb(II), Cd(II), Hg(II), Zn(II) and Cr(III).^{1,5,6,21,23,28-30} According to Wernick and Themelis, petroleum spent catalysts contain metals (molybdenum, vanadium, cobalt, and nickel).³¹ Glass additives and batteries also have metals that can be recovered.³¹ Electroplating and mining industries generate waste containing mercury, lead, cadmium, silver, copper, and zinc ions.^{5,6} Automobile catalysts contain more than 90 times the amount of precious metals (such as palladium) than the natural ores.³² Most of these metals are critical in various technologies. Figure 1-1, Figure 1-2 and Figure 1-3 indicate the criticality of some metals based on supply issues (in terms of their present abundance, geographical location and current rate of recycling of metals respectively). Therefore there is a need to recover critical metals²¹ from their waste streams to relieve pressure from the natural ores.

Remaining years until depletion of known reserves (based on current rate of extraction)																																			
5-50 years						50-100 years						100-500 years																							
1	H																2	He																	
3	Li	4	Be												5	B	6	C	7	N	8	O	9	F	10	Ne									
11	Na	12	Mg												13	Al	14	Si	15	P	16	S	17	Cl	18	Ar									
19	K	20	Ca	21	Sc	22	Ti	23	V	24	Cr	25	Mn	26	Fe	27	Co	28	Ni	29	Cu	30	Zn	31	Ga	32	Ge	33	As	34	Se	35	Br	36	Kr
37	Rb	38	Sr	39	Y	40	Zr	41	Nb	42	Mo	43	Tc	44	Ru	45	Rh	46	Pd	47	Ag	48	Cd	49	In	50	Sn	51	Sb	52	Te	53	I	54	Xe
55	Cs	56	Ba	57	La*	58	Ce	59	Pr	60	Nd	61	Pm	62	Sm	63	Eu	64	Gd	65	Tb	66	Dy	67	Ho	68	Er	69	Tm	70	Yb	71	Lu		
87	Fr	88	Ra	89	Ac†	90	Th	91	Pa	92	U	93	Np	94	Pu	95	Am	96	Cm	97	Bk	98	Cf	99	Es	100	Fm	101	Md	102	No	103	Lr		

Figure 1-1: Time remaining of rare and precious metal reserves based on present consumption and disposal rate¹

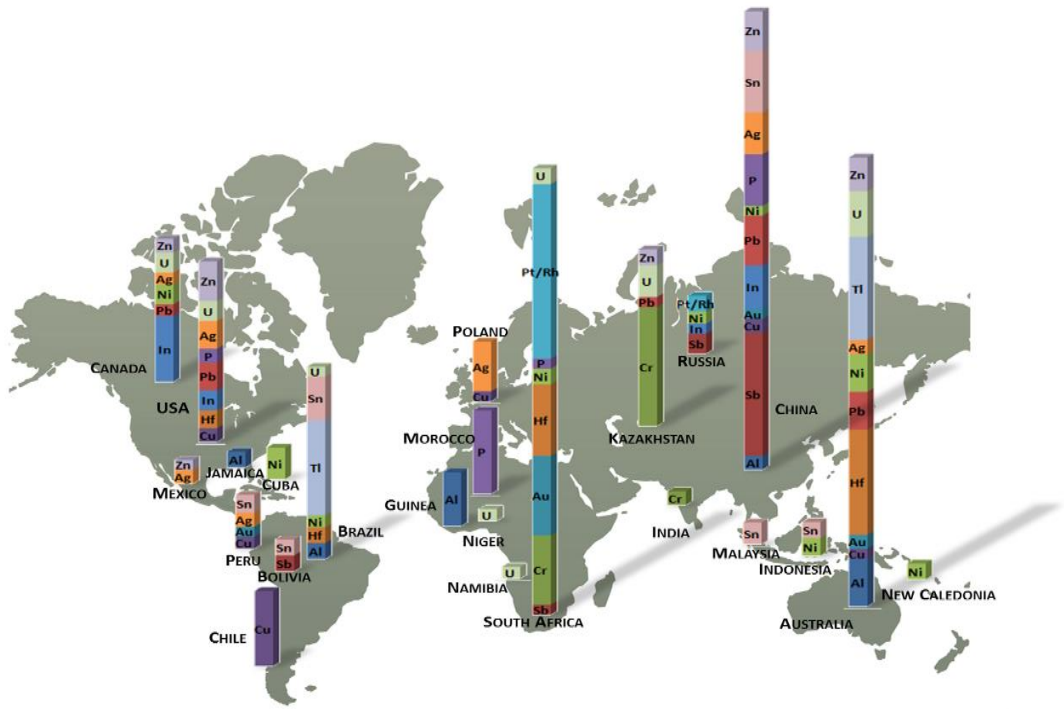


Figure 1-2: Uneven distribution of rare and precious metal reserves across the globe^{1,33}

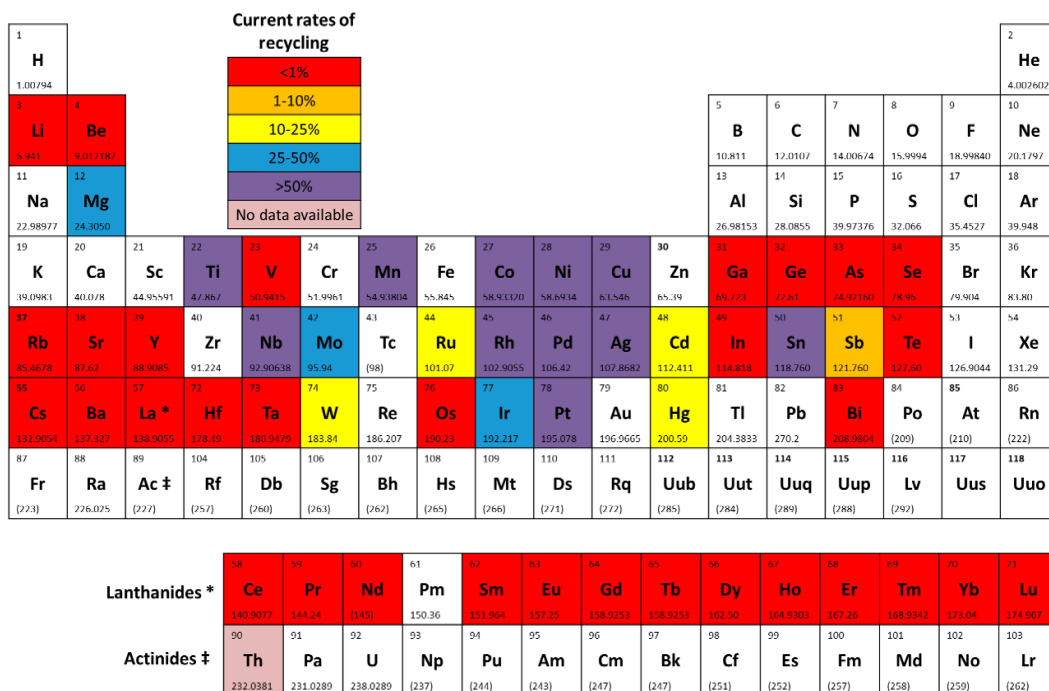


Figure 1-3: Current rate of recycling of different metals¹

Apart from sustainability issues, the recovery of metals from waste streams is also important as a lot of these metals are toxic or hazardous even at very low concentrations.^{6,34,35} Nagajyoti *et al.* reported that cadmium, copper, lead and mercury are major environmental pollutants, particularly in areas with high anthropogenic activities.³⁵ Therefore, it is essential to remove metal ions from industrial wastes before discarding them.³⁶ According to Osibanjo, used electronic equipment contain concentrations of heavy metals way above the permissible levels.³⁰ Thus, due to concern about sustainability and toxicity, continuous efforts are being made to remove heavy metals from the environment.^{31,37} According to Dodson *et al.* proper waste management of landfill sites, waste electrical and electronic equipment, contaminated waters, industrial wastes and mine tailings can aid the effective recovery of metals.¹ Similarly Hunt *et al.*³⁴ observed that recycling of metals from slags (secondary source of metals) or other waste will help reduce toxicity threat and ensure sustainability.

Therefore, there is a great necessity to search for alternative ways to use metals sustainably^{38,39} due to the increasing demand for metals in various applications and finite state of these resources.⁴⁰ Thus, extractive metallurgy can be used to recover metals from the environment.¹ Also according to Moss *et al.*,²¹ end-of-life recycling technologies can assist in metals sustainability and reduce the high-level consequences associated with these metals in the environment.^{31,37} On the other hand, Jadhav and Hocheng²⁹ stated that the process of recovering metals makes sense only if the cost of recovery is much less than the value of the metal while also employing an eco-friendly route for recovery. In addition, how metals are used initially influences the ability to recover them economically.³¹ Ordinarily, metals cannot be mineralised or decomposed,⁴¹ hence their properties could be fully restored. The selective recovery of metals from wastes still remains a challenge and continuous effort is being made to explore better ways of metals recovery using environmentally friendly means. One effective way of getting rid of excess heavy metals in say an aqueous waste stream is by using chelating agents possibly via a solvent extraction technique.³⁴ Chelating agents like EDTA (alone or supported on other solids) have been used for the recovery of rare earth and precious metals,^{42–45} as well as extraction of other heavy metals from soils and spent catalysts.^{46,47}

1.6 Chelating agents

Chelation is a process in which a metal ion coordinates with two or more donor atoms of the same ligand resulting in the formation of one or more rings.¹⁰ Therefore, chelating agents are molecules which can coordinate to metals with two or more donor atoms. The chelation formation reaction is always exothermic and in general the entropic contribution to the stability of the chelate is dominant.⁴⁸ The higher the donor atoms involved per ligand the higher is the strength of chelation.¹⁰ Chelating agents are used in

a variety of applications as they deactivate the charged metal ions by binding with them. Hence, they find use in paper pulp bleaching,^{41,49} detergents and cleaning,⁵⁰ water treatment and food industries.^{51,52} Chelants have also been used for the extraction of metals.^{41,53–60} Other applications where chelating agents are used include fertilisers,^{41,61–65} photography⁶⁶ and pharmaceuticals.^{67,68} They are also applied in nuclear industry, soil remediation^{69,70} and textile treatment.⁷¹ Additionally, chelators are used in many products to prevent; chemical degradation, discolouration, precipitation, emulsion instability and rancidity; thus increasing consumer appeal, shelf-life, and ultimate value.⁷² Chelants are also used for heavy metal detoxification,⁷³ treatment of antitumor⁷⁴ and in radioimmuno-diagnostics.^{75,76} They are potent agents for solubilising heavy metals from polluted soils^{71,77–79} and as root canal lubricants.⁸⁰ Sometimes chelating agents are used as precursors of catalysts.^{81,82} Chelants are also used to prevent scale.^{41,83} They can also enhance the growth of plants by removing toxic metals from the soil.^{84,85} Figure 1-4 below presents the percentage distribution of the most consumed chelating agents across different major sectors. More so, there has been increase in number of publications on application of chelating agents since 1950⁸⁶ which entails the wide need and use of these chemicals.

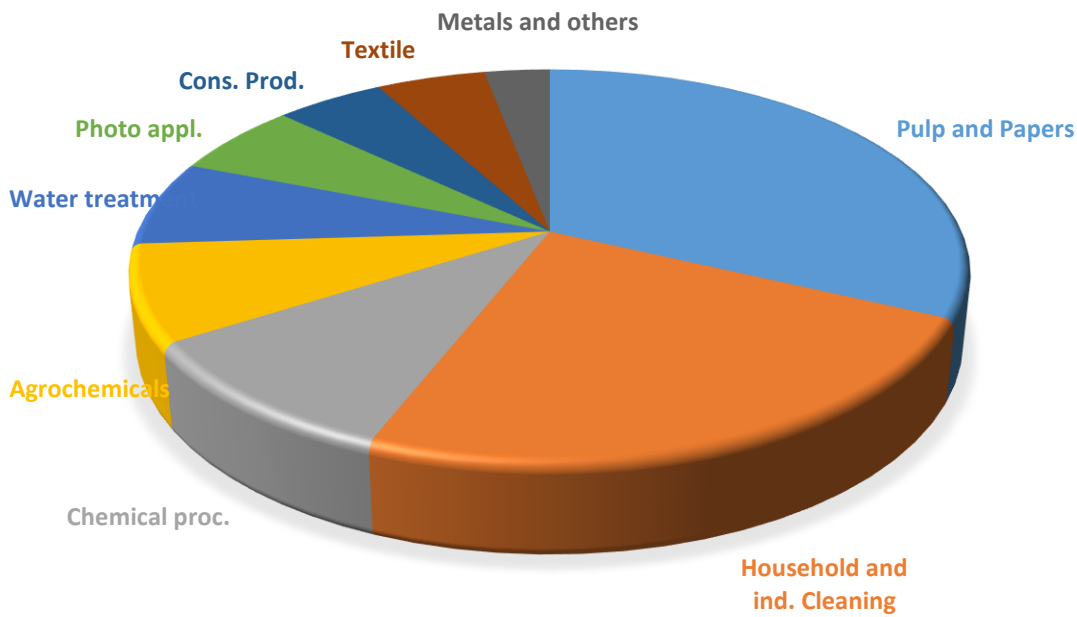


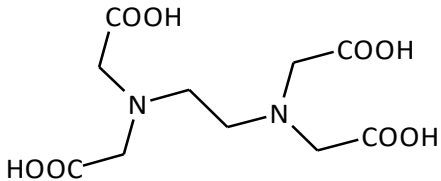
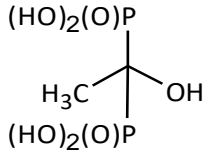
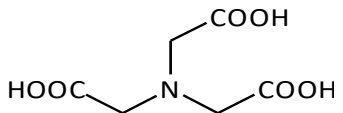
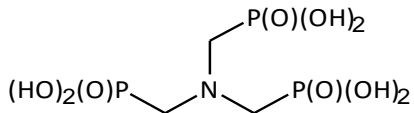
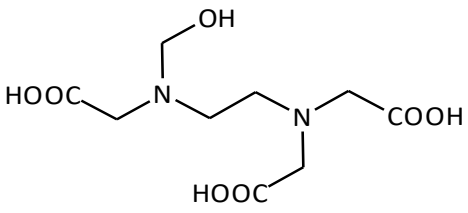
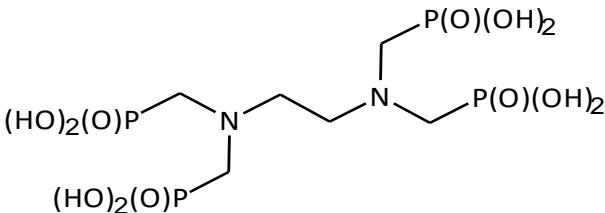
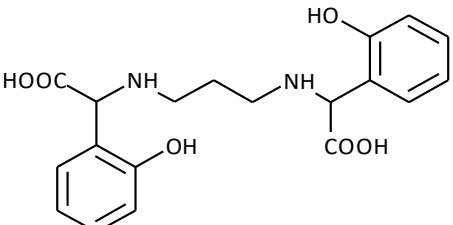
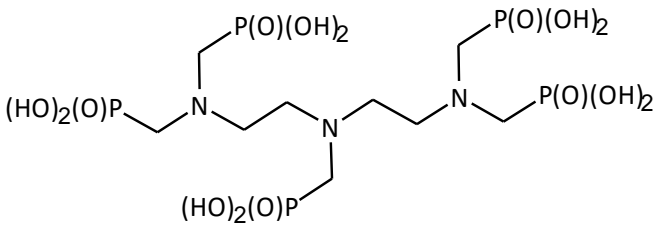
Figure 1-4: Percentages of applications of commonly used chelating agents, APCs (aminopolycarboxylates)⁸

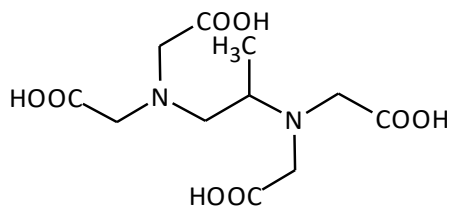
1.6.1 Traditional chelating agents

Traditional chelating agents such as aminopolycarboxylates, amino phosphonates and phosphates are used to chelate metals with substantial stability.⁵ Phosphonates are extensively used as scale inhibitors,^{8,87} and as ingredients in detergents for cleaning processes due to their ability to effectively bind Ca(II).⁸ Traditional phosphonate chelating agents include: Diethylenetriaminepentakis (methylenephosphonic acid), DTPMP; 1,2 -diaminoethanetetakis(methylenephosphonic acid), EDTMP; 1-hydroxy ethane (1,1-diylbis-phosphonic acid), HEDP; Phosphonobutanetricarboxylic acid, PBTC; Nitrilotris (methylenephosphonic acid), NTMP; N-phosphonomethylglycine, PMG.¹²² While the aminopolycarboxylates (APCs) chelants mostly used as chelators include ethylenediamine tetraacetic acid, EDTA; nitrilotriacetic acid, NTA; β -alanine diacetic acid, ADA; diethylenetriaminepentaacetic acid, DTPA; ethylenediaminedi(o-hydroxyphenylacetic acid, EDDHA; N- (hydroxyethyl) – EDTA, HEDTA.⁶⁷ APCs and phosphonates are among the most widely used chelating agents in the world, accounting

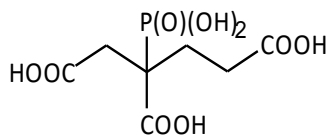
for 37.8% of consumption in 2009.^{5,15} There is a high demand for chelating agents' with an annual projected growth rate of 4%.¹⁵ Table 1-2 highlights some examples of traditional chelating agents.

Table 1-2: Some representatives of conventional chelating agents⁶⁷

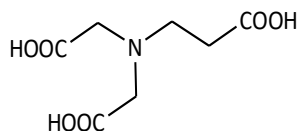
Aminopolycarboxylates	Phosphonic acids
 <p>EDTA-Ethylenediaminetetraacetic acid</p>	 <p>HEDP – 1-hydroxyethane – (1,1-diylbisphosphonic acid)</p>
 <p>NTA – Nitrilotriacetic acid</p>	 <p>NTMP – Nitrilotris(methylenephosphonic)-acid</p>
 <p>HEDTA; N-(hydroxyethyl)-ethylenediaminetriacetic acid</p>	 <p>EDTMP - 1,2-Diaminoethanetetraakis(methylene)-Phosphonic acid</p>
 <p>EDDHA- ethylenediaminedisuccinic acid</p>	 <p>DTPMP- Diethylenetriaminepentakis(methylenephosphonic acid)</p>



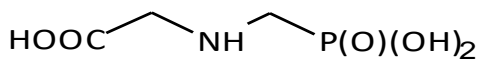
PDTA- 1,2-
diaminopropanetetraacetic acid



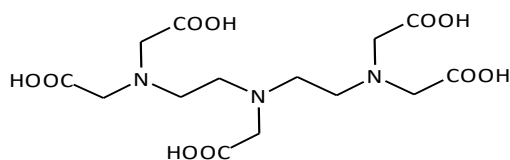
PBTC – Phosphonobutane-tricarboxylic acid



ADA- β-alanine diacetic acid



PMG – N-phosphonomethylglycine



DTPA – diethylenetriaminepentaacetic
acid

Other examples of chelating agents that are commonly used in metals recovery/extraction⁸⁸ are given in Figure 1-5 and include organophosphoric and phosphinic acids; versatic acids and naphthenic acids. Versatic acids and naphthenic acids are derived from distillation of crude oil which is a finite resource.⁸⁸ Carboxylic acids and phosphoric acids form dimers and polymers by hydrogen bonding (Figure 1-6) and this is also found in the metal complexes of these acid metals chelating extractants.⁸⁹ Metal extraction processes using acid chelating extractants operate by a cation exchange mechanism, where the extractant proton is substituted by a metal (see Equation 1-1).

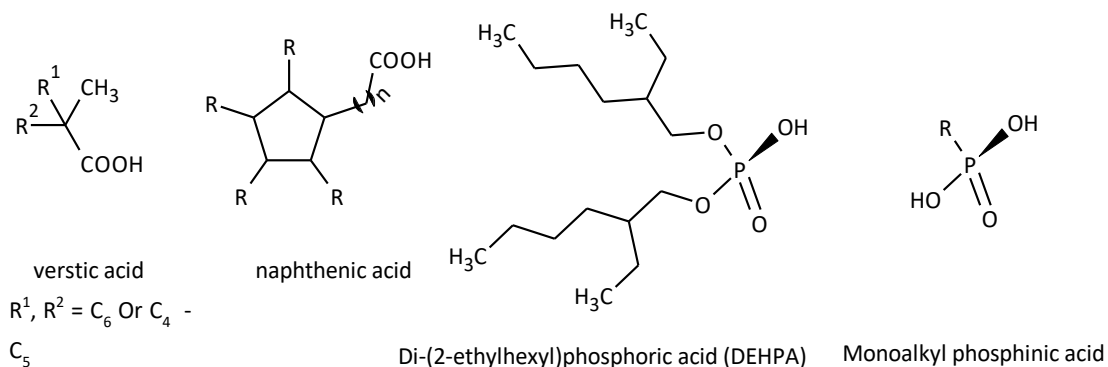


Figure 1-5: Some carboxylic and organophosphorus acid metals chelating extractants

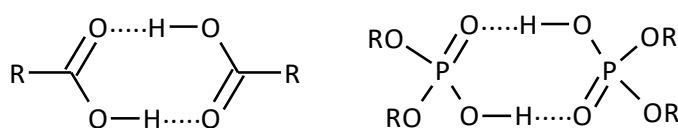
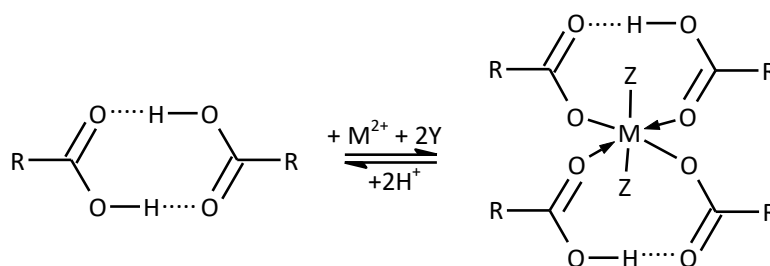


Figure 1-6: Dimers of carboxylic and phosphorus acids metals chelating extractants



Equation 1-1: Formation of metal complex with carboxylic acid dimers

Phosphoric acids have been used in chelating applications for a broad range of metals using a wide range of conditions, hence is considered to be a *universal extractant*. Among acidic organophosphorus extractants, di-(2-ethylhexyl) phosphoric acid (DEHPA) has been extensively used for the extraction of metal ions. Clarke, reported the use of DEHPA for the separation of uranium and zinc from cobalt and nickel.⁸⁸ Other processes using DEHPA include the extraction of iron, beryllium, gallium, vanadium, molybdenum and the rare earth.⁸⁸ Saji reported the recovery of vanadium (V), iron (III) and titanium (IV) from aqueous chlorides using organophosphorus extractants.⁹⁰ Oxygenated organic compounds such as alcohols, ketones, ethers and esters show basicity because of the

lone pair of electrons on the oxygen atom and can directly solvate metal ions resulting in their extraction.⁹⁰

1.6.2 Challenges of traditional chelating agents

Aminopolycarboxylates (APCs) chelators (like EDTA and NTA) and phosphonates have strong chelation effects for metals.^{8,11} Unfortunately, most of these compounds are not readily biodegradable.^{8,9,87} The infiltration of these chelants into the environment could cause dissolution of heavy metals from the sediments and soils, thereby mobilising them^{51,67,77,91} thus leading to increased levels of metals,⁴¹ except phosphonates that do not mobilise toxic metals.^{67,87} These strong chelants persist in the environment due to their high solubility in water and low biodegradability (except NTA).⁴¹ It has been stated that 800 µg/L of EDTA has been found in some U.S. industrial and municipal wastewater treatment plants and up to 12 mg/L in European bodies of water.⁸ Figure 1-7 shows the slow degradation of EDTA (a very common traditional chelator) which is carried out by the EDTA monooxygenases of strains BNC1 and DSM 9103. These enzymes oxidise EDTA to ethylenediaminetriacetate (ED3A) and then to ethylenediaminediacetate (EDDA), which in turn is oxidised by IDA oxidase to ethylenediamine (ED). The bacterium BNC1 may further metabolise ED to obtain the nitrogen present in it as reported by Chauhan *et al.*⁸⁶ EDTA is now among the EU priority list of substances for risk assessment.¹⁰

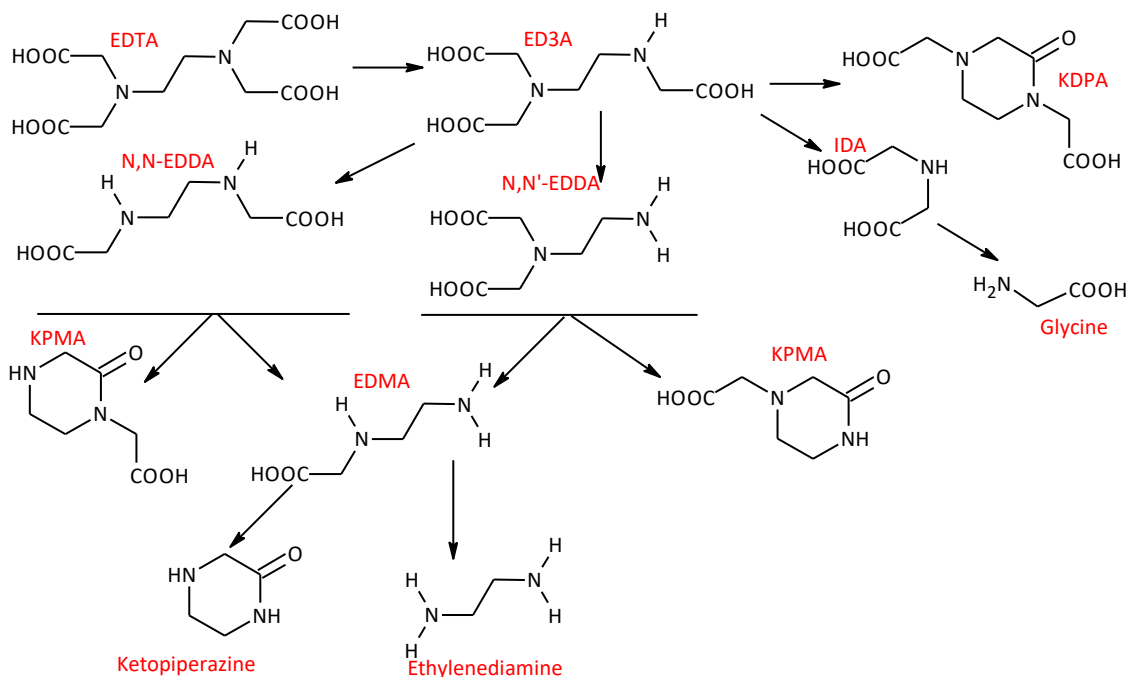


Figure 1-7: Identified degradation products and pathways of the EDTA⁸⁶

According to Sillanpaa,¹³ ethylenediamine tetraacetic acid (EDTA) contains 10% nitrogen which could harm aquatic organisms. Furthermore, the majority of the traditional chelating agents (APCs and phosphonates) are petroleum derived.^{17,92} Therefore, the consumption of traditional APC chelators is declining (−6% annually), because of the persisting concerns over their toxicity and negative environmental impact.¹⁵ Another concern is that most of these common chelants are produced from toxic substances like cyanide.^{8,93}

In addition, the EU is regulating the use of phosphates in consumer laundry detergents and consumer dishwasher detergents in order to reduce the eutrophication risks and costs of phosphate removal by wastewater treatment plants.^{94–97} Their persistence in the environment is because of their low biodegradability and high water solubility^{12,93} In addition, studies have shown that there is a decline in the high quality phosphorus rock reserves used to produce phosphate chelants which could lead to higher costs associated with obtaining phosphates and phosphonate products. The continuous dependence on

phosphates and phosphonate chelators will further accelerate the decline of finite high quality phosphate rocks.⁹⁸ Furthermore, phosphates are essential components in fertilisers (used for food production) and therefore the utilisation of phosphates as chelators is in direct competition with the food industry. Therefore, it is essential to look for alternative bioderived chelating agents in order to reduce the reliance on these traditional chelants.

1.6.3 Alternatives Greener chelating agents

More than 90% of organic chemicals are derived from fossil fuel refineries^{99,100} which is not sustainable. The continuous depletion of petroleum resources coupled with a shift to greener products by consumers means that it is vital to look for alternative greener chelating agents. Therefore in order to replace traditional chelants, the alternative chelating agents must have a strong ability to form complexes,^{10,101} as well as possess low nitrogen content so as to reduce the loading of nitrogen.¹⁰ In addition, they should be readily or at least inherently biodegradable.^{10,101} These alternative chelants (some of which are bioderived) are well favoured by environmental protection policies.^{9,102} Examples of benign alternative chelating agents include ethylenediamine disuccinic acid (EDDS), polyaspartic acid (PASA), methylglycinediacetic acid (MGDA),^{51,52} N,N-bis(carboxymethyl)-L-glutamic acid (L-GLDA). These have been proposed to replace the classical EDTA and diethylenetriaminepentaacetic acid (DTPA) chelators in various applications.^{8,10,103,104}

According to Hyvönen,¹⁰ alternative chelants have a lower chelating ability when compared to the traditional chelators, notwithstanding, this will make them less toxic. In 2013, these greener chelants represented approximately 15% of the total aminopolycarboxylic acids demand. This is expected to rise to around 21% by 2018,

replacing in particular the EDTA (ethylenediaminetetraacetic acid), NTA (nitrilotriacetic acid) and aminophosphonic acids used in cleaning applications.^{8,15,51} Although Mudgal⁹⁴ observed that at the moment some of these alternative chelants are proprietary products hence, they would become expensive.

1.6.3.1 *Glutamic diacetic acid (L-GLDA)*

L-glutamic acid *N,N*-diacetic acid is 86% bioderived from food-approved natural amino acid salt (monosodium *L*-glutamate or MSG).^{17,18} It's in turn obtained by fermenting sugar, molasses, corn or rice (renewable feedstock),¹⁷ and is marketed as Dissolvine GL-38.⁵¹ According to Dixon,⁵¹ GLDA is produced by a waste-free process and from renewable feedstock, which is in accordance with the 4th principle of green chemistry.⁵¹ Ammonia is generated as a by-product which is collected and re-used in industries. It is a strong chelating agent that is safe, readily biodegradable^{11,105} and is considered to be an adequate alternative to phosphates, NTA and EDTA, especially in cleaning applications.^{8,11,106} It is readily soluble in water at different pH values, which increases its performance rate.⁸ *L*-GLDA is stable over a different temperature than other APCs. *L*-GLDA, citrate and carbonate are incorporated in detergent formulations.¹⁰⁷ Aqueous solutions containing *L*-GLDA can be use as oil field chemicals to dissolve calcium carbonate scale and other subterranean carbonate formations to increase permeability and enhance the withdrawal of oil or gas.¹⁰⁸ The structure of *L*-GLDA is given as follows (Figure 1-8).

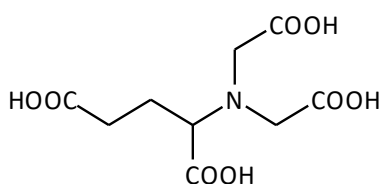
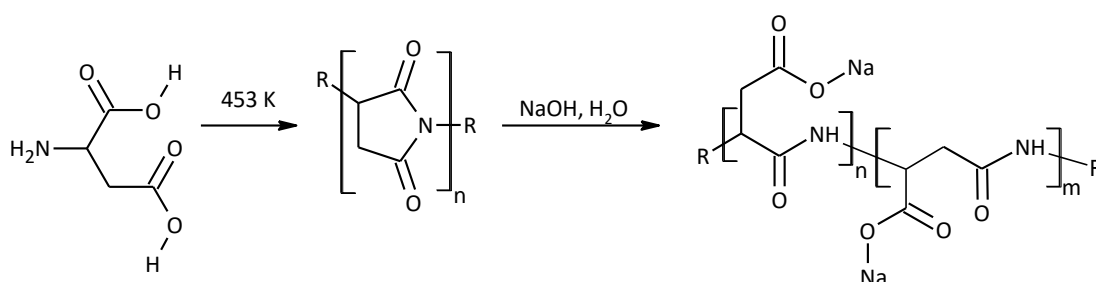


Figure 1-8: *L*-Glutamic diacetic acid (*L*-GLDA)

1.6.3.2 Polyaspartic acid (PASA)

There are different ways to obtain PASA¹⁰⁹ but the typical method for obtaining it is by heating aspartic acid to 453 K resulting in poly (succinimide) with elimination of water. The sodium hydroxide in the system then reacts with the polymer to partially cleave off the amide bonds, in which the (α and β) bonds are hydrolysed resulting in a sodium poly (aspartate) copolymer with 30% α -linkages and 70% β -linkages (see Equation 1-2).¹⁰⁹ Polyaspartic acid production (PASA) is cost-effective; hence it is available on a large scale. *L*-aspartic acid derived from plant sugars¹¹⁰ could be used for the sustainable production of PASA. Poly aspartate is used as a biodegradable anti-scaling agent, corrosion inhibitor and as a metal chelator.¹⁰⁹ Lingua *et al.*¹¹¹ described PASA as a green chelant used in agriculture to supply minerals to crop so as to improve the crop yield.

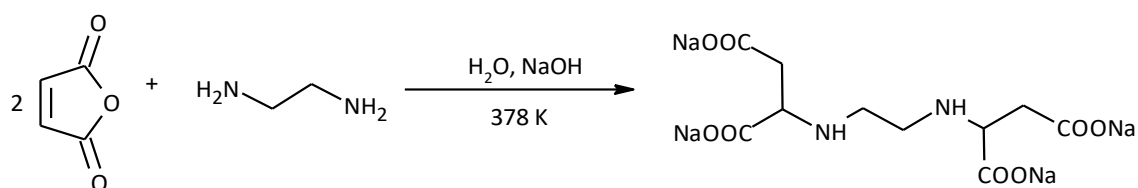


Equation 1-2: Synthesis of poly aspartate

1.6.3.3 Ethylenediamine disuccinic acid ([*S,S*]-EDDS)

Ethylenediamine disuccinic acid, [*S,S*]-EDDS is a naturally occurring compound and was first isolated from culture filtrate of the actinomycete *Amycolatopsis orientalis*. The biosynthesis of [*S,S*]-EDDS is from *L*-aspartate and serine^{105,112} or from oxaloacetate and 2,3-diaminopropionic acid.⁶² [*S,S*]-EDDS is also synthesised by the nucleophilic addition of ethylenediamine with sodium maleate affording stereoisomers of ethylenediamine-*N,N'*-disuccinic acid.^{112,113} Alternatively, [*S,S*]-EDDS is produced from the reaction of maleic anhydride and ethylenediamine to yield a mixture of the 3- isomer of EDDS. The

reaction of aspartic acid with 1,2-dibromoethane results in the formation of two isomers (*[R,R]*-EDDS and *[S,S]*-EDDS), depending on the isomer of aspartic acid used. Since aspartic acid can be derived from plant sugars it could also enhance the sustainable production of *[S, S]*-EDDS. It is also produced by fermentation of *A. orientalis*.⁶² *[S, S]*-EDDS is the structural isomer of EDTA, however it is readily biodegradable than EDTA.¹¹ Equation 1-3 describes the synthesis of this compound.



Equation 1-3: Synthesis of *[S, S]* EDDS

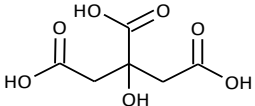
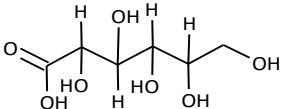
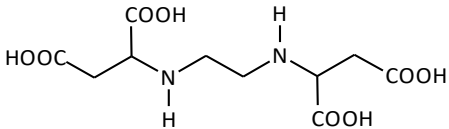
According to Dixon,⁵¹ *[S, S]*-EDDS production is in conformity with the 3rd principle of green chemistry; i.e. designing less hazardous chemical synthesis. It is one of the most promising biodegradable chelating agents^{66,77} and has a low nitrogen content¹⁰ making it less toxic.¹¹⁴ Furthermore, *[S,S]*-EDDS has zero NTA, formaldehyde or cyanide (toxic chemicals) unlike common traditional APCs chelants.¹⁰⁵

[S, S]-EDDS is effective in chelating several metals from soil.^{115–117} Furthermore, it is capable of binding transition metal ions in place of Mg(II) and Ca(II).^{51,105} According to work by Yang *et al.*¹¹⁸ *[S,S]*-EDDS at pH 5.5 is more suitable for Cu(II), Zn(II) and Pb(II) extraction. Ullmann *et al.*¹¹⁹ modified *[S, S]*-EDDS by attaching a lipophilic hydrocarbon chain to its nitrogen atoms in order to make a hydrophobic chelating agent.

Other bioderived metal chelants are low molecular weight organic acids; citric acids,^{69,120,121} gluconic acid,¹²² gallic acid⁹¹ etc. Citric acid is a green chelant used for the removal of heavy metals from contaminated sludge with higher extraction efficiency at

mildly acidic pH of around 2.30.^{120,123,124} It is also used as a chelant for removing Cr(III), Zn(II) and Mn(II) from printed circuit boards (PCBs).¹²⁵ Table 1-3 gives some of these environmentally-benign chelants; their sources and metal chelating functions.

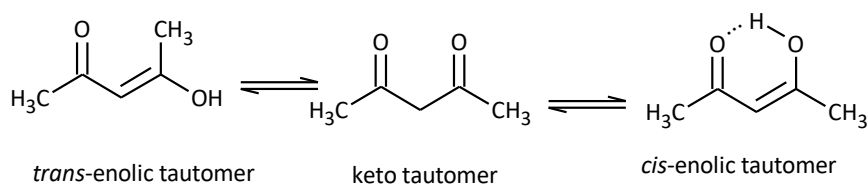
Table 1-3: Commonly used bioderived and green chelating agents for recovery of metals from wastes

Name	Structure	Sources	Common metals, % recovery	Optimum pH	Ref.
Citric acid		Fermentation of carbohydrate ¹²⁶ , synthesis and extraction from citrus fruits ^{127,128}	Cr(III), 100%; Cu(II), 88%; Ni(II), 98%; Zn(II), 100%; Pb(II), 95%	2.3	123,129,130
Gluconic acid		Oxidation of Glucose ^{47,131}	Ni(II), 43%; Cr(III), 60%; Cd(II), 63%; Zn(II), 70%; Pb(II), 80%; Cu(II), 8%	12.5	47
Ethylenediamine-N, N'-disuccinic acid, [S, S]-EDDS		L-aspartic acid ⁵¹	Cu(II), 80%; Zn, 64%; Pb(II), 91%; Cd(II), 52%	4	132,133

Polyaspartic acid, PASA		L-aspartic acid ⁸	Ca(II); Cr(III); Cu(II)	-	8
Glutamic diacetic acid, <i>L</i> -GLDA		Fermentation of sugar, molasses, corn, rice ⁸	Cd(II), 84% ; Cu(II), 94% ; Pb(II), 54% ; Zn(II), 62% ; Ni(II), 39%	4	133
Tartaric acid		Grapes, fermentation of wine-lees	Cd(II), 60%; Pb(II), 50%; Cu(II), 50%; Zn(II), 30%	3.5 – 4.0	134,135

1.7 Brief review on β -diketones

β -diketones are special dicarbonyl compounds that exhibit keto-enol tautomerism (see Equation 1-4).^{136,137} The amount of keto-enol is dependent greatly on the solvent,^{138,139} as highlighted in Table 1-4. The proton of the hydroxyl enol is quite labile and can be replaced easily with a metal. β -diketones are present in natural products, pharmaceuticals and other biologically active compounds and can also be used in producing them.¹⁴⁰ They have been used as ligands for over 120 years^{141,142} as well as NMR shift reagents, laser chelates, metals chelating agent, chemical and photochemical catalyst; antitumor, antioxidant, anti-inflammatory and antiviral agents.^{27,141} In addition, β -diketones are also used in the synthesis of many other derivatives such as pyrazole, isoxazole, and triazole¹⁴³ as described in the Figure 1-9.



Equation 1-4: keto-enol equilibrium of β -diketone

Table 1-4: Equilibrium constants for tautomerisation of acetylacetone in various solvents at 0.1 mole fraction solute

Solvent	Acetylacetone		Acetylacetone†	
	% enol	K_e^*	% enol	K_e^*
Hexane	95.00	19.00	93.60	14.70
Ether	95.00	19.00	90.40	9.40
Carbon disulphide	94.00	16.00	91.20	10.30
Benzene	89.00	8.10	87.20	6.70
Dioxane	82.00	4.60	79.40	3.90
Absolute ethanol	82.00	4.60	81.60	4.40
Pure solute	81.00	4.30	-	-
95% ethanol	77.00	3.40	78.00	3.60
Methanol	74.00	2.80	74.00	2.80
Acetic acid	67.00	2.00	78.00	3.50
Acetonitrile	62.00	1.60	67.20	2.10
Dimethylsulfoxide	62.00	1.60	76.00	3.20

$K_e = [enol]/[keto]$, $temp. = 306 \pm 2$ K; and † Measurements at 0.3 mole fraction of solute^{138,139}

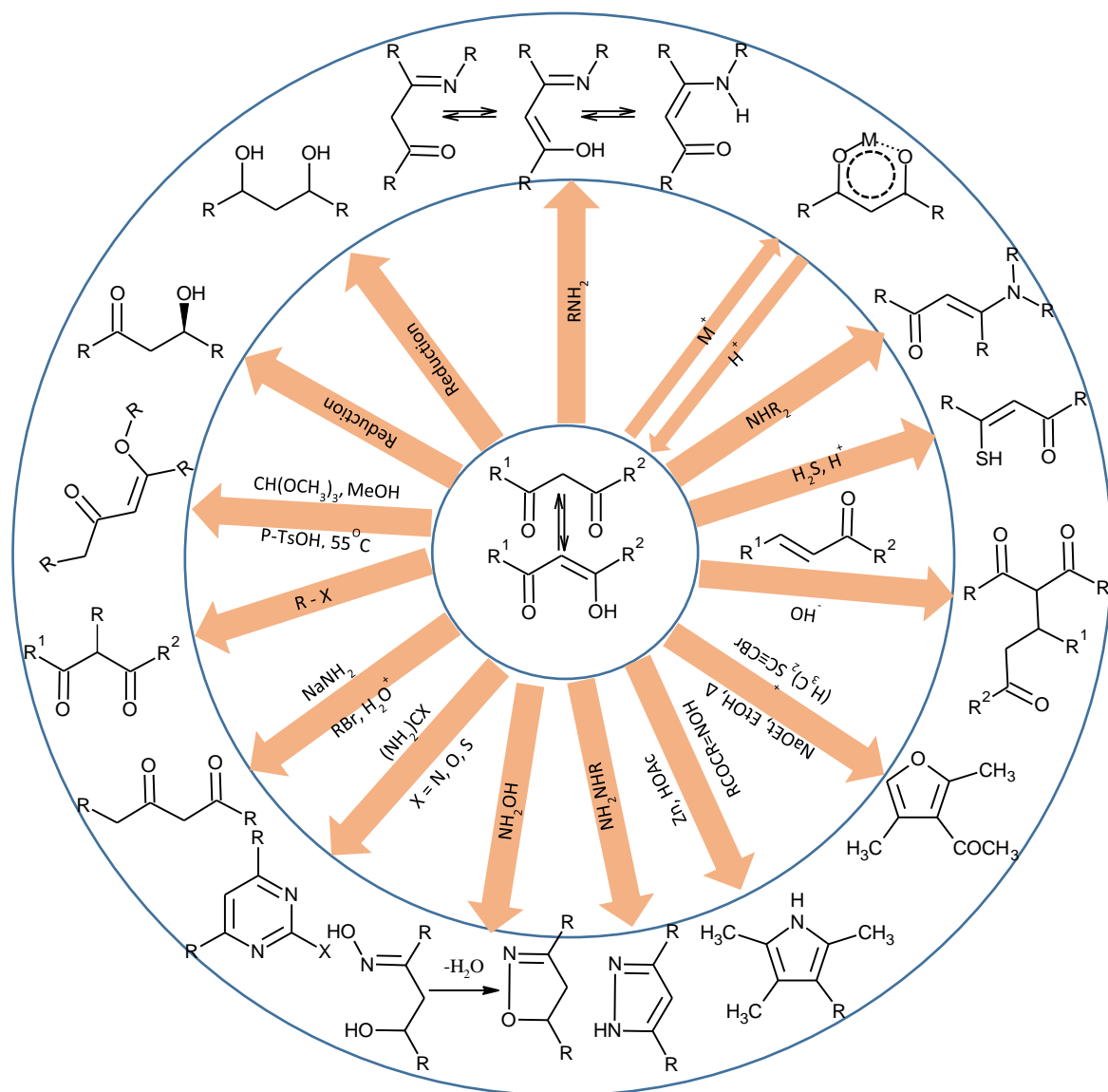


Figure 1-9: Some schemes of β -diketone derivatives

1.7.1 Synthesis of lipophilic β -diketones

Lipophilic β -diketones are obtained via chemical or biosynthetic means. A biosynthetic pathway to the synthesis of lipophilic β -diketone involves the insertion and retention of the carbonyl groups during the elongation process.^{144,145} C_{18} β -keto acyl chain is obtained by the addition of a C_2 unit to the palmitate. The β -keto group is protected and retained during elongation.¹⁴⁵ Further elongation takes place by the addition of C_2 units to the chain (with the protected β -diketone group) until a chain of length C_{32} is produced. Finally, decarboxylation of this C_{32} precursor and release of the protection on the

carbonyl groups takes place to form the complete β -diketone molecule as seen in Figure 1-10.¹⁴⁵

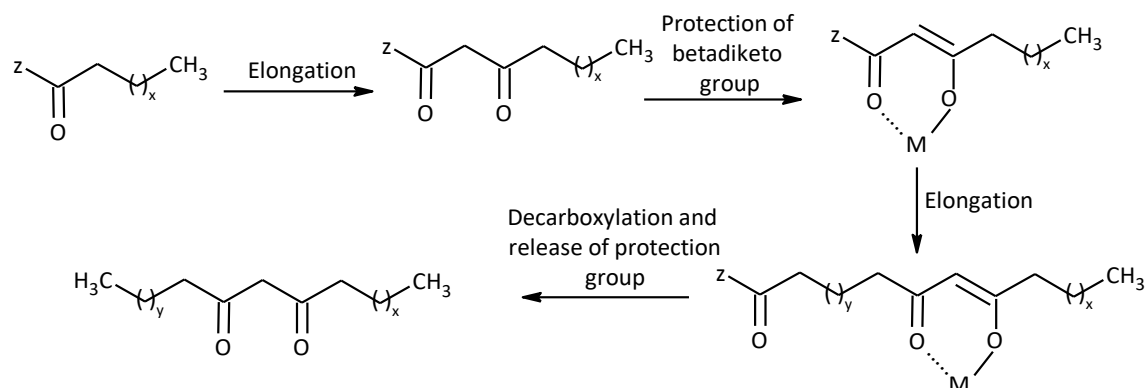
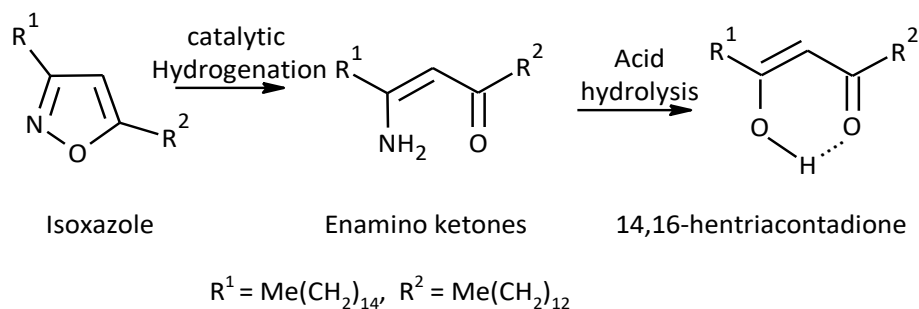


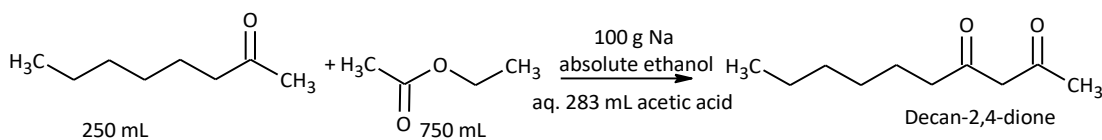
Figure 1-10: Scheme biosynthesis of β -diketone¹⁴⁵

Chemical synthesis of a lipophilic β -diketone (hentriacontanedione-14,16-dione) was proposed by Bianchi and Amici¹⁴⁶ as described in Equation 1-5 below;



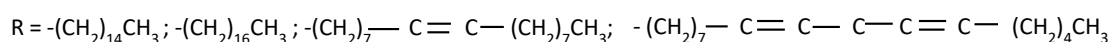
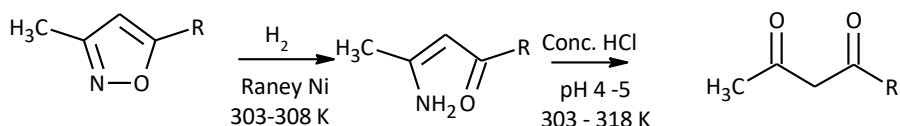
Equation 1-5: Synthesis of the 14, 16-hentriacontanedione

In addition, Equation 1-6 shows the Claisen condensation reaction of ethyl acetate and hexyl methyl ketone for the synthesis of 2,4-decanedione as reported by Gouveia *et al.*¹⁴⁷



Equation 1-6: synthesis of decan-2,4-dione using Claisen condensation reaction

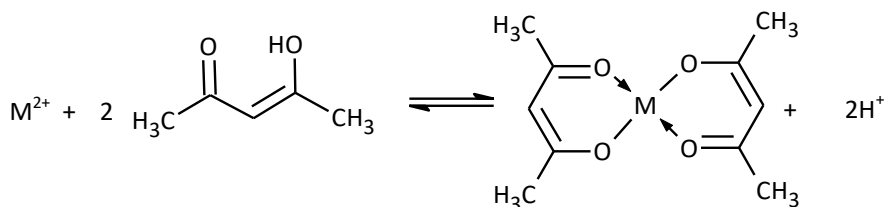
Kenar¹³⁹ also produced long chain aliphatic β -diketones by converting long-chain isoxazole compounds into their corresponding β -enaminones and subsequently hydrolysing them in the presence of concentrated HCl to form long chain β -diketones¹³⁹ as given in Equation 1-7.



Equation 1-7: Synthesis of long chain β -diketone

1.7.2 β -diketones as metal chelating agents

β -diketones are used as metal chelating extractants. They are known to chelate metals at slightly acidic medium and above.¹⁴⁸ Most commonly reported β -diketones in metal extraction are acetyl acetone (Hacac), benzoylacetone (Hbac) and dibenzoylmethane (Hdbm) as given in Figure 1-11. In addition, Koshimura and Okubo¹⁴⁹ used heptan-3,5-dione; 2,6-dimethyl heptan-3,5-dione; 2,2-dimethyl heptan-3,5-dione and 2,2,6,6-tetramethyl heptan-3,5-dione in the extraction of Pd(II), Fe(III), Al(III), Cu(II), Ni(II), Co(II), Zn(II), Cd(II) and Mn(II) with benzene as a diluent. Equation 1-8 illustrates a representative extraction of metals with β -diketone. Extraction of metals with lipophilic β -diketones into the organic phase occurs more readily than with non-lipophilic β -diketones. The stability constant of Hacac and Hdbm are similar, but the partition coefficient of metal dibenzoylmethanates is much higher in organic solvents than those of acetylacetonates because Hdbm is much more lipophilic.¹⁵⁰



Equation 1-8: Equation for extraction of metals using β -diketones as chelating extractant

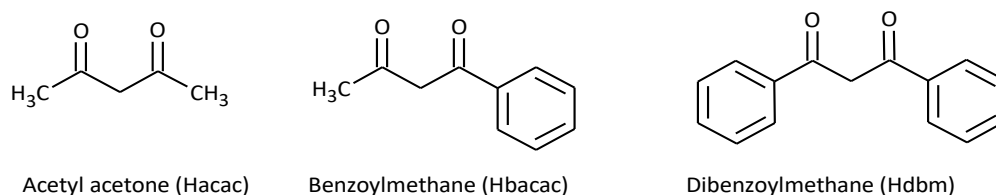


Figure 1-11: common β -diketones used in metals extraction

Fluorinated β -diketones (see Figure 1-12) like hexafluoroacetyl acetone and thenoyltrifluoroacetone are exclusively in the enol form (a favourable tautomer that chelates metals) even at high temperature and pressure.¹⁴⁸ This explains why fluorodiketones function better as metal extractants than non-fluorodiketones. Wai and Wang,¹⁴⁸ had also reported the use of fluorinated β -diketones as chelating agents in the supercritical fluid extraction of heavy metals, lanthanides and actinides. Stary¹⁵⁰ reported the use of thenoyltrifluoroacetone in the separation of actinide elements.

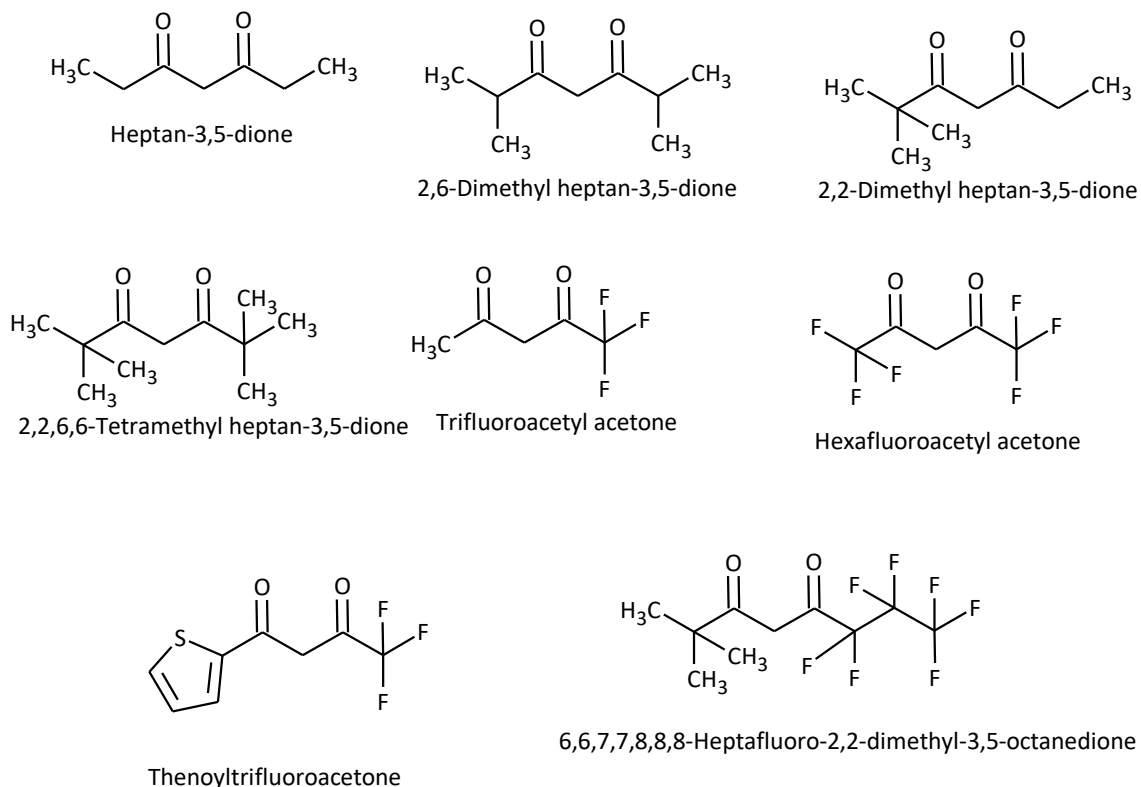
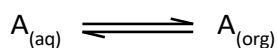


Figure 1-12: fluorinated and other nonfluorinated β -diketones used in metals extraction

1.8 Solvent extraction of metals

Solvent extraction is a separation procedure for isolating and concentrating substances from aqueous solution, by means of an immiscible organic solvent.⁸⁸ Separation can be achieved either by extracting the metal into the organic phase and keeping the unwanted materials in the aqueous phase; or by extraction of the unwanted substances into the organic phase and leaving the desirable metals in the aqueous phase. The species to be extracted into the organic solvent is expected to be electrically neutral or lipophilic. This technique has long been used for metal separation. In 1898, W. Nernst derived a distribution law encompassing the distribution of solute in the organic and aqueous phases. For an equilibrium reaction given in Equation 1-9;



Equation 1-9: An equilibrium reaction

$$K_{D,A} = \frac{\text{Concentration of the species (A) in organic phase}}{\text{Concentration of the species (A) in aqueous phase}} = \frac{[A]_{(\text{org})}}{[A]_{(\text{aq})}}$$

Equation 1-10: Distribution constant of solute (distribuend) A

Metal extraction involves the formation of a stoichiometric metal-extractant compound, which has a relatively high organic solubility. This process can be made selective for one metal over another, under suitable conditions as observed by Clarke.⁸⁸ In addition, Svärd¹⁵¹ observed that metal recovery from aqueous systems via liquid-liquid extraction is effective at high metal ion concentrations. In addition, most solvent extractions of metals are carried out at room temperature or slightly above room temperature. Hence, liquid-liquid extraction of metals is a highly energy effective technology. It is also particularly useful as there are possibilities of obtaining a target metal in high purity. Liquid-liquid solvent extraction is often favoured over traditional pyrometallurgy by industry because the reagents are recycled. Furthermore, liquid-liquid metal extractions plants do not emit SO₂ that is common with pyrometallurgy.⁸⁹ Wilson *et al.*⁸⁹ reported that hydrometallurgical plants involving liquid –liquid extraction processes are smaller so that they can be operated near the mining location.

Typically, in solvent extraction of metals, the aqueous feed solution is contacted with the solvent (containing the extractant occasionally with a modifier) resulting in metal extraction after a given contact time. Solvent extraction of metals with extractants are performed in extracting vessels such as columns or mixer settlers as shown in Figure 1-13. The advantage of using a mixer settler is that it allows proper contact between the extractant and the metal which is especially important when the chemical reaction between these two phases is slow.¹⁵² Furthermore, the extracted high-value metals can be kept while toxic metals can be safely disposed. In solvent extraction of metals, the

extractants such as hydrophobic chelating agent used could be recycled and re-use as described in in Figure 1-14.

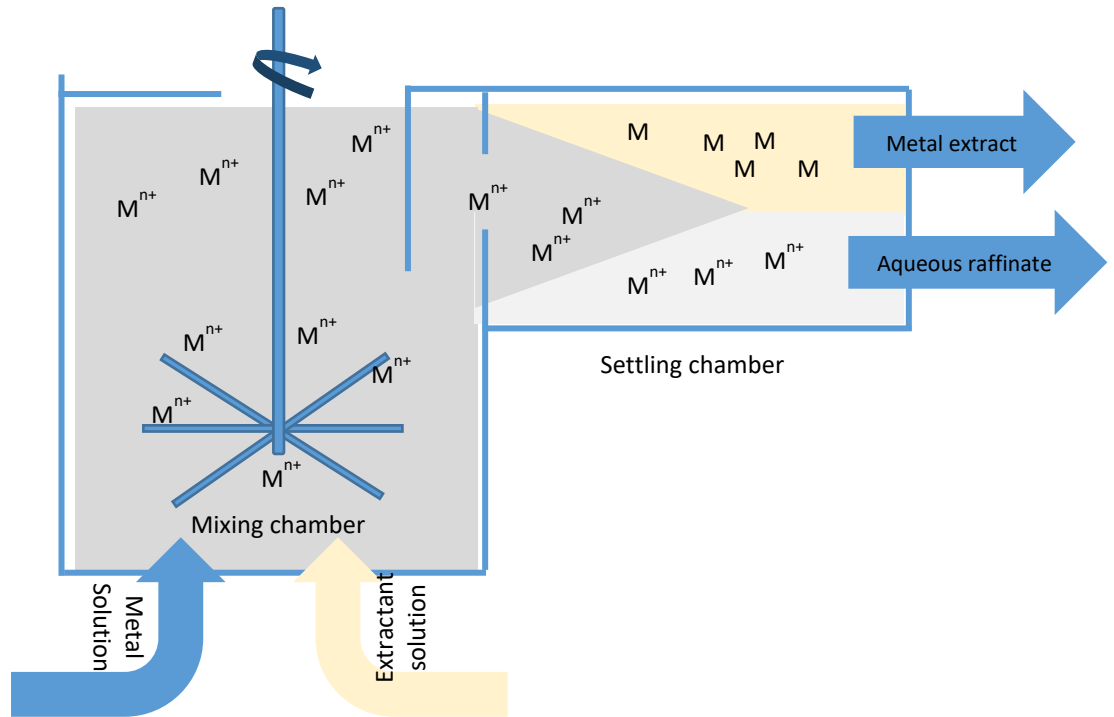


Figure 1-13: A typical traditional extracting vessel (mixer-settler) for solvent separation of metals

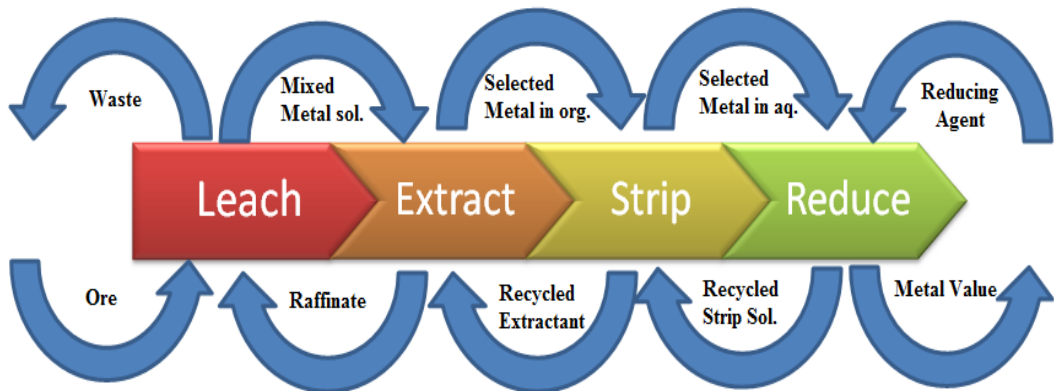


Figure 1-14: Incorporation of solvent extraction to achieve metal separation and concentration in a hydrometallurgical circuit which involves recycling of all reagents⁸⁹

In Figure 1-14; aqueous metal leached solution is contacted with the extractant in a mixer-settler (an extracting vessel). After the extraction and separation of metals, the resulting raffinate is recycled again into leachate and the metal extracts in the organic

layer are passed into another mixer-settler chamber to be stripped with an appropriate aqueous solution.⁸⁶ This gives a concentrated pure metal for reduction. In such a technique, the resulting chelate (formed after contacting the chelant and the metal ion) is stripped with strong acid (HCl or HNO₃) or any appropriate reagent resulting in the release of the captured metal in another aqueous phase. The metal ion is then reduced and concentrated to obtain the metal in the pure state.⁸⁹ As mentioned earlier, the stripped extractant is reused and the spent stripping agent is recovered and used in the subsequent process.⁸⁹

Saji⁹⁰ Wai and Wang¹⁴⁸ reported that compounds which are commonly used in solvent extraction of metals include oximes and other chelating agents previously discussed (such as β -diketones, organophosphoric acids, etc). Similarly, Przeszlakowski and Wydra¹⁵³ observed that chelating agents like β -diketones are well known for their metals chelation properties and are used in solvent extraction of metals. In the aqueous phase, water solvates the metal ions, however in the presence of an extractant with a more basic site (than the oxygen of water), the water is displaced resulting in the formation of the metal-complex. Even if the solubility of the extractant in the aqueous phase is quite low, it is assumed that the formation of the metal-complex takes place in the aqueous phase.

Solvent extraction is a widely applied method for the recovery of metals. He *et al.*,¹⁵⁴ reported that solvent extraction with a metal chelating extractant is considered to be an effective method for purifying metals from aqueous waste. In addition Cerna¹⁵² and Teng *et al.*⁹² have reported that solvent extraction is an acceptable method for the removal of heavy metals from waste waters of the chemical and electronic industries.^{92,152} Furthermore, there is a lot of focus on the extraction of trace metal ions in the

pharmaceutical and medical industries.⁹² Studies have shown that the extraction of copper from leachate is economically more efficient than the extraction of copper from ores.⁹³

Copper, palladium, platinum, silver and gold can be recovered from e-waste¹⁵⁵ by solvent extraction. Mackenzie¹⁵⁶ observed that solvent extraction of metals such as copper, uranium, cobalt and nickel have great economic significance, which has led to considerable interest in their extraction. Wang *et al.*¹⁵⁷ extracted metals from soils using low molecular weight organic acids. Abushi and Asayuki *et al.*¹⁵⁸ reported that many metals can be extracted by solvent extraction using β -diketones. Although the amount of precious metals currently recovered using solvent extraction is small, but the value of these metals is significant.¹⁵⁶ Solvent extraction of metals is efficient, eco-friendly and no hazardous by products are liberated during the process, thus this technology is more economical and favourable than most other technologies for metal recovery.⁸⁶ The possibility of recycling of chelators in solvent extraction of metal processes combined with good extraction efficiency reduces the process cost significantly and makes the process more attractive than other available methods.⁸⁶

The solvent extraction of metals is affected by factors such as equilibrium pH, concentration of metals and extractants, diluent, and counter ions etc.¹⁵⁹ In most cases these parameters are studied for the optimisation of the extraction process. Furthermore, Clarke stated that the distribution constant and coefficient are functions of the nature of the solute, the solvents involved, and the temperature.⁸⁸ The most crucial of these factors are the equilibrium pH, concentration of the extractant and the diluent. Most metal extractions are pH and extractant dependent. Furthermore, the extraction efficiency is enhanced by increasing the concentration of the extractant.

Again, the percentage extraction efficiency of Cu(II), Zn(II) and Pb(II) ions by the chelating agents; ethylenediamine tetraacetic acid (EDTA), ethylenediamine disuccinic acid (EDDS), nitrilotriacetic acid (NTA), methyl glycine diacetic acid (MGDA), IDSA were analysed and found to be strongly depended on pH.⁸⁶

1.9 Equilibrium slope analysis

Stoichiometry and equilibrium constants can be evaluated using the equilibrium slope method (analysis).^{92,160} During the experiment, the pH needs to be kept constant, meaning that pH affects the extraction constant, K_{ext} . Equation 1-11 is a typical example of a metal/ligand equilibrium;⁸⁹



Equation 1-11: Metal/ligand equilibrium

HR = Chelating Agent; x= stoichiometric coefficient of the chelating agent; org = organic phase, aq = aqueous phase and let K_{eq} = equilibrium constant or the extraction constant. K_{eq} is a function of D_{eq} , which is the equilibrium distribution ratio of the metal ion concentration in the organic and the aqueous phase. From Equation 1-11 above; the equilibrium or extraction constant, K_{eq} , or K_{ext} will be;

$$K_{eq} = \frac{[\text{CuR}_x][\text{H}^+]^x}{[\text{Cu}^{2+}][\text{HR}]^x}$$

Equation 1-12: An equation for equilibrium or extraction constant

The equilibrium distribution constant will be;

$$D_{eq} = \frac{[CuR_{xorg}]}{[Cu^{2+}]_{aq}}$$

Equation 1-13: Equilibrium distribution constant

Hence K_{eq} will now be;

$$K_{eq} = D_{eq} \frac{[H^+]^x}{[HR]^x}$$

Therefore, the linearized equilibrium constant equation for this metal/ligand equilibrium is as given Equation 1-14;

$$\text{Log } D_{eq} = x\text{pH}_{eq} + \text{lg } K_{eq} + x\text{lg } [HR]$$

Equation 1-14: linearize equation for determination of stoichiometry and extraction constant

Previous reports have utilised slope analysis for the determination of equilibrium equations in metal extraction.^{92,160,161} According to Teng *et al.*,⁹² at constant pH, a plot of $\text{lg } D_{eq}$ vs pH_{eq} can provide the number of protons released during the extraction and a plot $\text{log } D_{eq}$ vs $\text{log } [HR]$ can give the stoichiometric coefficient of the extracted metal ion. In addition, at constant pH, the plot of $\text{log } D_{eq}$ vs $\text{log } [HR]$ can give $\text{log } K_{eq}$ as the intercept. Solvent extraction is a rapid technique for the separation of metals and can be used to understand the system dynamics.¹⁶⁰

1.10 Metal ligand (M-L) interaction

A metal-ligand chelate formation (M-L) is affected by the electronic structure, size, oxidation state and coordination number of the metal ion. The M-L bond may be electrostatic (ionic) or covalent.¹⁰ The interaction between a metal ion and a chelant is based on the hard-soft-acid-base theory. The theory suggests that soft metals form the most stable complexes with soft ligand atoms (sulfur, phosphorus and chlorine) via

covalent bonds, and hard metals (oxygen, nitrogen and fluorine seekers) form stable complexes with hard ligands using electrostatic bonding. The metal ions coordinate or accept electron pairs from the donor groups of the ligand. Thus, metals are classified into soft/ hard acids as represented in Table 1-5.

According to Abushi and Asayuki,¹⁵⁸ hard metals (class a) are highly charged metals which are non-polarised like Mg(II), Ca(II), La(III), Fe(III), Co(III), Ga(III), Al(III), K(I), etc). while soft metals are small charged metals which are polarised like; Hg(II), Ag(I), Cd(I), Au(I), etc. Metals such as Pb(II), Zn(II), Cu(II) and Mn(II) are neither soft nor hard and are hence classed as borderline metal ions. Soft metals (class b) can form more stable complexes with neutral ligands than class a metals, while class a metals prefer ligands containing acidic functional groups such as polycarboxylic acids. However, the division of the metals into different classes is not clear cut, and there are several borderline ions. According to the hardness parameter derived from electronegativity by Parr and Pearson, the hardness order of the studied metal ions is $Mg(II) > Ca(II) > La(III) > Fe(III) > Zn(II) > Cd(II) > Mn(II) > Pb(II) > Cu(II) > Hg(II)$.

Carboxylic acids are ligands that contain highly electronegative donor atoms which are difficult to polarise, and are therefore classified as hard bases. Although nitrogen is classified as a hard donor atom, it is considered to be more suitable than oxygen for soft acids. Its lower electronegativity (3) as compared with oxygen (3.5) and its neutral character in the studied ligands makes it more suitable than oxygen for complexation with softer acids. On the other hand, both oxygen and nitrogen donors bond well with the large ions such Hg(II). Stable complexes result from the interactions between hard acids metals and hard bases (oxygen, nitrogen and fluorine) or between soft acids metals and soft bases (sulphur, chlorine and phosphorus).^{10,158} The stability of complexes of

divalent ions in the transition metal series with chelators containing oxygen or nitrogen donors often follows the Irving-Williams order: Mn(II) < Fe(II) < Co(II) < Ni(II) < Cu(II) > Zn(II).¹⁰

Table 1-5: M-L classification based on electronic structure, nature, ionic radii and hardness/softness of metal ions¹⁰

Metal ion	Type	Valence electrons	Class a/b/ borderline	Soft/hard/ borderline	Ionic radii
-	i	ns^2	(a)	(hard)	-
Mg(II)	ii	ns^2np^6	a	hard	72
Ca(II)			a	hard	100
Zn(II)	iii	$(n-1)d^{10}$	a	Hard-soft	74
Cd(II)			a-b	soft	95
Hg(II)			b	soft	102
Pb(II)	iv	$(n-1)d^{10}ns^2$	a-b	Hard-soft	118
Mn(II)	v	$(n-1)d^1$ to $(n-1)d^9$	a-b	Hard-soft	82
Transition metals					
Fe(III)			a	hard	64
Cu(II)			a-b	Hard-soft	73
La(III)	vi	$(n-1)(f^1 \text{ to } f^{13})ns^2np^6$ lanthanides n= 5	a	hard	106
Actinides n=6					

1.11 Wheat straw wax

Wheat straw wax is the hydrophobic components extracted from wheat straw. Wheat straw is an abundant and low value bio-feedstock in many countries, especially in Europe. In the UK alone, 10 million tonnes of wheat straw are produced annually, 4 million tonnes of which have no commercial market.¹⁶² Even though there are different applications for cereals straw in the UK, such as in livestock, energy and mushroom

growth, there is a surplus of 2- 3 million tonnes that could provide use in other areas.¹⁶³

Both Wales and Scotland are net importers of straw from England. 54% of agricultural straw production in the UK is currently derived from wheat¹⁶³ and 94% of wheat straw is produced in England. The different components making up wheat straw may be viewed in Figure 1-15.¹⁶⁴ The breakdown of wheat straw production in the UK is presented in Figure 1-16 while the main composition of wheat straw is highlighted in Table 1-6.

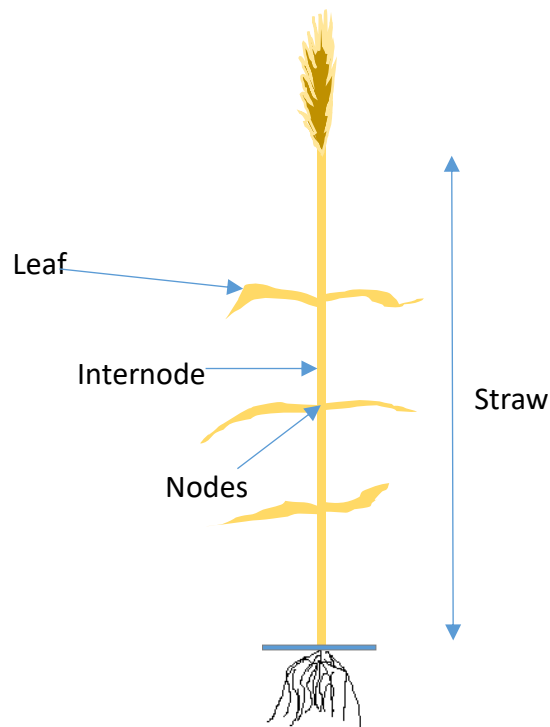


Figure 1-15: Description of a wheat straw

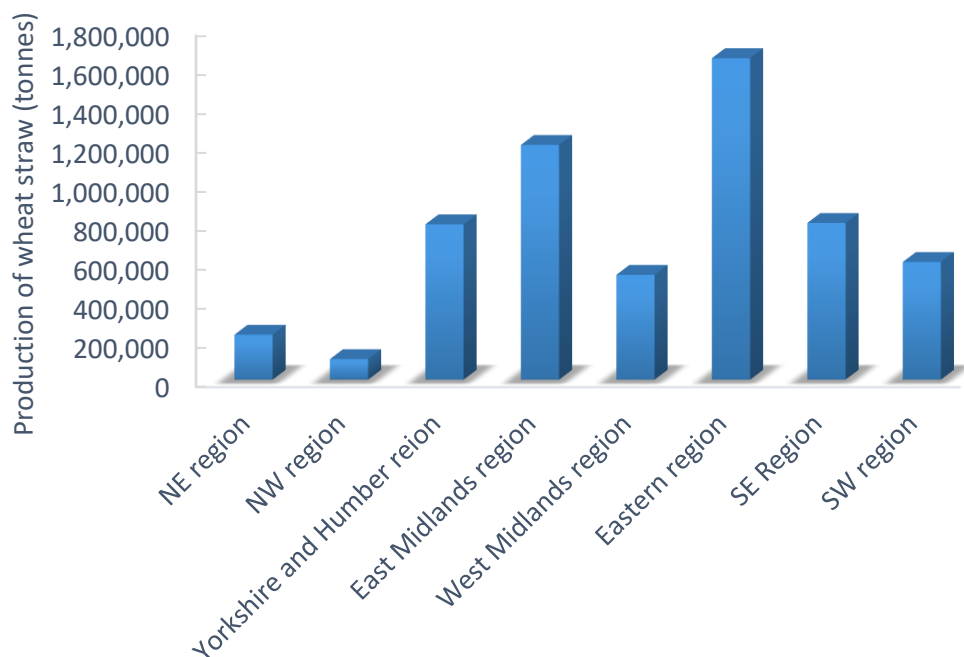


Figure 1-16: Breakdown of GB straw production (tonnes) by region in 2007

Table 1-6: Abundance of the main constituent in wheat straw^{164,165}

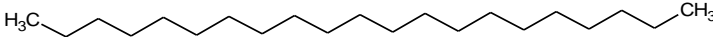
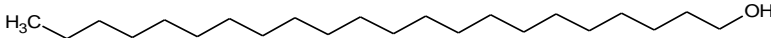
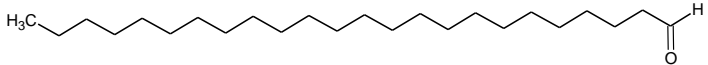
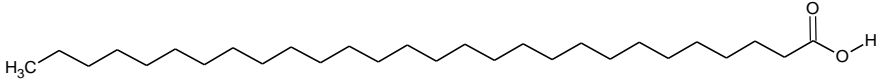
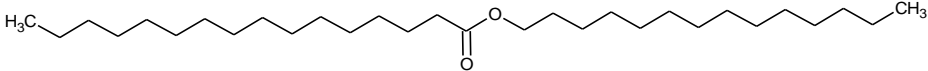
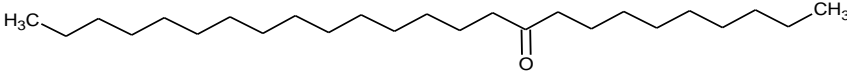
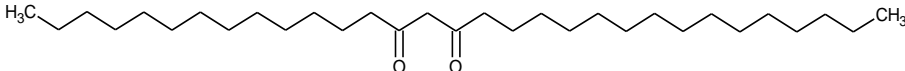
Components of wheat straw	%
Water-soluble	9.6
Total acetone extractives	2.7 (2.0 lipophilic and 0.7 polar)
Klason lignin	16.2
Acid-soluble lignin	1.5
Holocellulose	67.2 (36.5 cellulose and 30.7 hemicellulose)
Ash	6.6

Generally, waxes have many industrial uses in cosmetics, personal care products, polishes and coatings.¹⁶² Wheat straw wax has been highlighted as a potential renewable wax with many attractive characteristics to replace some existing commercial waxes in cosmetic applications.¹⁶⁶ Waxes offer protection against particle accumulation of pathogens by repelling water on the surface of the plant.¹⁶⁷ Furthermore, they prevent the formation of water films on the surface, which reduces gas exchange dramatically.

On wet leaves, which are covered with a liquid water film, the uptake of CO₂ for photosynthesis is reduced, because CO₂ diffuses 10 000 times more slowly through water than air.¹⁶⁷

The main components of wheat straw wax are long-chain aliphatic compounds and cyclic compounds;¹⁶⁶ these are primarily long-chain alkanes, fatty acids, fatty alcohols wax esters and sterols. Del Río *et al.*¹⁶⁵ reported that lipid quantity in the wheat straw constitutes 1 – 2%. Studies have shown that the lipophilic content of wheat straw comprises n-fatty acids (25%), n-fatty alcohols (20%), n-alkanes (5%), n-aldehydes (1%), high molecular weight esters (11%), monoglycerides (2%), diglycerides (1%), triglycerides (2%), β-diketones (10%), steroid hydrocarbons (< 1%) and steroid ketones (1%).¹⁶⁵ Furthermore, cyclic compounds including steroids, sterols, sterols glycosides and sterols esters were also present.¹⁶⁵ Sin reported the extraction of wheat straw waxes using organic solvents and scCO₂.¹⁶⁶ It is interesting to know that 14,16-hentriacontanedione is the second most abundant (875 mg/Kg fiber) single compound found in wheat straw wax, while octacosanol is the most abundant (1392 mg/Kg fiber) single compound in this wax.¹⁶⁵ A summary of some of these components of the wheat straw wax are as presented in the following Table 1-7.¹⁶⁶

Table 1-7: Representative of common components of wheat straw wax

Names	structure	Chain length	Common form
n-Alkanes		Odd (C ₂₁ - C ₃₇)	C ₂₇ , C ₂₉ and C ₃₁
n-fatty alcohols		Even (C ₂₂ - C ₃₆)	C ₂₆ , C ₂₈ , C ₃₀ , and C ₃₂
n-aldehydes		Even (C ₂₂ -C ₃₂)	C ₂₆ , C ₂₈ , C ₃₀ and C ₃₂
n-fatty acids		Even C ₁₆ -C ₃₂	C ₂₂ , C ₂₄ , C ₂₆ and C ₂₈
Waxy esters		Even C ₃₀ -C ₆₂	C ₄₀ and C ₅₀
ketones		Odd C ₂₃ -C ₃₃	C ₂₉ and C ₃₁
β-diketones		Odd C ₂₇ - C ₃₃	C ₃₁ and C ₃₃

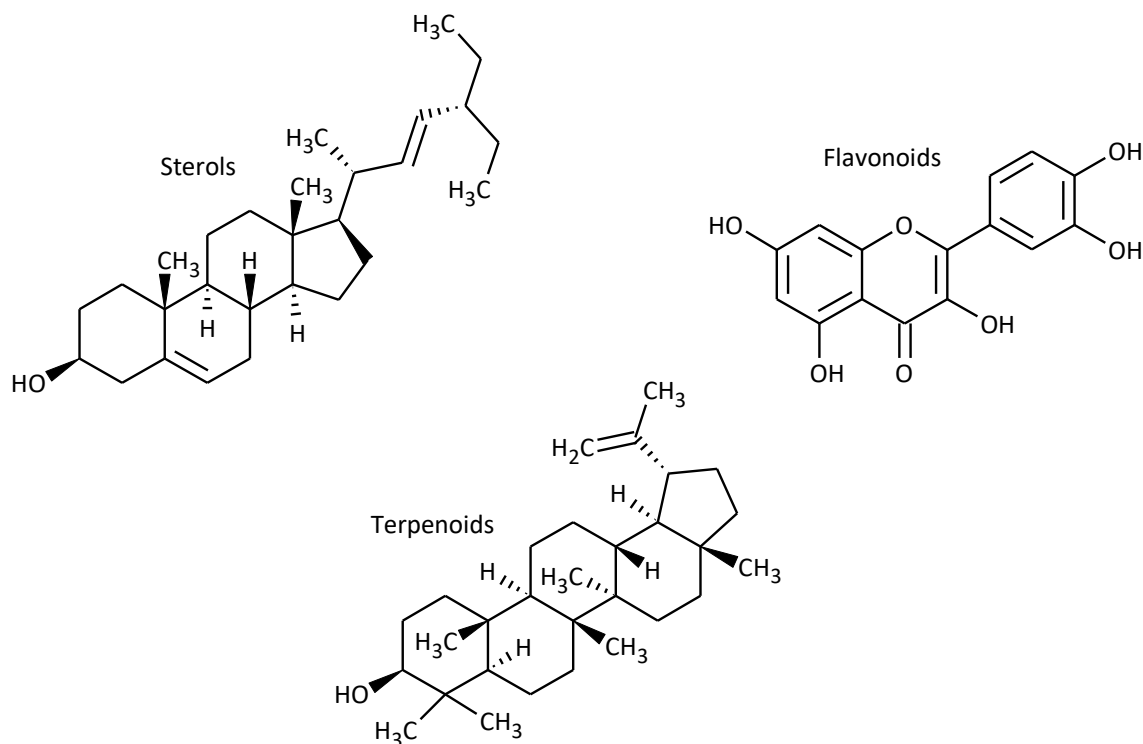


Figure 1-17: Major cyclic compounds in plant waxes

In addition, cereals such as wheat, barley, oats and rye contain 10-50% of hydrophobic β -diketones.^{168,169} Cereals also contain hydroxy- β -diketones, which are most likely derived from hentriacontane-14, 16-dione.¹⁶⁸ The keto groups are usually positioned at carbon 12, 14-, 14, 16- and 16, 18- in C_{31} and C_{33} straight-aliphatic chains. Occurrence of β -diketone in plant waxes plays an important ecological role in biotic or abiotic stress resistance of plants.¹⁷⁰ Since wheat straw waxes contains high amounts of β -diketones, this compound can be easily purified and used as a bioderived chemical in metal chelation and many other applications.

1.12 Use of supercritical carbon dioxide ($scCO_2$) for extraction/fractionation

A supercritical fluid (like a $scCO_2$) is a substance above its critical temperature and critical pressure.¹⁷¹ For instance, carbon dioxide reaches the supercritical state above 304.2 K and 73.8 bar,¹⁷² showing properties of both a liquid and a gas.¹⁶² The density, viscosity

and diffusivity of gases, liquids and supercritical fluids are given in Table 1-8 below and Table 1-9 describes the critical temperatures and pressures of some supercritical fluids.

Table 1-8: Order of density, viscosity and diffusivity of gases, liquids and supercritical fluids^{171,173}

Physical State	Density (g cm ⁻³)	Viscosity (g cm ⁻¹ s ⁻¹)	Diffusion (cm ² s ⁻¹)
Gas	10 ⁻³	10 ⁻⁴	10 ⁻¹
Liquid	1	10 ⁻²	<10 ⁻⁵
Supercritical fluid	10 ⁻¹ to 1	10 ⁻⁴ to 10 ⁻³	10 ⁻⁴ to 10 ⁻³
	Liquid like	Gas like	liquid like

Table 1-9: Critical temperatures and pressures of some fluids¹⁷³

Substances	T _c (K)	P _c (MPa)
Carbon dioxide	304.20	7.40
Water	647.10	22.10
Ethane	305.50	4.91
Propane	369.80	4.26
Methanol	513.00	7.95
Ethanol	516.10	6.39
Isopropanol	508.60	5.37
Acetone	508.00	4.76

The line between the triple point and the critical point is referred to as the gas-liquid (G-L) coexistence curve (Figure 1-20). As one moves along this curve, the density of the gas phase increases due to an increase in pressure while the density of the liquid phase decreases due to thermal expansion. Once the critical point is reached, the density of the two phases (gas and liquid) is equivalent and it is no longer possible to distinguish between the two phases. Therefore, the critical point may be seen as the maximum pressure and temperature where a substance is found as a gas and liquid in equilibrium

with one another. Beyond the critical point, an increase in pressure or temperature will not cause liquefaction; because the substance will exist as supercritical fluid above the critical point.¹⁷⁴ Small pressure changes cause an increase in the density of a supercritical fluid which enables liquid scCO₂ to solubilise compounds.¹⁷⁴ The critical point of CO₂ is described in Figure 1-18.

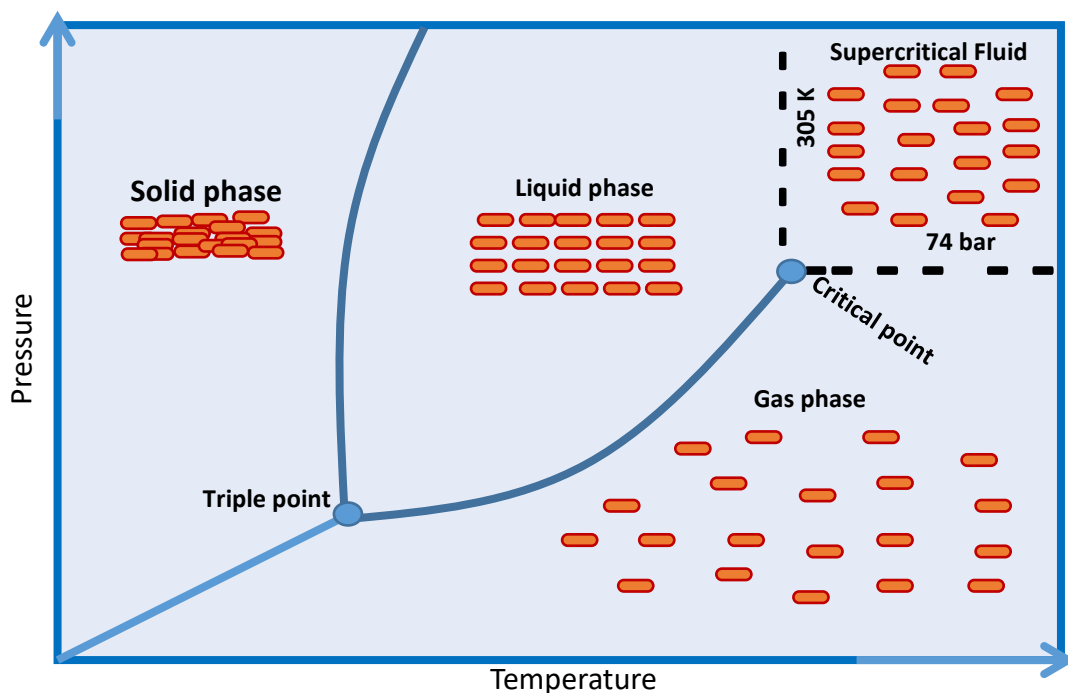


Figure 1-18: Phase diagram (P, V) for a pure compound in a close system. The triple point indicates the critical pressure of CO₂

Owing to their high penetration power of scCO₂, scCO₂ is good alternative solvent for extraction of chemicals from biomass. However, it is not adequate for the extraction of highly polar molecules such as sugars or amino acids, as well as most inorganic salts. More polar compounds can be extracted with scCO₂ using a polar co-solvent such as ethanol. The scCO₂ extraction technique is simple, fast, effective and a solvent-free sample pre-treatment technique.¹⁷⁵ Some other benefits of scCO₂ solvent includes;

Alternative solvent: scCO₂ is a non-toxic, non-flammable, selective, alternative solvent to hazardous organic solvents. ^{176–179}

Miscibility with gases: H₂, O₂, CO are not very soluble in liquid solvents, unlike scCO₂.^{178,180}

Increased mass transfer and diffusivity: scCO₂ unlike traditional organic solvents possesses lower viscosities and higher diffusivities like gases, enabling faster rates in terms of diffusion-limited reactions.^{174,175,181}

Good selectivity and Tuneable solvent properties: The high compressibility of scCO₂ makes it easy to manipulate its density. Changing the temperature and pressure (tuning the scCO₂) enhances reaction rates as well selectivity.^{177,178}

According to Mayadevi,¹⁸² scCO₂ is considered to be a green alternative solvent because it's eco-friendly unlike traditional organic solvents that are hazardous from use or release of VOCs (Volatile organic compounds). However, disadvantages of scCO₂ include; high operational pressure, solvent compression, elaborate recycling to make economical and high capital investment for equipment.¹⁷⁷

Prior to the extraction, liquid CO₂ is pumped through a heat exchanger to reach the required temperature. The scCO₂ is uniformly pumped into the extracting vessel containing the biomass to dissolve the soluble compounds.¹⁷⁶ In continuous flow mode, a high pressure pump, co-solvent pump, together with a back pressure regulator are connected to the reactor (or vessel). Typically, fractional separators are connected to a nozzle, through which the solutes dissolved in the supercritical CO₂ can expand rapidly into a region of much lower pressure. This process is called RESS (rapid expansion of supercritical solutions), resulting in a substantial drop in the solute's solubility and thus precipitation.¹⁷³ The scCO₂ is depressurised and the extracted substances collected while the CO₂ is vented out.¹⁸³ Recent studies have shown the successful extraction of natural

products with scCO_2 .^{175,181} In addition, scCO_2 containing suitable ligands have been used to extract metal ions from solid and liquid materials.¹⁸⁴

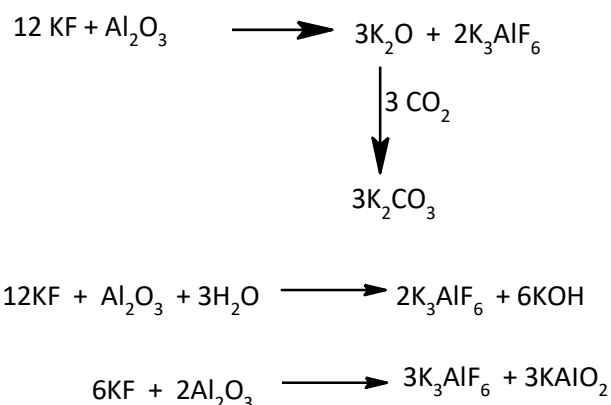
1.13 KF/alumina base catalyst

KF/alumina ($\text{KF}/\text{Al}_2\text{O}_3$) has been used as heterogenous base catalyst in many organic reactions including; Michael additions, Knoevenagel condensations, aldol condensations.¹⁸⁵ Some authors considered it as a weak or moderate base, while others consider it to be strong or even a super base.¹⁸⁵ Although KF/alumina has been widely applied in organic synthesis, the particular active site of KF/alumina remains contentious.¹⁸⁶ While some think that the fluoride ion is responsible, others feel that the active site of the catalyst is the aluminate ion. For instance Li¹⁸⁵ attributed the basic nature of this catalyst to: (a) the presence of active F^- , (b) the presence of $[\text{Al}-\text{O}]^-$ ion which generates OH^- when water is added, and (c) the cooperation of F^- and $[\text{Al}-\text{OH}]^-$. Weistock *et al.*¹⁸⁷ reported that the active species potassium hydroxide or the aluminate is responsible for the basic activity of KF/alumina^{187,188} and F^- has little or no direct role for the reactivity.¹⁸⁸ Powder x-ray and IR analysis showed the formation of potassium hexafluoroaluminate (K_3AlF_6)^{188,189} during the preparation of KF/alumina. Consequently, the formation of K_3AlF_6 must be accompanied by presence of KOH and aluminate as described in Equation 1-15. They categorically posited that, the high reactivity of this catalyst is due to reaction of F^- and alumina to form K_3AlF_6 , KOH and potassium aluminate.¹⁸⁸

On the other hand, Ando and co-workers concluded that the F^- ions are the source of the strong basicity.¹⁹⁰ Considerable literature may be found explaining the basic nature of the catalyst as a result of the hard F^- anion present on the surface.^{191,192} Clark *et al.*,¹⁹³ found that the activity arises as a result of the mixture of KF and alumina, rather than KF

or alumina alone. Alumina can act as a base, but KF on alumina is a very strong base.¹⁹⁴

The reaction of KF with Al₂O₃ mixture,^{189,195} is given in Equation 1-15.



Equation 1-15: Reactions of KF with alumina

However, activity of KF/alumina is well beyond just OH. F⁻ in the presence of alumina can act as a strong base as described below in Figure 1-19 which is consistent with the circumstances for the formation of K₃AlF₆ earlier noted.¹⁸⁹

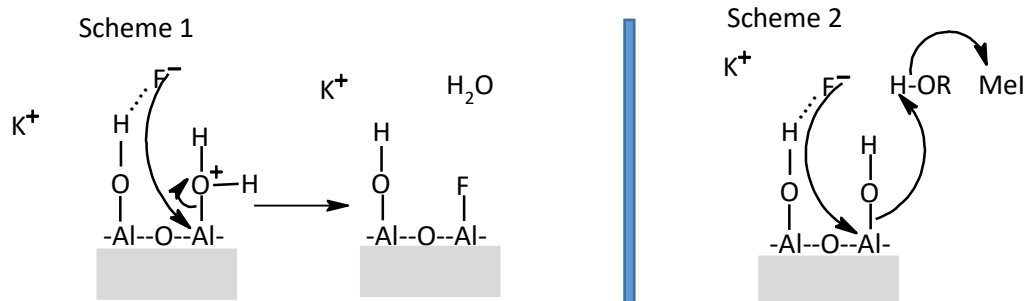


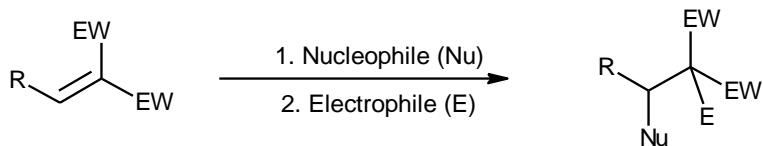
Figure 1-19: Cooperative basicity of F⁻ and alumina

Therefore, the reactivity of KF/alumina is not just due to KOH and aluminate alone, but the extra layer of KF when loading is above 0.6 mmol g⁻¹. The reactivity depends on the dispersion and increased surface area of KF giving co-ordinately unsaturated F⁻; liberation of strong base during preparation and the cooperative action of F⁻ and the hydrated alumina surface.¹⁸⁹ Schmittling and sawyer also contributed that the high basicity associated to KF-alumina is due to the presence K₃AlF₆, KOH, potassium aluminate and potassium carbonate.¹⁹⁵

The preparation of KF/alumina is enhanced by drying at high temperatures (300 °C) to remove the CO₂ and H₂O that may have blocked the active surface of the KF/Al₂O₃.^{191,192,196} In addition, the base can be prepared by simply mixing KF with alumina to produce the active base material;¹⁹³ which is often the same as when prepared from solutions.¹⁹³ However, other studies claimed that the activity of KF/alumina is strongly dependent on the residual water content,^{187,197} suggesting the importance of Bronsted basicity. KF/alumina is a recyclable basic catalyst.¹⁹⁸ It can be re-used up to four times without a drop in the yield through thorough washing with ethyl acetate and drying.¹⁹⁸ Other advantages of this catalyst include mild reaction conditions, easy work-up procedure and selective synthesis of the target molecules.¹⁹⁹

1.14 Michael addition reaction

The Michael addition reaction is an important C–C bond-forming reaction which involves nucleophilic addition of a carbanion (formed by the abstraction of a proton from a C–H bond of the organic donor molecule by a base) to α , β -unsaturated carbonyl compounds.¹⁸⁵ Michael addition has also been described as a reaction that involves the addition of nucleophiles (Michael donor) to an alkene or alkyne attached to electron withdrawing groups (Michael acceptor), followed by trapping of the anionic intermediate with an electrophile (in the simplest case, a proton) as expressed in Equation 1-16.²⁰⁰ The Michael addition reaction is a versatile method for the efficient coupling of electron poor olefins with a number of nucleophiles.^{201,202} It is also useful in polymer synthesis,²⁰¹ and it offers an environmentally benign approach to organic synthesis.²⁰³ Choudhary and Peddinti,²⁰⁴ Chowdhury,²⁰⁰ and Eder *et al.*²⁰⁵ observed that the Michael addition reaction is an atom economical reaction as it incorporates all the constituents of all the starting materials into the final product.^{200,204,205}



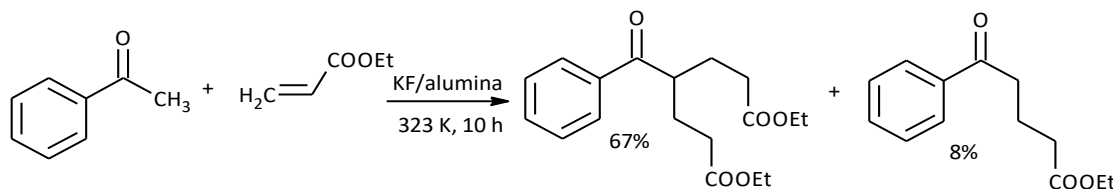
EW = Electron withdrawing group

Equation 1-16: General scheme of Michael Addition Reaction

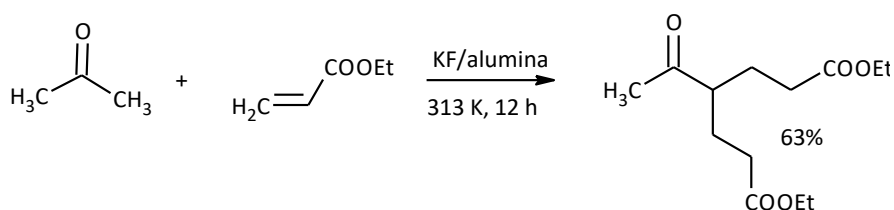
It has been reported that traditional strong bases (KOH, NaOH), metal-based catalysis and recently organocatalytic reagents are used to instigate this reaction.²⁰⁰ Environmental and economic concerns are bringing about the replacement of homogeneous bases by suitable solid catalysts. The latter are easy to separate, recover, and thus reuse. Hence solid base catalyst systems, such as Ba(OH)₂, MgO, KF/Al₂O₃, Na/NaOH/Al₂O₃, and modified Mg-Al hydrotalcite have now been commonly utilised in Michael additions.¹⁸⁵ In addition Li¹⁸⁵ reported that some transition metal complexes that are heterogeneous Lewis acid catalysts, such as montmorillonite-enwrapped scandium, nickel (II) and cobalt (II) complexes are used to perform Michael additions.¹⁸⁵ According to Basu and Paul,¹⁹⁹ several acidic and basic catalysts are used to influence this conjugate addition reaction. The choice of catalyst varies with the type of reactants. Choudhary and Peddinti²⁰⁴ performed a facile Michael addition using thiol, amines with nitroolefins in less than ten minutes. Meanwhile Eder *et al.*²⁰⁵ carried out the Michael addition of thiophenol to citral from the oil of lemon grass (*Cymbopogon citratus*) and other electron-poor alkenes using KF/Al₂O₃ under solvent-free conditions at room temperature. This led to the formation of 3,7-dimethyl-3-(phenylthio) oct-6-enal. It was observed that the Michael addition was enhanced under microwave irradiation.²⁰⁵

In the presence of a base catalyst, secondary condensations, polymerisations and double additions could be formed as side reactions,¹⁹⁹ notwithstanding, double addition have been commonly observed among these secondary reactions. Basu and Paul reported

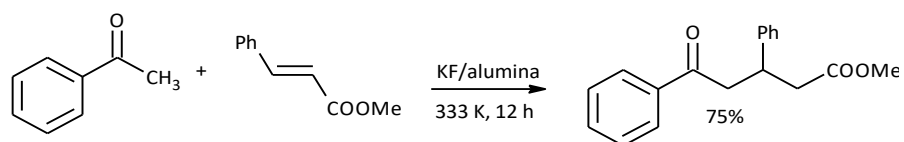
selective double and single Michael additions of aromatic and aliphatic methyl ketones to electron-deficient alkenes mediated over KF/alumina.¹⁹⁹ The schemes of these addition reactions are shown below in Equation 1-17, Equation 1-18 and Equation 1-19.



Equation 1-17: Scheme of double and single Michael addition



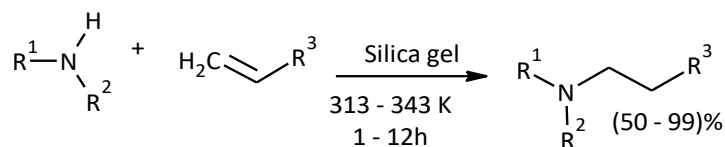
Equation 1-18: Selective double Michael addition



Equation 1-19: Selective single Michael addition

A double Michael addition reaction occurs with aliphatic and aromatic ketones. From Equation 1-18, acetone and ethyl acrylate react to yield a bis-adduct, diethyl 3-acetylheptanedioate (63% yield) keeping the other methyl group intact. The use of methyl cinnamate as an acceptor gives only the mono-adducts even at elevated temperature (as expressed in Equation 1-19). A possible reason for this may be attributed to the steric inhibition at the β -carbon of the conjugated olefins.¹⁹⁹ In some cases silica gel is also

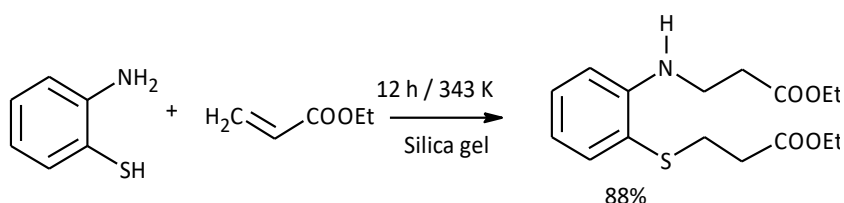
used to effect this Michael addition reaction,¹⁹⁹ as given below in Equation 1-20 and Equation 1-21. The reaction above proceeds under solvent-free conditions, with the exception of the work up processes.¹⁹⁹



$\text{R}^1 = \text{R}^2 = \text{H, alkyl, aryl}$

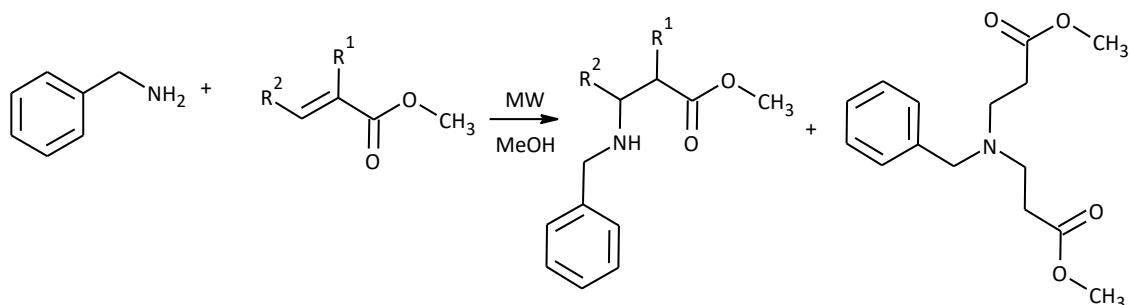
$\text{R}^3 = \text{COOEt, CN}$

Equation 1-20: The use of silica in Michael addition reaction of open chain amine



Equation 1-21: Michael addition reaction with silica gel involving aromatic amine

Escalante *et al.*,²⁰⁶ explained that the Michael acceptors methyl crotonate and methyl methacrylate formed only mono-adducts, but methyl acrylate formed both single and double addition even with short reaction times of 3 minutes, as expressed in the Equation 1-22 below;



Equation 1-22: Addition of amine to methyl crotonate, acrylate and methyl methacrylate

Some Michael addition reactions are performed using solvent-free conditions.¹⁹⁹ This would make the reaction environmentally benign as it avoids the generation of toxic

substances, like organic solvents and mineral acids. Traditionally, large amounts of organic solvents have been used to carry out reactions in commercial processes. The solvents allow the reactants to interact and they also provide a heat sink for any energy released in the processes. Solvents can be expensive, and therefore must be recovered and reused if possible. But 100% recovery is generally impossible, and some solvent is lost as vapour or is released into the environment thus expensive pollution control measures must be in place.²⁰⁷ These control measures are not 100% effective and some solvent is lost to the environment. Therefore, the solvent may become a contaminant in either soil, water, or the atmosphere.²⁰⁷ The chemical profession has increasingly turned to developing “green processes” which minimise the use of toxic materials and hence the use of solvent free reactions is becoming popular.²⁰⁷

Furthermore, microwave heating has been applied when carrying out Michael addition reactions. One notable advantage of using controlled microwave heating for chemical synthesis is the reduction in reaction times.^{208,209} It is a clean, efficient and cost-effective for the synthesis of a range of organic molecules²¹⁰ when compared to the traditional stirrer hot plate source of heating.²⁰⁸

1.15 Introduction to work in thesis

Attention has been focused on metals recovery from waste stream in the recent times in order to enhance metals sustainability. And the use of biobased materials in metals recovery is gaining more interest because such materials are environmentally benign and their supply in the future is certain. Therefore, this work is focused on biobased lipophilic chelants and their applications in metals recovery; and is divided into the following chapters.

Chapter 2 focuses on the purification of a known lipophilic hentriacontane-14,16-dione from wheat straw wax using petroleum ether and $\text{Cu}(\text{OAc})_2$. The bio-derived lipophilic β -diketone was characterised using DSC, TGA, GC-MS, GC-FID, NMR and FTIR techniques. Keto-enol equilibrium studies of this bioderived β -diketone in different deuterated solvents was investigated in comparison to acetyl acetone and dibenzoylmethane. The purified long alkyl chain β -diketone from the wheat straw wax exhibited similar properties to other β -diketones. Petroleum ether used in the purification of the lipophilic β -diketone has negative environmental impact. Therefore, alternative solvents were selected and tested in the purification of the long chain β -diketone.

Chapter 3 describes the use of alternative solvents; cyclohexane, *p*-cymene, cyclopentyl methyl ether (CPME) and 2,2,5,5-tetramethyl THF (TMTHF) in the isolation of the hydrophobic β -diketone from wheat straw wax. The advantages and disadvantages of these alternative solvents for the purification of the β -diketones were discussed. Furthermore, scCO_2 fractionation of wheat straw wax was studied as another alternative means for purification of 14,16-hentriacontanedione. The fractions collected were analysed using GC-FID and STA. Sequential scCO_2 fractionation using silica gel adsorbent was found to give at least better selectivity for lipophilic β -diketone when compared to alumina and celite adsorbents.

Chapter 4 looks into the use of the KF/alumina mediated Michael addition reaction for the modification of long chain bioderived lipophilic β -diketones (Htd) with methyl acrylate, methyl methacrylate, dimethyl itaconate and aconitate. The modified products were characterised by GC-FID, DSC, NMR and FTIR. There after methyl acrylate and dimethyl itaconate modified β -diketone were hydrolysed under alkaline condition. Also the yields and the efficiency of the reactions were assessed.

Chapter 5 deals with the liquid biphasic extraction of some selected metal ions with the unmodified β -diketone (Htd) and modified bioderived β -diketone. Furthermore, unmodified and modified Htd were used in the extraction of Pb(II), Mn(II), Ga(III), Cu(II), Ni(II), Co(II), Cr(III) and Fe(III) ions in comparison to acetyl acetone and dibenzoylmethane. The effect of the modification on the metals extraction were ascertained. The type of extraction mechanism of these unmodified and modified Htd was discussed. UV/visible spectra, $^1\text{H-NMR}$ spectra of some of the metal-Htd and metal-Dbm chelates were obtained and discussed.

Details of all experimental work carried out in this thesis are described in chapter 6.

Chapter 7 contains the concluding remarks and future work on the research.

Chapter 2

Purification of lipophilic β -diketone from wheat straw wax using petroleum ether

Aspects of the work described in this chapter have been presented as:

Kaana Asemave, Fergal Byrne, Andrew J. Hunt, Thomas J. Farmer and James H. Clark. Bioderived alternative chelating agent for metal recovery. Being a poster presentation at the RSC conference, titled: *Renewable chemicals from waste- securing the molecular value from waste streams*; London, UK. Nov. 20th, 2015

2 Chapter 2

2.1 Introduction

As highlighted in chapter one, β -diketones are versatile ligands^{141,142} used widely in coordination chemistry. They have also been applied as ligand for NMR shift reagents, metal extracting agents, chemical and photochemical catalyst, antioxidants, antitumor, anti-inflammatory and antiviral agents.^{27,141} β -diketones are present in natural products, pharmaceuticals and other biologically active compounds or can be used in their manufacture.¹⁴⁰ Keto-enol tautomerism has been observed as one unique nature of 1,3-dicarbonyls like β -diketones.^{136,137,211,212} The ratio of the keto-enol equilibrium is a function of factors such as the substituents on the β -dicarbonyl, the solvent, concentration and temperature.²¹³

Interestingly, hydrophobic β -diketones have been reported as wax components in cereals (such as wheat, barley, oats, and rye) and they are the major wax component in species such as eucalyptus, festuca, agropyron, and vanilla bean.^{139,168} However, up to now these naturally occurring β -diketone have not been well exploited for metal chelation and recovery. The lipids of *Vanilla fragrans* and *Vanilla tahitensis* (Orchidaceae) were found to contain 28% of four unsaturated long chain aliphatic β -diketones; 16-pentacosene-2,4-dione, 18-heptacosene-2,4-dione, 20-nonacosene-2,4-dione, 22-hentriacontene-2,4-dione, 24-tritriacontene-2,4-dione.²¹⁴ Wheat straw wax also has significant quantities of long chain β -diketones and is one of the most abundant compounds constituting the wax.¹⁶⁵ Leaf waxes from durum wheat varieties, pelissier and stewart 63 were found to contain hentriacontane-14,16-dione (35-36%) and 25(S)-hydroxyhentriacontane-14,16-dione (8-9%).²¹⁵ Cuticular waxes of glaucous-leaved *hosta* 'Krossa Regal' were analyzed and found to contain long chain β -diketones comprising as

much as 28.7%.¹⁷⁰ In order to be sustainable and avoid competition with the food industry, it would be ideal to obtain these molecules from feedstocks such as agricultural residues. Wheat straw in particular is an abundant bio-feedstock in many countries; in UK alone, 10 million tonnes of wheat straw are produced annually, of which 4 million tonnes have no commercial market.¹⁶²

There is little literature that focus on the isolation or purification of long chain lipophilic β -diketones from plant waxes. Chelation of β -diketones from organic solutions of plant waxes using copper(II) salts has been reported as an effective method for its isolation and purification.^{214,215} Horn *et al.*²¹⁶ reported the precipitation of lipophilic β -diketone from a petroleum ether solution of plant wax with $\text{Cu}(\text{OAc})_2$. Chromatographic separation of β -diketones from lipophilic extracts of beans has also been reported.²¹⁴ This chapter looks into the isolation of β -diketone from the wheat straw wax by chelation with cuprous acetate, $\text{Cu}(\text{OAc})_2$, and investigates improvements into the previously reported methodology.

2.2 Results and discussion on isolation of the lipophilic β -diketone using cuprous acetate - $\text{Cu}(\text{OAc})_2$

Isolation of the lipophilic β -diketone from wheat straw wax was performed by precipitation of the complex in petroleum ether in contact with a hot saturated $\text{Cu}(\text{OAc})_2$ solution. The wheat straw wax was firstly dissolved in petroleum ether and the resulting mixture filtered. The filtrate was subsequently contacted with hot saturated aqueous $\text{Cu}(\text{OAc})_2$, in a biphasic system. The lipophilic Cu-diketonate was formed and eventually accumulated at the interphase of the petroleum ether/water system. The Cu-diketonate was then collected from this mixture via filtration, dried, redissolved in fresh petroleum ether and stripped with concentrated HCl, thus converting back to the free diketone

form, yielding $18 \pm 5\text{wt}\%$ of a waxy solid. Evident from the above methodology is that the choice of solvent and the metal salt is vital to enable the precipitation of the lipophilic β -diketone. The extraction process is summarised in Figure 2-1 and Equation 2-1. This process of obtaining the β -diketone benefits from the fact that the wax is obtained from an abundant agricultural co-product, wheat straw.¹⁵⁸ Notwithstanding, due to chronic effect on human health and negative environmental impact associated with petroleum ether,²¹⁷ an alternative volatile green solvent would be ideal for this purification of the lipophilic β -diketone (Htd) from wheat straw wax.

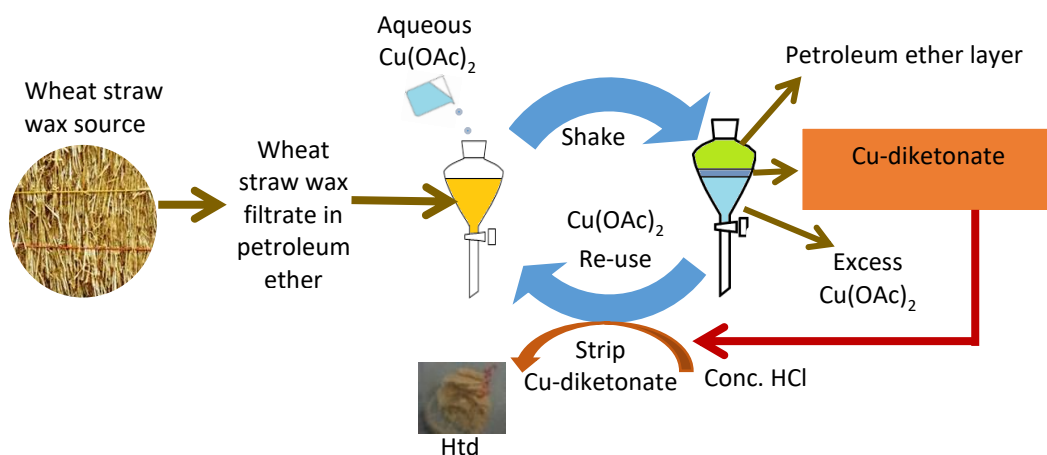
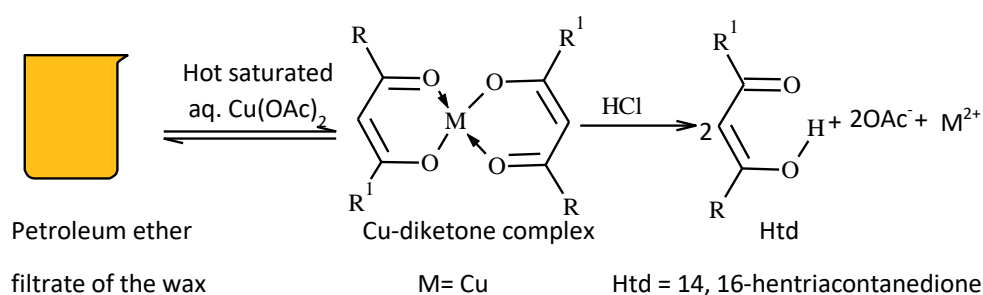


Figure 2-1: Isolation of Htd from wheat straw wax dissolved in petroleum ether with $\text{Cu}(\text{OAc})_2$



Equation 2-1: Formation of $\text{Cu}(\text{II})$ β -diketone complex and subsequent recovery of the Htd

Similar approaches for the isolation of lipophilic β -diketones from plant waxes had been reported in the literature.²¹⁴ Ramaroson-Raonizafinimanana *et al.*²¹⁴ isolated hydrophobic β -diketones from lipids of cured and green beans by column

chromatography using silica with *n*-hexane/diethyl ether (90:10 v/v, 200 mL). Eight fractions were obtained and the β -diketones (28%) were found in later eluting fractions (6-8).²¹⁴ Also the purification of the hydrophobic β -diketone from this lipidic extract (2.5 g) of the beans was achieved by crashing it from 70 mL hot *n*-hexane with 50 mL of saturated aqueous cuprous acetate.²¹⁴ Similarly, column purification of hentriacontane-14,16-dione (Htd) was performed by charging 10 g of Stewart wheat wax onto the front of a silicic acid column (400 g). By passing hexane through this column the first the long chain hydrocarbons were eluted followed by the esters, and subsequently the β -diketones (5.15 g) were eluted with hexane/CHCl₃ (4: 1).²¹⁵

A challenge with the methods thus far used for the isolation of the Htd found in plant waxes are that; the *n*-hexane and petroleum ether used for the purification of the lipophilic β -diketone are flammable and toxic solvents.^{217,218} Moreover, large volumes of solvent would be employed in liquid column chromatographic separation, which could likely contribute to significant negative environmental contamination. Thus, use of greener solvents and alternative isolation techniques such as scCO₂ separation for the purification of these lipophilic β -diketones would mean less negative impact on human health and the environment at large.

Thereafter, the characterisation of the known hydrophobic β -diketone, Htd, was carried out using techniques such as GC-FID, GC-MS, ESI-MS, TGA, DSC, FTIR and NMR spectroscopy. Solubility tests and keto-enol tautomerism studies were also carried out to obtain detailed insights about these fundamental properties

2.2.1 GC characterisation of the Htd

The GC-FID chromatogram and GC-MS of the Htd are presented below in Figure 2-2 and Figure 2-3.^{165,166} A fragmentation pattern for Htd is described in Figure 2-4;²¹⁹

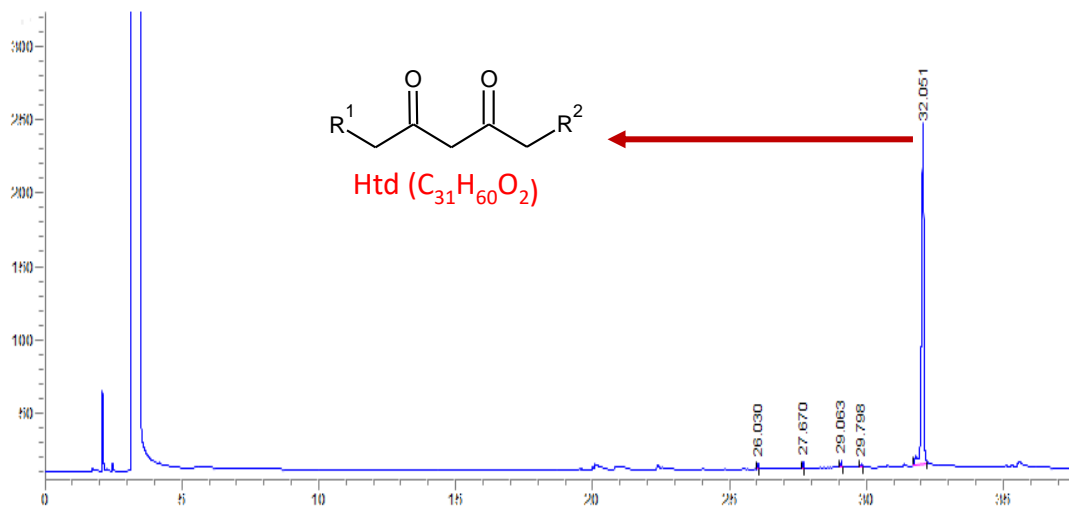


Figure 2-2: GC-FID chromatogram of the Htd

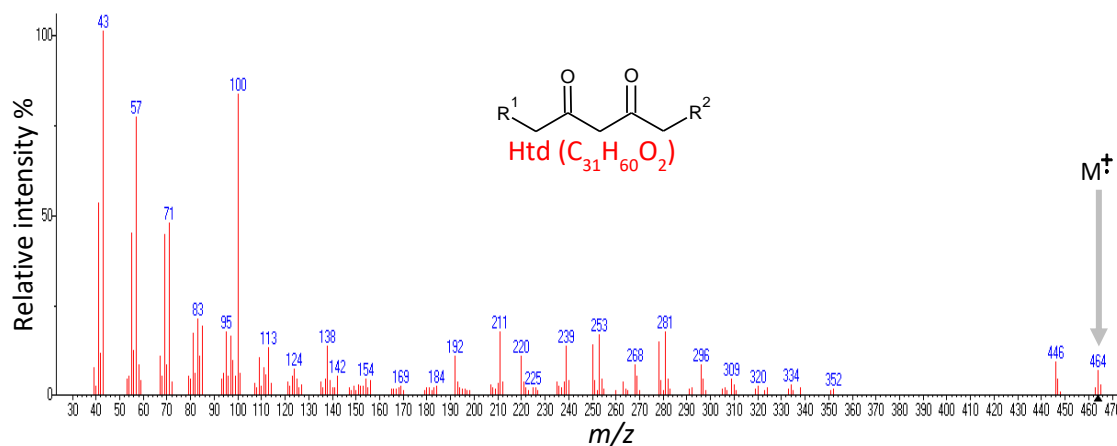
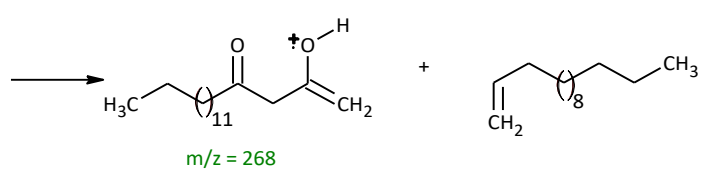
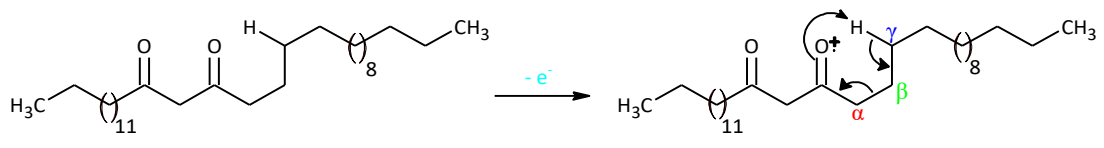
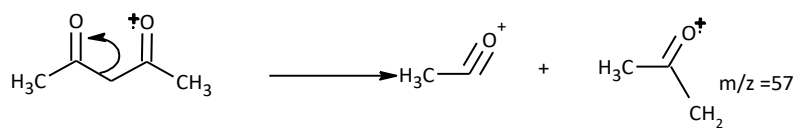
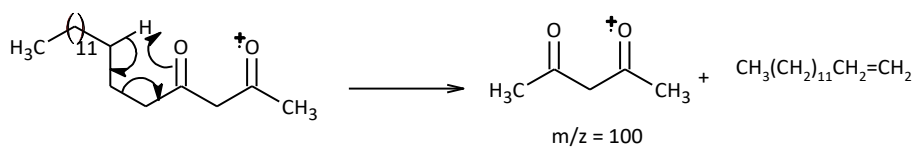
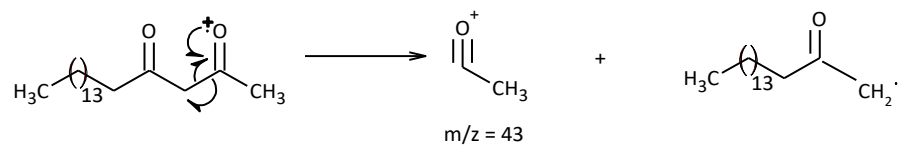
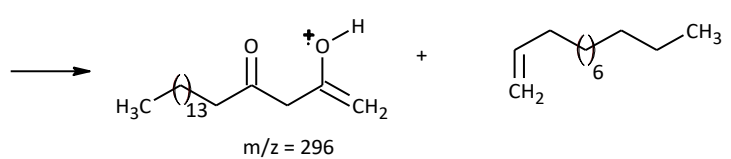
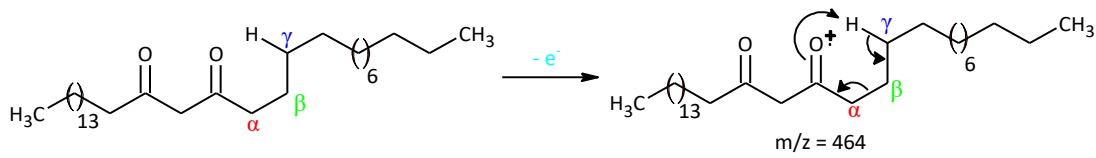


Figure 2-3: GC-MS of Htd



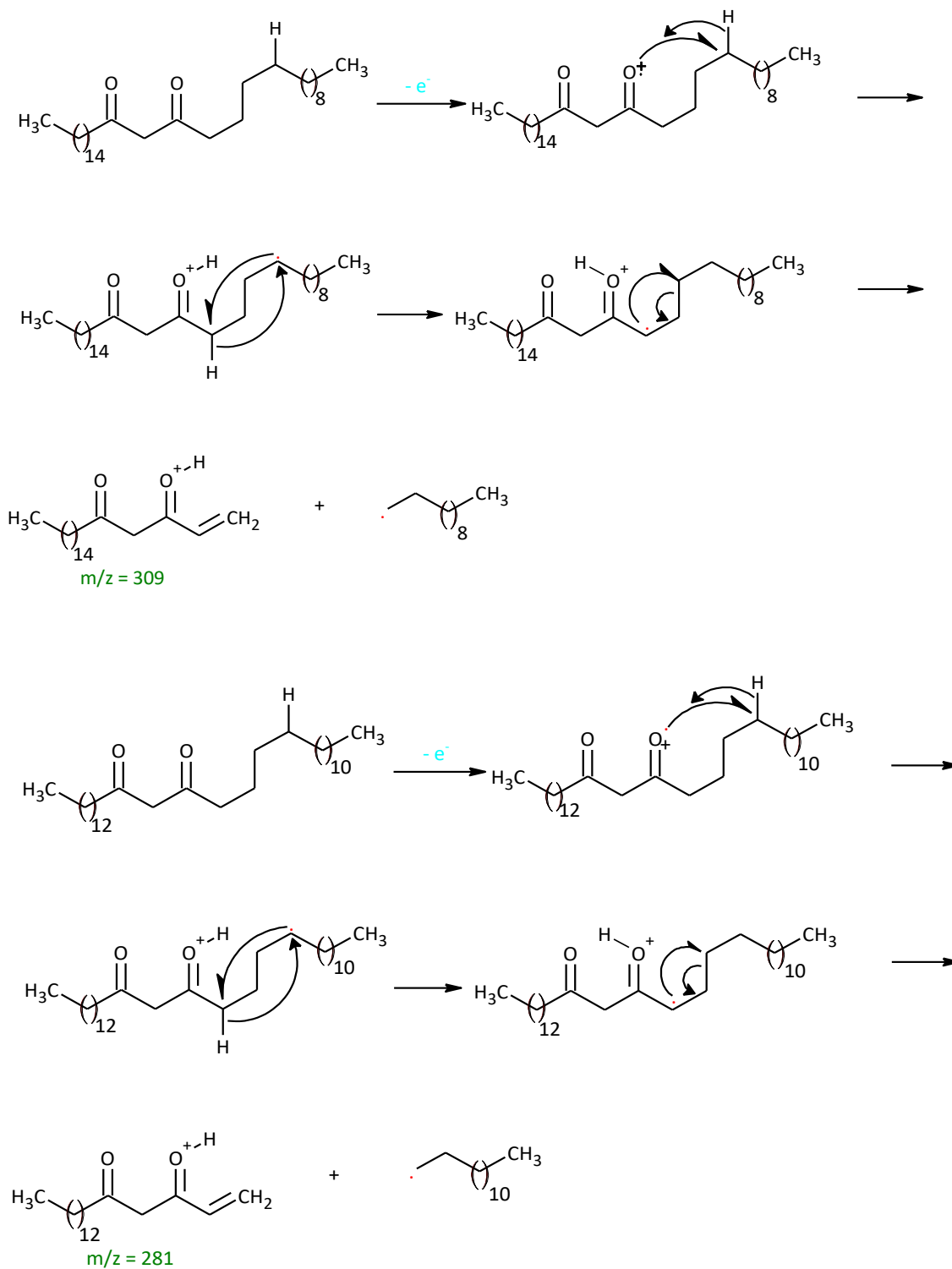


Figure 2-4: A Proposed fragmentation scheme of the bioderived β -diketone

The peak at 446 m/z arises because of the loss of water from the molecular ion (m/z 464). The fragments with a m/z of 296 and 268, 281 and 309 arise from the McLafferty rearrangement at both sides of the β -diketone as depicted by the scheme above.^{165,219} A typical fragment of 100 m/z for β -diketones was observed in this GC-MS. This ion arises

because of a McLafferty rearrangement at the first carbonyl group, which cleaves the long saturated alkyl group. Then followed by keto-enol tautomerism and subsequent second McLafferty rearrangement from the intermediate charged β -diketone moiety, cleaving the second alkyl chain to give rise to the peak 100 m/z . Rearrangement and loss of a methyl group from this ion gives a fragment ion of 85 m/z .¹⁶⁹ The ion fragments 43 m/z and 57 m/z are common characteristic peaks of β -diketones; resulting from the C-C(O) cleavage and loss of $[C_3H_5O]^+$ from 100 m/z fragment respectively. Therefore, the GC-MS shows that the bio-derived β -diketone isolated is indeed 14,16-hentriacontanedione; which is the most abundant β -diketone known to be found in wheat straw. The β -diketone structure was also identified using comparison to the NIST library 2008.

Ramaroson-Raonizafinimanana *et al.* reported five long chain aliphatic β -diketones found in epicuticular waxes of *Vanilla* bean species with their molecular peaks of 378 m/z ($C_{25}H_{46}O_2$), 406 m/z ($C_{27}H_{50}O_2$), 434 m/z ($C_{29}H_{54}O_2$), 462 m/z ($C_{31}H_{58}O_2$), and 490 m/z ($C_{33}H_{62}O_2$).²¹⁴ Furthermore, Kenar observed loss of water, presumably from the enol tautomer $[M - 18]^+$ and McLafferty rearrangements accounting for the fragment ion at m/z 100 in mass spectrum of long chain β -diketone.¹³⁹ The fragment ions at m/z 43 $[C_2H_3O]^+$ and m/z 85 $[C_4H_5O_2]^+$ likely resulted from α -cleavage to the carbonyl carbon, whereas the ion at m/z 57 results from a cleavage of a $[C_3H_5O]^+$ fragment.¹³⁹ Previous studies also showed that nonacosane-10,12-dione and hentriacontane-10,12-dione were also found to form a dehydration fragment, $[M - H_2O]^+$.¹⁷⁰

2.2.2 Electrospray ionisation mass spectrum (ESI-MS) of the Htd

In addition to the EI-MS, the ESI-MS of the Htd was determined. ESI is a soft ionisation analysis that causes little or no fragmentation of the parent compound. Proton,

potassium and copper adduct species of the Htd have been identified in the ESI-MS spectrum shown in Figure 2-5 and further described in Table 2-1 below. Copper may be accounted for in this spectrum since it comes from the cuprous acetate used to isolate the long chain Htd. Aravindhan *et al.*²²⁰ reported Na species of the metal and azo-metals complexes of embelin in their ESI-MS analysis.²²⁰

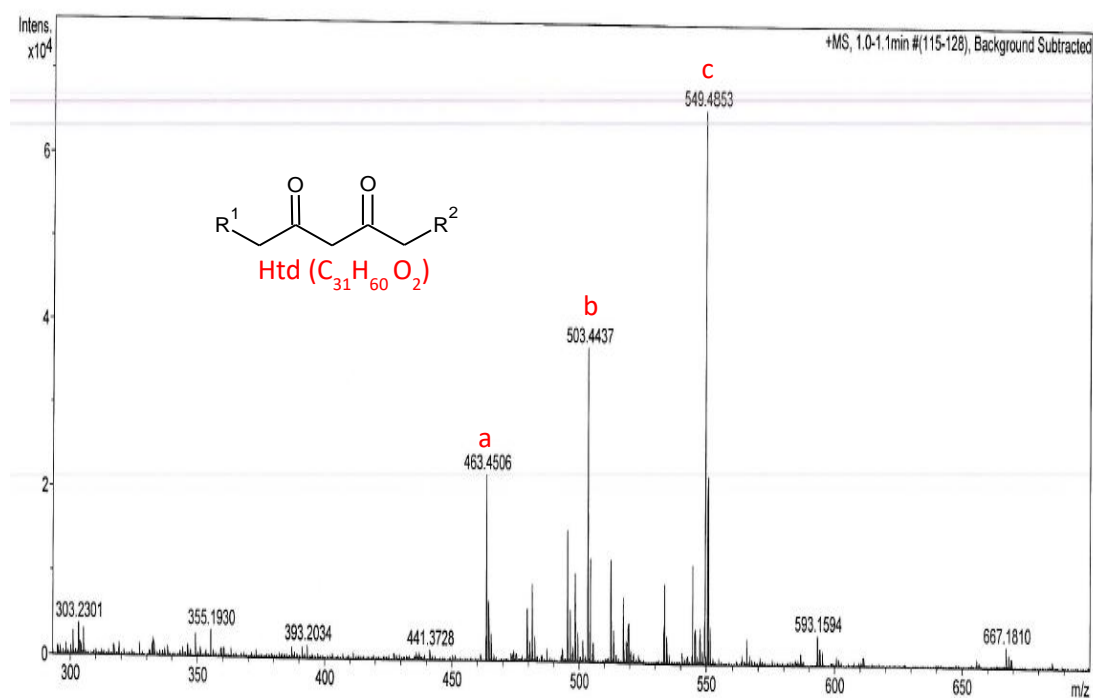


Figure 2-5: ESI-MS(+) for the Htd

Table 2-1: ESI-MS(+) interpretation of the Htd

Sample	<i>m/z</i> peak	Interpretation
	463.4506 (a)	[M] ⁺
14,16-hentriacontanedione	503.4437 (b)	[M+K] ⁺
	549.4853 (c)	[Htd-Cu ⁺ + Na - H] ⁺

2.2.3 FTIR spectrum and UV absorption of the Htd

The Htd was also characterised by measuring the FTIR spectrum (Figure 2-6) and determining the λ_{\max} in ethanol, limonene-R(+), and 2-methyl-THF. The characteristic FTIR absorption peaks of 2954.98 – 2828.74 cm^{-1} , 1639.48 cm^{-1} and 721.07 cm^{-1} were assigned to the functional groups C-H, -C=C-C=O and long chain -CH₂ respectively, as

presented in Table 2-2. Ramaroson-Raonizafinimanana *et al.* also reported the presence of 1610 and 1725 cm^{-1} in long-chain aliphatic hydrophobic β -diketones obtained from epicuticular wax of vanilla bean species.²¹⁴ Kenar reported the FTIR absorption bands of nonadecane-2,4-dione (1648 cm^{-1}), heneicosane-2,4-dione (1700 and 1648 cm^{-1}), heneicos-12-ene-2,4-dione (1712 and 1614 cm^{-1}) and heneicos-12,15-diene-2,4-dione (1705 and 1613 cm^{-1}).¹³⁹ These observations are comparable to the FTIR absorption of our isolated Htd.

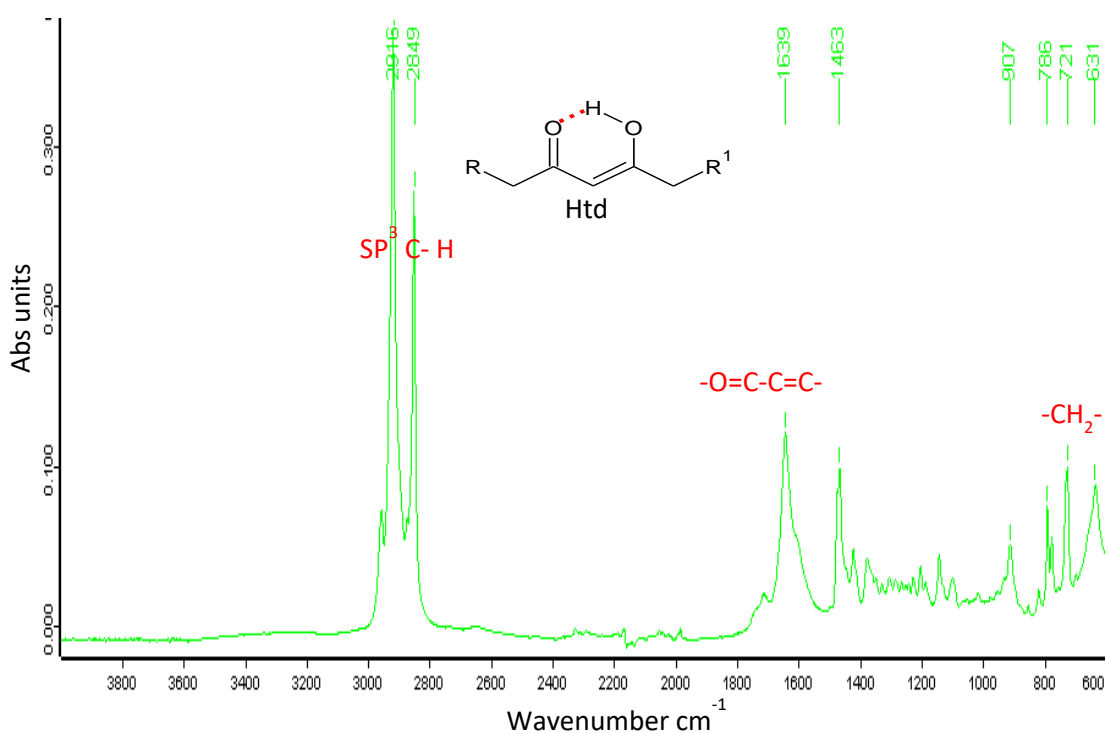


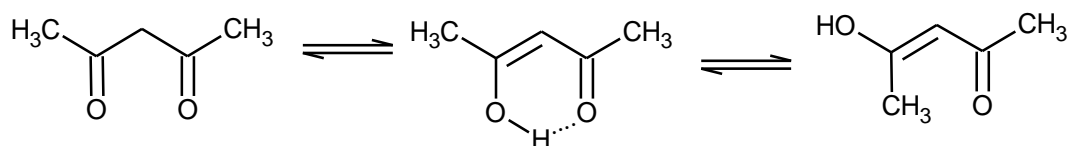
Figure 2-6: FTIR spectrum of the Htd

Table 2-2: FTIR assignments of the Htd

FTIR peaks (cm^{-1})	Assignments	Reference
2954.98, 2916.48 and 2948.74	C-H symmetric and antisymmetric stretch (sp^3)	221, 11, 222
1639.48	C=C-C=O	223, 224
1462.93	C- H scissoring, SP^3 (CH_3)	222
1419.29	O- H bend	

1374.87	C-H, methyl rock	
1302.68	C-O stretch	220
1223.10	C-O stretch	220
1199.78	C-O stretch	225
721.07	Long chain CH ₂	

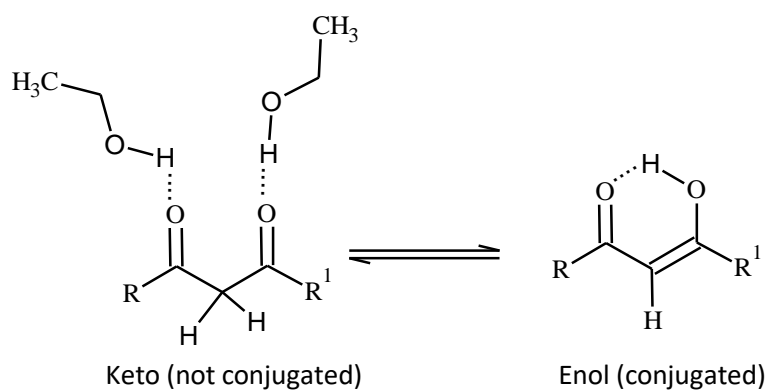
Abood and Ajam observed similar absorption bands for the β -diketones, acetyl acetone and dibenzoylmethane.¹³⁶ The FTIR of acetyl acetone in CCl₄ gave a strong and broad absorption band of 1610 cm⁻¹ and weak band near 1720 cm⁻¹. The absorption peak of 1610 cm⁻¹ is due to the superposition of C=O and C=C stretchings coupled with C-H in plane bending of the enol tautomer.¹³⁶ The weak band near 1720 cm⁻¹ was assigned to the C=O stretching of the keto form.¹³⁶ The high intensity of the 1610 cm⁻¹ peak indicates that acetyl acetone is highly enolised when dissolved in a nonpolar solvent. In addition, acetyl acetone has carbonyl absorption of 1695 cm⁻¹ for the non-chelated enol tautomer (Equation 2-2). This was supported by the fact that there was an absorption at 3350 cm⁻¹, where simple hydrogen bonded absorption (for O-H) occurs.¹³⁶ This kind of O-H absorption is broadened for the fatty acid dimer.¹³⁶ For dibenzoylmethane, the FTIR analysis showed a single band at 1605 cm⁻¹ due to the superposition of C=O and C=C stretching coupled with C-H in plane bending of the enol tautomer as earlier reported in acetyl acetone.¹³⁶



Equation 2-2: keto, chelated enol and non-chelated enol of acetyl acetone

The λ_{\max} for UV absorbance of Htd in ethanol, 2-methyl-THF and limonene– R (+) were 255 nm, 263 nm and 281 nm respectively. A red shift was observed in the UV absorption

of Htd from the polar solvent (ethanol) to Limonene-R (+), which is nonpolar. This is due to the ability of ethanol to form H-bonds with the ground state of Htd is stronger than 2-methyl-THF, while limonene-R (+) is not able to form hydrogen bond.²²⁶ The longer λ_{\max} of 263 nm and 281 nm observed when the Htd was dissolved in 2-methyl-THF and limonene shows conjugation (Equation 2-3) by virtue of the enolization of the Htd. However, Htd will not form significant conjugation in ethanol because of H-bonding between the ethanol and the carbonyl oxygen of keto tautomer being energetically preferential. The UV absorption band of 274 nm had been previously reported for the β -dicarbonyl moiety.²¹⁴ Such UV absorptions are linked to the $n-\pi^*$ transitions.²²⁶



Equation 2-3: Conjugated enol tautomer

2.2.4 $^1\text{H-NMR}$ and $^{13}\text{C-NMR}$ spectra of the Htd

From previous studies, the $^1\text{H-NMR}$ spectrum of Hacac has $\text{CH}_3^{\text{enol}}$ chemical shifts of 2.00 ppm; 5.60 ppm for CH^{enol} ; 15.5 ppm for OH^{enol} (quite small) and the chemical shifts with values of 2.10 ppm, 3.70 ppm for $\text{CH}_3^{\text{keto}}$ and $\text{CH}_2^{\text{keto}}$ respectively.²¹³ In $^{13}\text{C-NMR}$ spectrum (acetyl acetone), $\text{CH}_3^{\text{enol}}$ has chemical shifts of 24.60 ppm; CH^{enol} , 100.70 ppm; $\text{C}=\text{O}^{\text{enol}}$, 191.60 ppm; $\text{CH}_3^{\text{keto}}$, 30.70 ppm; $\text{CH}_2^{\text{keto}}$, 58.00 ppm and $\text{C}=\text{O}^{\text{keto}}$, 203.40 ppm.^{139,227} Kenar also reported such chemical shifts in long chain β -diketones, of 3.55 ppm and 5.47 ppm for $\text{CH}_2^{\text{keto}}$ and vinyl proton of the enol tautomer accordingly.¹³⁹ It was further observed that 81–85% of the β -diketone molecules existed in the enolic form in CDCl_3 .¹³⁹

These previous observations of similar compounds were compared to the NMR spectra of the Htd. In Figure 2-7 and Figure 2-8, the NMR spectra show that Htd existed more in enol form (81.42%) than keto tautomer (18.58%) in CDCl_3 as previously reported.^{139,227} The ^1H -NMR spectrum of the Htd in Figure 2-7 showed the chemical shift of the vinyl proton of the enol tautomer at 5.46 ppm, methylene protons of the keto tautomer at 3.53 ppm. There was also an intense chemical shift for α -proton adjacent to the $\text{C}=\text{O}^{\text{enol}}$ at 2.23-2.27 ppm and a less intense signal at 2.48 ppm due to α -proton adjacent to $\text{C}=\text{O}^{\text{keto}}$. The ^{13}C -NMR spectrum has signals at 193.29- 194.66 ppm for $\text{C}=\text{O}^{\text{enol}}$ and 99.13 ppm ($-\text{CH}=\text{C}$). CH_2 of the keto tautomeric form had chemical shifts of 58 ppm as similarly reported.^{139,221,223,139} The peak at 14 ppm is due to the CH_3 of $-\text{CH}_2\text{CH}_3$.¹³⁹ The $\text{C}=\text{O}^{\text{keto}}$ at about 200 ppm peak was absent due to the predominance of the enol tautomer.^{139,227}

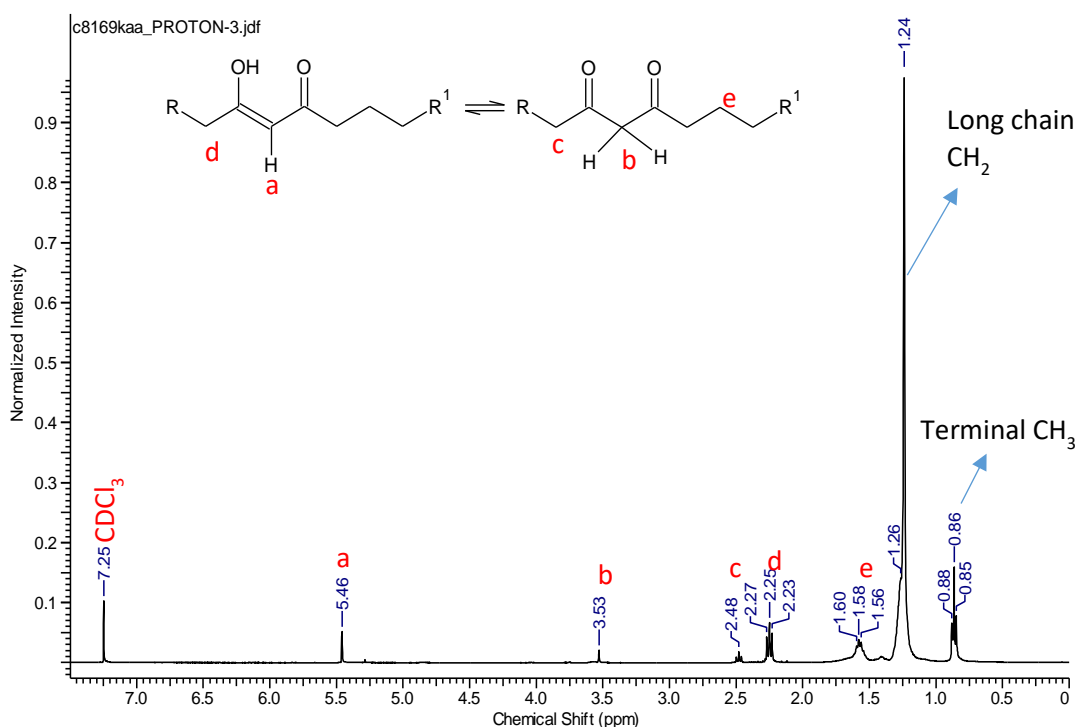


Figure 2-7: ^1H -NMR spectrum of the Htd in CDCl_3

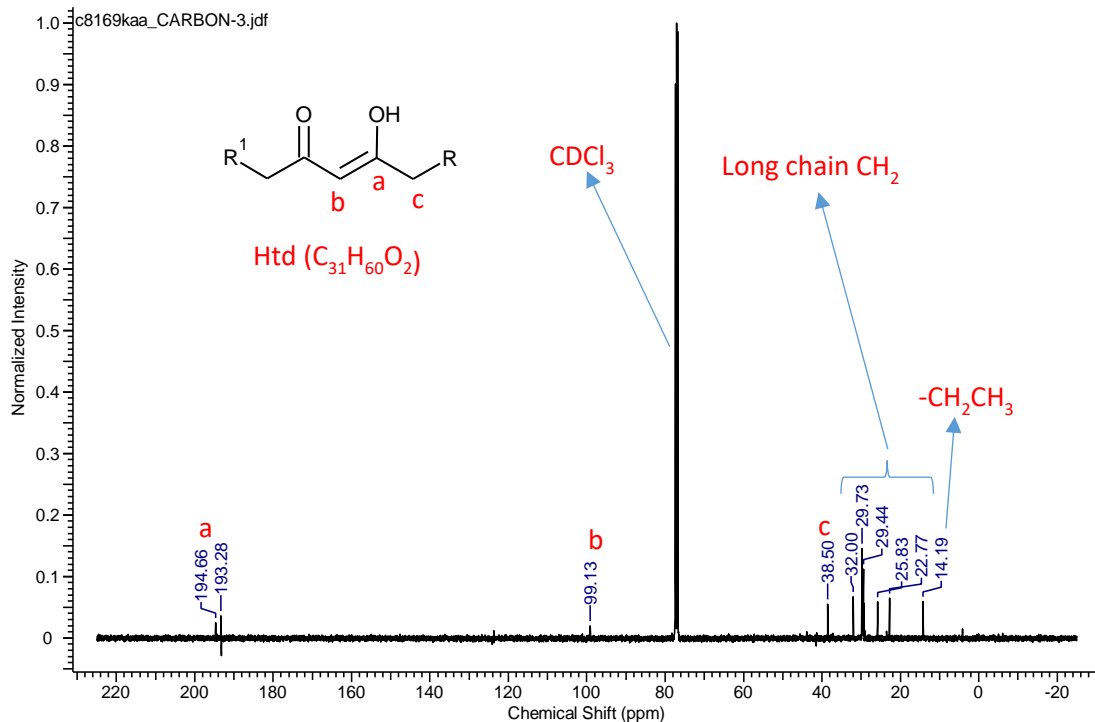
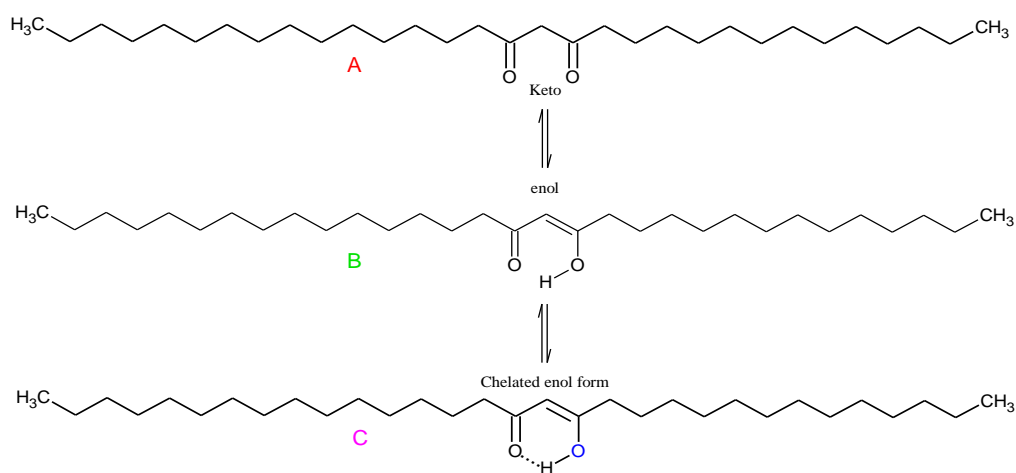


Figure 2-8: ^{13}C -NMR spectrum of the Htd in CDCl_3

The ^{13}C -NMR spectrum of the β -diketone were previously reported to show distinctive chemical shifts corresponding to both the keto and enol tautomeric forms.¹³⁹ The two carbon atoms of the carbonyl group in the keto tautomeric form had chemical shifts of roughly 204 and 202 ppm, whereas in the enol form these same carbon atoms' NMR peaks are 194 and 191 ppm.¹³⁹ Therefore, the structure of this known Htd is given in Equation 2-4 below.^{136,165,166}



Equation 2-4: Keto-enol tautomers of the Htd

2.2.5 Thermal gravimetric analysis (TGA) of the Htd

Thermogravimetric analysis is an excellent analytical tool to study the thermal behaviour of different materials under an inert atmosphere (typically N₂).²²⁸ The thermogram of the Htd in Figure 2-9 indicated that the compound is stable till 473 K. In addition, three stages of mass change were observed. From 373 – 473 K the mass change was 3.1% which is due to the loss of water. There was significant decomposition of the compound with a mass loss of 72.4% as the temperature was increased from approximately 473 K – 703 K. The third mass change (18.2%) occurred between 703 – 873 K, due to the formation of char from the compound. These trends were analogous to the literature findings, where loss of water has been encountered in various studies involving TG analysis.²²⁰ The TGA of Zn-embelin complex, [Zn(Emb)₂(H₂O)₂] showed a weight loss of 6.4% at the temperature range of 368 – 459 K which was attributed to loss of water molecules from the complex.²²⁰ The complex then decomposed at 586 – 688 K accounting for 65.2% weight loss.²²⁰

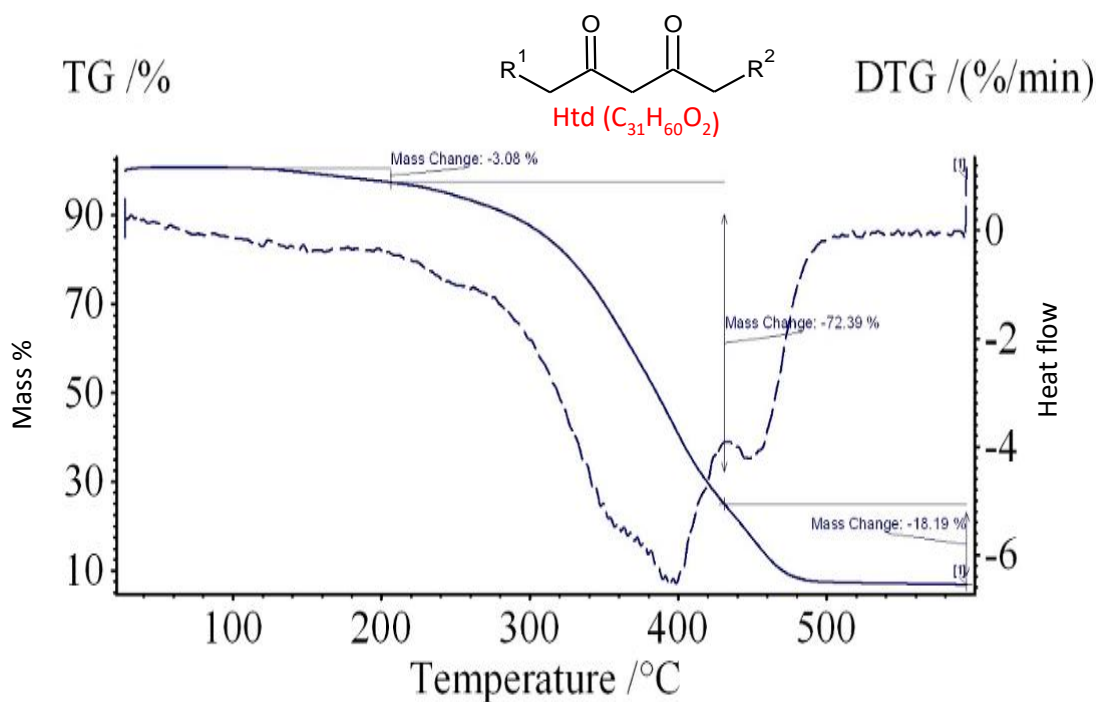


Figure 2-9: TGA thermogram of bioderived β -diketone (Htd)

Furthermore, from previous TGA studies of lipids of microalgal biomasses (lipid-extracted from *Chlorella* sp. and *T. suecica*), three mass changes were observed.²²⁸ The initial small change was taken as water removal at about 473 K.²²⁸ Subsequently, between 473 – 823 K, the volatiles present in the lipid were released.²²⁸ The final stage is the decomposition of the carbonaceous matter in the residues (> 823 K), where the carbonaceous matter was substantially decomposed, leaving behind the bio-char (predominately residual inorganic material and carbon).²²⁸

2.2.6 Differential scanning calorimetric measurement (DSC) of the Htd

The DSC technique is a useful diagnostic tool for studying the thermal transitions that occur in materials. Transitions such as melting, recrystallization, decomposition and glass transitions could be measured with DSC. In addition, Nassu and Goncalves, also determined the melting point of fats with DSC in comparison to the softening point method and found that DSC is an accurate and useful technique of melting point measurements above many other methods.²²⁹ Moreover, DSC has also been previously used for purity determination of materials such as waxes.²³⁰ An important advantage of DSC for melting point determination is that the measurements are more accurately reproducible.

Therefore, for these studies, the first heating cycle was carried out to remove any prior thermal character and thus all the results of the thermograms shown in Figure 2-10 are from the second heating cycle.

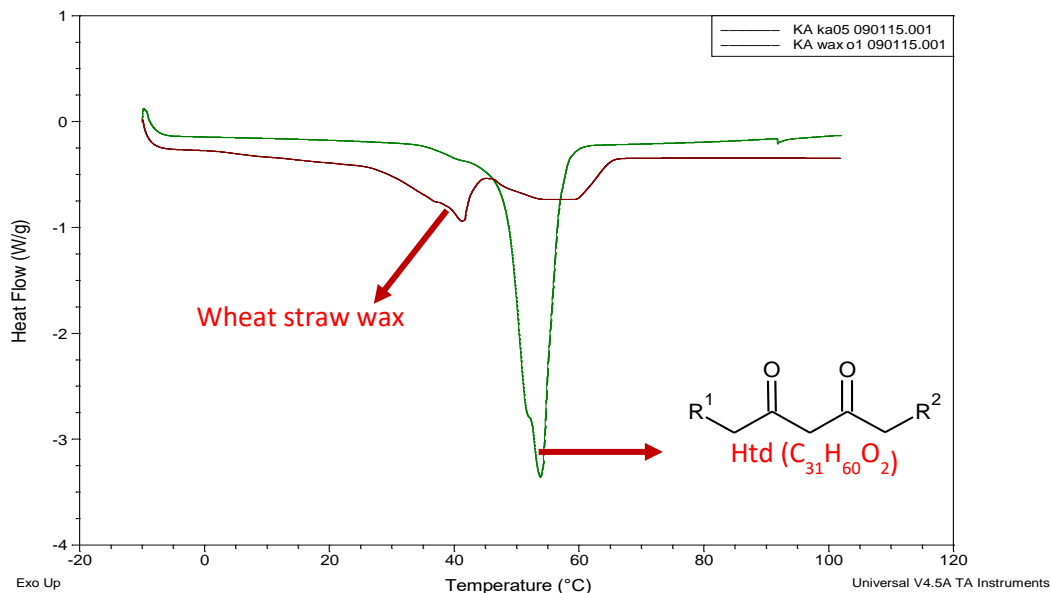


Figure 2-10: DSC thermogram of wheat straw wax and the Htd

From Figure 2-10 above it can be seen that the wheat straw wax has a broad DSC trace with two endothermic minima centred at around 313 K and 333 K. This is expected, as it is rare to find clearly defined transitions for waxes because they comprise of a complex mixture of hydrophobic compounds resulting in phase transitions occurring for families of compounds. On the other hand, the DSC curve of the Htd, as a pure compound, is a well-defined narrow peak (has a small shoulder) with an endothermic minimum of 326.9 K. The pronounced H-bonding via the β -diketone increases its melting point relative to similar hydrocarbons. Rugu *et al.* reported the melting points of lipid waxes in the range of 363.42 – 343.34 K with DSC technique.²³¹ The melting points variation was due to molecular composition and weight.

2.2.7 Solubility study of the Htd

In order to find suitable solvents that can dissolve the Htd efficiently, the solubility test of the β -diketone was investigated in various solvents, some with less negatively environmental impact.²³² Most of these solvents were selected primarily using the GlaxoSmithKline (GSK) solvent guide, for greener solvents as given below in Table 2-3.²¹⁷

In addition 2,2,5,5-tetramethyl THF (TMTHF) developed at the Green Chemistry Centre of Excellence (University of York) was selected as a new emerging bio-derived alternative to toluene.

Approximately 20 mg of the β -diketone was shaken in 1 mL of each of the solvents for 2 min and then the mixture allowed standing at room temperature for 30 min. The ability of these solvents to dissolve Htd was then visually determined as complete or incomplete dissolution. The results show that the hydrocarbons and ethers used were able to completely dissolve the Htd with the exception of heptane. Ethyl acetate and ethanol dissolved at least more than half of 20 mg Htd.

Table 2-3: GSK quick solvent guide²¹⁷

Solvents	Few issues (boiling point)	Some issues (boiling point)	Major issues
Chlorinated	Substitute for chlorinated solvents; TBME, isopropyl acetate, 2-methyl THF or dimethyl carbonate		Dichloromethane†, carbon tetrachloride†, chloroform†, 1,2-dichloromethane†
Greenest option	Water (373 K)		
Alcohols	1-butanol (391 K), 2-butanol (373 K)	Ethanol (351 K), 1-propanol (370 K), t-butanol (355 K), 2-propanol (355 K), methanol (339 K)	2-methoxyethanol†

Esters	t-butyl acetate (368 K), isopropyl acetate (368 K), Propyl acetate (375 K), dimethyl carbonate (364 K)	Ethyl acetate (370 K), methyl acetate (330 K)	
Ketones		Methyl isobutylketone (390 K), acetone (329 K)	Methylethylketone
Aromatics		p-xylene (411 K), toluene† (384 K)	Benzene
Hydrocarbons		Isooctane (372 K), cyclohexane (354 K), heptane (371 K)	Petroleum spirit, 2-methylpentane, hexane
Ethers		t-butyl methyl ether (328 K), 2-methyl THF (351 K), cyclopentyl methyl ether (379 K)	1,4-Dioxane†, 1,2-dimethoxyethane†, THF, diethyl ether, Diisopropyl ether†

Dipolar aprotics

Dimethylsulfoxide (462 K)

Dimethyl formamide†, N-methyl pyrrolidone†,
N-methyl formamide†, dimethyl acetamide†,
acetonitrile

† EH regulatory issues

Table 2-4: The results of the solubility studies of Htd at 293 K and the Kamlet-Taft parameters²³²⁻²³⁴ of the selected solvents

Solvent	Hydrogen bond donor (α)	Hydrogen bond acceptor (β)	Polarisability (π^*)	Nature of solubility
Heptane	0.00	0.00	-0.08	Incomplete
Cyclohexane	0.00	0.00	0.00	Complete
Toluene	0.00	0.11	0.54	Complete
2-methylTHF	0.00	0.45-0.58	0.53	Complete
CPME	0.00	0.53	0.42	Complete
TMTHF				complete
Limonene	0.00	0.00	0.16	complete
<i>p</i> -Cymene	0.00	0.13	0.39	complete
<i>tert</i> -butanol	0.42	0.93	0.41	Incomplete
Methanol	0.98	0.66	0.60	Incomplete
Ethanol	0.86	0.75	0.54	Incomplete
Octanol	0.77	0.81	0.40	Incomplete
Ethyl acetate	0.00	0.45	0.55	Incomplete
DMSO	0.00	0.76	1.00	Incomplete
1-butanol	0.84	0.84	0.47	Incomplete
Acetone	0.08	0.43	0.71	Incomplete
water	1.17	0.47	1.09	Incomplete

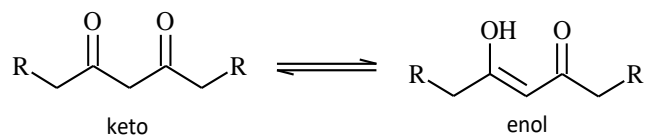
TMTHF = 2,2,5,5-tetramethyl THF

Cyclopentyl methyl ether (CPME), *p*-cymene, TMTHF, limonene, cyclohexane, toluene and 2-methylTHF with H-bond donor of 0.00 completely dissolve the Htd unlike heptane, DMSO and ethyl acetate with same H-bond donor (Table 2-4). In addition, it can be seen that ethyl acetate has polarisability and H-bond acceptor close to toluene and 2-

methylTHF in which case it incompletely dissolves Htd unlike toluene and 2-methylTHF that efficiently dissolve the Htd. It could be broadly observed that ethyl acetate is at least more polar than 2-methylTHF and toluene; hence, it was less effective in dissolving this lipophilic Htd. Therefore, it is evident from this solubility test of these selected solvents that the hydrocarbons and ethers have shown more ability to dissolve this long chain Htd than the alcohol, esters, ketones, DMSO and water, showing that Htd is evidently more lipophilic in character. This aligns with our hope that Htd could be used as a lipophilic chelator.

2.2.8 Keto- enol tautomerisation studies of the Htd in comparison to Hacac and Hdbm

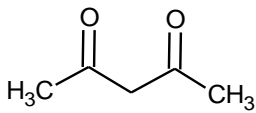
In the literature it has been shown that β -diketones exhibit keto-enol tautomerism.¹³⁶ The ability to form stable complexes with metals is a direct consequence of the occurrence of such compounds to revert to their enol form (as an enolate when in the presence of positive metal ions).²¹¹ The ratio of the keto–enol equilibrium is a function of the substituents on the β -dicarbonyl, the solvent,²³⁵ concentration,²¹³ temperature,²¹³ and the presence of other species in solution that are capable of forming hydrogen bonds. The presence of electron-donating groups on carbonyl groups and increasing the temperature decreases the enol tautomer.^{236,237} ¹H-NMR spectroscopy is a viable method for measuring tautomeric equilibrium (see Equation 2-5) because the equilibrium is slow on the NMR timescale^{136,213,238} and the equilibrium constants are calculated from the integrated intensities of keto-enol signals.²³⁷



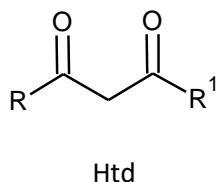
Equation 2-5: Keto-enol tautomerism of β -diketone

Therefore, the keto-enol tautomerism of the Htd was investigated in comparison to Hacac and Hdbm with NMR spectroscopy in five different solvents. The keto-enol equilibrium constant (K_{eq}) and the corresponding free energy (ΔG°) for the keto-enol equilibrium were evaluated in a similar way as was carried out in the literature.²³⁹ The $^1\text{H-NMR}$ chemical shift positions of the keto-enol tautomers and the other protons were found to be solvent dependent. The data is summarised in Table 2-5 below.

Table 2-5: $^1\text{H-NMR}$ chemical shifts (δ , ppm) for Htd in comparison to Hacac and Hdbm in different deuterated solvents

Compound	Solvent	δ_{H}
 Hacac	Cyclohexane- d_{12}	$^1\text{H-NMR}$ (400 MHz, cyclohexane- d_{12}) δ ppm 1.89 (s, 6H; methyl of keto tautomer) 1.96 (s, 3H; methyl of enol side) 2.05 (s, 3H; methyl keto side) 3.33 (s, 2 H; methylene protons) 5.31 (s, 1 H; vinyl proton)
	Toluene- d_8	$^1\text{H-NMR}$ (400 MHz, toluene- d_8) δ ppm 1.58 (s, 9H; methyl on the keto tautomer plus on the enol side) 1.62 (s, 3H; methyl proton on the keto side) 2.74 (s, 2H; methylene protons) 4.91 (s, 1H; vinyl proton)
	CDCl_3	$^1\text{H-NMR}$ (400 MHz, CDCl_3) δ ppm 2.03 (s, 9H) 2.23 (s, 3H) 3.58 (s, 2 H; methylene protons) 5.49 (s, 1H; vinyl proton)
	Acetone- d_6	$^1\text{H-NMR}$ (400 MHz, acetone- d_6) δ ppm 1.98 (s, 9H; methyl on the keto tautomer plus on the enol side) 2.13 (s, 3H; methyl on the keto side) 3.64 (s, 2 H; methylene proton on keto tautomer) 5.61 (s, 1H; vinyl proton of enol tautomer)

^bTHF-d₈ ¹H-NMR (400 MHz, THF-d₈) δ ppm 1.95 (s, 6H; methyl of keto tautomer) 2.01 (s, 3H; methyl of enol side) 2.08 (s, 3H; methyl on the keto side) **3.53 (s, 2H; methylene protons)** **5.53 (s, 1H; vinyl proton)**



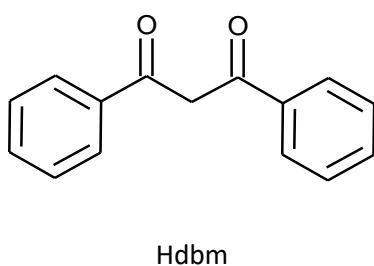
Cyclohexane-d₁₂ ¹H-NMR (400 MHz, cyclohexane-d₁₂) δ ppm 0.83 - 0.92 (m, 7 H) 1.28 (s, 46 H) 1.40 - 1.47 (m, 3 H) 1.54 - 1.64 (m, 5 H) 2.17 (t, *J*=7.56 Hz, 4 H) **3.46 (s, 2 H; methylene protons)** **5.31 (s, 1 H; vinyl proton)**

Toluene-d₈ ¹H-NMR (400 MHz, toluene-d₈) δ ppm 0.91 (t, *J*=6.64 Hz, 8 H) 1.15 - 1.36 (m, 54 H) 1.45 - 1.58 (m, 5 H) 2.04 (br. s., 2 H) 2.13 (br. s., 1 H) 2.22 (br. s., 1 H) **2.99 (s, 2 H; methylene protons)** **5.25 (s, 1 H; vinyl protons)**

CDCl₃ ¹H-NMR (400 MHz, CDCl₃) δ ppm 0.86 (t, *J*=6.87 Hz, 9 H) 1.15 - 1.35 (m, 64 H) 1.50 - 1.65 (m, 8 H) 2.25 (t, *J*=7.79 Hz, 4 H) 2.48 (s, 1 H) **3.53 (s, 2 H; methylene protons)** **5.46 (s, 1 H; vinyl proton)**

Acetone-d₆ Acetone did not dissolve the β-diketone

^bTHF-d₈ ¹H-NMR (400 MHz, THF-d₈) δ ppm 0.79 - 0.91 (m, 7 H) 1.19 - 1.35 (m, 45 H) 1.49 - 1.61 (m, 4 H) 2.17 - 2.27 (m, 4 H) 2.43 (br. s., 1 H) **3.49 (s, 2 H; methylene protons)** **5.52 (s, 1 H; vinyl proton)**



Cyclohexane-d₁₂ ¹H-NMR (400 MHz, cyclohexane-d₁₂) δ ppm **4.43 (s, 2 H; methylene protons)** **6.76 (s, 1H; vinyl proton)** 7.31 - 7.42 (m, 6H; gamma and delta proton to C=O) 7.91 - 7.95 (m, 4H; beta proton of phenyl to the C=O)

Toluene-d₈ ¹H-NMR (400 MHz, toluene-d₈) δ ppm **4.03 (s, 2 H; methylene protons)** **6.57 (s, 1 H; vinyl proton)** 6.92 - 7.03 (m, 6 H; gamma and delta proton to C=O) 7.77 - 7.84 (m, 4 H; beta proton of phenyl to the C=O)

CDCl₃ ¹H-NMR (400 MHz, CDCl₃) δ ppm **4.63 (s, 2 H; methylene protons)** **6.86 (s, 1H;**

vinyl proton 7.45 - 7.59 (m, 6 H) 7.95 - 8.03 (m, 4H)

Acetone-d₆ ¹H-NMR (400 MHz, acetone-d₆) δ ppm **4.80 (s, 2 H; methylene protons) 7.24 (s, 1 H; vinyl proton) 7.49 - 7.66 (m, 6 H) 8.02 (dd, J=8.47, 1.14 Hz, 2 H; beta protons of phenyl on keto end) 8.10 - 8.19 (m, 2H; beta protons of phenyl on keto end)**

THF-d₈ ¹H-NMR (400 MHz, THF-d₈) δ ppm **4.66 (s, 2 H; methylene protons) 7.11 (s, 1 H; vinyl proton) 7.43 - 7.57 (m, 6H; gamma and delta proton to C=O) 8.04 - 8.10 (m, 4H; beta proton of phenyl to the C=O)**

^b= THF methylene protons THF and the keto tautomer overlap

It has been reported that polar solvents such as chloroform, THF and acetone (i.e. at least in comparison to cyclohexane) form hydrogen bonds with the α -protons of the keto tautomer,²¹³ which affect the ¹H-NMR chemical shifts of β -diketones.¹³⁸ This is due to the simultaneous breaking of solute-solute intramolecular hydrogen bonds and the re-forming of solute-solvent intermolecular hydrogen bonds.¹³⁸ Therefore, the chemical shifts (δ) for the methylene protons in Hacac increased as follows: 2.74 ppm, 3.33 ppm, 3.53 ppm, 3.58 ppm, and 3.64 ppm for toluene- d₈, cyclohexane-d₁₂, THF-d₈, CDCl₃ and acetone-d₆ respectively. The chemical shifts for the vinyl proton of the Hacac increased as: 4.91 ppm, 5.31 ppm, 5.49 ppm, 5.53 ppm, and 5.61 ppm for toluene- d₈, cyclohexane-d₁₂, CDCl₃, THF-d₈, acetone-d₆. The following Figure 2-11 describes how the keto-enol values were evaluated from the ¹H-NMR spectra. In each case the integral value for the keto peak was divided by 2 hence the % of keto was determined relative to the integral value of the enol peak.

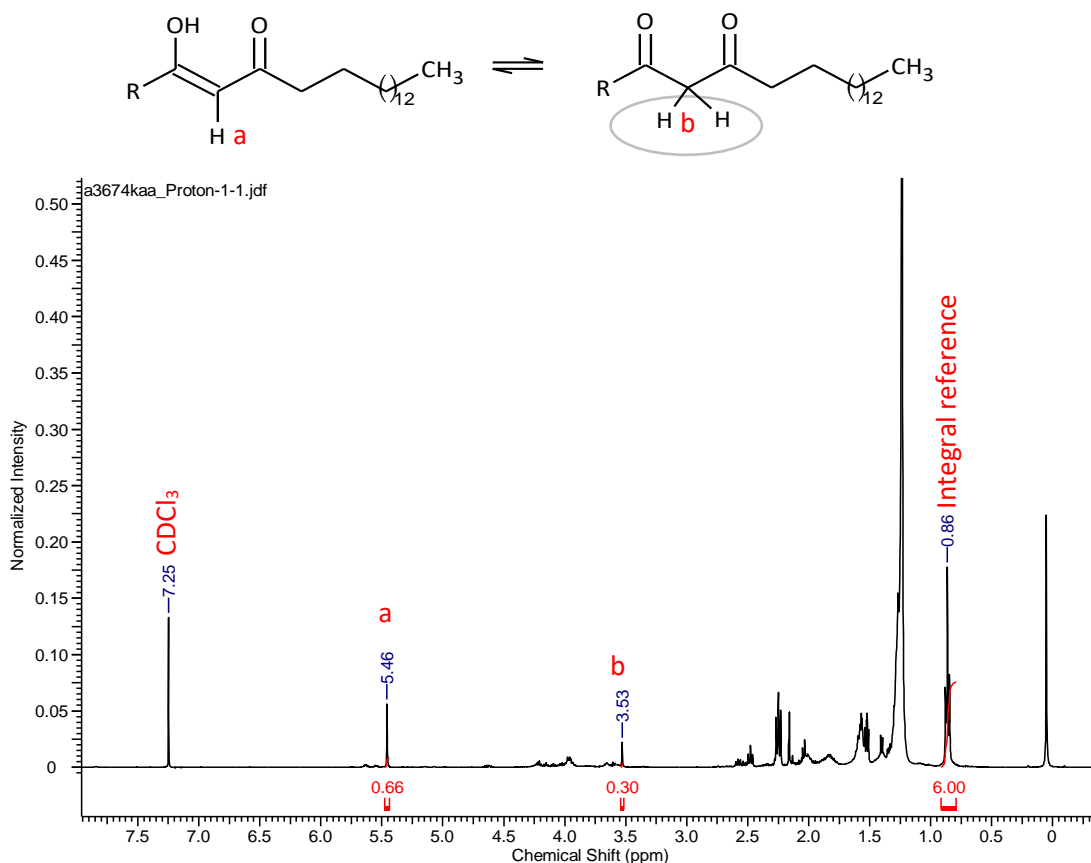


Figure 2-11: Keto-enol Integrated $^1\text{H-NMR}$ spectrum of Htd

For the Htd, the $^1\text{H-NMR}$ chemical shifts (δ) of its keto tautomer in the different solvents were 2.99 ppm, 3.46 ppm, 3.49 ppm, and 3.53 ppm for toluene- d_8 , cyclohexane- d_{12} , THF- d_8 and CDCl_3 respectively; while in the enol tautomer the shifts were 5.25 ppm, 5.31 ppm, 5.46 ppm, 5.52 ppm for toluene- d_8 , cyclohexane- d_{12} , CDCl_3 , THF- d_8 respectively. For the Hdbm, the H^{keto} chemical shifts were 4.03 ppm, 4.43 ppm, 4.63 ppm, 4.66 ppm, 4.80 ppm in toluene- d_8 , cyclohexane- d_{12} , CDCl_3 , THF- d_8 , acetone- d_6 respectively; while in the H^{enol} , the chemicals shifts were 6.57 ppm, 6.76 ppm, 6.86 ppm, 7.11 ppm, 7.24 ppm for toluene- d_8 , cyclohexane- d_{12} , CDCl_3 , THF- d_8 , and acetone- d_6 respectively. The combined effect of H-bonding acceptor, donor and polarizability of the solvents deshielded the keto-enol protons, hence the values shifted downfield with increasing polarisability of the solvents. The effect of varying the solvent did not only affect the chemical shifts of

methylene and vinyl protons of the keto-enol tautomer but all other chemical shifts of the compounds. Reeves also reported that there is no solute-solvent interaction of Hacac and cyclohexane.²¹³ Similarly Ferrari *et al.*²⁴⁰ reported the carbon and proton chemical shift for 3-Acetyl-4-oxopentanoic acid as a function of the polarity of D₂O, MeOD and DMSO- d₆.

Table 2-6 below gives the % keto-enol of Htd, Hacac and Hdbm in different solvents (cyclohexane, toluene, acetone, THF and CDCl₃). The keto-enol equilibrium constants and the free energy were determined using the following equations respectively.

$$K_e = \frac{\% \text{ enol}}{\% \text{ keto}}$$

Equation 2-6: Keto-enol equilibrium constant

$$\Delta G^\circ = -RT \ln K_{eq}$$

Equation 2-7: Gibbs free energy

Where R= gas constant (8.3145 J/mol·K or 1.9872035cal/mol) K_{eq} = equilibrium constant and T= absolute temperature (K)

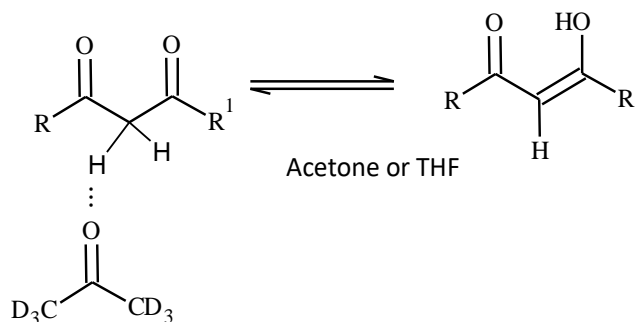
Plot for the effect of these solvents properties such as polarizability, dipole moment and hydrogen bond acceptor (β) versus % enol for each of these β -diketone was made. The % enol values in THF were not used for these plots because there was inaccuracy in their determination as explained in Table 2-6 footnote. Moreover, there was better correlation in the plot without using the % enol values in THF. Therefore, it was observed that, % enol content for Htd in these solvents is in the order: cyclohexane > toluene > CDCl₃ > acetone. The % enol of the long chain Htd is very similar to that of Hacac because both Htd and Hacac have chemically similar alkyl groups attached to the

two carbonyl groups. In contrast, there is a higher degree of enolisation in Hdbm than in Htd and Hacac due to the mesomeric effect of phenyl groups which enhances the stabilization of the enol tautomer. Similarly, phenyl groups in β -ketoamide were found to stabilize and enhance the enol tautomer than the keto form.²³⁹ The overall trend of the keto-enol studies of Htd, Hacac and Hdbm is also in agreement to keto-enol tautomerisation studies of Hacac, Hdbm and Hbac as reported by Abood and Ajam.¹³⁶

In addition, it was observed that in Figure 2-12, the % enol of Htd, Hacac and Hdbm decrease gradually as the polarizability (π^*) of the solvents increases from cyclohexane (π^* , 0.00), toluene (π^* , 0.54), CDCl_3 (π^* , 0.58) to acetone (π^* , 0.71) because solvents with higher π^* (polarisability) solvate and stabilise the keto tautomer more than enol. On the other hand, lower polarizability solvents (such as cyclohexane and toluene)²⁴¹ stabilise the enol tautomer more and hence form higher % enol in them. Hence there was higher % enol of these β -diketones in cyclohexane and toluene than in CDCl_3 , THF and acetone. Same trend was previously reported as given in Table 2-7, where the % enol of Hacac, Hdbm and Hbac were found to decrease as the polarisability of the solvents increase.¹³⁶ Furthermore, a plot of the % enol of Htd, Hdbm and Hacac against hydrogen bond acceptor (β) of these solvents is given in Figure 2-13. This plot also shows that % enol decreases with increase in hydrogen bond acceptor of cyclohexane, toluene, CDCl_3 and acetone in that order. This again implied that solvents with higher β can stabilize the keto tautomer above enol, hence % enol is decreased. Previous work has shown that higher hydrogen bond acceptor solvents (such as acetone at least compare to cyclohexane) decrease the enol content of β -diketone by bonding to the methylene proton as shown in Equation 2-8.²³⁹ The interaction of the lone pairs of oxygen electrons in the acetone

solvent may destabilise the usual six- membered ring, thus decreasing the % enol.²³⁹

There is no much difference in hydrogen bond donor, α of these solvents, cyclohexane (0.00), toluene (0.00), CDCl_3 (0.20) and acetone (0.08), hence the % keto-enol was essentially influenced more by the π^* and β properties of these solvents as explained above.



Equation 2-8: Influence of acetone on the keto- enol equilibrium

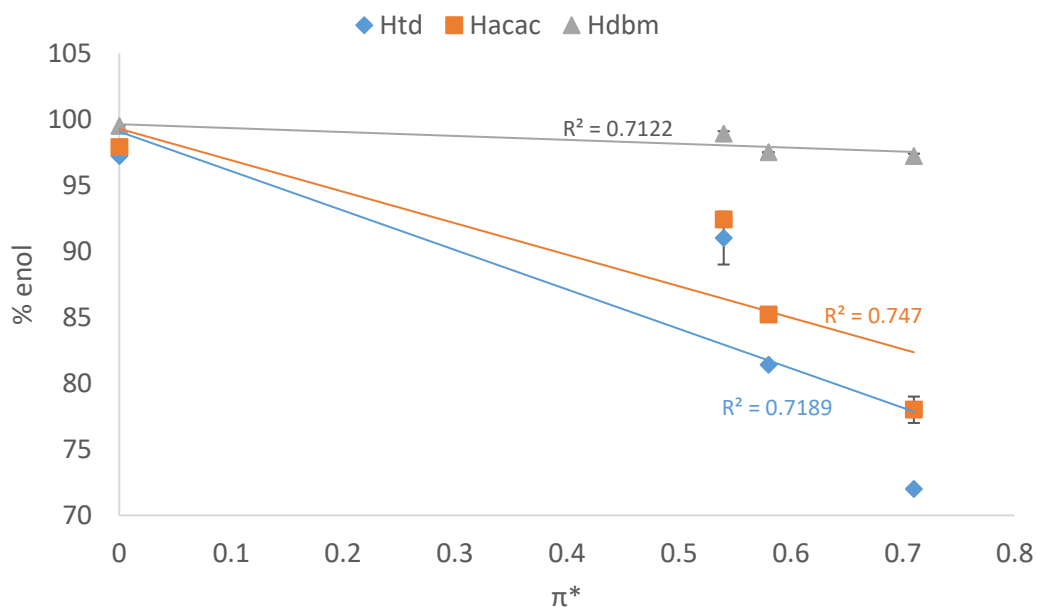


Figure 2-12: % enol of Htd, Hacac and Hdbm versus solvents polarizability

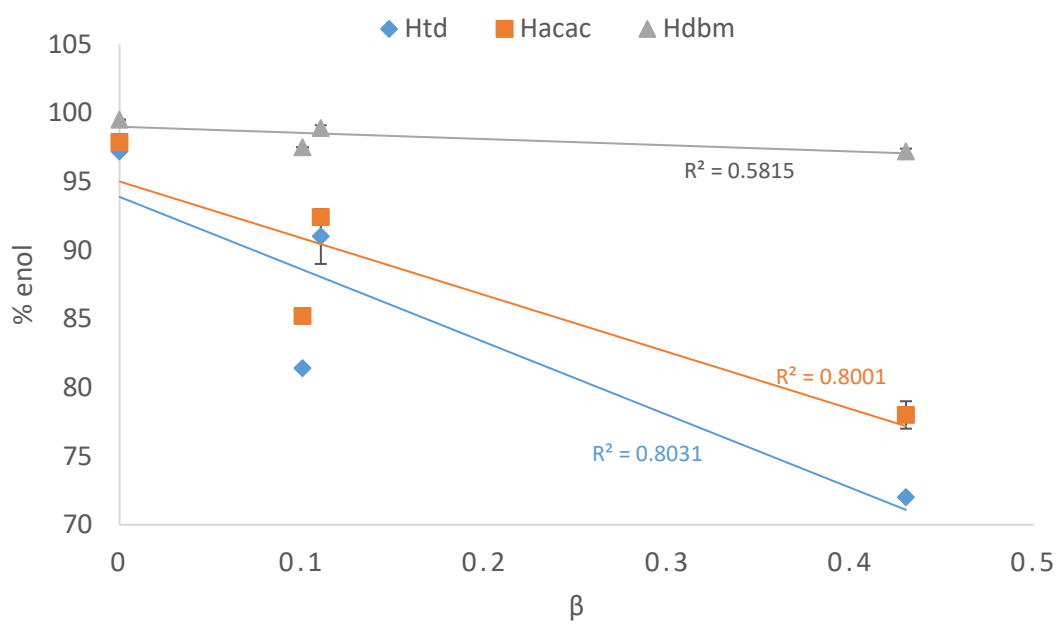
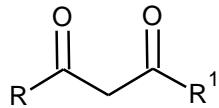
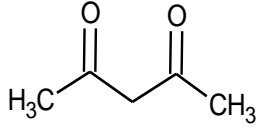
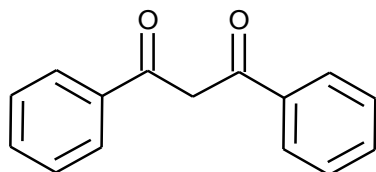


Figure 2-13: % enol of Htd, Hacac and Hdbm versus solvents hydrogen bond acceptor

Table 2-6: Keto-enol content, equilibrium constant (K_{eq}) and ΔG° of Htd in comparison to Hacac and Hdbm in five different solvents at 295 K

	Solvent	π_{233}^*	β	α	% enol	% keto	K	$\Delta G/$ kcal.mol ⁻¹
 Htd	Cyclohex.-d ₁₂	0.00	0.00	0.00	97.20 ±0.10	2.80 ±0.10	34.00 ±2.00	-2.00 ±0.03
	Toluene- d ₈	0.54	0.11	0.00	91.00 ±2.00	9.00 ±2.00	10.00 ±2.00	-1.30 ±0.10
	Acetone-d ₆	0.71	0.43	0.08	72.00 ^a	28.00 ^a	2.60	-0.60
	THF-d ₈	0.58	0.55	0.00	87.80 ^b	12.20 ^b	7.20	-1.20
	CDCl ₃	0.58	0.10	0.200	81.40 ±0.1	18.60 ±0.10	4.38 ±2.00	-0.90 ±0.10
 Hacac	Cyclohex.-d ₁₂	0.00	0.00	0.00	97.90 ±0.03	2.08 ±0.03	47.10 ±0.70	-2.25 ±0.01
	Toluene- d ₈	0.54	0.11	0.00	92.42 ±0.04	7.58 ±0.04	12.19 ±0.07	-1.50 ±0.10
	Acetone-d ₆	0.71	0.43	0.08	78.00 ±1.00	22.00 ±1.00	3.50 ±0.20	-1.00 ±0.04
	THF-d ₈	0.58	0.55	0.00	76.44 ^b	23.56 ^b	3.24	-0.69
	CDCl ₃	0.58	0.10	0.200	85.20 ±0.10	14.80 ±0.10	5.77 ±0.07	-1.03 ±0.04



Hdbm

Cyclohex.-d ₁₂	0.00	0.00	0.00	99.50 ±0.04	0.50 ±0.04	200.00 ±16.00	-3.10 ±0.05
Toluene- d ₈	0.54	0.11	0.00	98.90 ±0.20	1.10 ±0.20	90.00 ±14.00	-2.63 ±0.09
Acetone-d ₆	0.71	0.43	0.08	97.20 ±0.20	2.80 ±0.20	34.00 ±3.00	-3.00 ±0.05
THF-d ₈	0.58	0.55	0.00	98.70 ±0.20	1.30 ±0.20	76.00 ±12.00	-3.00 ±0.09
CDCl ₃	0.58	0.10	0.200	97.50 ±0.10	2.50 ±0.10	39.65 ±0.07	-2.15 ±0.04

NB: Htd= 14, 16- hentriacontanedione and Hdbm= dibenzoylmethane; Hacac= acetyl acetone; π^* = Kamlet-Taft polarisability, ^b = in these values THF solvent overlaps with Htd and Hacac; and ^a = in these values acetone sparingly dissolves the Htd

Furthermore, it has been observed that the keto tautomer of β -diketones predominate in solvents with a higher dipole moment,^{237,243,244} while the enol tautomer is favoured in solvents with lower dipole moment.^{243,245} Therefore, a plot of % enol versus the dipole moment of these solvent was made as is presented in Figure 2-14. And it was observed also that the % keto was increased with increasing dipole moment from cyclohexane (μ , 0.00), toluene (μ , 0.31), CDCl_3 (μ , 1.15) to acetone (μ , 2.88), while the % enol was decreased from cyclohexane to acetone. The present results were generally similar to a reported solvents effect on keto-enol tautomerisation of Hacac, benzoylacetone (Hbac) and Hdbm,¹³⁶ as presented in Table 2-7 and also in terms of the structure of the β -diketones. The Gibbs free energy obtained for the keto-enol equilibria as given in Table 2-6 were all negative implying that the equilibrium for the formation of enol is spontaneous. In addition, the equilibrium constant for the keto-enol equilibria in all these solvents were greater than 1, which implies that enol formation is more favoured in these solvents as previously reported.^{136,138}

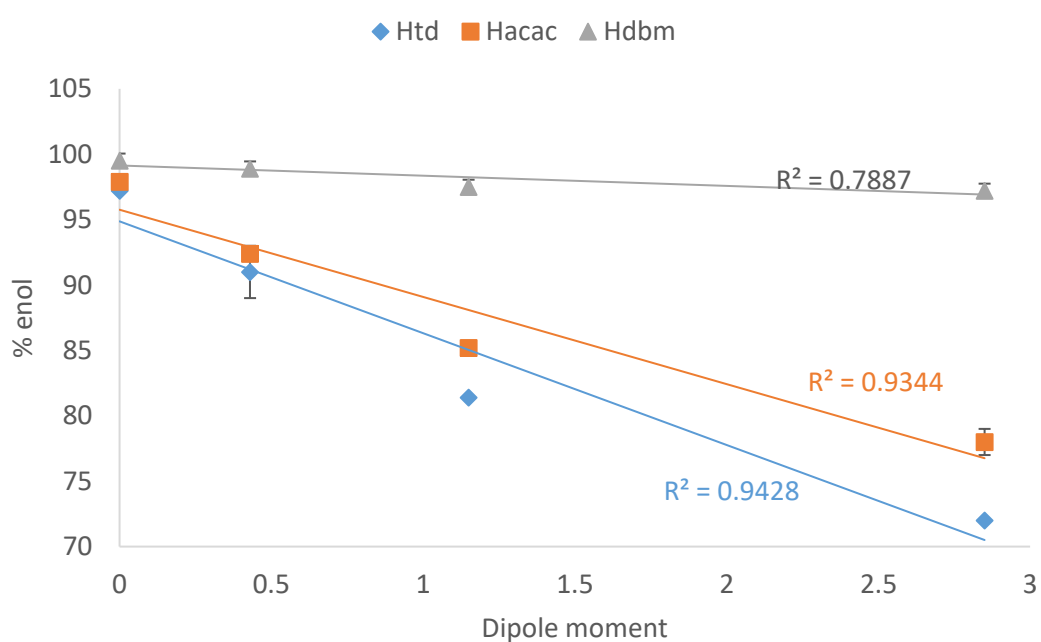


Figure 2-14: % enol of Htd, Hacac and Hdbm versus solvents dipole moment

Table 2-7: % enol and equilibrium constant in different solvents determined with FTIR¹³⁶

1,3-diketone	% enol	K _e	π*	Dipole moment ²⁴³	solvent
Hacac	91.20	10.36	-0.04	0.08	n-hexane
	82.80	4.78	0.28	0.00	CCl ₄
	74.00	2.84	0.58	1.05	CDCl ₃
	77.90	3.51	0.59	0.00	Benzene
	70.70	2.40	0.54	1.69	ethanol
	57.00	1.32	0.55	0.45	1,4-dioxane
	98.20	54.40	-0.04	0.08	n-hexane
Hbac	93.00	13.30	0.28	0.00	CCl ₄
	70.00	2.33	0.58	1.05	CDCl ₃
	92.50	13.10	0.27	1.15	diethyl ether
	81.50	4.40	0.55	0.45	1,4-dioxane
	72.00	2.47	0.60	1.70	methanol
	67.00	2.03	0.54	1.69	ethanol
	100.00	ND	0.28	0.00	CCl ₄
Hdbm	Incompletely soluble		-0.04	0.08	n-hexane
	100.00	ND	0.58	1.15	CDCl ₃
	100.00	ND	0.55	0.45	1,4-dioxane
	98.20	54.40	0.27	1.15	Diethyl ether
	Incompletely soluble			1.70	methanol

Furthermore, it has also been reported that the keto tautomer of β-diketones are more favoured in hydroxylic solvents like methanol, because these solvents are H-bond donors which leads to competition with the intramolecular H-bonds formed in the enol tautomer resulting into decrease in the enol content.¹³⁶ That is, polar protic solvents provide extra stabilisation to the keto tautomers, when compared with polar aprotic

solvents of the same polarity, because of hydrogen bonding.²³⁵ Similarly Clark *et al.* reported that acetic acid and propionic acid have a tendency to interfere with the enol hydrogen-bonding system, thus making this tautomer less energetically favourable than otherwise expected.²⁴¹ But the biobased β -diketone, Htd in particular was quite insoluble in methanol which prevented studies in MeOD. Keto-enol studies are obviously always far more meaningful in solvents that dissolve the solutes fully.²⁴²

2.3 Conclusion

The lipophilic β -diketone (Htd) was isolated by crashing out from a petroleum ether solution of wheat straw wax with $\text{Cu}(\text{OAc})_2$. A recovery yield of $18 \pm 5\%$ was thus obtained. The Htd was characterised using different techniques; GC-FID, GC-MS, TGA, FTIR and NMR spectroscopy, DSC and ESI-MS. Keto-enol tautomeric studies of Htd were investigated with different deuterated solvents; CDCl_3 , acetone- d_6 , cyclohexane- d_{12} , THF- d_8 and toluene- d_8 and directly compared to acetyl acetone and dibenzoylmethane. The % keto-enol of Htd was influenced by the π^* , β and dipole moment of these solvents. Hydrocarbons and ethers were efficient solvents for dissolving the long chain lipophilic Htd, while DMSO and water were found to be least effective for dissolving it. Most studies investigating the extraction of plants waxes and consequently purification of the hydrophobic β -diketones involve the use of toxic solvents including hexane, petroleum ether, chlorinated solvents and so on, which constitute damage to human health and to the environment. Therefore, in the next chapter, four greener alternative solvents will be tested for the isolation of the Htd from wheat straw wax and compared to the petroleum ether and hexane.

Chapter 3

Purification of the lipophilic β -diketone with greener solvents

3 Chapter 3

3.1 Introduction

In chapter two, the purification of lipophilic bioderived β -diketone from wheat straw wax using cuprous acetate and petroleum ether (333 – 353 K) was effectively demonstrated. Similar methodologies for isolating long chain β -diketones from plant waxes have previously been carried out in the literature, whereby petroleum ether (typically a C5 and C6 alkane mixture) or hexane were the solvents of choice.²¹⁴ However, these solvents are non-renewable and have a number of toxicological and safety issues associated with them. Hexane is an extremely flammable, forms explosive mixtures with air and was found to be a neurotoxin, having detrimental effects on the nervous system.²⁴⁶ Furthermore, hexane has been listed as a hazardous air pollutant by the Environment Protection Agency (EPA) in the Clean Air Act (1990).²¹⁸

Therefore, substituting these hazardous, non-renewable solvents with greener solvents is vital in order to move towards a cleaner, more sustainable process. In the work shown in this chapter, a range of green solvents were explored as possible replacements to hexane and petroleum ether for the purification of the β -diketone from the wheat straw wax. One potential alternative solvent is supercritical carbon dioxide (scCO₂).¹⁸² Extraction/fractionation using scCO₂ is a green technique, in which the CO₂ is abundantly obtained as a co-product from fermentation, production of bioethanol, production of ammonia and the generation of hydrogen.^{166,247} The scCO₂ is nontoxic unlike most traditional volatile organic solvents used in extraction/fractionation of plant waxes. In addition, it is possible to carry out fractionation of crude products with scCO₂ using fractional separators found in series.²⁴⁸ This leads to wax products of higher value and makes isolation of certain compounds, such as β -diketones, more straightforward.

However, the deployment of scCO_2 technique for extraction/fractionation entails high operational costs; it is energy intensive and involves high pressures.

Cyclohexane, *p*-cymene, 2,2,5,5-tetramethylTHF (TMTHF) and cyclopentyl methyl ether (CPME) have greener credentials of environmental health safety (EH) compared to most traditional solvents.^{217,244} Hence, they were also considered as alternatives for the purification of the Htd from wheat straw wax. In addition to green credentials, the ability of these alternative solvents to dissolve the wheat straw wax is a critical property, without which the purification would not be possible. Jessop reported that there is currently a growing interest in using greener solvents so as to reduce solvent-related environmental damage.²⁴⁹ One key parameter here is finding a low/moderate boiling point green solvent in order to avoid energy-intensive processes such as distillation and hence reduce energy costs.²⁴⁹ Up to now no literature can be found looking into using green solvents in the purification of long chain saturated β -diketone. Therefore, this chapter investigate the purification of the Htd using better EH solvents; scCO_2 , *p*-cymene, CPME, TMTHF and cyclohexane.

3.2 Results and discussion on alternative solvents used in the purification of Htd

The isolation of the Htd from wheat straw wax was achieved with CPME, TMTHF, *p*-cymene and cyclohexane. All these solvents were found to adequately dissolve the wheat straw wax as previously described in chapter two. Hence the precipitation of the Htd was carried out with cuprous acetate. The recovered yields are presented in Table 3-1 below. Typically, all these solvents were found to be effective in crashing out the Htd with cuprous acetate. However, from an energy perspective, some of these solvents would be difficult to implement in an industrial process. The removal of *p*-cymene

(boiling point of 450 K) from the product for example was carried out at substantially reduced pressure and 373 K. This is very energy intensive and would not be viable from an economical point of view, and also resulted in residual *p*-cymene being left in the final isolated product. One possible way to reduce traces of the *p*-cymene in the product is to dissolve the copper-diketone complex in a more volatile green solvent prior to the decomposition of the complex with HCl to obtain the free Htd. CPME and TMTHF were readily removed at 333 K with reduced pressures of about 50 – 60 mbar.

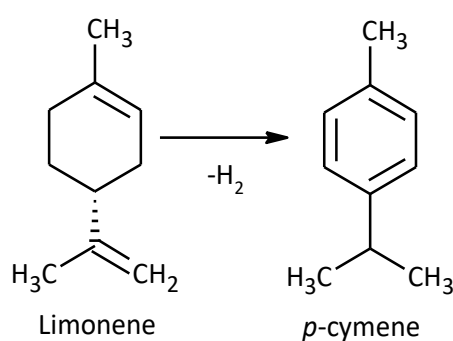
Table 3-1: Comparison of the isolated β -diketone's yield and benefits of the alternative solvents to petroleum ether

Solvent	Yield (%)	Boiling point (K)	Advantage	Disadvantage
Petroleum ether	18.0	333-353	Low boiling point and immiscible with water	Toxic and Flammable
<i>P</i> -Cymene	8.2	450	Immiscible with water and it is bioderived	High boiling point
Cyclohexane	6.0	354	Low boiling point and immiscible with water	Flammable
CPME	7.8	379	Moderate boiling point	slightly miscible with water (1.1 g/100 g) and flammable
TMTHF	21.4	385	Moderate boiling point; it is bioderived	slightly miscible with water (1.6g/L)

Therefore, CPME, TMTHF and cyclohexane could be used as viable alternatives for petroleum ether (333-353 K) for the purification of the Htd. The properties of these alternatives solvents used for the isolation of Htd are given in Table 3-2. Each solvent is

given a score from 1 (red, bad) to 10 (green, good) to express their properties as compared to the traditionally used petroleum ether and hexane in the isolation of Htd. This guide has been previously reported by Henderson *et al.*²¹⁷ and Alder *et al.*²⁵⁰

Some other advantages of these alternative solvents used for isolation of Htd like TMTHF and *p*-cymene is that they are bioderived. TMTHF can be produced by the mycelium of tuber borchii.²⁵¹ In addition, Green Chemistry Centre of Excellence (University of York) has developed a method for synthesis of bio-based TMTHF with an intention of replacing toluene with it. On the other hand, *p*-cymene can be easily derived quantitatively from limonene through sequential isomerisation and dehydrogenation as presented in Equation 3-1.²⁵² Limonene in turn is available in large quantities from citrus waste.²³⁴ Although the feedstock is limited by the geographical location and seasonality of the crop, fortunately extracting limonene from citrus rind does not compete with food production. Limonene itself is a suitable bio-solvent that is able to replace non-polar petroleum-based solvents.²⁵²



Equation 3-1: Synthesis of *p*-cymene from limonene²³⁴

Table 3-2: Properties of the alternative solvents used in the purification of Htd from wheat straw wax in comparison to petroleum ether and hexane.²¹⁷

Solvent	Bp (K)	Waste recycling, incineration, VOC and bio treatment issues	Environmental impact fate and effects on the environment	Health Acute and chronic effects on human health and exposure potential	Flammability & Explosion Storage and handling	Reactivity/stability Factors affecting the stability of the solvent	Life cycle score Environmental impacts to produce the solvent	Legislation Alerts on regulatory restrictions
Cyclohexane	354	5	5	7	2	10	7	
Petroleum spirit	333- 353	6	2	2	3	10	7	Substitution recommended – existing regulatory restrictions apply
Hexane	342	5	3	4	2	10	7	Substitution recommended - Future

							restriction may apply
CPME	379	6	4	4	5	8	4
2-MTHF	353	4	5	4	3	6	4
p-cymene	450	9	3	5	6	9	
TMTHF	385	<i>Not found</i>					

Whereas cyclohexane is petrol derived (i.e. occurs naturally in crude oil and is obtained industrially by hydrogenation of benzene). On the other hand CPME has benefit of moderate boiling point (379 K) with better properties such as low formation of peroxides,²⁵³ low solubility in water, relatively stable under acidic and basic conditions.²⁵³ Hence it is found as an excellent replacement for THF, 2-MeTHF, dioxane (carcinogenic) and 1,2-dimethoxyethane.²⁵³ Therefore, cyclohexane, TMTHF and CPME are good alternative to hexane and petroleum ether than *p*-cymene for the isolation of Htd based on the advantages highlighted above.

However, from Table 3-2 above it may be seen that, in as much as petroleum ether and hexane are recommended for substitution because of their toxic nature, there is less environmental impact (such as less consumption of energy) in producing hexane and petroleum ether than CPME. In the case of cyclohexane, it has life cycle credential as hexane and petroleum ether. Moreover, the life cycle assessment of MTHF, *p*-cymene have not yet been fully characterised, therefore they cannot be clearly compared to petroleum ether and hexane at this time. Thus effort should be made in reducing environmental impact in the case of producing solvents and also to produce new biobased solvents with good life cycle.

3.2.1 The scCO₂ extraction/fractionation of the wheat straw wax for the Htd

The density of scCO₂ has a crucial effect on the amount of lipids extracted from biomass. The highest scCO₂ density is achieved at low temperature and high pressure²⁵⁴; with the latter in particular taking pre-eminence in scCO₂ fractionation/extraction. Fractionation with scCO₂ makes use of fractional separators arranged in series.²⁴⁸ Each fractional separator is set at a different pressure and temperature which therefore causes a change in the density of CO₂. Lipid molecules that are only soluble at a particular density range

will crash out when entering a fractional separator having a different CO₂ density, while those molecules that are soluble will flow into the subsequent separator.

Matricardi *et al.*²⁵⁵ showed that for an effective fractionation, waxes are often adsorbed onto a solid support, such as celite. This is done in order to decrease the particle sizes and give larger amounts of surface area to facilitate diffusion as well as an increased number of ruptured cells resulting into higher fractional yields. Therefore, several experiments were conducted to find suitable conditions for crashing out the Htd from our wheat straw wax. The parameters varied include pressure, the type of adsorbent and wax: adsorbent ratio.

The presence of solutes in the supercritical phase act as a co-solvent which significantly enhances the solubilising ability of scCO₂, a phenomenon referred to as the entrainer effect as previously described by Dobbs and Johnston.²⁵⁶ For this reason, simultaneous fractionations carried out starting from high to low pressures were compared to stepwise (sequential) fractionation, which were performed starting from low to high pressures in order to check the entrainer effect. The results of the fractional extracts were compared to the GC-FID chromatograms of the crude wheat straw wax (in Figure 3-1). The components of the wheat straw wax were identified as ketones, fatty acids, alkanes, alcohol, aldehydes, β -diketones, sterols and wax esters by Sin as illustrated in Figure 3-1 below.¹⁶⁶

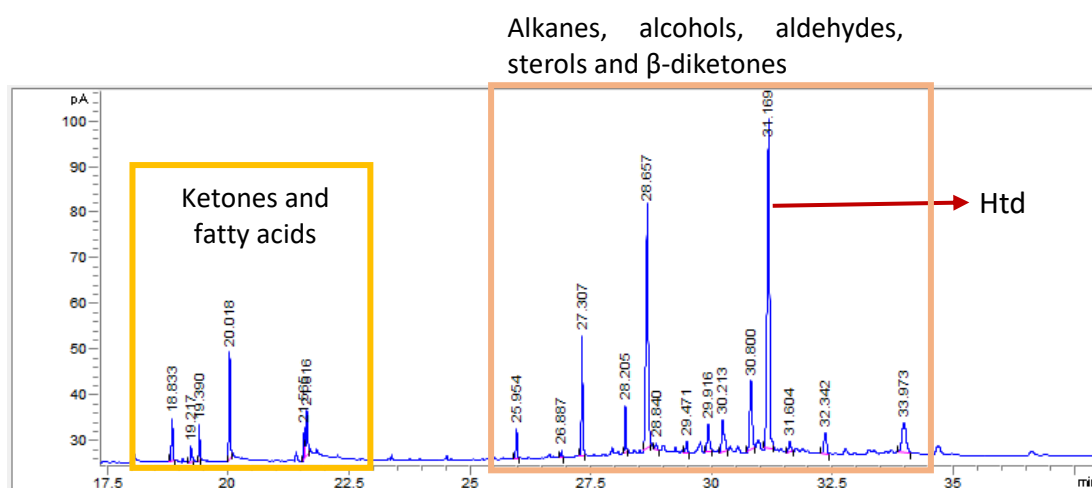


Figure 3-1: GC-FID chromatogram of the wheat straw wax before fractionation

3.2.2 Simultaneous scCO_2 extraction/fractionation of the wheat straw wax for Htd using celite adsorbent

Fractionation of the wax for Htd using liquid scCO_2 was first carried out using a 155 g wax: 165 g celite ratio. The automated back pressure regulator was fixed at 350 bar and the sequential fractional separators were set at 250 bar, 150 bar, 75 bar and 1 bar. The experiment was run for 6 h with a scCO_2 flow rate of 40 g/min. The quantities of material recovered are summarised in Table 3-3.

Table 3-3: Masses of the fractional extracts for the simultaneous scCO_2 extraction/fractionation using 155 g wax: 165 g celite

Pressure (bar)	250	150	75	1
Tempt. (K)	323	323	308	308
Mass g (%)	22.60 (14.58)	20.59 (13.28)	9.10 (5.87)	3.00 (1.94)

There was no observed selectivity among the four fractions collected using GC analysis. This could be because of the entrainer effect explained previously. When using this ratio of 155 g wax: 165 g celite, the fractional masses of the materials collected were directly proportional to the pressure of the fractional separator. 22.60 g (14.58%), 20.59 g (13.28%), 9.10 g (5.87%) and 3.00 g (1.94%) of the fractional materials were obtained at

250 bar, 150 bar, 75 bar and 1 bar respectively. This result is comparable to other works carried out on scCO₂ extraction of lipids in terms of the masses obtained with respect to the pressure applied. Cheung²⁵⁷ found that the extraction rates of lipids from red seaweed increased as the pressure was also increased. Figure 3-2 below shows the fractional samples collected.

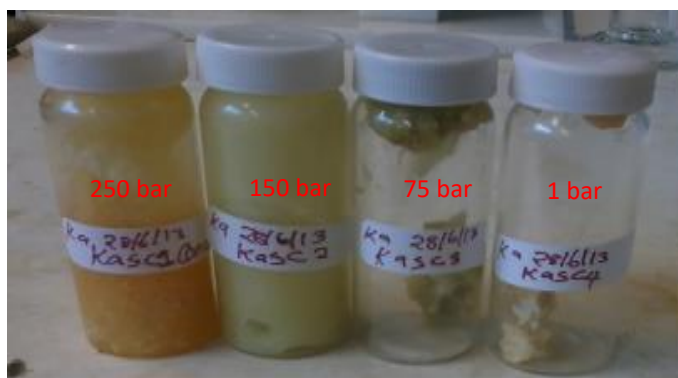


Figure 3-2: Fractions from the simultaneous scCO₂ extraction/fractionation using 155 g wax: 165 g celite adsorbent

Sin reported that the appropriate temperature and pressure to fractionate the hydrophobic β -diketone from wheat straw waxes is 305 K and 1 bar,¹⁶⁶ but no such observation was found yet in the above fractionation conditions. Therefore, in the subsequent fractionation experiment, the wax loading on the adsorbent (celite) was reduced, using a 200 g celite: 10 g wax ratio and a 200 g celite: 1 g wax ratio in order to enhance selective extraction of Htd. The various conditions used for these fractionations and the materials collected are as given in Table 3-4 below.

Table 3-4: The various quantities of fractions from simultaneous scCO₂ extraction/fractionation of the wax (A = 1 g wax: 200 g celite & B= 10 g wax: 200 g celite) for 4 h

Pressure (bar) gradient	Tempt. (K)	Fractional masses mg (%) in A	Amount of Htd mg (%) in A	Fractional masses g (%) in B	Amount of Htd mg (%) in B
300	323	63.30 (6.33)	5.71 (0.57)	3.91 (39.06)	575.85 (5.76)
150	323	6.90 (0.69)	0.29 (0.03)	1.61 (16.10)	206.33 (2.06)
80	305	60.10 (6.01)	1.66 (0.17)	1.13 (11.26)	96.40 (0.96)
1	305	574.30 (57.43)	98.97 (9.90)	3.05 (30.54)	615.29 (6.15)
Total % Htd			10.66 wt%	14.94 wt%	

The Htd was spread across four separators as highlighted in the red boxes in Figure 3-3 and Figure 3-4 respectively. One conspicuous difference among the fractions was that there were more materials extracted at 300 bar and 1 bar than at 150 bar and 80 bar as displayed in Table 3-4 above. More components were identified in the fraction collected at 1 bar, 305 K. The fractionation results from 1 g wax: 200 g celite and 10 g: 200 g celite are consistent with previous reports by Sin, whereby higher concentrations of β -diketone were collected in the fraction at 1 bar and 305 K.¹⁶⁶ Interestingly, the GC chromatograms revealed that alkanes selectively crashed out at 80 bar, 305 K from 10 g wax: 200 g celite adsorbent and 1 g wax: 200 g celite adsorbent. The same selectivity was observed when using a 155 g wax: 156 g celite. Therefore, it can be concluded that the solvation properties of scCO₂ were enhanced by the entrainer effect which affected the selectivity for Htd. For this reason, a sequential fractionation was performed whereby the extraction was carried out at the lowest pressure (75 bar) first.

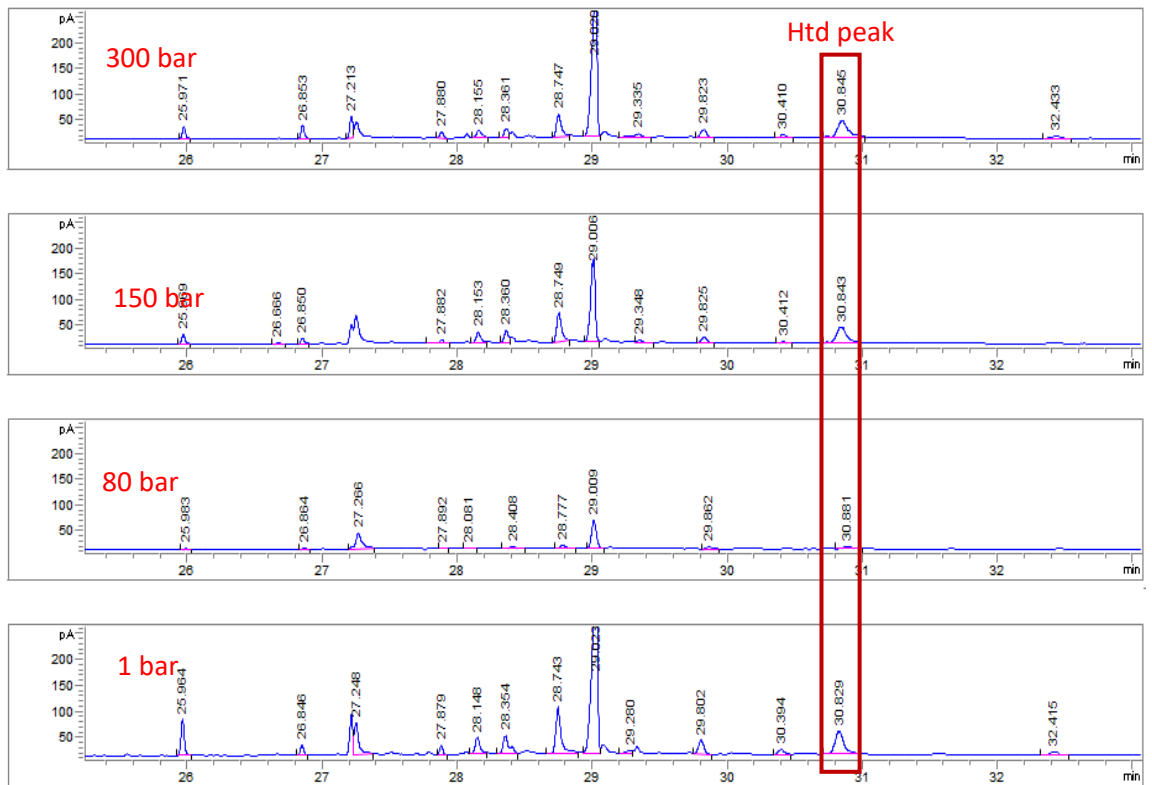


Figure 3-3: GC-FID chromatograms of the simultaneous $s\text{CO}_2$ extraction/fractionation of wheat straw wax for Htd from 10 g wax: 200 g clay

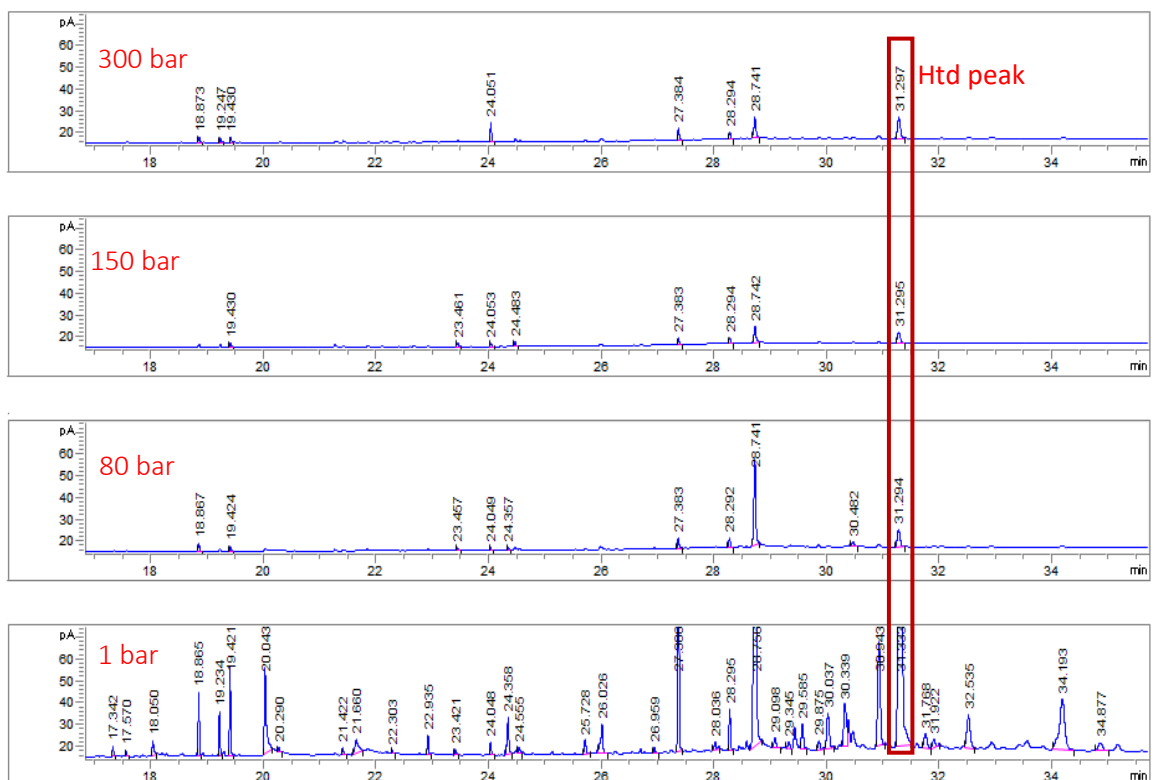


Figure 3-4: GC-FID chromatograms of the simultaneous $s\text{CO}_2$ extraction/fractionation of wheat straw wax for Htd from 1 g wax: 200 g celite adsorbent

3.2.3 Sequential scCO₂ extraction of the wheat straw wax for Htd using celite adsorbent

Sequential extraction using 1 g wax: 200 g celite was performed with flow rate 40 g/min at 313 K. As stated above, the first part of the extraction was carried out at the lowest pressure (75 bar). After 40 min, the extraction was stopped and the extract was collected. The pressure was then increased to 100 bar and the process was repeated. This was carried out using five different pressures of; 75 bar, 100 bar, 200 bar, 300 bar and 400 bar. The fractional amount of materials was; 78.30 mg (7.83%), 338.90 mg (33.89%), 115.20 mg (11.52%), 22.90 mg (2.29%), 11.70 mg (1.17%) at 75 bar, 100 bar, 200 bar, 300 bar and 400 bar respectively (see Table 3-5). Therefore, the highest amount of fractional extract, 338.90 mg (33.89%) consisting of 171.36 mg (17.14%) Htd was collected at 100 bar. And the fraction at 400 bar shows smallest amount of the Htd, 0.80 mg (0.08%). The GC chromatograms of the fractional extracts are given in Figure 3-6. Figure 3-5 presents the fractional samples collected with dichloromethane after the fractionation. The different colour of the fractions indicates their varying compositions.

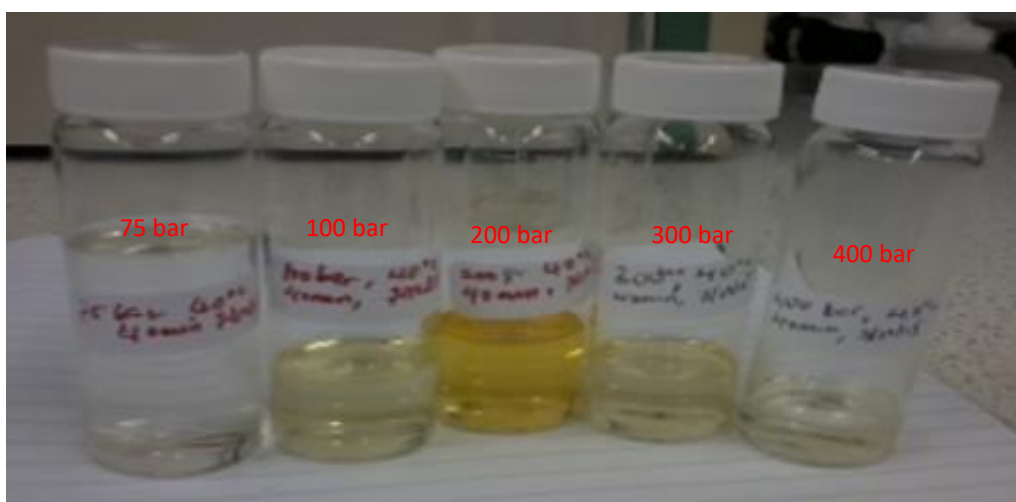


Figure 3-5: Fractional extracts from sequential scCO₂ extraction of the wax from 1 g wax: 200 g celite adsorbent at 313 K and 40 min

Table 3-5: Materials collected from sequential scCO₂ extraction with 1 g wax: 200 g celite adsorbent at 313 K and 40 min

Pressure (bar)	Fractional masses mg (%)	Amount of Htd in mg (%)
75	78.30 (7.83)	14.37 (1.44)
100	338.90 (33.89)	171.36 (17.14)
200	115.20 (11.52)	21.75 (2.18)
300	22.90 (2.29)	2.54 (0.25)
400	11.70 (1.17)	0.80 (0.08)
Total Htd		21.10 wt%

The observed total mass of the lipid fractions is smaller when compared to the total mass of extracts obtained during the simultaneous extraction/fractionation. Since the time allotted for each pressure was only 40 min, a total of 3 h 20 min was taken to collect all the five fractions. Increasing the amount of time for extraction at each pressure would likely further enhance the total mass recovery. It can be seen from Figure 3-6 that at a low pressure of 75 bar, more fatty acids and alkanes were detected than at higher pressures (100–400 bar), which is consistent with previous observations by Deswarte *et al.*¹⁶² Hunt *et al.*²⁵⁴ and Cheung.²⁵⁷ Whereas more waxy esters, and fatty alcohols were found at higher pressures (100–400 bar) than at 75 bar.

Hunt *et al.* observed that in the liquid scCO₂ extraction of lipids from C₄ biomass and fractionation of sugarcane bagasse, there were larger concentrations of wax esters at higher pressures (250 bar and 150 bar) than at lower pressures (150 bar and 1 bar); while at lower pressures higher concentrations of fatty acids were found.²⁵⁴ Furthermore, Deswarte *et al.* fractionated wheat straw using liquid scCO₂ and observed that at relatively low pressures, the extract contains a high amount of alkanes whereas at higher pressures the extracts contain higher quantities of fatty alcohols.¹⁶² Once again, no

selective isolation of the β -diketone was observed. Therefore, the influence of other adsorbents (silica and alumina) on the fractionation of the wax for Htd was investigated.

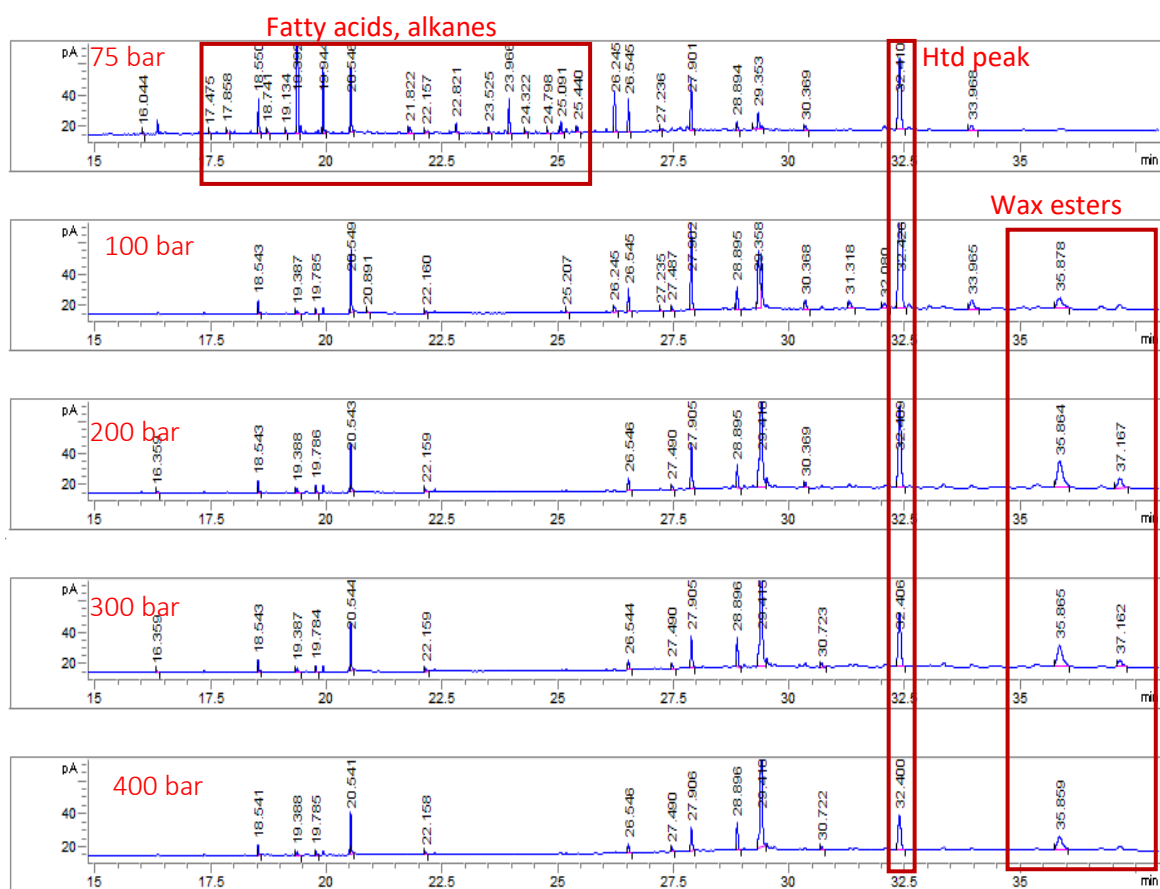


Figure 3-6: GC-FIDs chromatogram of the fractions from the sequential scCO_2 extraction using 1 g wax: 200 g celite adsorbent at 313 K and 40 min

3.2.4 Sequential scCO_2 extraction of the wheat straw wax for Htd using silica adsorbent

Various pressures between 75–400 bar were also applied for the sequential scCO_2 extraction of the wheat straw wax using 1 g wax: 200 g silica adsorbent at 313 K for 40 minutes. The GC chromatograms for the fractional extracts are given in Figure 3-7 and the differences in the composition are also highlighted. There were higher compositions of alkanes, fatty acids, aldehydes and ketones at pressures of 200 – 75 bar. For the silica adsorbent, smallest amount of the Htd, 0.94 mg (0.09%) was found at 75 bar, while highest quantity of the Htd, 81.42 mg (8.14%) was obtained at 200 bar. Therefore, doing the sequential fractionation of the wheat straw wax for longer time of 3 h at 75 bar, 313

K could leave behind a fraction with concentrated Htd. In addition, the sequential fractionation from 1 g wax: 200 g silica at 300 bar, 313 K for 40 min has a reasonable selectivity for the Htd as shown in Figure 3-7 below, while the fractional masses are found



Figure 3-7: GC-FIDs chromatogram of the fractions from the sequential scCO₂ extraction using 1 g wax: 200 g silica adsorbent at 313 K and 40 min

Table 3-6: Masses collected from sequential extraction of wax using 1 g wax: 200 g silica adsorbent at 40 min at 313 K

Pressures (bar)	Fractional masses mg (%)	Amount of Htd in mg (%)
75	2.60 (0.26)	0.94 (0.09)
100	137.90 (13.79)	20.53 (2.05)
200	148.20 (14.82)	81.42 (8.14)
300	97.00 (9.70)	36.57 (3.66)
400	63.60 (6.36)	20.94 (2.09)
Total Htd		16.04 wt%

3.2.5 Sequential scCO₂ extraction of the wheat straw wax for Htd using alumina adsorbent

Alumina adsorbent was also tested for the sequential scCO₂ fractionation of the wax. 400 g of the alumina was used with 1 g of the wax instead of 200 g in order to sufficiently load the extractor. Previously, 200 g of celite and silica: 1 g wax were found to be sufficient for the scCO₂ extractor. The results of the fractions collected from this sequential scCO₂ fractionation of the 400 g alumina: 1 g wax are shown in Figure 3-8 and Table 3-7 as follows.

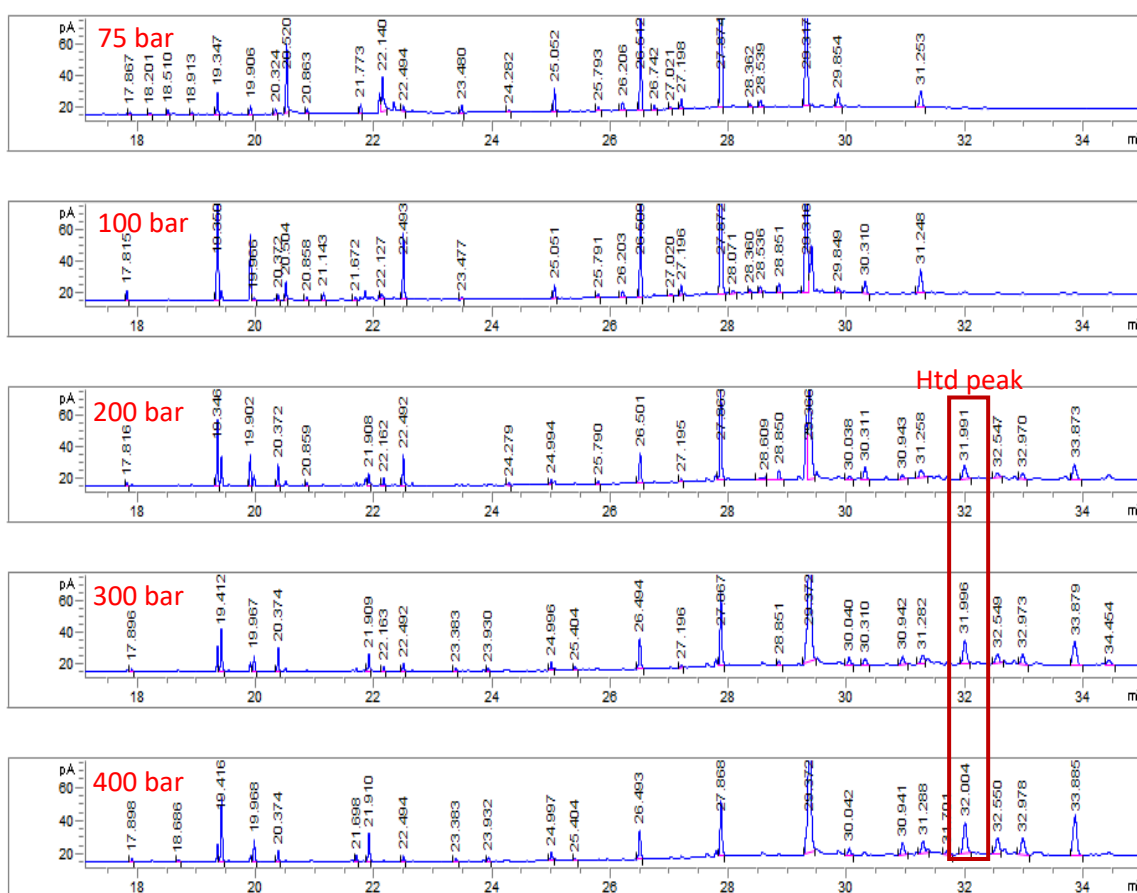


Figure 3-8: GC-FIDs chromatogram of the fractions from the sequential scCO₂ extraction using 1 g wax: 400 g alumina adsorbent at 313 K and 40 min

The sequential extraction of this wax with alumina adsorbent shows that the Htd was not detected in fractions at 75 and 100 bar, while fractions 200-400 bar contain the Htd with other components. Therefore, 0.17 mg (0.02%), 0.32 mg (0.03%) and 0.16 mg (0.02%) of Htd were detected in the fractions at 200, 300 and 400 bar respectively. In

which case, the fractionation using the alumina adsorbent was not selective as may be seen in Figure 3-8 unlike as it was previously observed for silica. For better understanding, the amount of the Htd in most of the liquid scCO₂ fractions collected are summarise in Table 3-8 as follows;

Table 3-7: Masses collected from sequential extraction of wax using alumina adsorbent at 40 min

Pressures (bar)	Fractional masses in mg (%)	Amount of Htd in mg (%)
75	1.00 (0.10)	ND
100	16.50 (1.65)	ND
200	12.60 (1.26)	0.17 (0.02)
300	6.50 (0.65)	0.32 (0.03)
400	3.10 (0.31)	0.16 (0.02)
Total Htd		0.1 wt%

Table 3-8: Amount of lipophilic β -diketone (Htd) determined from the scCO₂ fractions obtained from wheat straw wax

Simultaneous extraction/fractionation of the wheat straw wax for Htd				Sequential extraction of the wheat straw wax for Htd				
Pressure (bar)	Tempt. (K)	Amount Htd mg (%) from 1 g wax: 200 g celite	Amount Htd mg (%) from 10 g wax: 200 g celite	Pressure (bar)	Tempt. (K)	Amount Htd mg (%) from 1g wax: 200 g celite	Amount Htd mg (%) from 1 g wax: 200 g silica	Amount Htd mg (%) from 1g wax: 400 g alumina
300	323	5.71 (0.57)	575.85 (5.76)	75	313	14.37 (1.44)	0.94 (0.09)	ND
150	323	0.29 (0.03)	206.33 (2.06)	100	313	171.36 (17.14)	20.53 (2.05)	ND
80	305	1.66 (0.17)	96.40 (0.96)	200	313	21.75 (2.18)	81.42 (8.14)	0.17 (0.02)
1	305	98.97 (9.90)	615.29 (6.15)	300	313	2.54 (0.25)	36.57 (3.66)	0.32 (0.03)
				400	313	0.80 (0.08)	20.94 (2.09)	0.16 (0.02)
Total % Htd		10.66wt%	14.94wt%			21.10wt%	16.04wt%	0.10wt%

In the simultaneous extraction/fractionation, 1 bar and 300 bar were observed as the fractional conditions that produced higher amount of Htd. While in the sequential extraction of the wax for Htd using 1 g wax: 200 g of celite, silica and 400 g alumina at 313 K in the pressure range of 75–400 bar showed that fractions with higher amount of the Htd were obtained at 100 bar, 171.36 mg (17.14%) for celite adsorbent; 200 bar, 81.42 mg (8.14%) for silica adsorbent and 300 bar, 0.32 mg (0.03%) for alumina adsorbent. A total of 21.10wt%, 16.04wt% and 0.10wt% of the Htd were all together collected using celite, silica and alumina respectively per gram of the wax with the sequential fractionation.

Comparing the two approaches of the fractionation with celite as adsorbent, higher quantity of the Htd were obtained at 300 bar, 5.71 mg (0.57%) and 1 bar, 98.97 mg (9.90%) for simultaneous fractionation. On the contrary higher amount of 171.36 mg (17.14%) Htd was found at 100 bar in the case of sequential fractionation. Of these two fractionations, sequential fractionation gave highest amount of Htd (171.36 mg) in a single fraction. In addition, 10.70wt% and 21.10wt% were the total Htd collected for the simultaneous and sequential fractionation respectively.

The order of effectiveness of the adsorbents tested for the fractionation of Htd was silica > celite > alumina. The fractionation of the wax using the silica adsorbent appeared more promising in terms of selectivity towards the Htd. However, further optimisation studies should be investigated about temperature, pressure and wax: silica ratio to further improve the fractionation process.

3.2.6 Simultaneous thermal analysis (STA) of some fractional extracts from the fractionation of wheat straw wax

STA is a combination of TGA and DSC, whereby the TGA thermograms gives the thermal stability while the DSC provides details of the different phase changes of a substance including, crystallization, melting point and so on. Although it was difficult to isolate the Htd from liquid scCO₂ fractionation, the different fractions obtained would still have specific properties²⁵⁸ such as melting point,²⁵⁴ due to their varying composition. As mixture of compounds, waxes are often characterised by their melting points,¹⁶² which is a useful indicator for application in areas such as cosmetics, candles, polishes, coating containers, impregnating paper, etc. The fractions were analysed using simultaneous thermal analysis (STA) to obtain the melting point ranges of each fraction as shown in Table 3-9 (see Figure 3-9, Figure 3-10, Figure 3-11 and Figure 3-12).

Table 3-9: Masses and melting point ranges of the fraction obtained from simultaneous scCO₂ fractionation with 10 g wax: 200 g celite adsorbent

Fractions	1	2	3	4
Pressure (bar)	250	150	75	1
Tempt. (K)	323	323	308	308
Fractional mass g (%)	4.30 (43.00)	1.51 (15.10)	0.54 (5.40)	2.48 (24.80)
Endothermic minima (K)	330.80	311.10	335.50	327.80

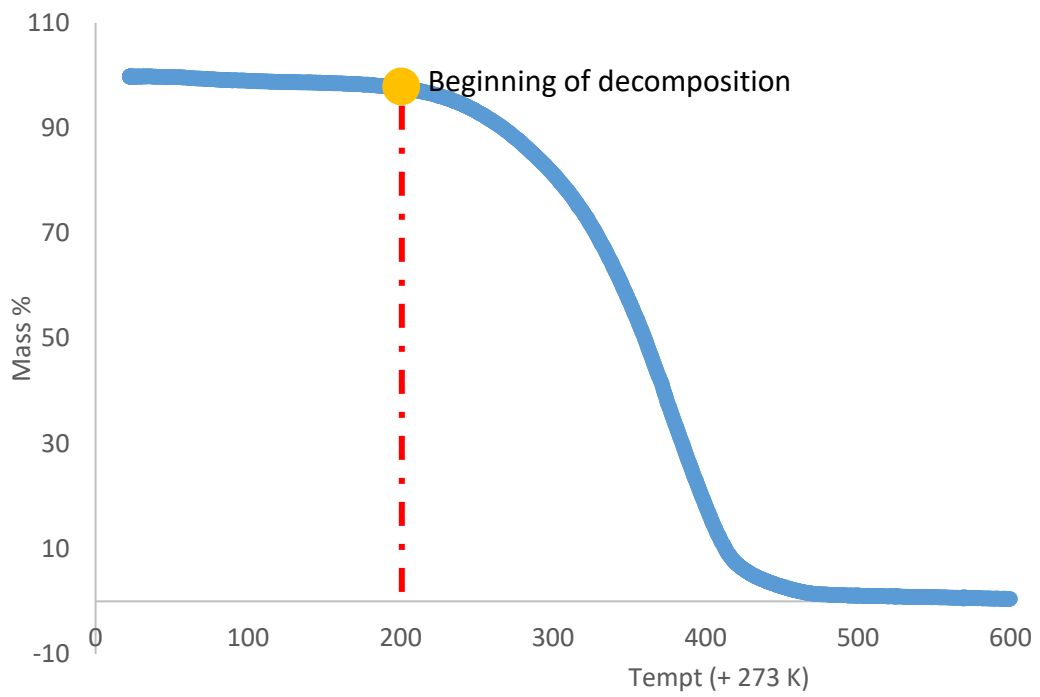
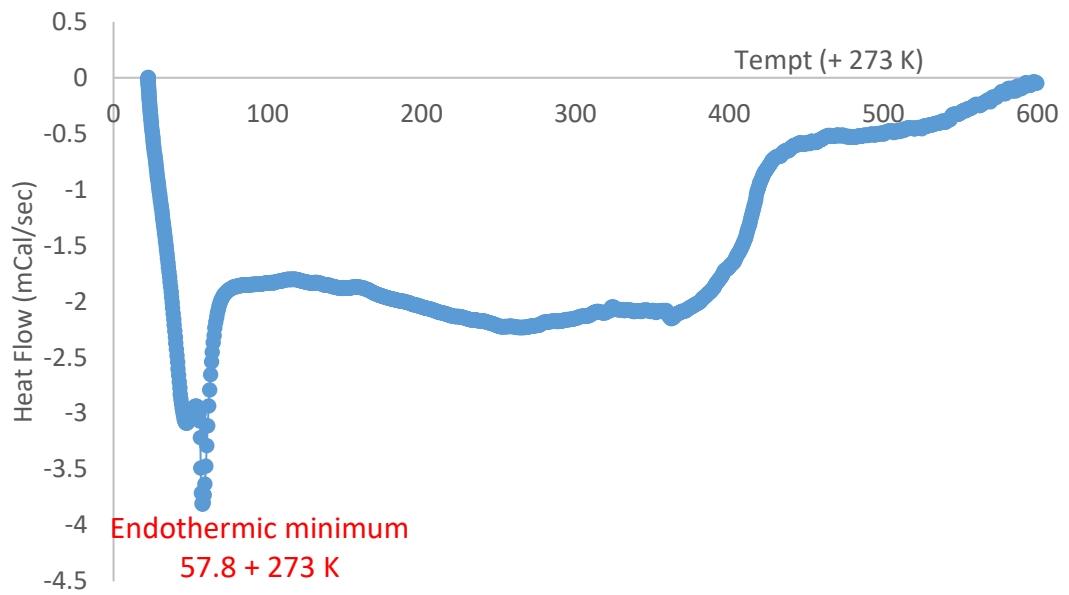


Figure 3-9: STA of the fraction at 250 bar and 323 K for the simultaneous scCO₂ fractionation of wax using 10 g wax: 200 g celite adsorbent

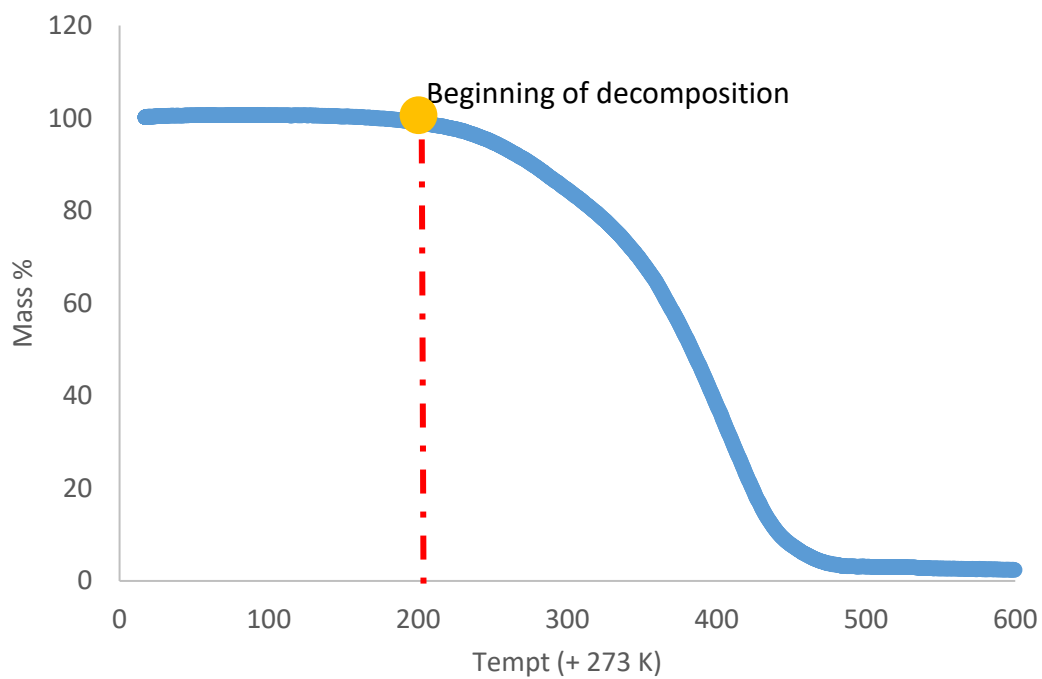
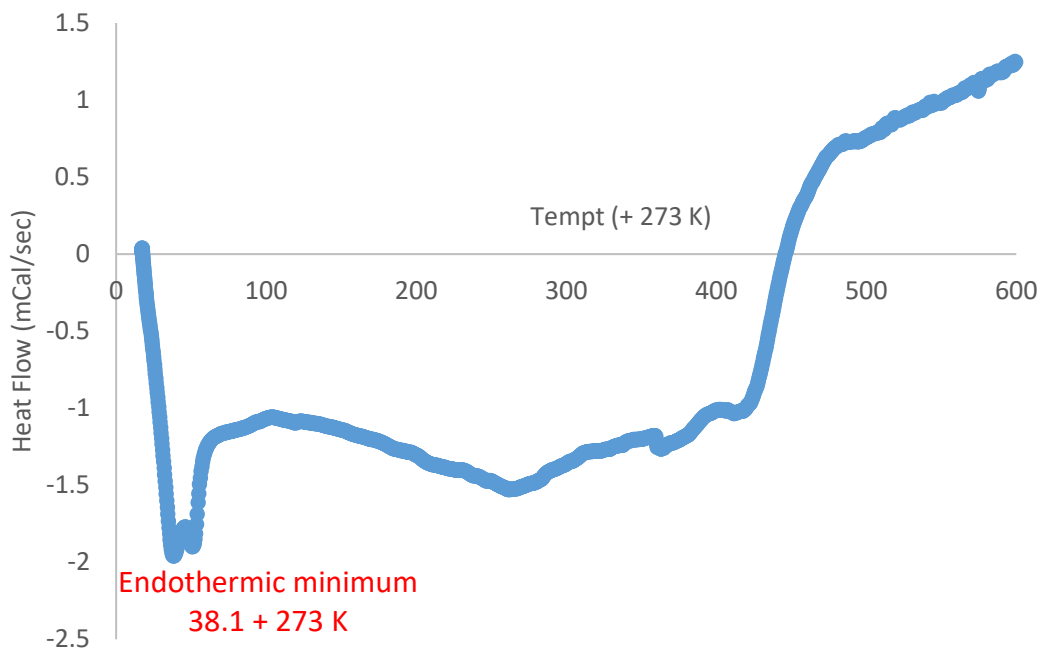


Figure 3-10: STA of the fraction at 150 bar and 323 K for the simultaneous scCO₂ fractionation of wax using 10 g wax: 200 g celite adsorbent

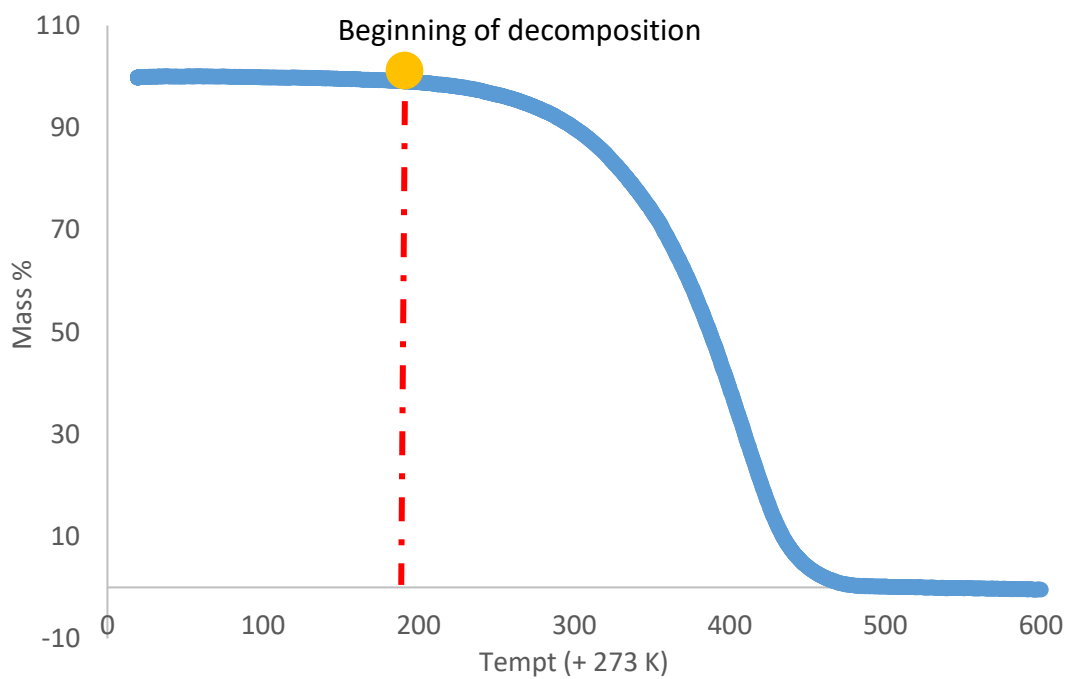
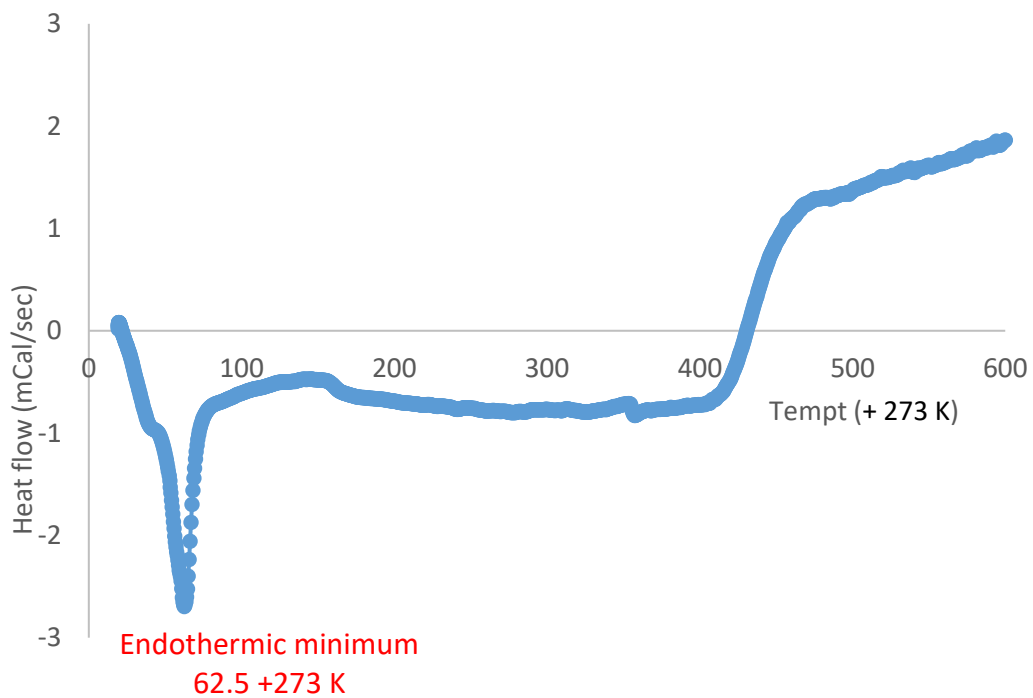


Figure 3-11: STA of the fraction at 75 bar and 308 K for the simultaneous scCO₂ fractionation of wax using 10 g wax: 200 g celite adsorbent

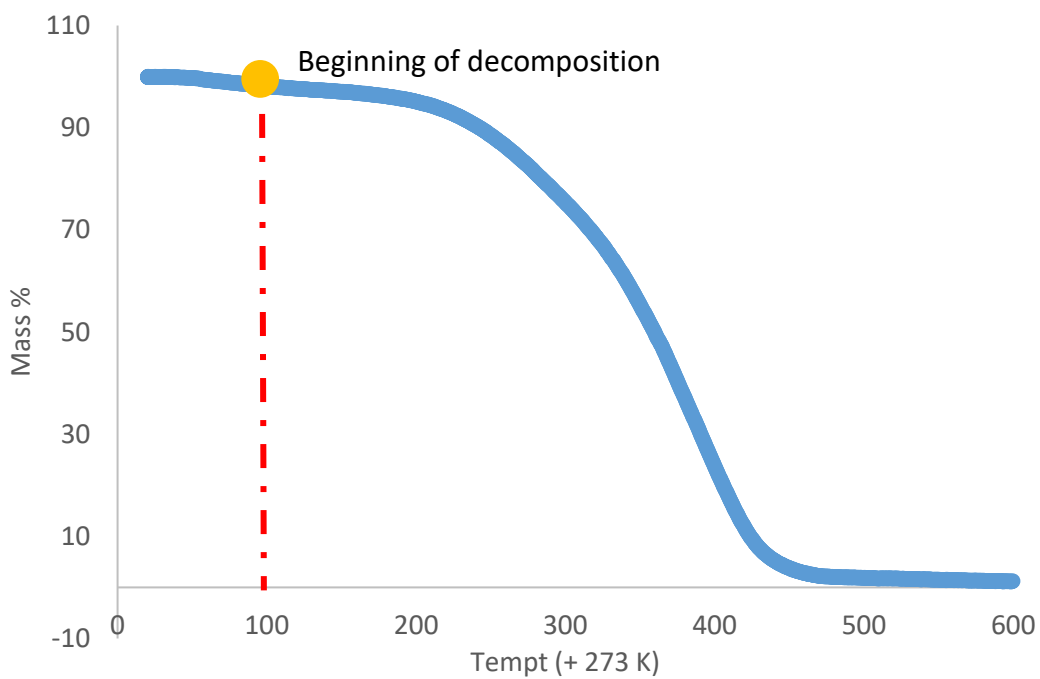
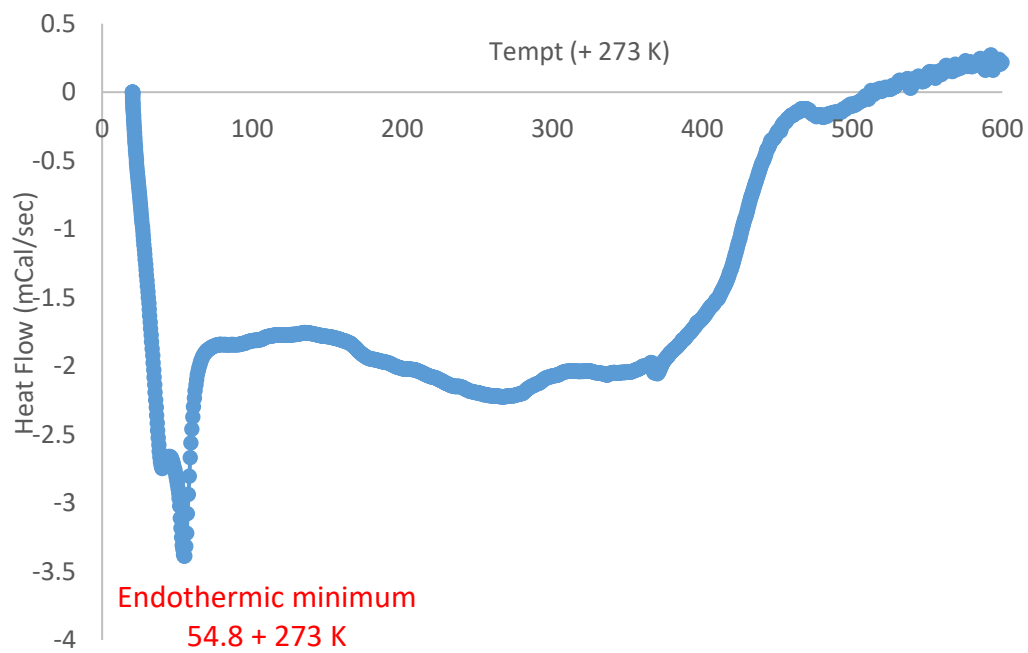


Figure 3-12: STA of the fraction at 1 bar 308 K for the simultaneous scCO₂ fractionation of wax using 10 g wax: 200 g celite adsorbent

The STA thermograms indicate that the four fractions collected were different in terms of their melting point ranges. The fractions at 250 bar, 150 bar, 75 bar and 1 bar had endothermic minima centred at 330.80 K, 311.5 K, 335.5 K and 327.80 K respectively. From the TGA thermograms it can be seen that the fractions began decomposing between 373– 473 K. This corresponds to water being driven off from the substance resulting in the small mass change observed in all the TGA thermograms of the four fractions. Subsequently, between 474– 873 K, there was a significant mass reduction due to a great proportion of these fractions becoming volatized and finally charred.

Since the chemical compositions of the extracts constitutes over 100 different compounds, it is challenging to identify which single compound is corresponding to which particular thermal transition.¹⁶⁶ Even if this was possible, it would not give useful information as it has been shown that different wax groups within complex mixtures interact and behave in a different way.¹⁶⁶ The fraction collected at 150 bar and 323 K had a softer texture than the rest. Therefore, it could be useful in skin care formulations as previously observed.¹⁶⁶ The rest of the fractions had melting points in the range of 327 - 335.50 K and could therefore be good ingredients for lip-sticks, mascara formulations and many others. Some useful applications of wheat straw wax components are given in Table 3-10 below.

Table 3-10: Potential applications of different wheat straw wax components¹⁶⁶

Wax group	Top compounds	Potential applications
Fatty acids	Hexadecanoic acid, Octadecadienoic acid, octadecenoic acid, octadecanoic aid	Soap, detergent, lubricating oils, cleaning compounds/polishes
Hydrocarbons	Nonacosane, hentriacontane	Paraffin wax, coatings

Fatty alcohols	octacosanol	Surfactants, cosmetics
Aldehydes	octacosanal	Food flavouring
Wax esters	Octacosanyl hexadecanoate	Hard wax polishes, coatings, cosmetics, plasticisers
Sterols	β -sitosterol, stigmasterol, campesterol	Nutrient supplement, cosmetics, surfactants
β -diketones	Htd	Metal ions chelating agent

3.3 Conclusion

This chapter demonstrated that Htd can be successfully isolated from wheat straw wax with $\text{Cu}(\text{OAc})_2$ using alternative greener solvents to hexane and petroleum ether (333 – 353 K). Cyclohexane, TMTHF and CPME were found to be adequate replacements for the purification of the long chain β -diketone. In which case TMTHF gave the highest yield of 21.40wt% among these alternative solvents tested. *p*-cymene could also be used but it has a higher boiling point which will consume more energy during distillation to separate *p*-cymene from the Htd. However, scCO_2 was also tested for fractionation of the wheat straw wax in order to obtain the Htd using different adsorbents (celite, silica and alumina) and varying pressures. The fractions collected were analysed with GC-FID and STA. Sequential scCO_2 fractionation of 1 g wax: 200 g silica at 300 bar, 313 K for 40 min was found to give at least better selectivity for the Htd than with alumina and celite adsorbents under similar condition.

Chapter 4

Modification of the bioderived lipophilic β -diketone

Aspects of the work described in this chapter have been presented as:

Kaana Asemave. Bioderived alternative chelating agents for metals extractions. Being a talk presented at Northern Sustainable chemistry (NORSC), 5th PG symposium; King's Manor, York, UK. Sept. 23rd, 2015

4 Chapter 4

4.1 Introduction

Although β -diketones are useful metal chelating agents, modifying them with carboxylate groups could enhance their metals chelation capacity. The modification of β -diketones such as acetyl acetone and dibenzoylmethane with saturated and unsaturated organic halide has long been reported.^{259–261} The alkylation of acetyl acetone with isopropyl alcohol in the presence of boron trifluoride has also been previously carried out.²⁶² Ferrari *et al.*²⁴⁰ modified acetyl acetone with tert-butyl bromoacetate using sodium hydride in THF at room temperature for about 24 h to form tert-Butyl-3-acetyl-4-oxopentanoate.²⁴⁰ However little information has been published on the modification of long chain lipophilic β -diketones such as 14,16-hentriacontanedione.

Unsaturated (α , β) carbonyl esters can be added to α -position of β -diketones using the Michael addition reaction and then hydrolyse the modified β -diketones for enhancing the chelation ability as has been suggested by Fanou *et al.*²⁶³ Nowadays microwave heating is also efficiently used to perform Michael addition reaction and many other chemical transformations. In addition, neat Michael addition reactions have recently been reported. KF/alumina has found use as an effective solid heterogeneous base catalyst for effecting Michael addition reactions and many other reactions.^{191,186} This catalyst has attracted widespread interest because it is convenient and environmentally benign.^{203,205}

Classical hydrolysis conditions for esters involves the use of NaOH, KOH, or LiOH in pure H₂O, MeOH, EtOH or MeOH/H₂O and EtOH/H₂O solvents.²⁶⁴ Alkaline system (usually KOH

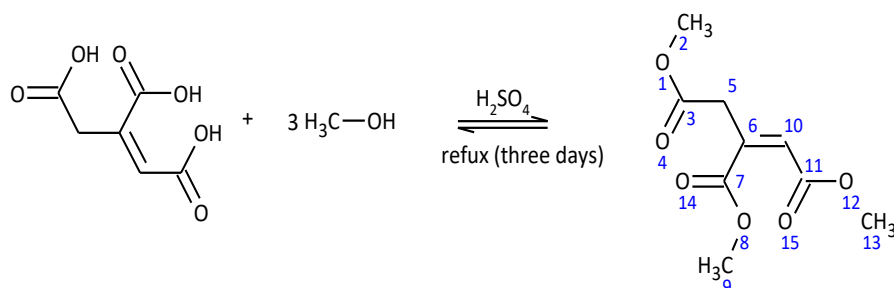
and NaOH) hydrolysis is carried out with a slight excess of base in ethanol. This is a sufficiently mild procedure that most fatty acids are unaltered.²⁶⁴ Similarly, according to Salimon *et al.*,²⁶⁴ 1.75M of ethanolic KOH at 338 K for 2 h was used to hydrolyse *Jatropha curcas* seed oil. Gupta and Ho reported the hydrolysis of methyl paraben and propyl paraben esters with 10% KOH in alcohol-water (80-20).²⁶⁵ According to Khurana *et al.*,²⁶⁶ methanol is the solvent of choice for rapid hydrolysis of esters at ambient condition with KOH, whereas hydrolysis of esters with KOH-ethanol and KOH-n-propanol are poor. This is because KOH is more soluble in methanol than the ethanol and n-propanol. Also that addition of water as co-solvent slows the hydrolysis and reactions were incomplete even after 6 h at 308 K.²⁶⁶ Esters of aromatic acids readily give a solid metal carboxylate within a few minutes of the reaction unlike esters of aliphatic acids. It was observed that methyl esters are hydrolysed quicker than esters with bulkier alkyl group.²⁶⁶ Aliphatic esters with alpha hydrogens are not readily hydrolysed, as aromatic esters due to competing aldol type condensations and the tendency to form stabilized anion after deprotonation.²⁶⁶ Recently, Theodorou *et al.*²⁶⁷ reported an efficient hydrolysis of esters in DCM/MeOH. Therefore, this chapter deals with the modification of the Htd by applying Michael addition reaction catalysed by KF/alumina medium to form α , β -unsaturated carbonyl esters, followed by the hydrolysis of the modified bioderived β -diketones and characterisation of these modified compounds.

4.2 Results and discussion of modification of the β -diketone

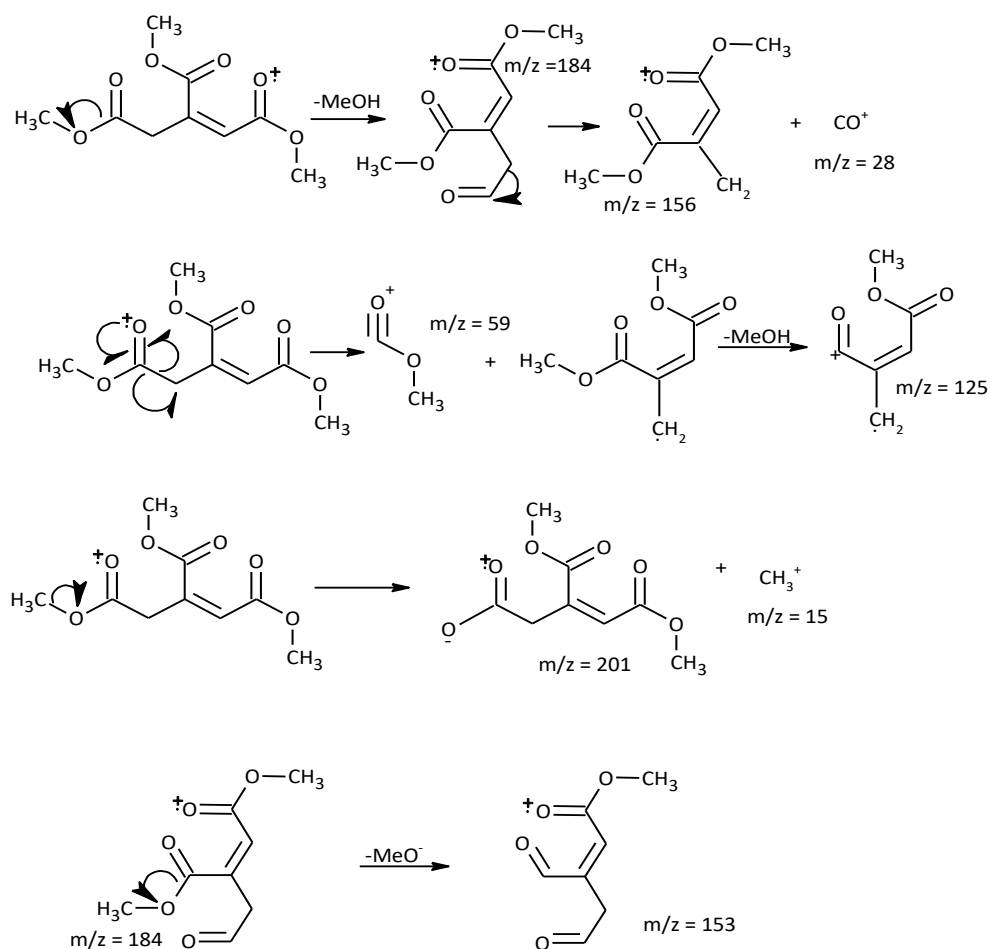
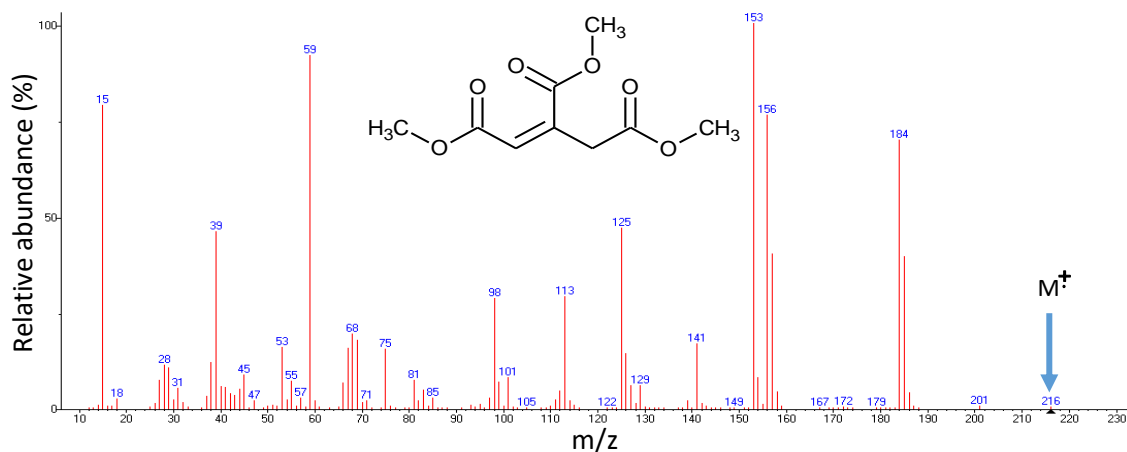
The α -protons in the β -diketone are acidic and can be removed by relatively weak bases including; ammonia, sodium hydroxide, piperidine or pyridine; but a much stronger base is required for the second deprotonation.²³⁶ Thus advantage is taking of the acidic nature of β -diketone to effect the modification. Prior to the modification of the bioderived β -

diketone, $\text{KF}/\text{Al}_2\text{O}_3$ mediated modification of acetyl acetone (1 equivalent) with methyl acrylate (5 mole equivalents) was carried out in order to establish a basis. The reaction was carried out in solventless condition in accordance with the 1st and 5th principle of green chemistry so as to minimise waste. Double and single addition of the methyl acrylate onto acetyl acetone was observed as it has been reported in similar reactions.²⁰⁶ Escalante *et al.* conducted Michael addition of amines to methyl acrylates under microwave irradiation and also observed double addition.²⁰⁶

In addition, trimethyl aconitate was prepared from aconitic acid to be use as an agent for bioderived β -diketone modification. The preparation of trimethyl aconitate from aconitic acid as described in Equation 4-1 resulted into complete conversion as confirm with GC-MS in Figure 4-1. The GC-MS spectrum shows the molecular ion of aconitate as 216 m/z, which is consistent with the molecular weight of the compound. The fragmentation (as described in Scheme 4-2) is typical of carbonyl compounds, involving cleavage of $\text{C}(\text{O})-\text{C}$ bond which has been similarly reported by Parsons.²⁶⁸ Other major peaks found in the spectrum are due to the fragmentation of the aconitate molecule. The chemical shifts of the protons on the ester groups are; 3.62 ppm (3 H, s; 13), 3.70 (3 H, s; 2) and 3.75 (3 H, s; 9) which implied the formation of the trimethyl aconitate as well.



Equation 4-1: Preparation of trimethyl aconitate in acidified methanol medium

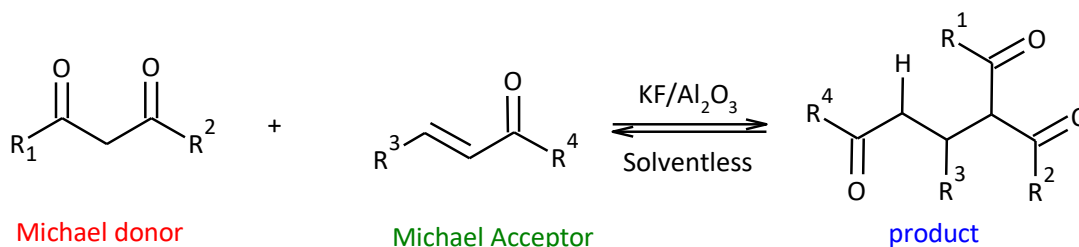


Scheme 4-2: A proposed fragmentation pattern for the trimethyl aconitate

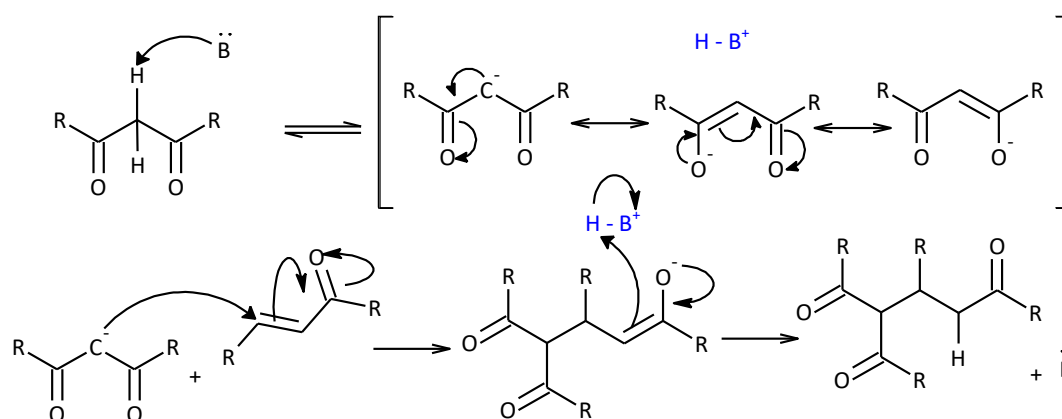
4.2.1 The modification of the Htd

The $\text{KF}/\text{Al}_2\text{O}_3$ mediated Michael addition modification of the Htd was tested with; methylacrylate, methylmethacrylate, dimethyl itaconate and trimethyl aconitate (see

Table 4-1) because they contain unsaturated carbonyl moiety that can act as Michael acceptors. The Michael addition modification reaction and the scheme are described in Equation 4-3 and Scheme 4-4.



Equation 4-3: Modification of the Htd using Michael addition reaction



Scheme 4-4: Detail scheme of Michael addition modification reaction

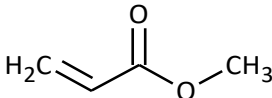
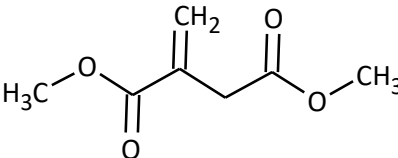
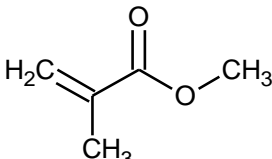
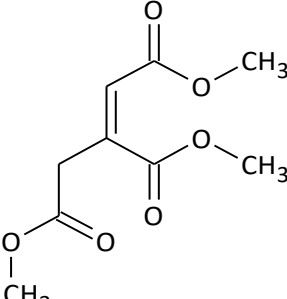
The reaction involves the use of the heterogeneous base catalyst KF/alumina.¹⁹⁹ The reaction begins with deprotonation of the β -diketone by the base,¹⁸⁶ resulting to formation of a resonance stabilized carbanion (nucleophile). This nucleophile is then added to the electrophile (the unsaturated carbonyl moiety) and subsequently the transfer of protons from the base to the Michael product.²⁰¹

ESI (+)-MS, GC-FID and $^1\text{H-NMR}$ techniques were used to identify the Michael products formed. Evidence obtained showed that, methyl acrylate, methyl methacrylate and dimethyl itaconate were added to the Htd unlike aconitate. The conversion was quite

low using methyl methacrylate with this condition. The observed increasing order of the modification conversion with these acceptors is; aconitate < methylmethacrylate < itaconate < methylacrylate. Methyl acrylate in particular is a good Michael acceptor as described by Escalante *et al.*²⁰⁶ Therefore, details studies of the modification of the Htd focussed on methyl acrylate and dimethyl itaconate. Bhatt and Nimavat²⁶⁹ had similarly demonstrated the modification of 2-bromo benzoic acid with acetylacetone into 2-(2,4-dioxopentan-3-yl)benzoic acid.

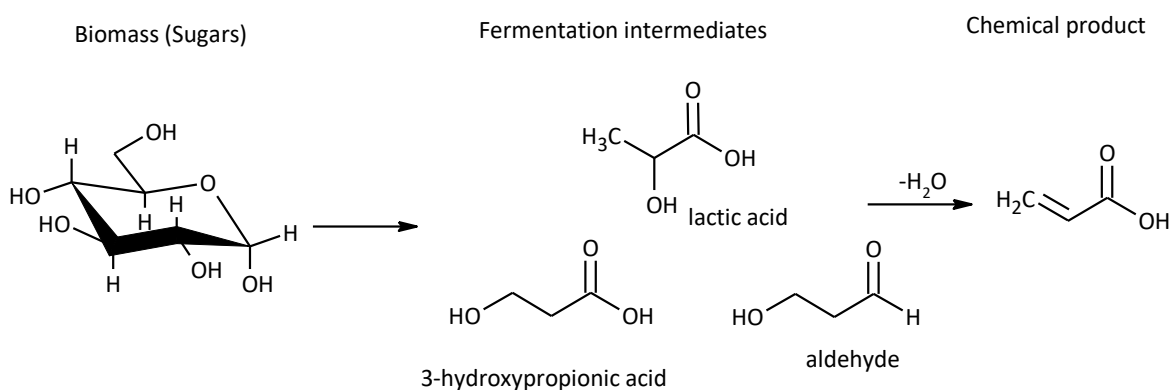
Michael addition reactions are often carried out in polar solvents such as MeOH, acetone, DMSO, THF,²⁴⁰ MeCN.²⁷⁰ In the present studies, these reactions were carried out under solventless condition as similarly reported by Ravichandran and Karthikeyan²¹⁰ in order to simplify the process, prevent solvent wastes, hazards, and reduce the potential toxicity.^{271,272} Solvent-free microwave mediated Michael addition has also been performed by Rao and Jothilingam.²⁷³ They found that the solvent-free condition was better than using polar aprotic solvent such as DMSO.²⁷³ The modification under microwave heating benefits from the fact that, ketones are medium microwave absorbers like water which can be heated efficiently,¹⁹⁴ plus minimal by-product formation, high functional group tolerance and high conversions.²⁷⁰ Solventless and microwave are recent concepts that have been embraced in many chemical transformations by the research community.^{272,274}

Table 4-1: The Michael acceptors that were tested for the modification of Htd

Names	Structures
Methyl acrylate	
Dimethyl itaconate	
Methyl methacrylate	
Trimethyl aconitate	

Furthermore, this work is tailored towards sustainability. Therefore, the sources of principal chemicals that are used in the studies for modifying Htd such as methyl acrylate and dimethyl itaconate are highlighted as follows. Currently, a significant proportion of the acrylic acid supply (from which methyl acrylate could be obtained) comes from petroleum as reported by Straathof *et al.*²⁷⁵ Acrylic acid can be alternatively derived from dehydration of 3-hydroxypropionic acid (3-HPA). Hence, there has been effort to produce 3-HPA from biomass^{275–277} as given in the Equation 4-5 below. Relatedly, Danner *et al.*²⁷⁸ has proposed a renewable production of acrylic acid from lactic acid,²⁷⁸ by converting

carbohydrates to lactic acid by fermentation, followed by dehydration to acrylic acid.^{278,279}



Equation 4-5: Renewable routes to acrylic acid ²⁷⁶

At the present time the economic feasibility of this bio-derived acrylic acid is still on going because of the low yield of acrylic acid after the dehydration.²⁷⁹ Furthermore, because of the existence of acrylic acid pathways in some microorganisms, strain improvement and metabolic engineering is another route to produce acrylic acid directly from biomass by fermentation.²⁷⁹ Whereas dimethyl itaconate is derived from the itaconic acid which is produced from fermentation of glucose,²⁸⁰ (from carbohydrate) using fungi, *Aspergillus flavus*.²⁸¹⁻²⁸⁴ Fungal species are best used for production of itaconic acid than bacterial species.²⁸⁰ Itaconic acid is used in synthetic resins, synthetic fibres, plastics, rubbers, surfactants and oil additives which has led to an increased demand for this product,^{281,285,286} but at the moment itaconic acid production capacity exceeds the demand.

4.2.2 Electrospray ionisation mass spectroscopy (ESI (+)-MS) of the carboxylate esters of modified bioderived β -diketone

ESI-MS is a less energetic ionisation technique, where a sample is protonated in gas phase to form cationic species not radical (as is the case of impact ionisation

approach).²⁶⁸ Therefore, the modified Htd were identified using ESI-MS technique. The ESI (+)-MS of the methyl acrylate, dimethyl itaconate and methyl methacrylate modified Htd are presented in Figure 4-2 and Figure 4-3 and the peaks are interpreted (assigned) in Table 4-2. The ESI(+)-MS of dimethyl itaconate modified 14,16-hentriacontanedione (Ita) had minor peaks, 407.2757 m/z and 379.2460 m/z in addition to the major product ion (645.5051 m/z). These are likely due to loss of 239 (C₁₆H₃₁O) from the parent compound as shown in Figure 4-3. The remaining fragment with mass of 383 m/z then combine with Na⁺ to produce 407.2757 m/z ion approximately. Loss of CO (28) from the 407.2757 m/z ion will form 379.2460 m/z. Loss of CO in such compounds has been previously reported by Brent *et al.*²⁸⁷ Alternatively, ion 379.2460 m/z may have come from losses of 211 (C₁₅H₃₁) and 32 (MeOH) from the Ita. Similarly, Na⁺ and K⁺ adducts were seen in the ESI-MS of the methyl acrylate modified β-diketone (Ma). The ESI(+)-MS spectrum of Ma had major peaks; 589.4794 m/z and 675.5179 m/z for potassium adduct for single and double addition of methyl acrylate products respectively, then 659.5216 m/z as sodium species of double addition of the methyl acrylate product. There was much more formation of the double addition product (M_d) than single addition (M_s) using methyl acrylate as Michael acceptor as similarly explained in chapter one. The minor peaks 421.2924 m/z, 449.3213 m/z and 479.2984 m/z in the ESI-MS of the Ma are due to formation of these species [M_d -239 +Na]⁺, [M_d -211 +Na]⁺ and [M_d - 239 + 2Na +K - 2H]⁺ respectively as earlier pointed out. This means that there was fragmentation of Ita and Ma. ESI-MS peaks are obtained mostly as potassium and sodium adducts.²⁸⁸ The ESI-MS spectra of the modified β-diketones are described below.

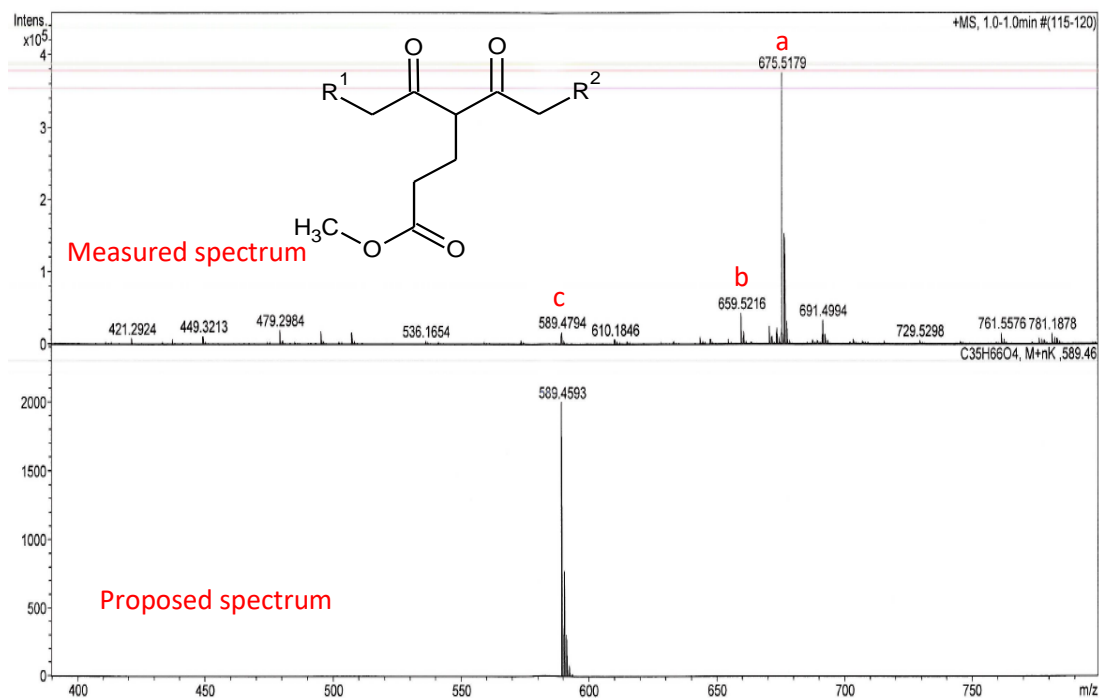


Figure 4-2: ESI (+)-MS of the Ma

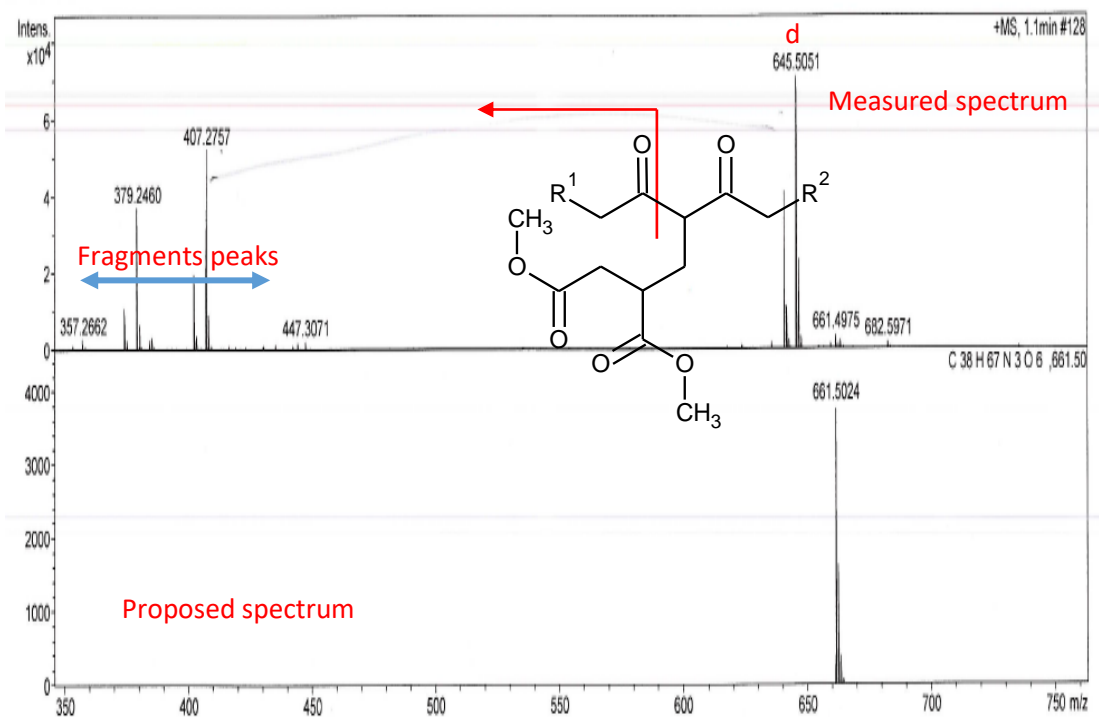


Figure 4-3: ESI(+)-MS of Ita

Table 4-2: ESI-MS peaks and interpretation for the Ma and Ita

Cationic species	Peaks (m/z)	Molecular weight	Interpretation	Cross Ref.
		464 (M)	Htd	
$[M_s + K]^+$	589.4794	550	Single addition of methyl acrylate – Ma_s	Figure 4-2 (c)
$[M_d + K]^+$	675.5179	636	double addition of methyl acrylate – Ma_d	Figure 4-2 (a)
$[M_d + Na]^+$	659.5216	636	Double addition of methyl acrylate – Ma_d	Figure 4-2 (b)
$[M + Na]^+$	645.5051	622	Single addition of dimethyl itaconate- Ita	Figure 4-3 (d)
$[M + K]^+$	503.4413	464	Unreacted β -diketone- Htd	

Note: Molecular weight of Hacac, methyl acrylate and dimethyl itaconate are about 100, 86 and 158 $g\text{mol}^{-1}$ respectively

Methylacrylate is a good Michael acceptor²⁰¹ both single and double additions were formed as previously reported.^{201,289,290} Escalante *et al.*²⁰⁶ showed that methyl acrylate can form double addition even at short time of 3 min with equimolar amount of the amines and methyl acrylate. This double deprotonation resulting to double addition in this studies has proven that KF/alumina is a strong base.¹⁰⁹ The addition of itaconate to Htd was also successful with good conversion as already highlighted above. Whereas, the modification of Htd with methyl methacrylate has low conversion and no double addition was observed with methyl methacrylate. This may be due to the fact that, methyl methacrylate is relatively poor Michael acceptor than methyl acrylate and itaconate by virtue of the methyl group on methylene carbon of the methyl methacrylate as previously reported.²⁰¹ Thus, additions with methyl methacrylate are better at longer time and high temperatures.²⁰⁶ In the case of aconitate, no evidence to indicate that

there was an addition of the aconitate to the Htd. Steric hindrance due to the structure of aconitate may have affected its addition to the Htd.

4.2.3 GC-FIDs chromatogram of the modified Htd

In addition to the ESI-MS identifications, the GC-FID chromatograms for these modified bioderived β -diketones; Ma and Ita (in Figure 4-5 and Figure 4-6) were obtained as further evidence of their formations. Figure 4-4 is the GC-FID for the Htd which was obtained with the same GC-FID method of analysis as those of Ma and Ita. With this evidence of the modification of the Htd with these acceptors, the modification conditions (temperature, time and catalyst loading) were varied to obtain an optimal condition using the traditional stirrer hot plate and microwave heating

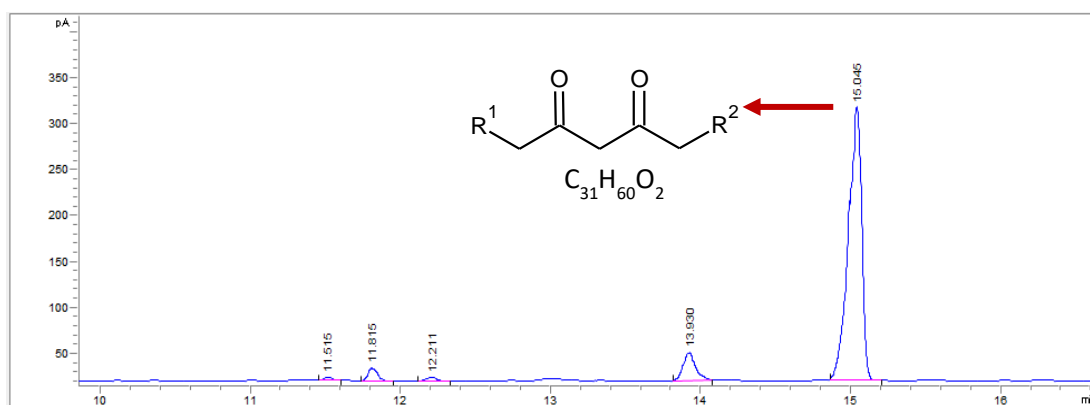


Figure 4-4: GC-FID chromatogram of the Htd

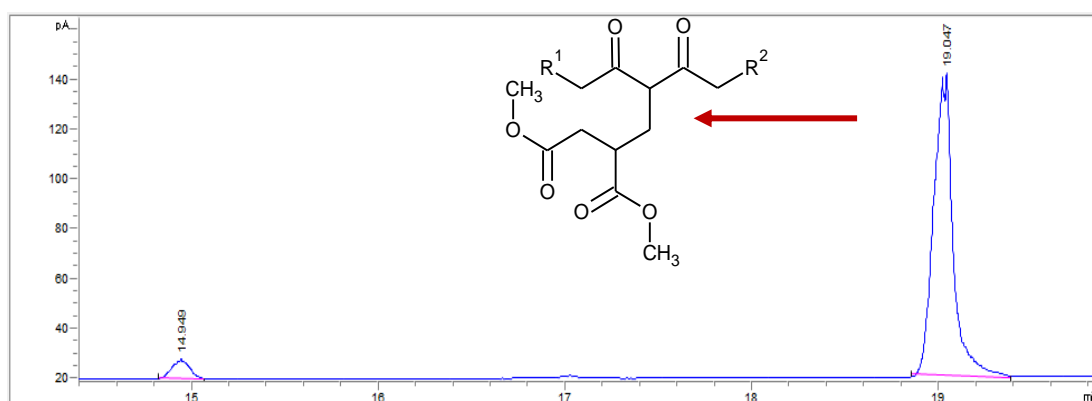


Figure 4-5: GC-FID chromatogram of the Ita

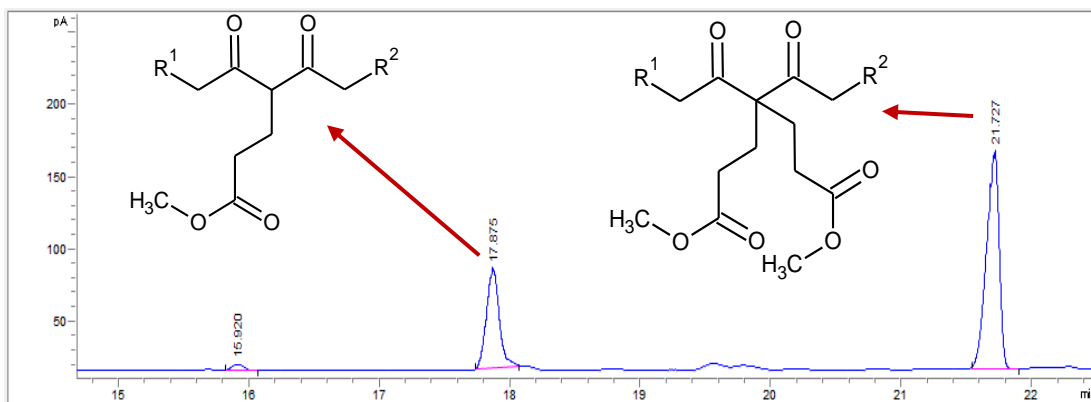


Figure 4-6: GC-FID chromatogram for the Ma (single and double addition of methyl acrylate)

4.2.4 Effect of Michael acceptors on the modification of the Htd

The influence of different Michael acceptors for the modification of the Htd with methyl acrylate, methyl methacrylate and dimethyl itaconate were carried out using conventional and microwave heating. The % conversions were analysed with $^1\text{H-NMR}$ technique. The results are shown in Figure 4-7 and Figure 4-8.

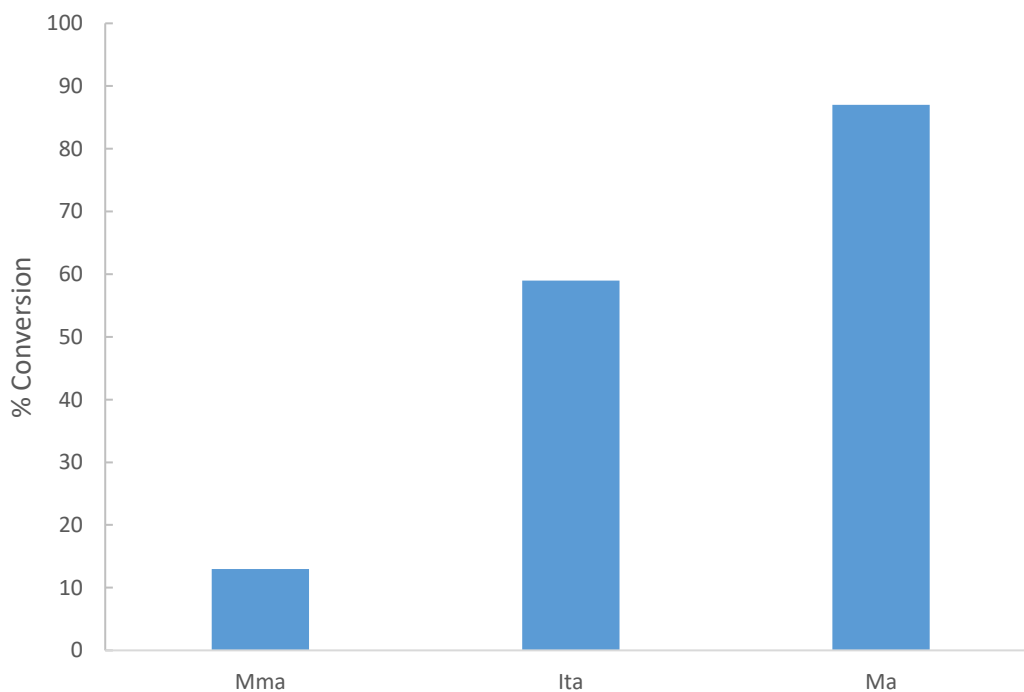


Figure 4-7: % conversions of the modification of the Htd for 5 min at 423 K using conventional heating (Mma = methyl methacrylate product, Ita = itaconate product and Ma = methyl acrylate product)

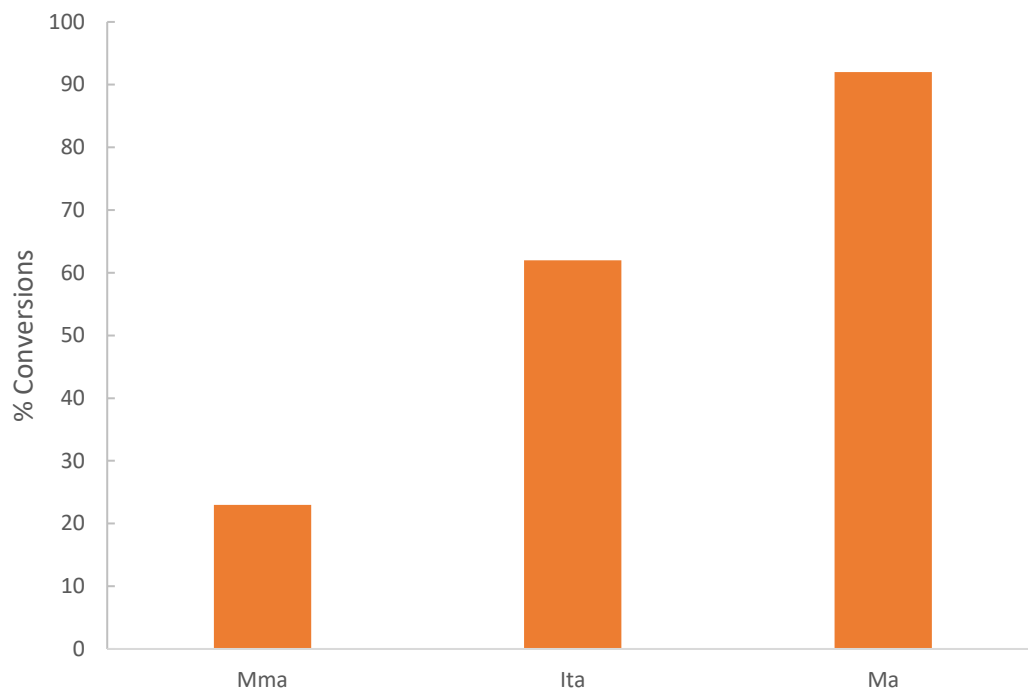


Figure 4-8: % conversions of the modification of the Htd for 5 min at 423 K using microwave heating (Mma = methyl methacrylate product, Ita = itaconate product and Ma = methyl acrylate product)

The percentage conversions under conventional heating were; 13%, 59%, 87% (as found in Figure 4-7) and for the microwave heating were; 23%, 62% and 92% (see Figure 4-8) with respect to methyl methacrylate, itaconate and methyl acrylate respectively. The % conversions with methyl acrylate were higher than itaconate and methyl methacrylate. At this modification condition, methyl methacrylate was least effective due to the electron donating effect of the methyl group as reported in the literature.²⁰⁶ This also shows that the reaction condition was suitable in microwave irradiation as similarly performed.^{270,291}

4.2.5 Effect of temperature on the modification of the Htd

Various temperatures of 333 – 453 K were tested for the modification and it was found that at 393 K, optimal conversions were obtained as 84% and 85% for dimethyl itaconate and methyl acrylate respectively as found in Figure 4-9.

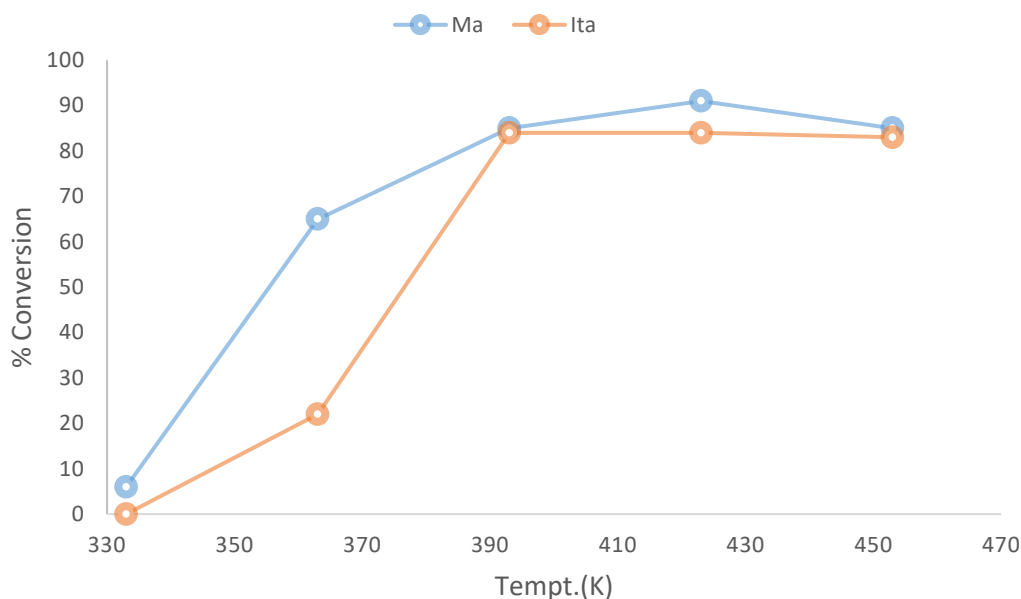
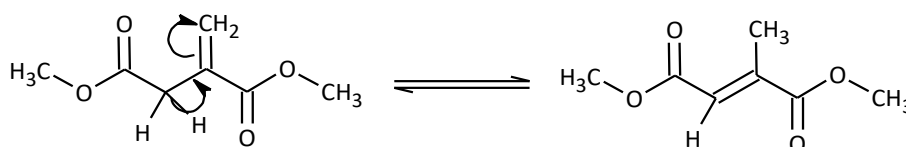


Figure 4-9: % conversions of the modification of the Htd with methyl acrylate and dimethyl itaconate for 5 min at different temperatures

The effective conversions found at 393 K is due to the further activation of the catalyst by driving off water that might have stuck to the surface. In addition, the reaction still occurs even at lower temperature, just as it has been similarly observed,²⁰⁶ importantly with methyl acrylate. Going beyond this optimal temperature of 393 K for the modification will not be necessary as this will increase side reactions. It was also found that, dimethyl itaconate isomerises (see Equation 4-6) at high temperature of 363 K and above in the presence of the KF/alumina at the condition of this experiment. This could also affect the conversion of the modification of the Htd with dimethyl itaconate.



Equation 4-6: Isomerisation of dimethyl itaconate in the presence of KF/alumina at temperature of 363 K and above

4.2.6 Effect of time on the modification of the Htd

Figure 4-10 and Figure 4-11; Figure 4-12 and Figure 4-13 respectively are the results of the modification of the Htd at different times with the dimethyl itaconate and methyl acrylate with conventional and microwave heating. From 1 to 3 min there was increase in conversions in both the microwave and conventional heating experiments. At 10 min holding time, the conversion using microwave heating reached a maximum based on this scale of the reaction unlike the conventional heating. The higher conversions in microwave heating is mostly due to the slightly longer time incurred from ramping phase. It is thought that if the overall time (including ramping period of about 3 minutes) is used in the conventional heating of the reaction, the difference in the conversions between the microwave and the conventional heating may become less noticeable.

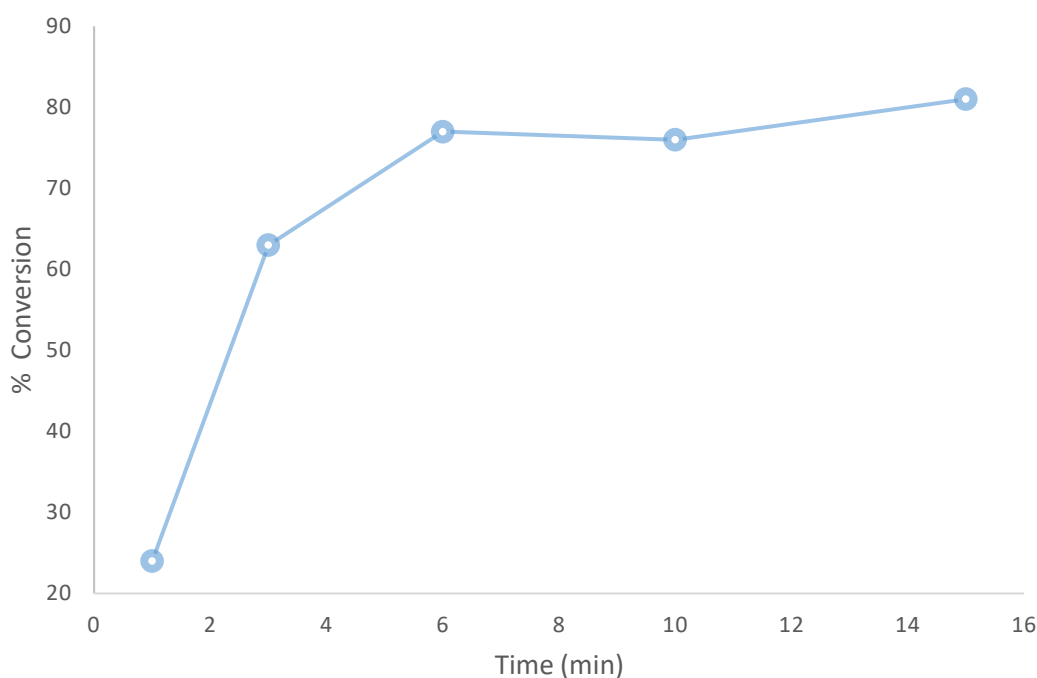


Figure 4-10: % conversion of the modification of Htd with dimethyl itaconate at 423 K at varying time (between 1-15 min) under conventional heating

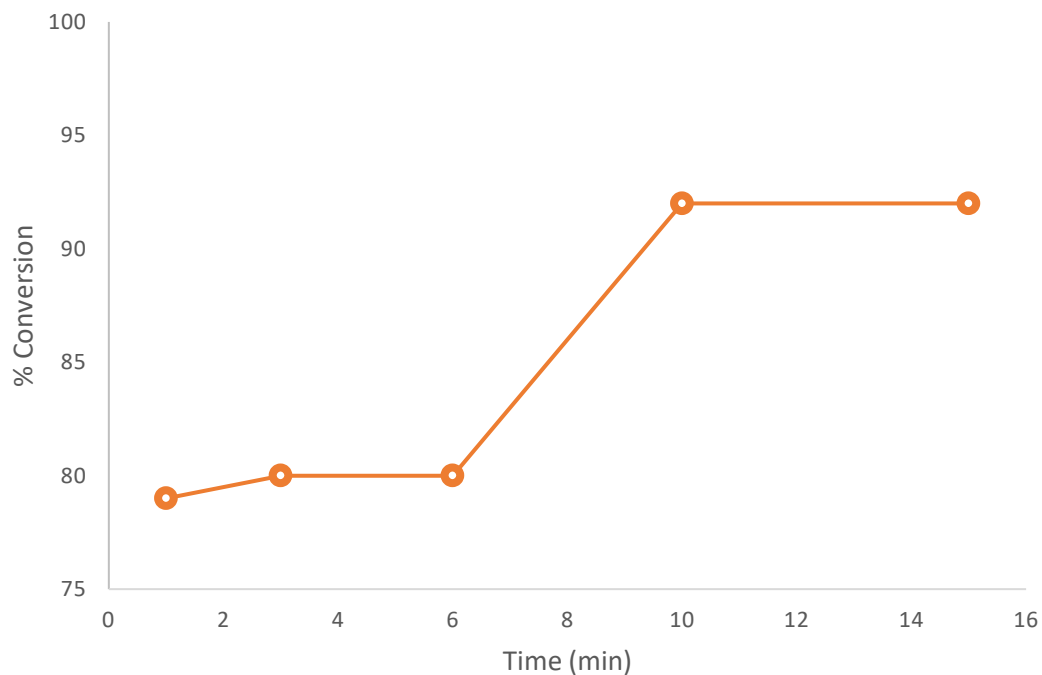


Figure 4-11: % conversion of the modification of Htd with dimethyl itaconate at 423 K at varying time (between 1-15 min) under microwave heating

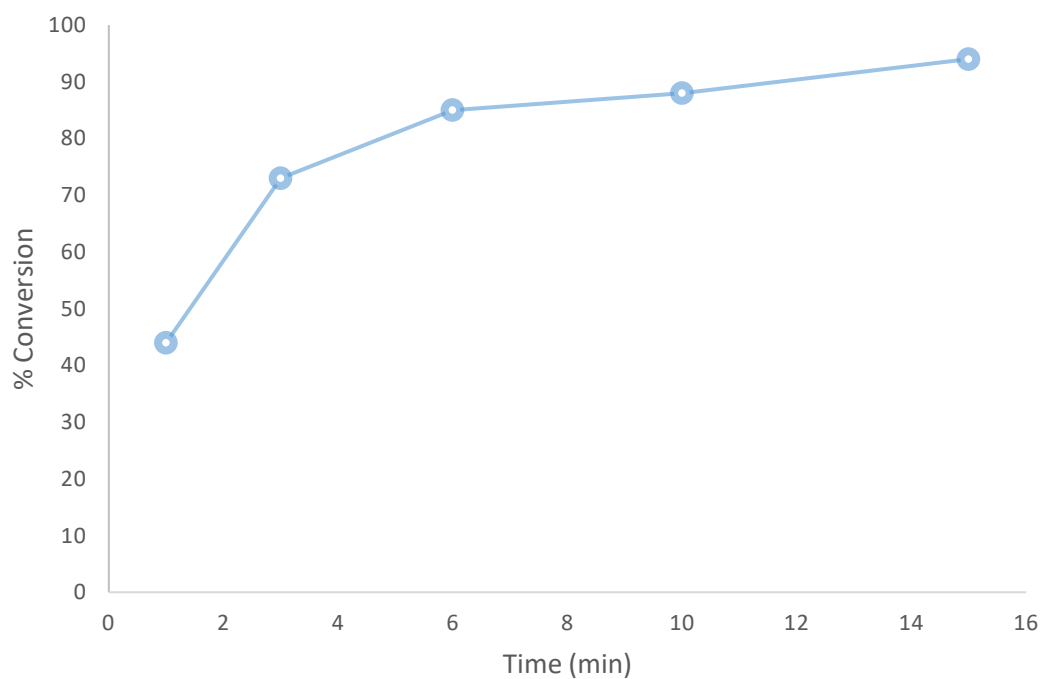


Figure 4-12: % conversions of the modification of the Htd with methyl acrylate at 393 K at different time under conventional heating

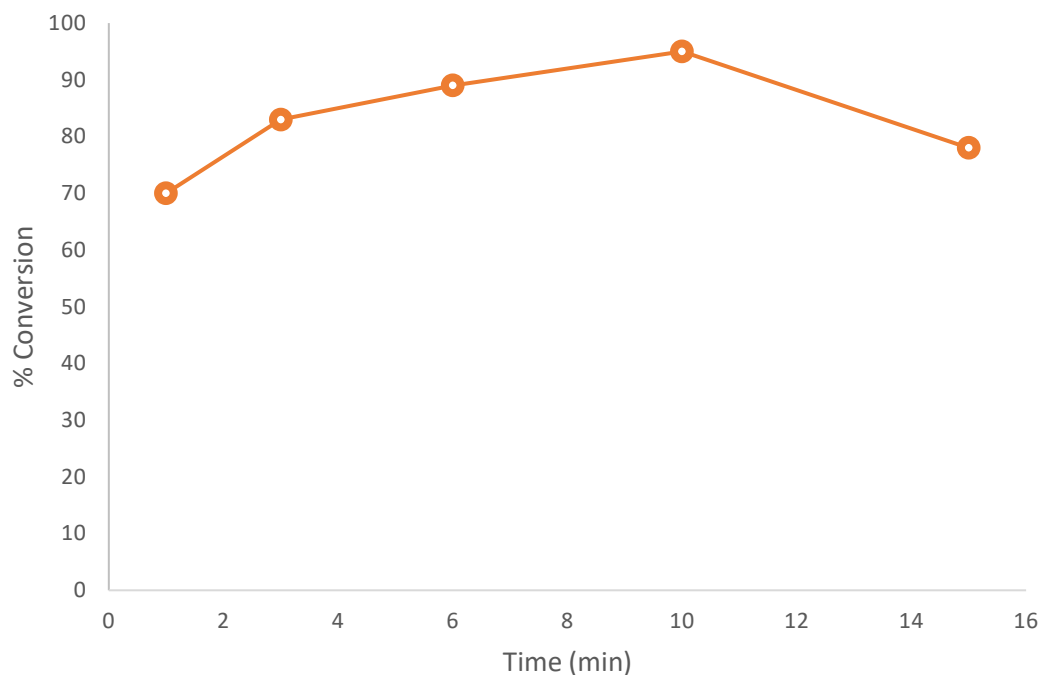


Figure 4-13: % conversions of the modification of the Htd with methyl acrylate at 393 K at different time under microwave heating

4.2.7 Effect of amount of KF/alumina on the modification of the Htd

The effect of changing the amount of catalyst (KF/alumina) on the % conversions of the modification of Htd using dimethyl itaconate and methyl acrylate were investigated. As given in Figure 4-14, the % conversions increased faster as the amount of the catalyst increase from 15 mg through to 50 mg, but increasing the amount of the catalyst to 80 mg resulted into lower increment in the % conversions at the scale of this reaction. The modification indeed depends on the KF/alumina loading. Thus, it is reasonable from this result, to say methyl acrylate and dimethyl itaconate can be used for the modification of this Htd at 393 K or 333 K (methyl acrylate).

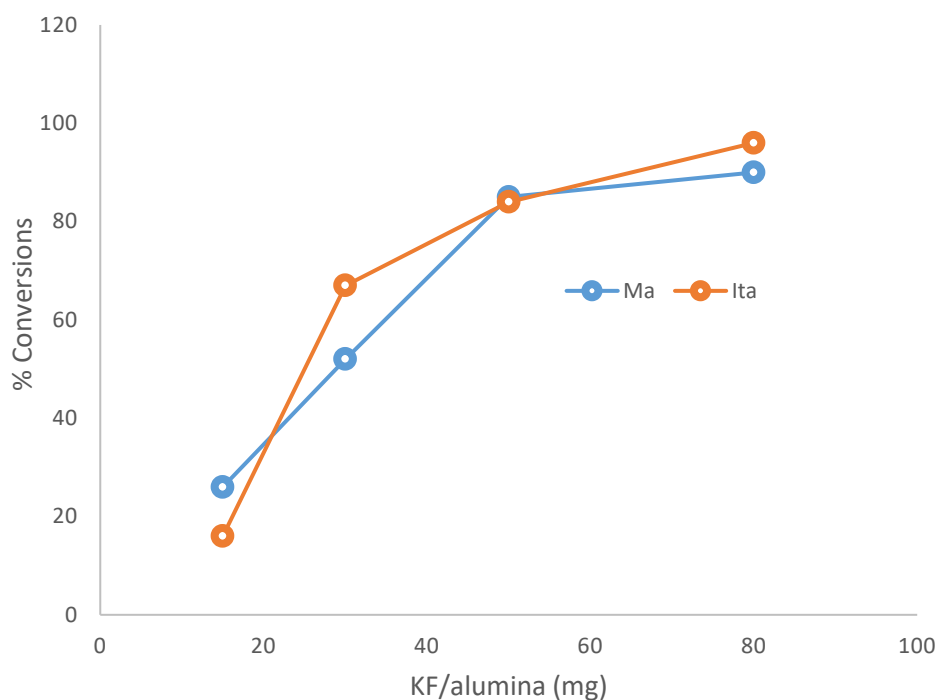


Figure 4-14: Effect of amount of catalyst (KF/alumina) on the modification of Htd with dimethyl itaconate and methyl acrylate

4.2.8 Separation/purification of the modified Htd

The modified compounds were separated/purified using flash chromatography. The TLC obtained prior to the separation of the Ma and Ita are presented in Figure 4-15 and Figure 4-16 respectively. It was found that using a mobile phase of 20% ethyl acetate and 80% cyclohexane gives a good separation of the Htd from the Ma and Htd from the excess dimethyl itaconate and the Ita. The TLC spots in Figure 4-15 were revealed with phosphormolybdate stain. Figure 4-16 is the TLC for the separation of Ita which was read with UV lamp and the spots marked with pencil. Alternatively, the excess dimethyl itaconate was distilled from the reaction mixture using a Kugelrohr distillation; leaving behind the Htd and Ita.

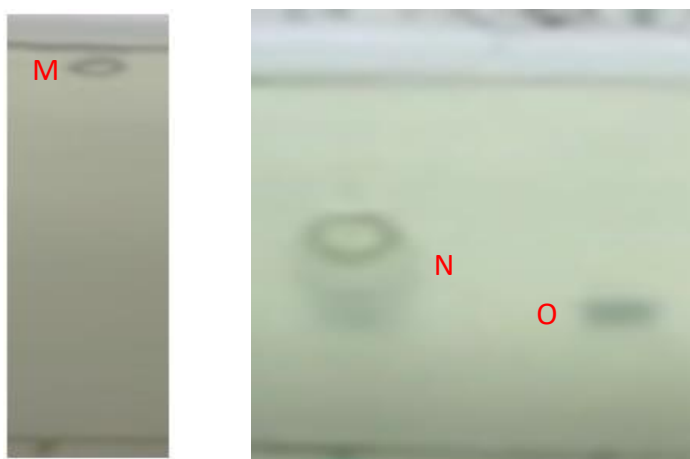


Figure 4-15: TLC for Ma using 80% cyclohexane and 20% ethyl acetate (M = Htd; and N, O = products, Ma_s and Ma_d respectively)

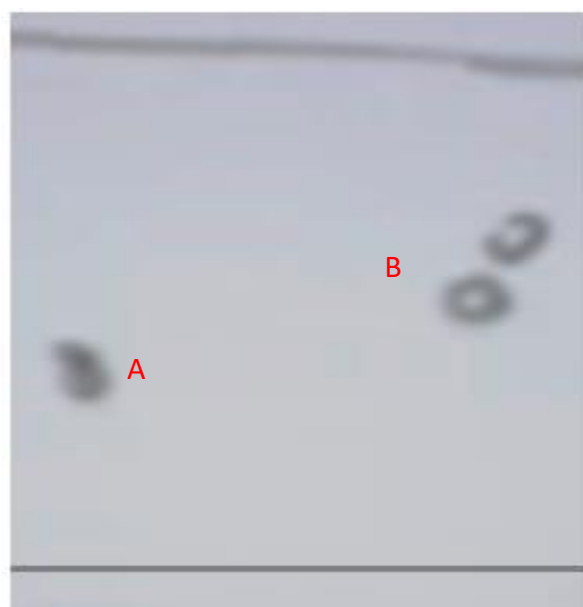


Figure 4-16: TLC for Ita using 80% cyclohexane and 20% ethyl acetate (The spot marked A= excess dimethyl itaconate and B= Ita)

Thereafter, the r_f values were evaluated (see Table 4-3 below) and used in the flash chromatographic separation of the modified β -diketones. The Figure 4-17 and Figure 4-18 below are the UV chromatogram of the components in the two modified mixtures as obtained during the chromatographic separation. In Figure 4-17, the first two peaks are due to the Htd and then follow by the products, Ma (single and double addition of methyl acrylate respectively). Similarly, in Figure 4-18, the first peak with a shoulder is

the starting material (Htd), follow by the product, and lastly the excess dimethyl itaconate. Some of the separated fractions of Ma mixture are as found in Figure 4-19; while the isolated Ita is given in Figure 4-20. The recovery yield obtained is about 60% (41% double addition and 19% single addition) for Ma; and 20% Ita.

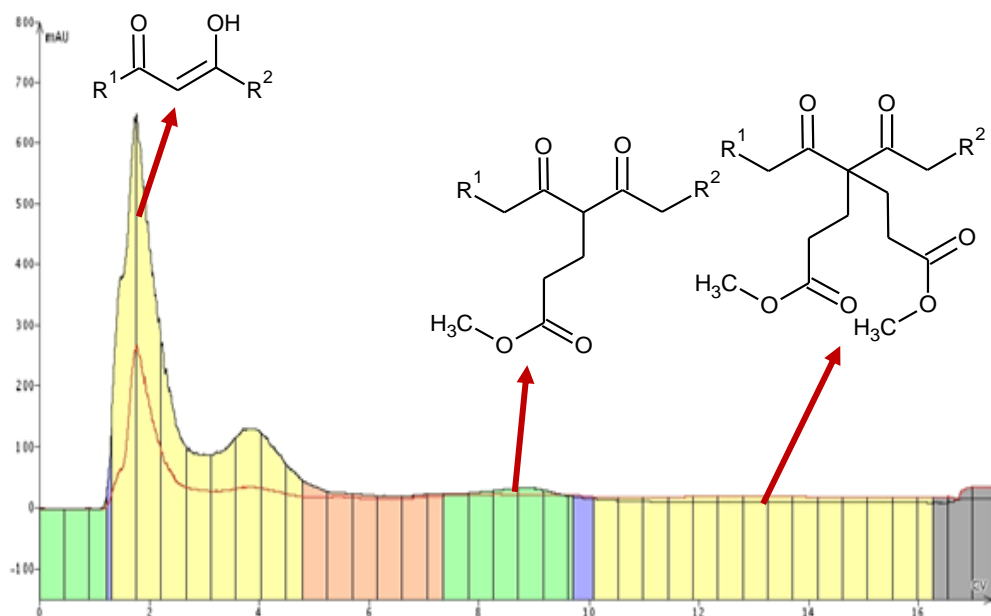


Figure 4-17: UV chromatogram for the separation Ma

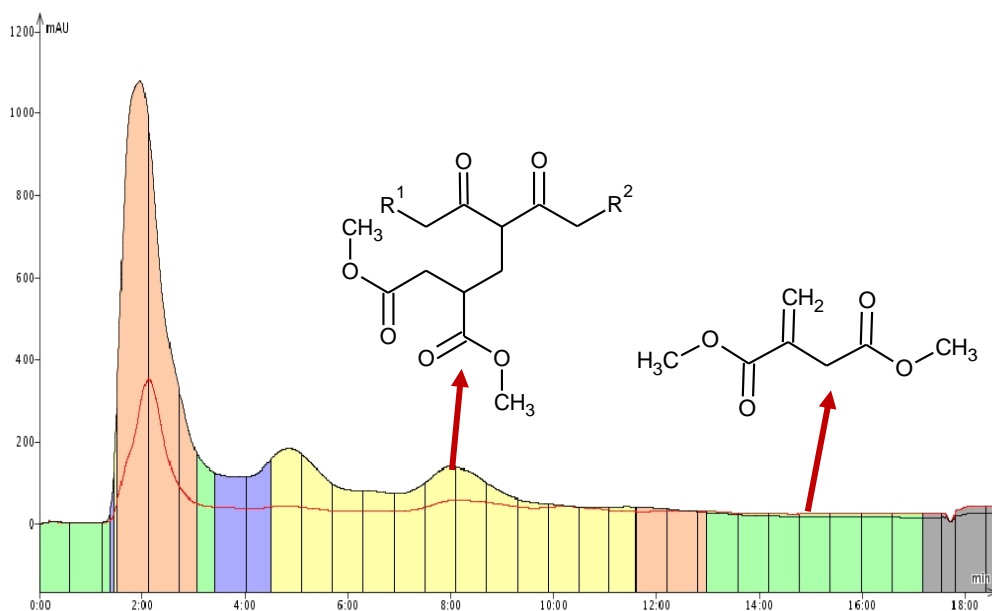


Figure 4-18: UV chromatogram for the separation Ita



Figure 4-19: Fractions collected from the purification of Ma

Ma_s = single addition product; Ma_s & Ma_d = mixture of single and double addition products, Ma_d = double addition product, a = the unreacted Htd



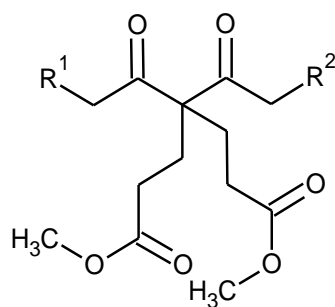
Figure 4-20: Sample of purified Ita

Table 4-3: The r_f of the Htd, Ma_s , Ma_d , and Ita using 80% cyclohexane and 20% ethyl acetate

Compounds	$r_f \pm 0.02$	structure
Htd	0.89	
Ma_s	0.59	

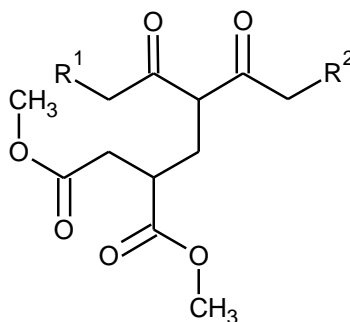
Ma_d

0.41



Ita

0.51



4.2.9 NMR spectra of modified Htd

The $^1\text{H-NMR}$ spectra were also used to characterise the Ma and Ita (see Figure 4-21 and Figure 4-22). The integral areas of the ester protons (a) on the modified β -diketones and the six terminal protons (y) on the either sides of the saturated long chain were compared. This was to check if the addition of the dimethyl itaconate and the methyl acrylate to Htd is single or double. From the integral ratios in Table 4-4, it can be deduced that the addition was only single for dimethyl itaconate and a mixture of single and double with methyl acrylate.

Table 4-4: Determination of the molar composition of the modified Htd

Sample	Integral ratio of protons (y: a)	Composition of the addition
Ma	6.00: 5.55	1: 2 (1 mole Htd: 2 moles methyl acrylate) – double addition of methyl acrylate
Ita	6.00: 5.30	1: 1 (1 mole Htd: 1 mole dimethyl itaconate)- single addition of dimethyl itaconate

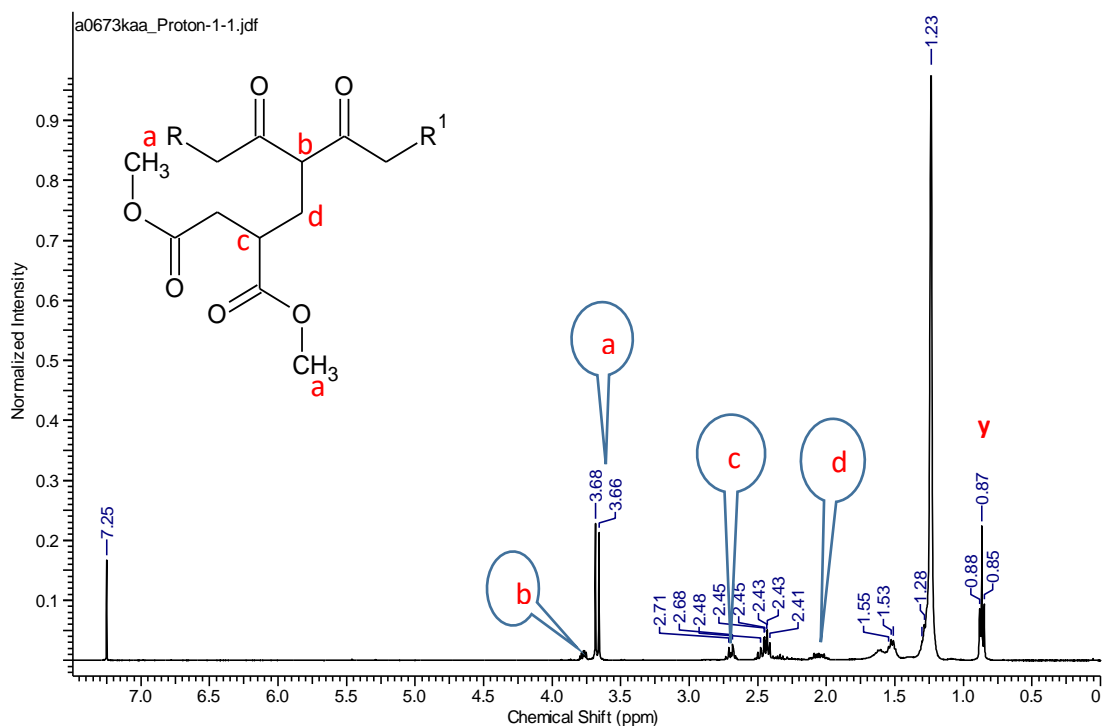


Figure 4-21: $^1\text{H-NMR}$ spectrum of Ita

For the modification with dimethyl itaconate, only single addition was observed. Thus, the methylene proton peak is shown in the Figure 4-21 above marked as 'b'. For the Ma, there was double addition, hence there was no signal of the of methylene proton. Chemical shift of about 3.65 ppm in both $^1\text{H-NMR}$ spectra in Figure 4-21 and Figure 4-22 is confirmation of ester protons on the Ita and Ma as it has been previously reported.²⁶⁸ The $^{13}\text{C-NMR}$ spectra of these modified β -diketones in Figure A-1 and Figure A-2 (as found in the appendix 1) has the carbonyl carbon peaks of 205 - 208 ppm^{keto}, 171 - 173 ppm^{ester} and 193 ppm^{enol}. These chemical shifts are consistent with previous literature report for β -diketones and esters carbonyl carbons.¹³⁹ This further confirmed the structure of Ma and Ita products.

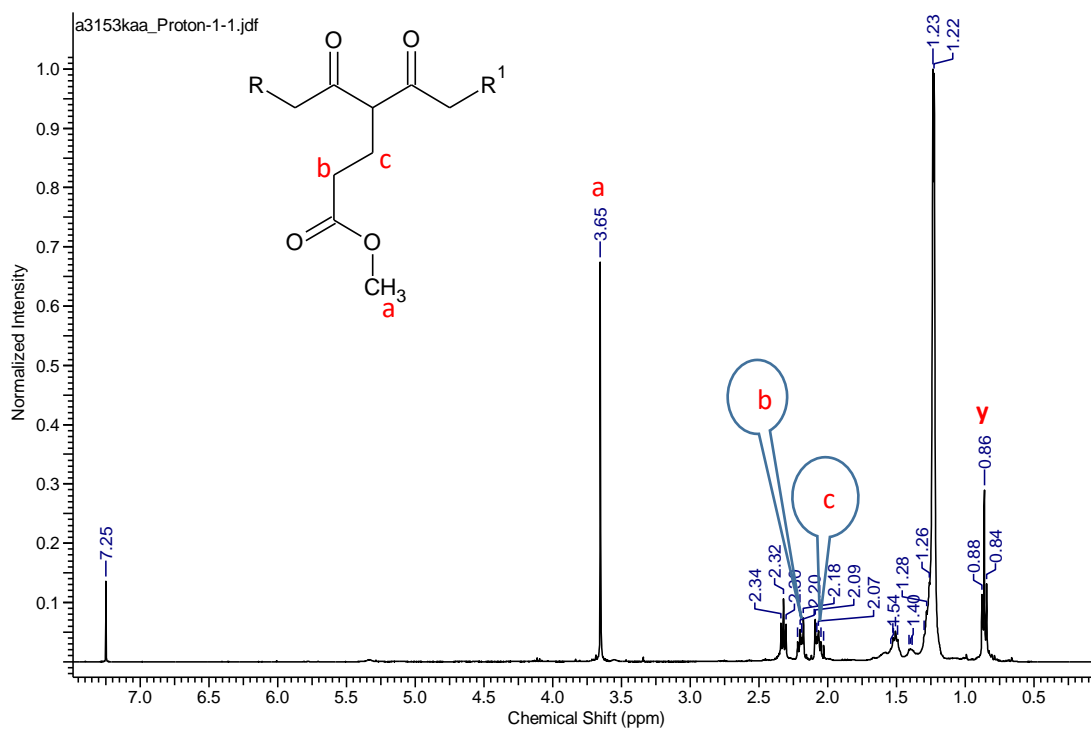


Figure 4-22: $^1\text{H-NMR}$ spectrum of Ma

4.2.10 FTIR of the modified Htd

The FTIR spectra of the modified Htd were collected as presented in Figure A-3 and Figure A-4 (see appendix 1) and the characteristic peaks are assigned in Table 4-5. The FTIR absorption of the most peaks of these modified β -diketones are similar to the unmodified Htd as earlier been pointed out in chapter two. However, there are significant differences in the FTIR absorptions of the carbonyl groups of the unmodified and these esters modified β -diketone.

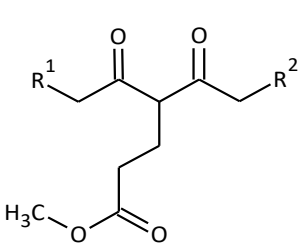
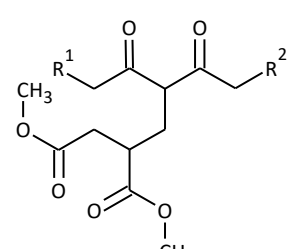
Table 4-5: Characteristic carbonyl peaks of the unmodified Htd and modified Htd

Samples	Characteristic IR (cm ⁻¹)	Ref
Unmodified Htd	1710 (keto C=O), 1640 (chelated enol C=O)	222,224,268
Ma	1723 (ester C=O), 1689 (enol C=O)	222,225,268
Ita	1735 (ester C=O), 1729 (ester C=O), 1717, 1692 (enol C=O)	222,225,268

4.2.11 DSC of the modified Htd

The melting points of the Ma and Ita were determined as 310 K and 319.7 K respectively (see Table 4-6) using DSC analysis. These values are lower than the melting point of the unmodified Htd (326.9 K) as presented in chapter two. This may be due the substantial H-bonding found in the unmodified Htd than in the Ma and Ita. Secondly, the Ma sample gave so much lower melting point compared to the Htd because of the sample is mixed of single and double addition products. The DSC thermograms are expressed in Figure 4-23.

Table 4-6: Determination of melting points of the Ma and Ita by DSC

Samples	Name	Melting points (K)	Heat flow(W/g)
	Ma	310.00	-1.6
	Ita	319.70	-3.4

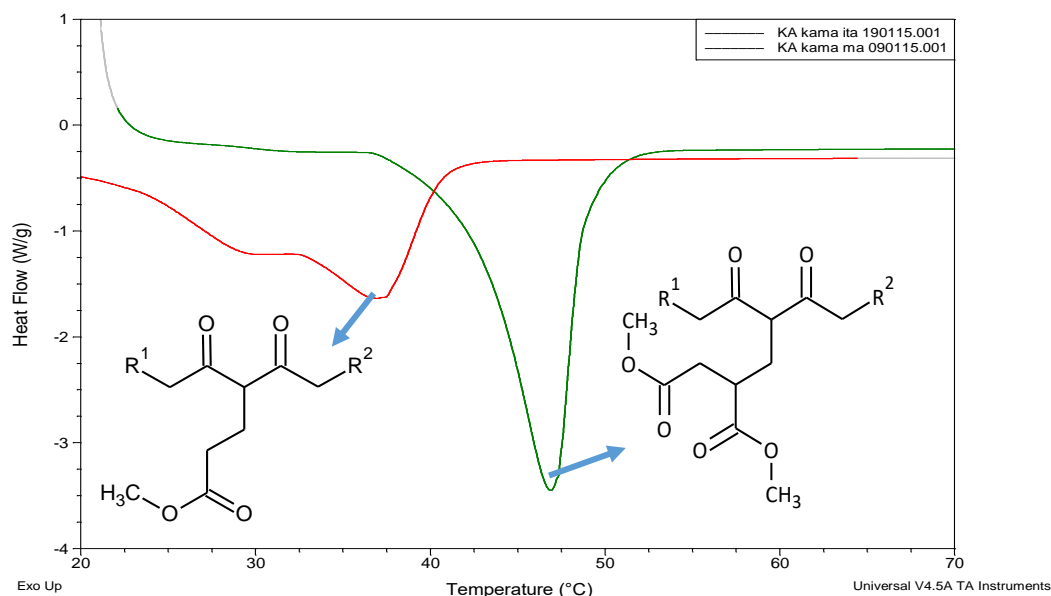
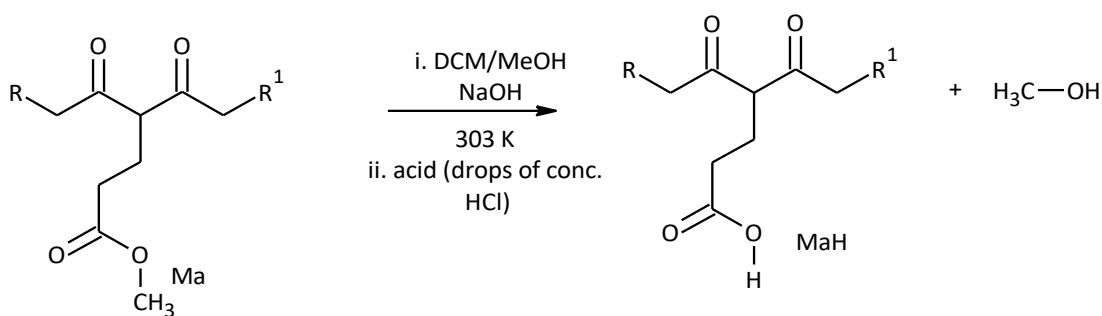


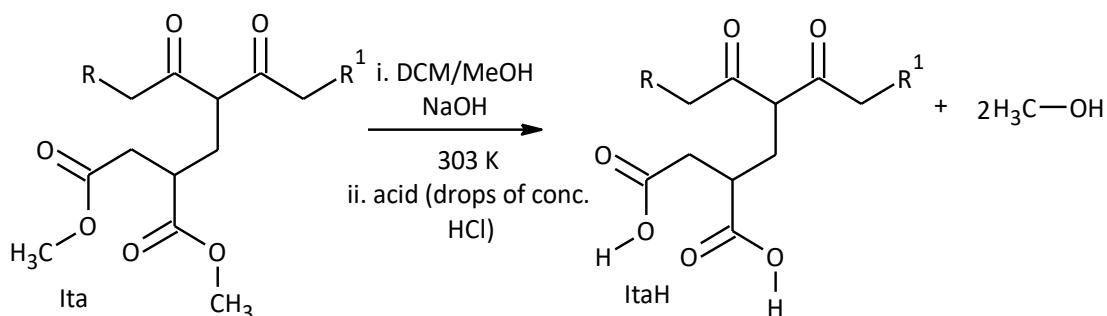
Figure 4-23: DSC thermograms of Ma and Ita

4.2.12 Preparation of the carboxylate acid of the modified Htd

Before the preparation of acid carboxylate of Htd, the hydrolysis of methyl palmitate and cinnamate were firstly investigated to find an appropriate condition to apply on the hydrolysis of modified bioderived β -diketones. Use of polar aprotic solvents for base hydrolysis of ester makes the reaction goes faster.²⁹² The complete hydrolysis of methyl palmitate took longer time than methyl cinnamate as is being reported.²⁶⁶ Therefore, the preparation of the carboxylate acid of methyl acrylate and dimethyl itaconate modified Htd (see Equation 4-7 and Equation 4-8) were performed following these predetermined conditions and the procedure reported by Theodorou *et al.*²⁶⁷ The better solubility of the modified Htd in DCM/MeOH enhances the hydrolysis. From pale yellow mixture at the start, the mixture eventually formed a white lump of sodium carboxylate salt of these modified β -diketone compounds.



Equation 4-7: Preparation of the carboxylate acid of the methyl acrylate modified bioderived β -diketone (MaH)



Equation 4-8: Preparation of the carboxylate acid of the dimethyl itaconate modified bioderived β -diketone (ItaH)

4.2.13 NMR spectra of the carboxylate acid of the modified β -diketones

The ^1H -NMR spectra for the MaH and ItaH indicate formation of carboxylate acid functional group (see Figure A-5 and Figure A-6 in the appendix 1) because the ester protons (with chemical shift of 3.66 ppm) in the ^1H -NMR spectra of the unhydrolysed modified β -diketones as previously presented in section 4.2.9 were lost. Similarly, the alkaline hydrolysis of these modified compounds were conducted at long time (24 h) like the hydrolysis of methyl palmitate. According to Khurana *et al.*,²⁶⁶ the hydrolysis of aliphatic esters are known to take a longer time than aromatic esters.

The integral ratio of peaks **a**: **b** in ^1H -NMR spectra before and after hydrolysis of the Ma and Ita were the same. This indicates that the original backbone of the compound did

not decompose; but only the ester unit that had been converted into the carboxylate acid group. In addition, the ^{13}C -NMR spectra of the ItaH and MaH in Figure A-7 and Figure A-8 (in the appendix 1) showed the chemical shifts at 179 - 180 ppm which is due to carbon of the carboxylate acid functional group. 130 ppm peaks in these spectra are attributed to the alpha enol carbon adjacent to the carbonyl centre for these carboxylate acids modified β -diketones. Again the chemical shifts of 207 – 210 ppm observed in the ^{13}C -NMR of these carboxylate acids are due to carbon peaks for the keto groups on the long chain β -diketone moiety. The chemical shifts for MaH and ItaH are quite similar which implies similar chemical structures. In addition, apart from the carbonyl regions, the rest of the ^{13}C -NMR shifts in of the MaH and ItaH are quite alike as was observed in the ^{13}C -NMR of the Ma and Ita.

4.2.14 ESI-MS of the carboxylate acids of modified Htd

Electrospray ionization mass spectroscopic technique (ESI-MS) has already been established as a powerful tool in the characterization of small and large molecules.²⁹³ Thus ESI- mass spectra of the MaH and ItaH were collected in order to further confirm their structures. These ESI-MS spectra are presented in Figure 4-24, Figure 4-25 and Figure 4-26 with the labelled peaks. Then the ions (m/z) are interpreted (assigned) in Table 4-7, Table 4-8 and Table 4-9.

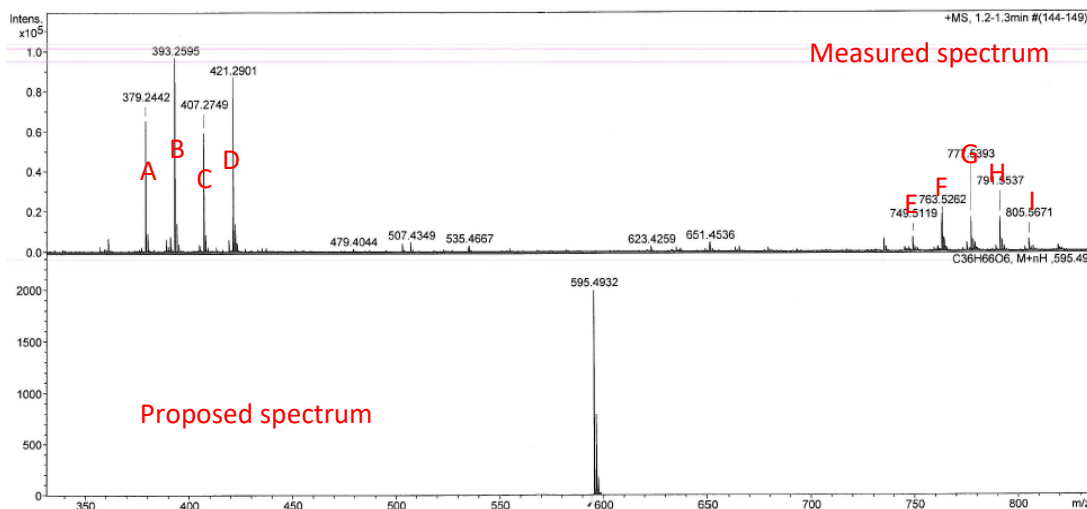


Figure 4-24: ESI (+)-MS of the ItaH

Table 4-7: Proposed assignment of the ESI (+)-MS peaks of the ItaH

ESI(+)-MS peaks (m/z)	Label	Interpretation
-	M	Expected molar mass (594)
379.2442	A	Loss of CO (28) from C, 407.2749 m/z
393.2595	B	Loss CO (28) from D, 421.2901 m/z
407.2749	C	$[594-211^* + \text{Na}]^+$
421.2901	D	$[M-211^* + \text{K}]^+$
749.5119 - 805.5671	E - I	Impurities

211* ($\text{C}_{15}\text{H}_{31}$) is dissociated fragments of the β -diketone as described in Figure 4-27

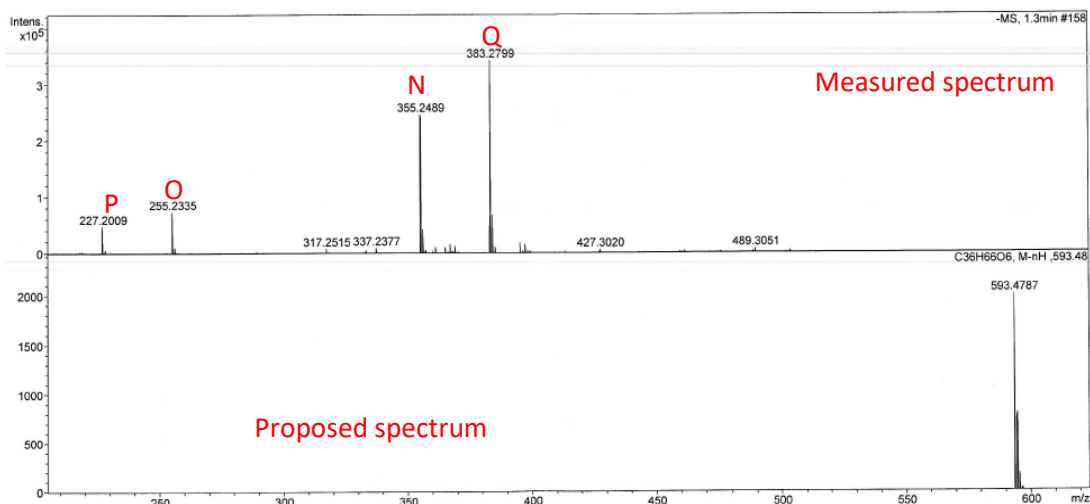


Figure 4-25: ESI (-)-MS of the ItaH

Table 4-8: Proposed assignment of the ESI (-)-MS of the ItaH

ESI(-)-MS peaks (m/z)	Label	Interpretation
-	M	Expected molar mass (594)
383.2799	Q	$[M-211]^-$
355.2489	N	$[M-239]^-$
255.2335	O	$[383 - 128 (C_5H_4O_4)]^-$
227.2009	P	$[255-128]^-$

Note: 239* ($C_{16}H_{31}O$) is a dissociated fragment from the β -diketone as described in Figure 4-27

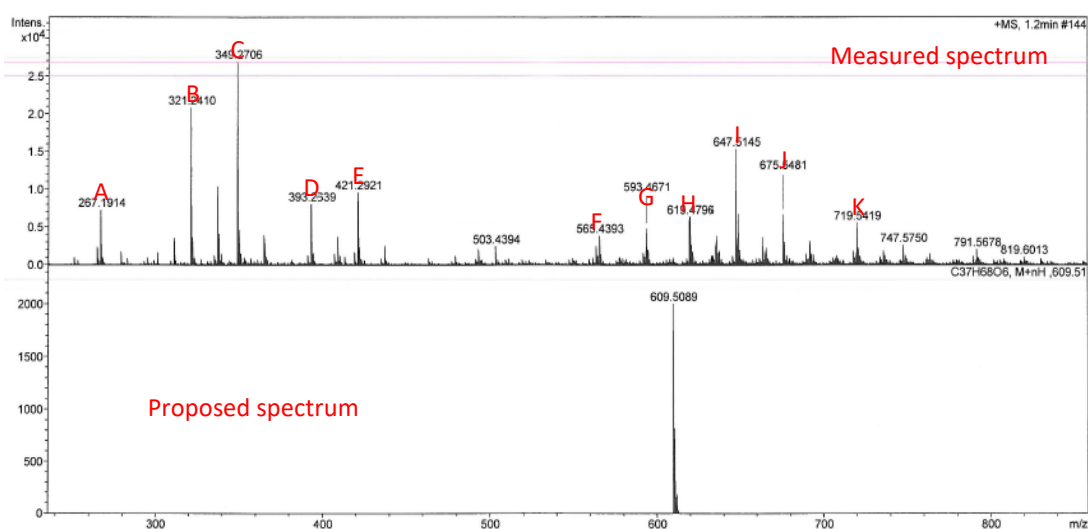


Figure 4-26: ESI (+)-MS of the MaH

Table 4-9: Proposed assignment of the major ESI (+)-MS peaks of the MaH

ESI(+)-MS peaks (m/z)	Label	Interpretation
-	Ma_s and Ma_d	Expected molar mass (536 and 608)
321.2410	B	Loss of CO from C, 349.2706 m/z
349.2706	C	$[Ma_s - 211 + 23]^+$
393.2639	D	Loss of CO (28) from E, 421.2921 m/z or M-239
421.2921	E	$[Ma_d - 211 + Na]^+$
565.4393	F	Loss of 28 (CO) from G, 593 m/z
593.4771	G	$[Ma_s + K + H_2O]^+$

619.4796	H	Loss of 28 from J, 647.5145 m/z
647.5145	I	[Ma _d +K] ⁺
675.5481	J	Loss COO from 719.5419 m/z
719.5419	K	[Ma _d +5Na – 4H] ⁺

Ma_s = Product of the single addition of acrylate and Ma_d= Product of the double addition of methyl acrylate

As earlier explained, ESI-MS is one of the soft ionization technique which usually produce predominantly sodium, potassium and proton ionic species of the molecule in question. Such less ionization was also observed in this study for the analysis of the Htd; the Ma and Ita. However, with the MaH and ItaH, there were more ions in addition to the sodium and potassium cationic species which is due to some fragmentation. Protonated species, [M+H]⁺ common in ESI(+)- MS were absent as it has been similarly reported.²⁹⁴ Prominent ions observed in the spectra (see Figure 4-24 and Figure 4-26) are as result of the splitting of the carboxylate acids modified Htd as described in Figure 4-27. The Loss of 211 (C₁₅H₃₁) or 239 (C₁₆H₃₁O) masses were observed for both the Ma and Ita (as earlier discussed in section 4.2.2) and also in the MaH and ItaH. But the fragmentation was more pronounced in the case of the MaH and ItaH (see Figure 4-27) than the carboxylate esters analogues. Ramaroson-Raonizafinimanana *et al.*²¹⁴ had also observed similar fragmentation of such lipophilic β-diketones as it was found in the mass spectrum of 2,4-diketone silyl ether derivatives described in Figure 4-28.

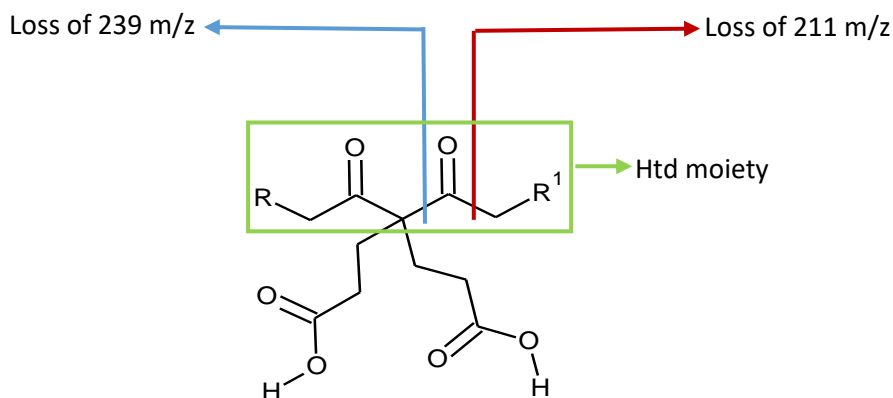


Figure 4-27: Proposed dissociation (fragmentation) of Htd derivatives as found in ESI-MS(+)

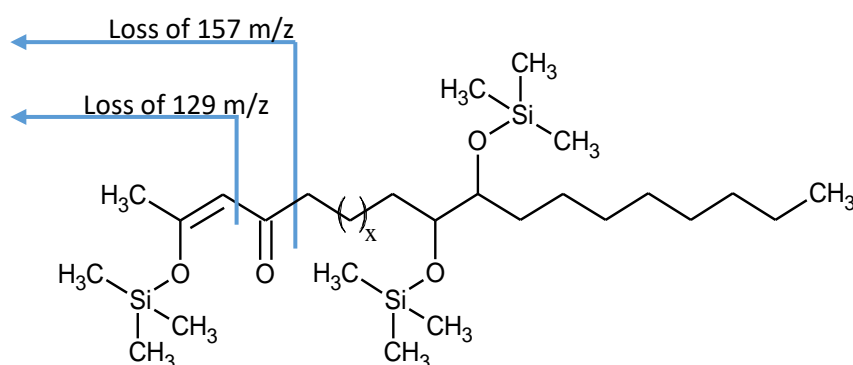
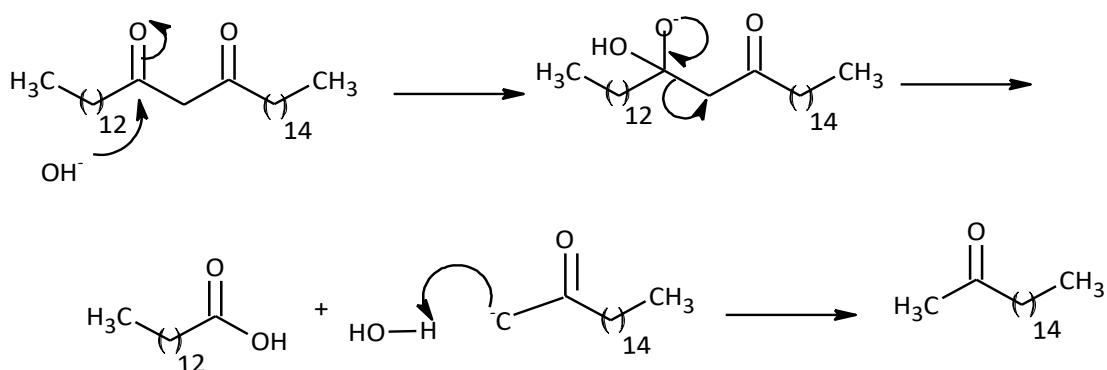


Figure 4-28: Fragmentation of long chain 2,4-diketone silyl ether derivatives

This proposed dissociation was used to interpret most of the peaks found in the ESI(-)-MS of these MaH and ItaH in Table 4-7, Table 4-8 and Table 4-9. According to Leenheer *et al.*,²⁹⁴ the ESI(+)-MS of fulvic acid has been shown to lose CO, COO, H₂O, carbon and proton. Furthermore, Brent *et al.*²⁸⁷ reported losses of COO (m/z 44), H₂O (m/z 18), CO (m/z 28) or combinations of losses CO and H₂O (m/z 46), COO and H₂O (m/z 62) in coupled IC/ESI-MS/MS characterisation of branched aliphatic monoacids, branched and straight chain aliphatic diacids. These show that group of atoms could be lost even from soft ESI-MS technique. In addition, 407.2757 m/z and 421.2924 m/z; 407.2749 m/z and 421.2921 m/z were observed in the Ita and ItaH; Ma and MaH respectively. These show that there was fragmentation of these compounds during the ESI-MS analysis.

On the other hand, side reaction like retro-Claisen (see Equation 4-9 below) may occur on the backbone of the β -diketone especially the one without α -proton in the presence of OH^- bringing about its decomposition.²⁹⁵ If this was the case, then hydrolysis of the predominantly double addition product of Ma will result into significant decomposition. Also Ita should be stable under alkaline condition because it has an alpha proton. However, the evidence obtained in this work show that the modified β -diketones may not have been decomposed appreciably during the hydrolysis. Both $^1\text{H-NMR}$, ESI(+)-MS and FTIR spectra of the hydrolysed modified Htd have common pattern of peaks. Similarly, it was suggested that, retro-Claisen is not able to complete on 14,16-hentriaconatane,¹⁶⁶ likely due favourable enolate formed in the presence of OH^- .



Equation 4-9: Retro-Claisen pathway for β -diketone¹⁶⁶

4.2.15 FTIR of the MaH and ItaH

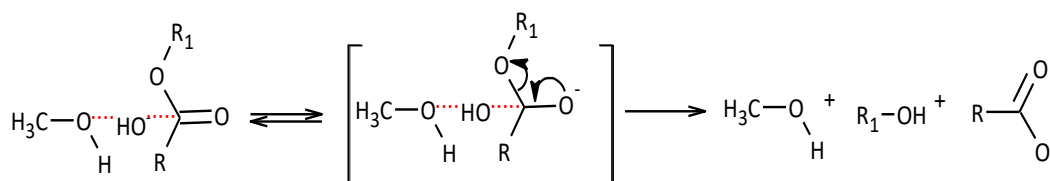
The FTIR spectra of the Ma and Ita after hydrolysis were compared to the unhydrolysed modified Htd. The C=O stretching frequencies of the MaH and ItaH (see Figure A-9, Figure A-10 in appendix 1 and Table 4-10) were different from the C=O absorption frequencies found in the Ma and Ita as previously discussed in section 4.2.10

Table 4-10: FTIR of the carboxylate acid of the modified Htd

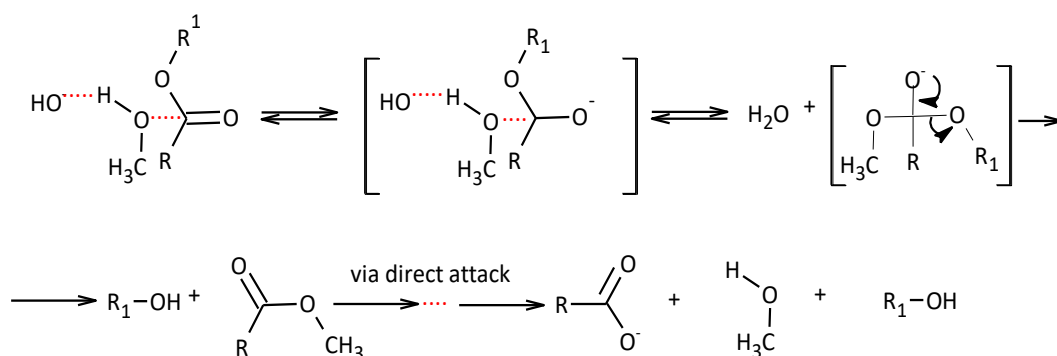
FTIR (cm ⁻¹)	Interpretation	Literature reference for such functional group
3600 - 2800	Broad; O-H stretching vibration for intermolecular H-bonding	222
2916 – 2849	Strong; C-H stretching vibration	222
1698- 1693	Strong, C=O stretch vibration	296
1463 -1433	CH ₂ scissoring deformation	296
1426-1379	Strong; C-H bending vibrations, SP ³	222
1283-1289	C-OH stretch	296
1235	C-O	220
1110	C-O	225
933-941	CH ₂ and CCOO twist deformation	296

FTIR carbonyl stretch for the carboxylate acids of the modified β -diketones were observed as 1698 and 1693 cm⁻¹ which has been similarly reported.²⁹⁶ All the FTIR carbonyl frequencies of the Ma and Ita as previously determined are higher than their carboxylate acids analogues. Max and Chapados²⁹⁶ reported that the acetic and acrylic acid carbonyl bands were situated at 1706 and 1703 cm⁻¹ respectively which is different from the average carboxylate carbonyl absorption band of 1723 cm⁻¹, these low positions are attributed to the formation of dimers through hydrogen bonds that weaken the carbonyl bond. The carboxylate acids of these modified β -diketones also have comparable carbonyl vibration bands of about 1700 cm⁻¹. This showed pronounced dimerization of the carboxylate acid of the modified Htd. Furthermore, broad FTIR absorption at 3600 – 2800 cm⁻¹ signifies O-H stretching vibration for intermolecular H-

bonding of the carboxylic functionality in these compounds after hydrolysis as highlighted in Table 4-10 above. The O-H vibration of these MaH and ItaH were observed to overlap with the C-H absorption. The 3000 and 2600 cm^{-1} bands in carboxylate acids were previously assigned to the carboxyl OH groups that are hydrogen-bonded to other carboxyl groups.²⁹⁶ Therefore, the mechanism for these hydrolysis is expressed in Scheme 4-10 and Scheme 4-11 below as it was proposed by Theodorou *et al.*²⁶⁷



Scheme 4-10: Scheme for the formation of the carboxylate acids of the modified Htd via direct hydrolysis



Scheme 4-11: Scheme for the formation of the carboxylate acids of the modified Htd via alcoholysis

4.3 Conclusion

In this chapter the Htd has been modified by a KF/alumina mediated Michael addition reaction under solventless condition with methyl acrylate and dimethyl itaconate using microwave and conventional heating. Methyl acrylate formed single and double addition with the bioderived β -diketone, while the itaconate formed only single addition. The optimal temperature for this reaction was 393 K. The modification was also dependent

on the amount of $\text{KF}/\text{Al}_2\text{O}_3$ used and the time of reaction. The recovery yield for the acrylate modified β -diketone of 60% was higher than recovery yield of dimethyl itaconate modified Htd (20%). After separation/purification of the modified β -diketones, the products were characterised using the techniques NMR, FTIR, ESI-MS, GC-FID and DSC. The Ma and Ita were hydrolysed to form MaH and ItaH which were again characterised with FTIR, ESI-MS and NMR analyses. The whole purpose of this is to make better metal-chelating Htd through modification.

Chapter 5

Metals extraction with the unmodified and modified bioderived β -diketone

Aspects of the work described in this chapter have appeared as:

Kaana Asemave, Andrew J. Hunt, Thomas J. Farmer, James H. Clark and Fergal Byrne. Alternative bioderived chelating agent (chelant) for metal recovery. Being a poster abstract for 2nd international conference on Past and Present Research Systems of Green Chemistry; Orlando, USA. Sept. 14-16, 2015

5 Chapter 5

5.1 Introduction

Metals are applied in modern low-carbon energy technologies such as; nuclear, solar, wind, bioenergy, carbon capture and storage (CCS), electricity grids,^{21,22} and manufacturing of consumer goods such as cell phones, television and computers.^{31,297} However, the natural deposits of metals are depleting with time, hence there is need to recover metals dispersed in the environment. Recently metals recovery using bio-derived materials has seen increased attention for the sake of long-term elemental sustainability.^{47,121,156,298–300} Chelating agents can be used to extract metals from the environment in order to enhance metal recovery, prevent toxic emissions and for removal of unwanted metals in chemical processes or products, such as in the case of removing metal catalysts from pharmaceuticals.

The extraction of metals with β -diketone chelators has been widely reported.^{86,153,301} Other classes of chelators, such as carboxylic acids, ketones, alcohols, ethers and esters have also been used as metals extractants.⁹⁰ Recently alternative more-benign chelating agents are preferred for metals recovery in order to avoid negative environmental impact from continuous use over variety of applications.^{10,302} More so, hydrophobic metal chelating extractants are crucial because they will not be so easily lost into the environment via aqueous waste streams.³⁰³ This has led to the search for new low-cost chelants where biomass is seen as preferred feedstock, thus further improving the sustainability of the concept of metal recovery.⁴¹ Thus, bio-derived lipophilic β -diketones will be useful in this regards. In addition, these lipophilic β -diketones will not be easily released into the environment like the commonly used chelants; hence they will have a

less negative impact on the environment. However, there is currently limited evidence on the use of bio-derived lipophilic β -diketones and their modified analogues (3-substituted lipophilic β -diketones) in metal recovery, despite the obvious promise of their use.

Moreover, metal extraction via chelation is regarded as an economical process,⁸⁶ especially with lipophilic extractants, because the chelant can be recycled and reused. Furthermore, solvent extraction techniques are among the most studied methods for the production and recovery of various metal ions from different sources because of their simplicity, speed and wide scope.³⁰⁴ It has also been highlighted that solvent extraction technologies are particularly good for recovery of metals from secondary sources, such as low grade ores and mixed metals and can lead to excellent material and energy balances.⁸⁹ Hence, this chapter describes the use of unmodified or modified (carboxylates esters and acids) Htd to remove metal ions; Ni(II), Co(II), Cu(II), Fe(III), Cr(III), Pb(II), Mn(II) and Ga(III) in liquid biphasic system in comparison to currently commercially available Hdbm and Hacac.

5.2 Results and discussion on the extraction of metals with the unmodified and modified Htd

Before looking at the comparison of different metal extracted with different chelators we first wanted to understand better the key factors affecting metal extraction such as time, solvent, pH, ionic strength and temperature. This initial study was carried out solely for the extraction of Cu(II) with the Htd because Cu-diketonates are known to be stable over a broad pH range.¹⁰ More so the complexes of transition metals are found to be highly stable compared with those of non-transition elements.¹⁰ Attention is also given

to copper recovery partly because of its technological and biological importance. Additionally copper species such as $\text{Cu}(\text{OH})^+$, $\text{Cu}_2(\text{OH})_2^{2+}$ and CuCO_3 are reported as toxic, and as such that reduced emission into the environment is highly desirable.³⁰⁵ Also slope analysis for the extraction of $\text{Cu}(\text{II})$ was studied. In addition, UV/visible, FTIR and $^1\text{H-NMR}$ spectra evidence of some of the selected metal β -diketonates with the Htd were obtained. Furthermore, the effect of pH and initial metal ion concentration for the extraction of $\text{Cu}(\text{II})$ was carried out using the Ma, MaH, Ita and ItaH modified β -diketones in comparison to Htd (unmodified) and Hdbm (commercial fossil-derived chelator). Based on this initial results the study was further expanded to the extraction of $\text{Pb}(\text{II})$, $\text{Mn}(\text{II})$, $\text{Ga}(\text{III})$, $\text{Ni}(\text{II})$, $\text{Co}(\text{II})$, $\text{Cu}(\text{II})$, $\text{Fe}(\text{III})$ and $\text{Cr}(\text{III})$.

5.2.1 Influence of contact time on the removal of $\text{Cu}(\text{II})$ from $\text{Cu}(\text{OAc})_2$ solution

A study into the influence of time on $\text{Cu}(\text{II})$ extraction from 0.03 M $\text{Cu}(\text{OAc})_2$ solution with 3 mM Htd and Hdbm (in limonene) was conducted at 1, 3, 5, 10, 30, 60 and 120 min contact time. Maximum extraction of 105 mg/L and 128 mg/L of $\text{Cu}(\text{II})$ (with Htd and Hdbm respectively) was found in at least after 30 min. This rapid contact time for $\text{Cu}(\text{II})$ extraction has also been reported in various other accounts in the literature.^{263,306–309} This result is as presented in Figure 5-1.

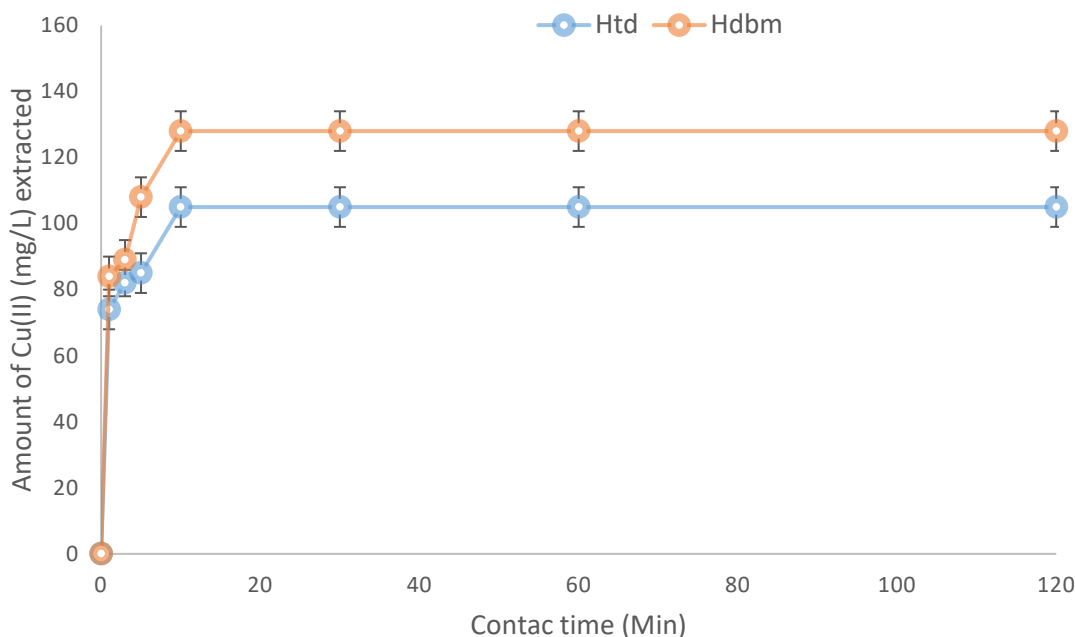


Figure 5-1: Effect of contact time on the removal of Cu(II) from Cu(OAc)₂ solution using Htd and Hdbm (in limonene; M: L; 10:1)

A similar contact time effect was also observed using β -diketone-functionalized styrene-divinylbenzene copolymeric resin³¹⁰ where an equilibrium for the extraction of the metals ions; Pb(II), Ni(II), Cd(II), Cr(VI) and Co(II) was reached within 60 - 100 min.³¹⁰ According to Fanou *et al.*,²⁶³ a contact time of 30 min was used for the extraction of Pb(II), Cu(II), Zn(II) and Fe(III) from aqueous solution by δ -diketones for this reason. Gerald *et al.*³¹¹ also reported performing an extraction of Co(II) from aqueous solution using β -diketone (1-phenyl-3-methyl-4-(p-nitrobenzoyl)pyrazolone) for 30 min.³¹¹ Similarly Begum *et al.*³¹² also observed that the contact times required to achieve equilibrium for the extraction of Cu(II), Ni(II) and Zn(II) with the commercial extractant, Cyanex 272 were all less than 20 min. In most previously reported cases it appears that the extraction equilibrium of copper using β -diketones such as Hacac, Hbac and Hdbm is typically reached in only a few minutes. Furthermore, Gupta and Singh reported extraction of Pt(IV) and Pd(II) with Cyanex 923 and found that a minimum of just 3 min and 4 min

shaking time was sufficient for attaining maximum extraction of Pt(IV) and Pd(II) respectively, and that excess shaking did not affect the eventual extraction of these metal ions.³¹³

5.2.2 Effect of Htd concentration on removal of Cu(II) from Cu(OAc)₂ solution

The influence of substrate concentration on a reaction or process is usually found to be an important factor affecting rates and overall yields, the same likely being application to the process of extraction. Therefore, an extraction of Cu(II) was tested using varying concentrations of Htd to determine the influence of Htd concentration on the extraction process. The results of extraction of Cu(II) from 0.02 M Cu(OAc)₂ with 4.31 – 0.34 mM of the Htd show increases in the levels of Cu(II) ions extracted (19 – 95 mg/L) with increasing amounts of the extractant; this is obviously linked to the fact that the total number of active chelating sites increased with increasing chelant present. The result is displayed in Figure 5-2 below. Similarly, evaluation of the % of free Htd from the varying concentration of Htd used in this Cu(II) extraction implied increased in free Htd as the initial amount of the Htd was increased. That, the % free Htd for using 4.31 mM was 65% whereas, 15% free Htd was deduced from using smaller amount of Htd (0.345 mM) for this particular extraction of Cu(II). The plot of Cu(II) extracted against the percentage of free Htd is as given in Figure 5-3.

Previous studies have indicated the same enhanced extraction of metals ions with increasing amount of the metal extractant.^{86,153,263,314} Furthermore, during the extraction of copper from ammoniacal solutions, Sengupta *et al.*³¹⁴ observed an increase in copper extraction rates with an increase extractant (oxime) concentration. It was again reported

that the % extraction of Cu(II), Zn(II) and Ni(II) was increased by increasing the concentration of Cyanex 272.³¹²

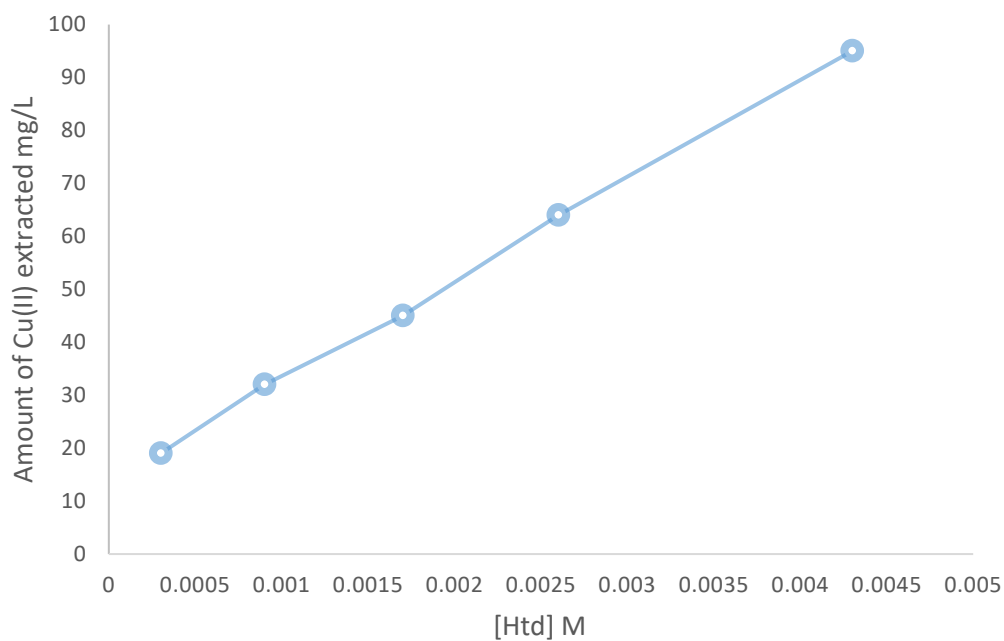


Figure 5-2: Cu(II) extraction from Cu(OAc)₂ solution with different amount of the Htd

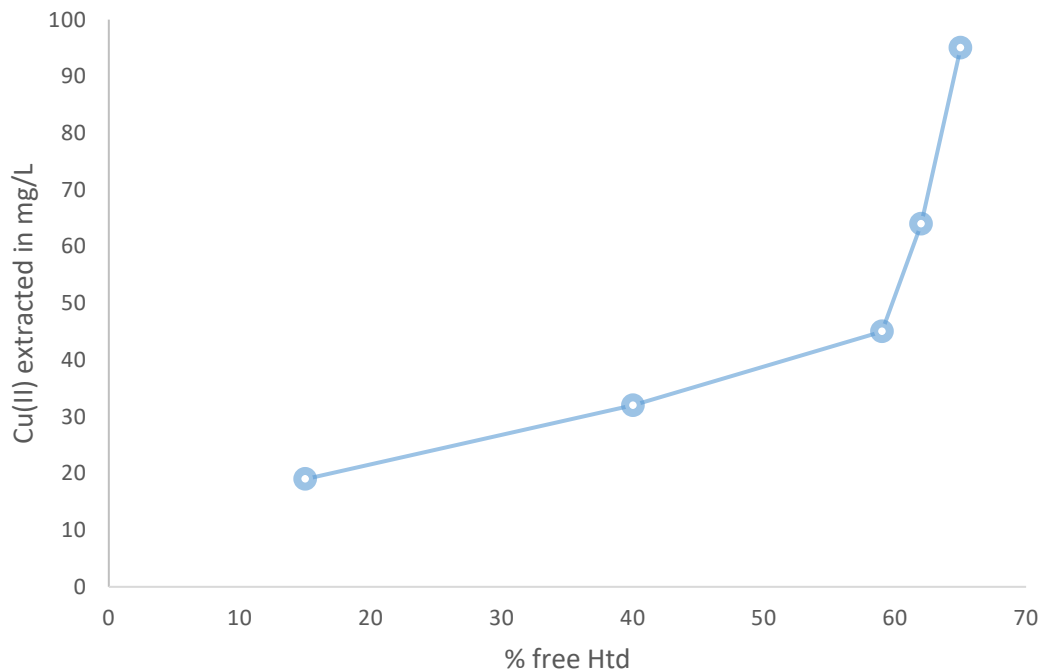


Figure 5-3: Cu(II) extracted (i.e. from 0.02 M Cu(OAc)₂) versus % free Htd (initial concentration of Htd = 4.31 – 0.34 mM)

5.2.3 Slope analysis for Cu(II) extraction from Cu(OAc)₂ solution with Htd

Slope analysis is a common method for stoichiometric assessment in the solvent extraction of metals. In order to achieve this, the distribution constants for the removal of Cu(II) from Cu(OAc)₂ solutions with different concentration of the Htd and pH were carried out. Then equilibrium slope analysis for the extraction were obtained as plots of logD vs [Htd] and logD vs ΔpH as given in Figure 5-4 and Figure 5-5. These plots show the dependence of distribution constant on the amount of chelator and pH as previously found.³⁶ Generally the slope of such plots are taken as the mole of the ligand (in this case the β-diketone) required for 1 mole of the metal ion, or as the mole of H⁺ release for extraction of 1 mole of metal respectively.^{311,315} Sepulveda *et al.*³¹⁶ also reported plots of logD as function of equilibrium pH and log [chelator] from which the slope was used to obtain the stoichiometry of the equilibrium of extraction equation. Table 5-1 is the determined distribution of Cu(II) based on the concentration of the β-diketone.

Table 5-1: Dependence of distribution of Cu(II) on concentration of the Htd

[Htd], M	Log [Htd]	D	Log D	ΔpH	Log D
0.00156	-2.8069	0.16662	-0.7783	0.48	-0.7783
0.00094	-3.0269	0.08258	-1.0831	0.26	-1.0831
0.00062	-3.2076	0.05006	-1.3005	0.10	-1.3005
0.00031	-3.5086	0.02945	-1.5309	0.02	-1.3010

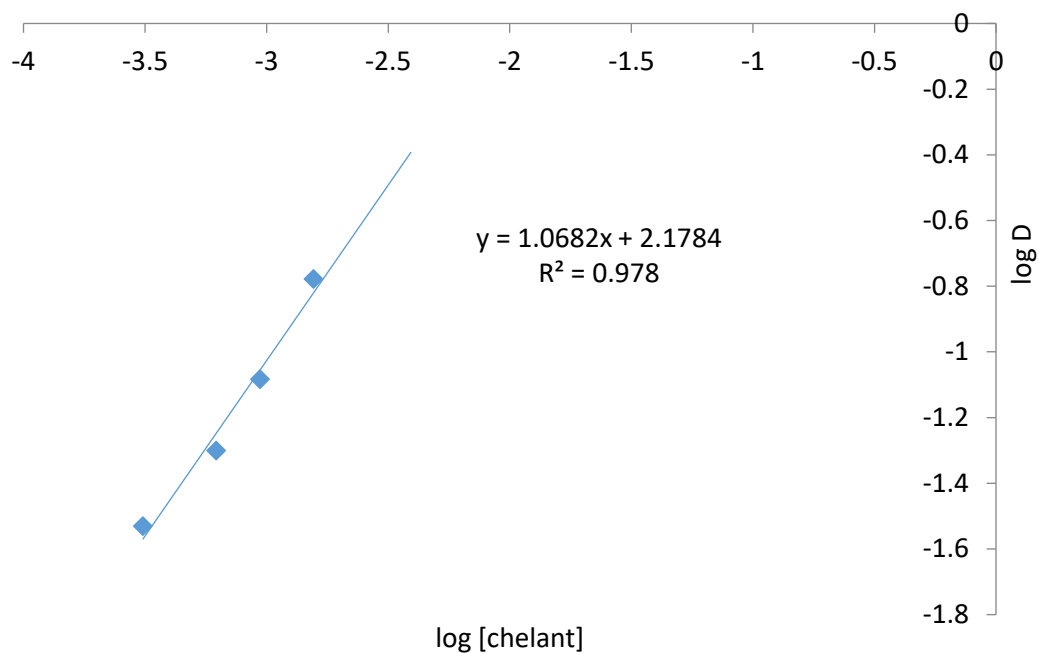


Figure 5-4: Plot of the $\log D$ vs $\log [\text{Htd}]$ for the extraction of $\text{Cu}(\text{II})$ from $\text{Cu}(\text{OAc})_2$ solution

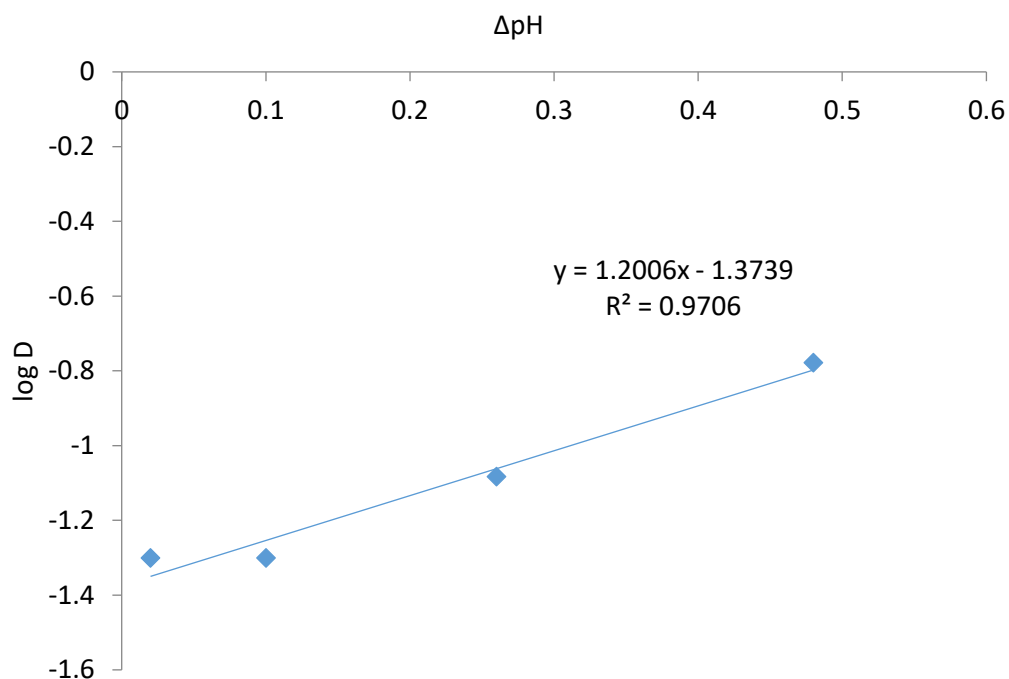
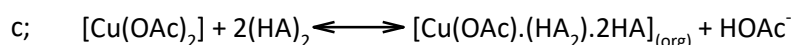
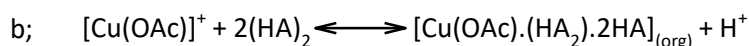
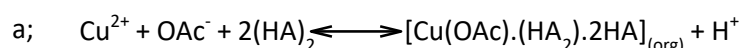


Figure 5-5: Plot of $\log D$ vs ΔpH for the extraction of $\text{Cu}(\text{II})$ from $\text{Cu}(\text{OAc})_2$ solution with the Htd

The plots of $\log D$ vs $\log [\text{Htd}]$ and plot of $\log D$ vs ΔpH have slopes of approximately 1 implying that there is involvement of one mole of β -diketone and release of one proton

for each mole of Cu(II) extracted. Therefore, the stoichiometry for the removal Cu(II) from Cu(OAc)₂ solution with the Htd under this condition is 1:1, Cu: L.

Begum *et al.*³¹² performed Cu(II), Zn(II) and Ni(II) extraction with cyanex 272 (dissolved in hexane) and found that at lower OAc⁻ ion concentration (0.01 to 0.05 M), the distribution ratio of Cu(II) increased with increase in OAc⁻ ion, after that the distribution ratio was independent in the OAc⁻ concentration in the medium range of 0.05 to 0.25 M. Subsequently, at higher OAc⁻ ion concentration of 0.25 - 0.5 M, the extraction efficiency decreased. This happened because OAc⁻ ion concentration increased in the aqueous phase, the species Cu(II), [Cu(Ac)]⁺ and [Cu(Ac)₂] were formed gradually (see Scheme 5-1).³¹²

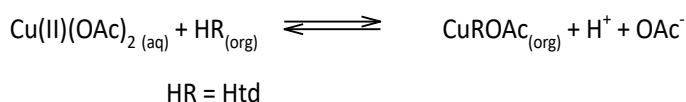


Scheme 5-1: Equilibria for Cu(II) extraction with Cyanex 272 at low (a), medium (b) and high OAc⁻ concentrations

Begum *et al.*³¹² also found out that for nickel extraction, the percentage of extraction increased with increase in acetate ion concentration (0.01 to 0.5 M). For the extraction of zinc, the extraction percentage was increased slowly with acetate ions. These facts imply the involvement of OAc⁻ ion in the copper complex formed in the organic phase. Therefore, in the present studies also, there is that high chance that there was involvement of OAc⁻ in the Cu-diketone complex as previously reported especially that

the experiments were conducted with at least 5-fold excess amount of the Cu(OAc)₂ solution.

Others have also reported that stoichiometry depends largely on the concentration of ligand.^{161,311} According to Gerald *et al.*,³¹¹ plot of log D of Co(II) against log [1-phenyl-3-methyl-4-(p-nitrobenzoyl)pyrazolone, HPMNP] has a slope of 1.0 at lower concentrations of HPMNP and a slope of 2.0 at higher concentration of HPMNP. It was assumed that Co(II) was initially extracted as Co(PMNP)⁺ and at higher concentration, the cationic species changes to Co(PMNP)₂. Such charged metal complex was also found by Lertlapwasin *et al.*³⁰⁷ while extracting Cu(II) with ionic liquid combined with 2-aminothiophenol ligand. Furthermore, Begum *et al.*³¹² also plotted log D vs equilibrium pH of the extraction Cu(II), Ni(II) and Zn(II) with Cyanex 272 and observed it was linear with a slope of 1 implying the release of H⁺ during the extraction of the metal ions. In addition, β-diketones are known to form neutral complexes by cation exchange.³¹⁶ Therefore, based on this present studies of the equilibrium slope analysis, a proposed equilibrium for the Cu(II) extraction with the Htd is given below in Equation 5-2. Such cationic exchange equilibria of extraction of metal with Htd have been similarly reported in other works.^{58,316}



Equation 5-2: The equilibrium equation for extraction of Cu(II) with Htd

5.2.4 Effect of pH on the extraction of Cu(II) from Cu(OAc)₂ with Htd

Solvent extraction of metal ions is dependent on the equilibrium pH as well,¹⁶¹ because chelators are effective at different pH. Moreover, each metal ion has a peculiar pH value

requirement for its extraction. An influence of pH on extraction of Cu(II) from 0.03 M Cu(OAc)₂ solution was studied here at three different pH values (7.40, 6.41 and 3.00) with 0.001 M Htd as presented in Figure 5-6. At pH 6.41 (no adjustment), 32 mg/L Cu(II) was removed. When the pH was adjusted from 6.41 to 7.41 with NaOH, 426 mg/L Cu(II) was quantitatively extracted. The high levels of Cu(II) extracted at pH 7.41 may have been due to some Cu(II) ions precipitation with OH⁻ as well. Lowering the pH from 6.41 to 3.00 by adding HCl resulted into no extraction. According to Shigematsu *et al.*,³¹⁷ Cu(II) ions can be extracted in the pH range of 5-9 using β-diketone. Begum *et al.*³¹² found that the pH of 5.3 and 7.45 are optimal for extraction of Cu(II) and Zn(II) using Cyanex 272. The point here is that, the β-diketones are effective chelators under basic condition as it has been reported.^{89,153} Hence, increase in pH favours the extraction of Cu(II) from the Cu(OAc)₂ solution. It has been reported that for the extraction of metal ions from acidic medium, higher concentration of β-diketone is required.³¹⁸

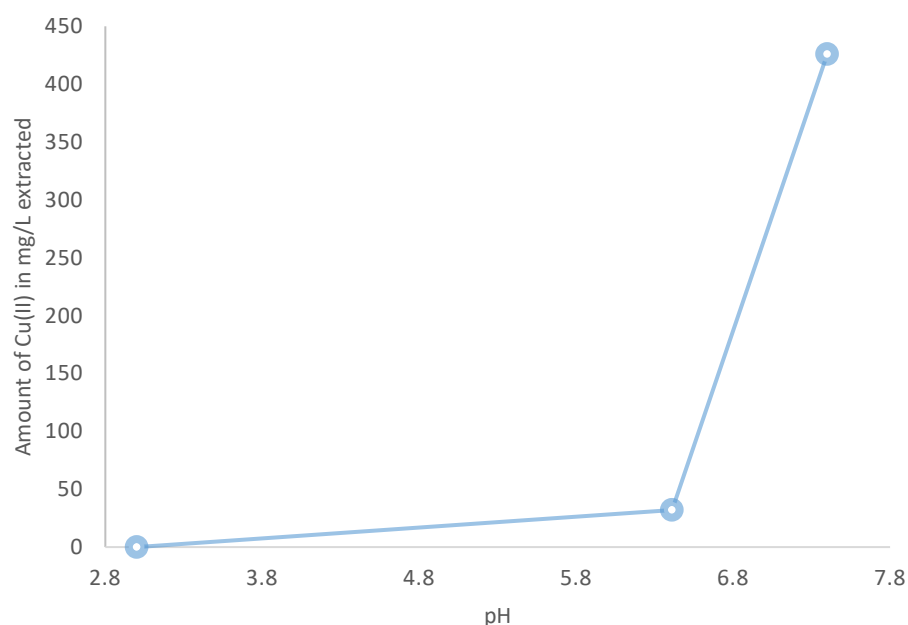


Figure 5-6: Effect of pH on extraction of Cu(II) from Cu(OAc)₂ solution using the Htd

5.2.5 Effect of solvent on the extraction of Cu(II) from CuCl₂ solution with Htd

Solvents are also used in optimising metals extraction processes. Diluents are supposed to show high solubility for the chelator and metal-chelate but low solubility in water. And their boiling point should be high for safety reasons.³¹⁹ Chelating agents coordinate the metal ion by replacing coordinated water molecules as well as neutralising the charge of the metal and therefore enhances the solubility of metal chelate.^{310,320} Toluene,³¹¹ dichloromethane,²⁶³ chloroform,^{311,317} butyl acetate^{311,317} and benzene³⁰⁹ are often used in extraction of metals³¹⁸ due to their ability to dissolve the metal-diketonate formed, hence enhance the metal extraction. Using carbon tetrachloride is better because it has higher density than water and separation of the two phases is less difficult (less emulsion),³¹⁸ but is not regarded as safe or green.

For this studies, cyclohexane, limonene, toluene and CPME were tested as solvent carriers for the extraction of Cu(II) from CuCl₂ solution with the Htd in M: L, 10:1 because cyclohexane, limonene and CPME are greener solvents as highlighted in chapter 2 and toluene was chosen for comparative purpose and these three solvents are capable of solubilizing Htd. The amount of Cu(II) removed were; 20 ±3 mg/L, 108 ±8 mg/L and 105 ±6 mg/L for toluene, cyclohexane and limonene respectively. No extraction of Cu(II) was detected or the extracted Cu(II) may have been below the detection limit while using CPME under this experimental condition and measurement technique (See Figure 5-7). The increasing order of these solvents in the recovery of Cu(II) is; CPME < toluene < cyclohexane. Cyclohexane is observed to be a better solvent than toluene and CPME for extraction of Cu(II) ion as far as the Htd is concern.

From similar previous studies, extraction of Cu(II) with D2EHPA (di-(2-ethylhexyl) phosphoric acid) was of the order dodecane > CPME > toluene.³¹⁹ Furthermore, Gupta and Singh reported extraction of Pt(IV) and Pd(II) with Cyanex 923 using different organic diluents, nitrobenzene, cyclohexanone, chloroform, toluene, xylene, kerosene and n-hexane.³¹³ No correlation was observed between the extent of extraction of these metal ions and the dielectric constant or chemical nature of the diluents. Toluene was preferred as a diluent since it provides quicker phase separation.³¹³

Extraction of metals using toluene as a diluent are commonly reported³⁰⁶ probably due to the ability of toluene to effectively dissolve most hydrophobic chelators. Otherwise the Htd form higher enol in cyclohexane (97%) than in toluene (91%), which is a crucial feature that enables β -diketone to chelate metal ions. More so, limonene is essentially non-polar solvent, thus would enhance enol formation to similar extent like cyclohexane. Therefore, the Htd in cyclohexane and limonene is being more efficient and comparative in terms of extraction of Cu(II) than toluene and CPME. The inefficiency of CPME as a diluent compare to cyclohexane is due to the fact that CPME is a bit polar hence partly dissolves in water³¹⁹ (1.1 g/100 g water at 296 K). In addition, the enol content of the Htd in CPME will be less than cyclohexane at least as explained in chapter two. Therefore, the higher polarity of cyclopentyl methyl ether than toluene and cyclohexane may have been the cause of poor extraction of Cu(II). Recent studies suggested that, if longer alkyl chain is appended on the cyclopentane this will lessen hydrophilicity of CPME and make it a better diluent.³¹⁹ Moreover, CPME could participate in the coordination to metal ions because of the ethereal oxygen.

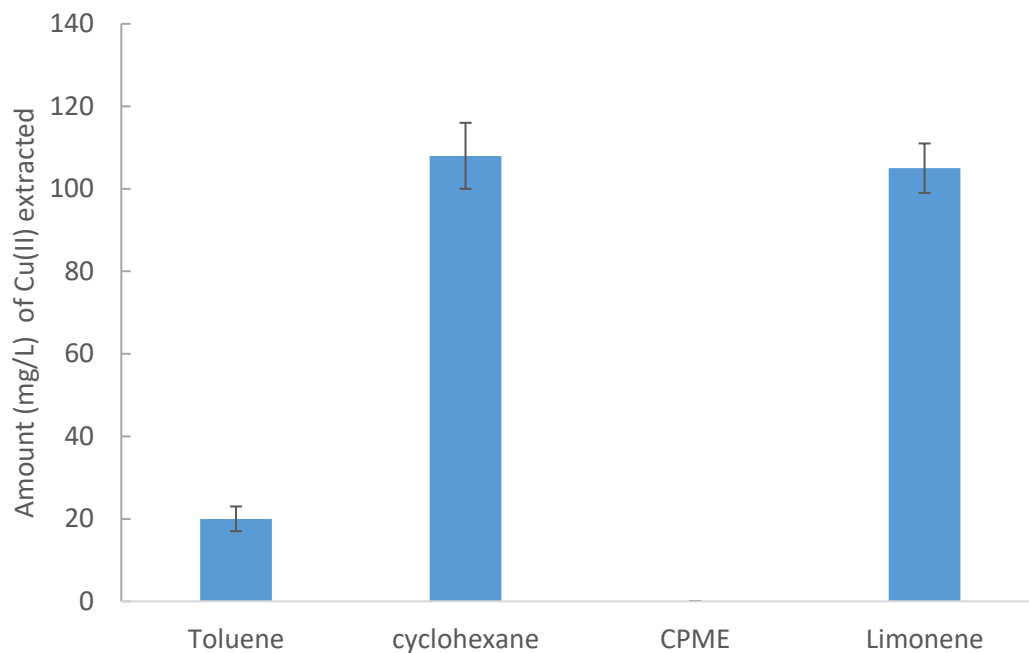


Figure 5-7: Extraction of Cu(II) from CuCl₂ solution with Htd in toluene, limonene, cyclohexane and cyclopentylmethyl ether (CPME)

5.2.6 Temperature effect on extraction of Cu(II) from CuCl₂ solution with Htd

Metals extraction is also temperature dependent and often time this parameter is investigated.³⁶ The extraction of 15 mM Cu(II) was investigated at different temperatures from 293 – 323 K with the 3 mM Htd and the results is given in Figure 5-8. It was found that, 26 ±4mg/L, 15 ±5 mg/L, 10 ±3mg/L and 15 ±3mg/L of Cu(II) were extracted at 293 K, 303 K, 313 K and 323 K respectively as shown in Figure 5-8. Carrying out the extraction of Cu(II) at higher temperatures beyond 293 K resulted into decreased in Cu(II) extraction efficiency. Such similar temperature effect has been reported in literature.^{55,263,309} In addition, the extraction of Cu(II) has been reported to be temperature independent.³²¹ However according to Fanou *et al.*,²⁶³ Pb(II) extraction was efficient at 303 K. Then further increase in temperature resulted to decline in the Pb(II) removal. Sary and Hladky³⁰⁹ had reported extraction of metal ions with Hacac, Hdbm and Hbac at 293 K. More so the extraction and separation of platinum and palladium using Cyanex 923 at

283 – 323 K showed decrease in percent extraction with the increasing temperature because of the exothermic nature of the process.³¹³ However Pranolo *et al.*³²² suggested that extraction of aluminium is best at 313 K.

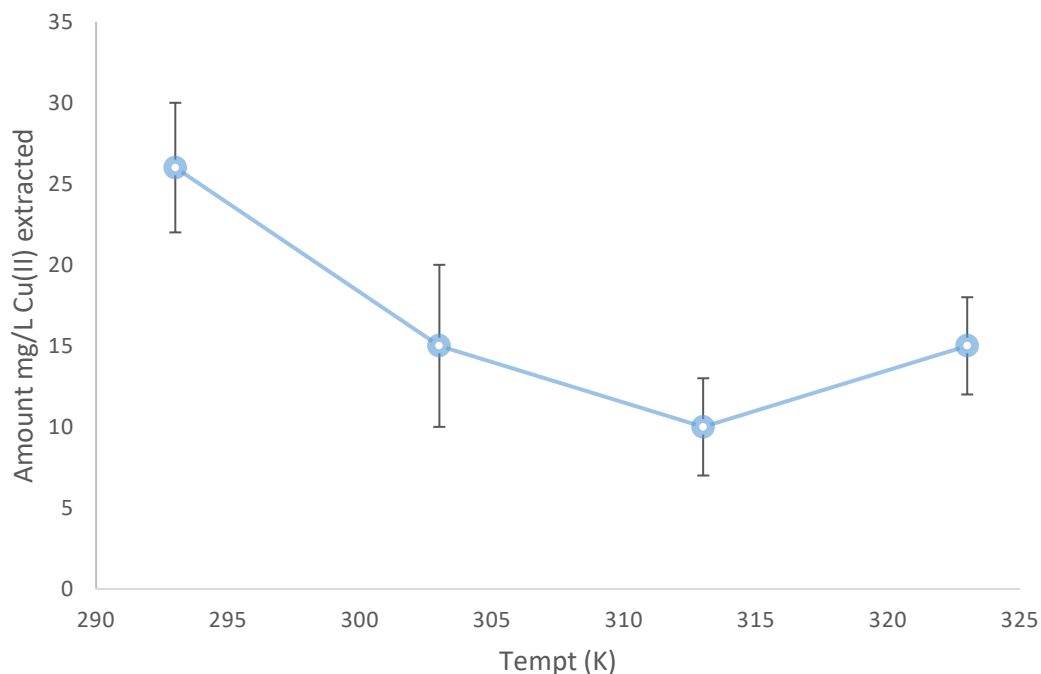


Figure 5-8: Effect of temperature on extraction of Cu(II) from CuCl₂ solution with Htd

5.2.7 Effect of ionic strength on extraction of Cu(II) from CuCl₂ solution

Influence of ionic strength was tested by adding KCl as similarly reported in the literature³⁰⁴ on the removal of Cu(II) with the Htd M:L (5:1). 10.3 mg, 20.40 mg, 31.01 mg and 40.2 mg of KCl were respectively added into 5 mL 15 mM solution of CuCl₂ and the Cu(II) extracted with 3 mM Htd. There was slight decrease in the amount of Cu(II) removed with the Htd as the ionic strength increased in the range of 0.05 – 0.13 M (see Table 5-2 below). The levels of Cu(II) removed were between 26 mg/L – 13 mg/L.

Other studies of extraction of metals showed that, increase in ionic strength enhances the extraction efficiency³²³ where the added salt could be acting as salting out agent and weak complexing agents.^{304,324} However, the use of larger amount of metal ions versus

chelator ratio (5:1) in the present studies may have brought about the opposite trend of the influence of added KCl during the extraction of the Cu(II) ions.

Table 5-2: Effect of adding various amount of KCl on removal of Cu(II) from CuCl₂ solution with the Htd at M: L (5:1)

Ionic strength	Mg/L
0.05	26.00
0.07	19.00
0.1	19.00
0.13	20.00
0.15	13.00

5.2.8 Removal of metal ions with Htd in comparison to Hdbm and Hacac

The metal ions; Cu(II), Ni(II), Co(II), Cr(III) and Fe (III) extraction with Htd, Hdbm and Hacac were compared as given Figure 5-9. Unlike Htd and Hdbm, extraction of these metal ions with Hacac into cyclohexane was poor under this experimental conditions due to non-lipophilic nature of Hacac. Although Hacac was observed to have removed small amount of Co(II) and Fe(III) into cyclohexane. It was found that Hacac form complex with Fe(III) almost in less than 5 min of contact time to form dark-red complex in the aqueous phase which was different from the initial orange colour of solution of FeCl₃. But the complex was not quite extractable into the cyclohexane phase in the presence of Hacac.

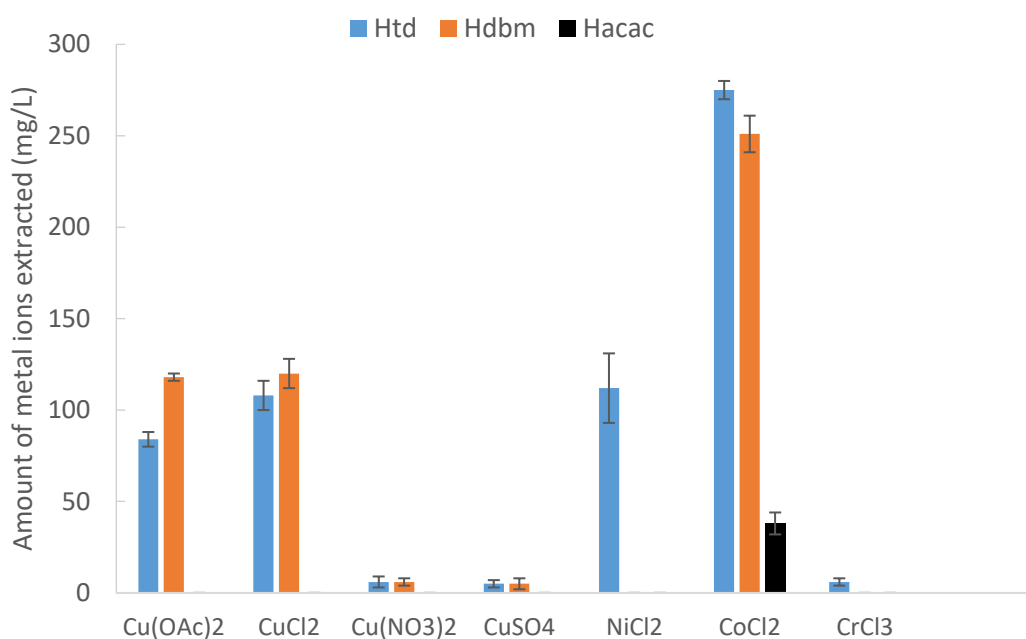


Figure 5-9: Extraction of the metal ions using Htd, Hdbm and Hacac

Shigematsu *et al.*³¹⁷ reported that, it is often problematic to compared lipophilic β -diketones to Hacac in metals extraction because the metal acetyl acetonates partition coefficient in most organic solvent of an aqueous/organic biphasic system is significantly less than metal chelates of lipophilic β -diketones. Furthermore, Sekine *et al.*³²⁵ observed that the solvent extraction of divalent metal ions with Hacac is very often partial as a results of low extractability of the *bis*-acetylacetonato chelates. From this standpoint, lipophilic β -diketones like Hdbm and the Htd whose molar volume is much greater than Hacac but their ability to form complexes is similar readily extracted metal ions into organic phase as may be seen in Figure 5-9 above. Moreso, according to Stary,¹⁵⁰ the partition coefficient of Hacac and lipophilic β -diketones are much different.

Therefore, the distribution coefficients of the Hacac, Hdbm and Htd were tested. 5 mL distilled water was contacted with 5 mL of each of 3 mM β -diketones (Htd, Hdbm and Hacac in cyclohexane) for 30 min and subsequently allowed to stand for 24 h. The GC

peaks area of the β -diketones in the organic layer were compared to those of their original standards. Then amount of the β -diketones present in water was evaluated by difference, hence the apparent distribution coefficients were determined. These results (Table 5-3) was compared to the literature distribution constants of Hacac and Hdbm as presented in Table 5-4 and Table 5-5.

Table 5-3: Distribution constant of Hacac, Hdbm and Htd at 298 K in cyclohexane

Samples	K_D	Log K_D
Hacac	0.88	-0.06
Hdbm	Undefined	-
Htd	Undefined	-

Table 5-4: Distribution constants of β -diketones at 298 K in aqueous-organic phase³²⁵

	Aqueous		Log K_d			
	I(M)	pK _a	Hexane	CCl ₄	Benzene	CHCl ₃
Hacac	0.1	8.67	-0.05	0.51	0.70	1.36
	1	8.99	-0.14	0.40	0.59	1.26
	3	9.75	-0.24	0.22	0.40	1.09
Hbac	0.1	8.39	2.03	2.81	3.02	3.64
	1	8.55	1.96	2.73	2.96	3.57
	3	9.19	1.91	2.70	2.94	3.44
Hdbm	0.1	8.59	3.95	4.90	5.20	-
	1	8.57	3.93	5.10	5.30	-
	3	9.00	3.99	5.20	5.30	-

Table 5-5: Distribution constants of Hacac, $\log K_{D(HA)}$ between water and various organic solvents, 298 K³²⁶

Solvent	I, M		
	0.001	0.1	1.0
n-Hexane	-0.02 ±0.01	-	-0.06 ±0.04
Cyclohexane	0.00 ±0.01	-	-0.04 ±0.04
Benzene	0.77 ±0.01	0.74 ±0.02	0.64 ±0.02
Toluene	0.66 ±0.01	0.62 ±0.01	0.55 ±0.02
Xylene	0.57 ±0.01	-	0.52 ±0.01
Dichloromethane	1.41 ±0.02	1.32 ±0.02	-
3-Methyl butanol	-	-	0.54 ±0.02

Note: $K_D = \text{Conc. in org}/\text{conc. aq phase}$ ³²⁶

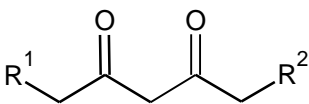
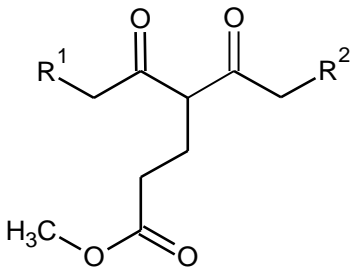
These data in Table 5-5 shows that the Hacac is most distributed in dichloromethane and CHCl_3 than in hexane and cyclohexane.³²⁵ It is seen from Table 5-4 also that the distribution constant is higher by a factor of about 200 and above by the substitution of methyl group of Hacac with phenyl group.³²⁵ These evidences show that Hdbm and the Htd are much more lipophilic than Hacac. The Hdbm and Htd were not detected in the aqueous phase as given in the Table 5-3 above because of their higher lipophilicity. Similarly, the β -diketones; dipropiylmethane, diisobutyrylmethane, pivaloyacetylmethane and dipivaloylmethane were also found to be just slightly soluble in water.¹⁴⁹ This difference in the partition coefficient will obviously affect the extraction of metals with Hacac and hydrophobic β -diketones. Hence, there will be technical difficulty in comparing metals extraction pattern of Hdbm and Htd to Hacac because the former are insoluble in water, or rather Hacac is more soluble in water. The results of the extraction of these metal ions with Htd, Hacac and Hdbm were also affected by some

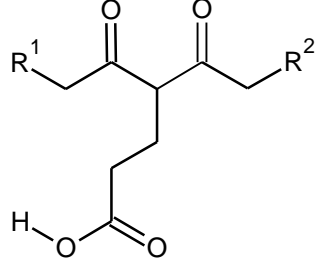
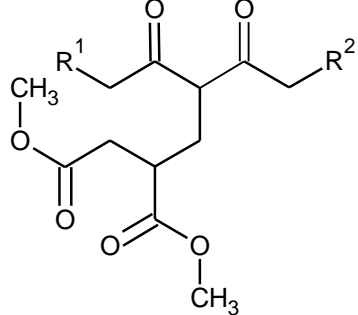
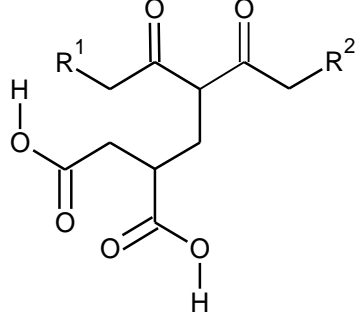
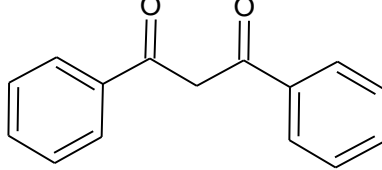
factors as counter ion, contact time and pH which will be discussed in the following sections of this chapter. More so, because of the solubility issues, further studies of these metals extractions were conducted with these bioderived lipophilic β -diketones in comparison to Hdbm.

5.2.9 Extraction of the different metal ions with unmodified and modified Htd

The most common chelating agents contain nitrogen, phosphorus, sulphur and oxygen to bond metals cations.^{61,90} Although, bioderived chelators with less nitrogen content are among the preferred chelants these days.^{327,328} Better still, hydrophobic chelating agents have advantage of being reuse in solvent metals extraction. For this reason, Htd, Ma, Ita, MaH, and ItaH (see Table 5-6 for details of their structures) were used for the extraction of some metal ions; Cu(II), Ni(II), Co(II), Fe(III), Cr(III)) in comparison to Hdbm.

Table 5-6: The unmodified and modified Htd tested as metals chelators in comparison to Hdbm

Names	Structure	Abbreviations used
Bioderived lipophilic β -diketone (14,16-hentriacontanedione)		Htd
Methyl acrylate modified β -diketone		Ma

Carboxylate acid of methyl acrylate modified β -diketone		MaH
Dimethyl itaconate modified β -diketone		Ita
Carboxylate acid of dimethyl itaconate modified β -diketone		ItaH
Dibenzoylmethane		Hdbm

5.2.10 Effect of initial metal ion concentration on Cu(II) extraction with the Htd, Hdbm, Ma, Ita, MaH and ItaH

The effect of initial metal ion concentration was assessed by considering molar ratios of M: L as 2:1 and 10:1 for the extraction of Cu(II) from CuCl₂ solutions with these Htd, Ma, Ita, MaH, and ItaH in comparison to Hdbm. The increase in the initial concentration of CuCl₂ results into enhanced removal of Cu(II) using the bioderived chelators. For the M: L, 10:1, dibenzoylmethane, Htd, Ma, Ita, MaH and ItaH extracted 120 ±8 mg/L, 108 ±8

mg/L, 107 ±19 mg/L, 102 ±19 mg/L, 88 ±13 mg/L and 86 ±6 mg/L Cu(II) respectively at pH 4-5 as presented in Table 5-7. When the ratio of the M: L was reduced to 2:1, then the amount of Cu(II) ions removed were lesser; 19 ±4, 25 ±4, 6 ±4, 9 ±4, 6 ±4 and 10 ±5mg/L for Htd, Hdbm, Ma, Ita, MaH and ItaH respectively. As would be expected, increase in initial metal ion concentration increases the overall chemical interaction between the donor groups of the chelants and the metal ions³²⁹ therefore, the amount of metal ions extracted is also increased. Similarly the extraction of Pb(II) with δ -diketones was also observed to be enhanced with increasing amount of the initial Pb(II) concentration as reported by Fanou *et al.*²⁶³ Similarly, the potential to remove Zn(II), Cd(II) and Mn(II) from aqueous solutions through biosorption using maize stalks as an agriculture waste was found to increase with increasing initial metal ion concentrations.³²⁹

Table 5-7: Effect of initial Cu(II) ion concentration on Cu(II) extraction with the these bioderived chelators and Hdbm

	Molar ratio M: L; 2:1	Molar ratio M: L; 10: 1
Htd	19 ±4	108 ±8
Hdbm	25 ±4	120 ±8
Ma	6 ± 4	107 ±19
Ita	9 ± 4	102 ±19
MaH	6 ±4	88 ±13
ItaH	10 ±5	86 ±6

5.2.11 UV/Visible spectrophotometric determination of Cu(II) extraction

Extraction of Cu(II) was performed from CuCl₂, Cu(OAc)₂, CuSO₄.5H₂O and Cu(NO₃)₂.3H₂O solutions to check the influence of counter ions. Figure 5-10 gives amount (mg/L) of

Cu(II) extracted with these bioderived molecules in comparison to Hdbm from CuCl₂ and Cu(OAc)₂ solutions at pH range of 4 – 6. Previous reports have also shown that recovery of Cu(II) with Hacac, Hbac, Schiff base and alkyl-substituted β-diketones can be achieved at pH 4-6.^{304,308,330} There was no difference in the pattern of extraction of Cu(II) from CuCl₂ solution with these Htd, Ma, Ita, MaH, and ItaH in comparison to Hdbm. Furthermore, 84 ±4, 118 ±2, 16 ±3, 232 ±3, 29 ±3 and 226 ±15 mg/L of Cu(II) was extracted from Cu(OAc)₂ solution by Htd, Hdbm, Ma, MaH, Ita and ItaH respectively. The extraction of Cu(II) is more effective from Cl⁻ than OAc⁻ when using Htd. In the case of Hdbm, extraction of Cu(II) from Cl⁻ or OAc⁻ were comparable. In addition, Ma and Ita extracted 16 ±3mg/L and 29 ±3 mg/L amount of Cu(II) from Cu(OAc)₂ solution which were less than those of Htd and Hdbm. This demonstrates that, the Ma and Ita with the carboxylate esters are less effective Cu(II) ion removal from OAc⁻ medium than the Htd. Whereas, the MaH and ItaH with the carboxylate acid groups removed 232 ±3 mg/L and 226 ±15 mg/L of Cu(II) from Cu(OAc)₂ higher than those extracted by Ma, Ita, Htd and Hdbm. In which case all these chelators can be applied for metals extraction in Cl⁻ and OAc⁻ solutions.

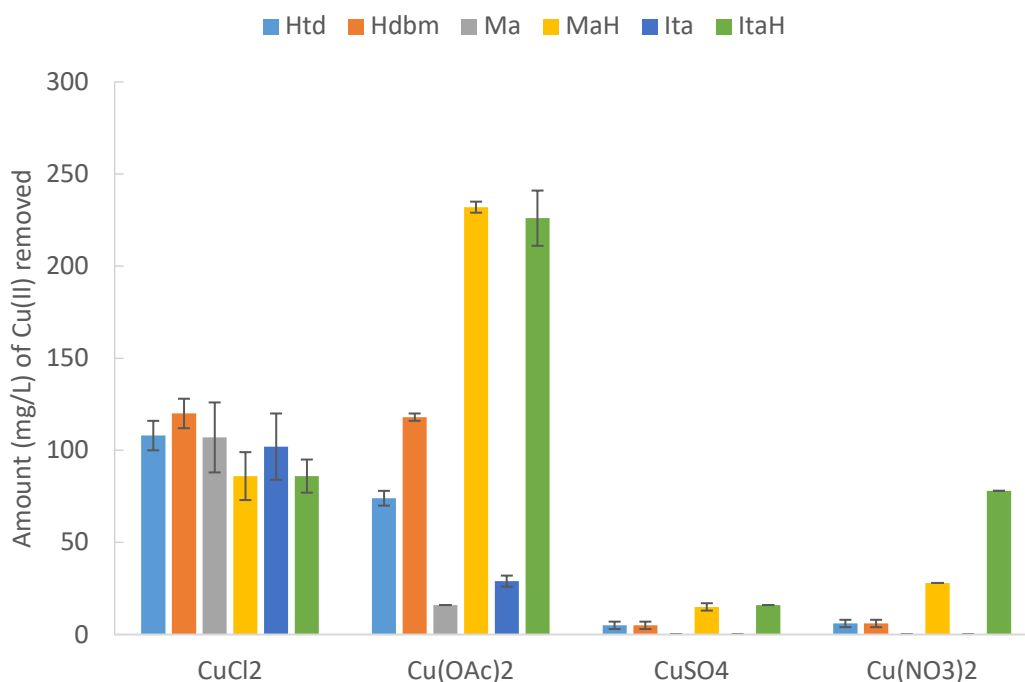


Figure 5-10: Removal of Cu(II) with the bioderived chelators and Hdbm

Recovery of Cu(II) from CuSO₄ and Cu(NO₃)₂ solutions at pH of about 5 showed that Htd and Hdbm efficiency is comparable. MaH and ItaH extracted 15 ±3 and 16 ±3 mg/L Cu(II) from Cu(SO₄)₂ better than all the rest of chelators. This means that the carboxylate acids of the modified lipophilic β-diketone has potentials as a better chelator for Cu(II) from SO₄²⁻ medium than Htd, Ma and Ita. Similarly, the Cu(II) ion extraction from Cu(NO₃)₂.3H₂O solution indicated that, ItaH and MaH removed 78 ±5 and 28 ±4 mg/L respectively of the Cu(II) ions which were higher than the amounts extracted by Hdbm, Ita, Ma and Htd. This shows that the modified Htd with carboxylate acid groups are better extractants for Cu(II) from OAc⁻ medium.

In general, the pH of Cu(OAc)₂, CuCl₂, Cu(NO₃)₂.3H₂O and CuSO₄.5H₂O solutions for the Cu(II) extraction were 6.13, 4.17, 5.00 and 4.84 respectively (pH range of 4 – 6). As the pH were not adjusted, the removal of Cu(II) with these bioderived β-diketones showed that, CuCl₂ and Cu(OAc)₂ solutions were favourable for the removal of Cu(II) ion as it has

been similarly reported^{89,331,332} than from $\text{Cu}(\text{NO}_3)_2$ and $\text{Cu}(\text{SO}_4)_2$. Majority of metal extraction systems are carried out in sulphate medium,³¹⁶ but extraction of most metals is favoured in Cl^- medium⁸⁹ because Cl^- is a strong inner sphere ligand.

It has been reported that the extraction of $\text{Cu}(\text{II})$ from SO_4^{2-} medium using hydrophobic pyridyl ketoximes was found to be inefficient, but the extraction was enhanced with added chloride ions.³³¹ Begum *et al.*³¹² performed $\text{Cu}(\text{II})$ and $\text{Ni}(\text{II})$ extraction with 0.1 - 0.05 M Cyanex 272 and found that the extraction was independent at lower concentration of sulphate, 0.02 - 0.1 M. But the extraction of both $\text{Cu}(\text{II})$ and $\text{Ni}(\text{II})$ decreased by increasing the concentration sulphate from 0.1 - 0.5M due to formation of non-extractable $\text{Cu}(\text{II}) \text{SO}_4^{2-}$ and $\text{Ni}(\text{II}) \text{SO}_4^{2-}$.

However, increasing the amount of β -diketone and pH could enhance the extraction of $\text{Cu}(\text{II})$ from CuSO_4 and $\text{Cu}(\text{NO}_3)_2$ solutions as earlier explained. Previous report showed that quantitative recovery of metals are enhanced with increasing pH of the aqueous medium and increasing the concentration of the β -diketone.³¹⁸ More so β -diketones are weak chelator and work better at alkaline medium. Therefore, higher concentration or pH will be needed for quantitative removal of metals with these molecules from SO_4^{2-} , NO_3^- , Cl^- and OAc^- media. In addition, it was also observed that, the removal of the $\text{Cu}(\text{II})$ from solutions of CuCl_2 , $\text{Cu}(\text{OAc})_2$ and $\text{Cu}(\text{SO}_4)_2$ was of the order: $\text{CuCl}_2 > \text{Cu}(\text{OAc})_2 > \text{Cu}(\text{SO}_4)_2$ as presented in Table 5-8.

Table 5-8: Extracted Cu(II) from CuCl₂, Cu(OAc)₂ and CuSO₄·5H₂O solutions with Htd determined with ICP-MS and UV/visible spectrophotometric methods

Cu salt solution	%E of Cu(II) – from	Amount Cu(II) mg/L– from
	ICP-MS method	UV/Visible Spec. method
	1:1 (M:L)	10:1 (M:L)
CuCl ₂	36	108
Cu(OAc) ₂	31	84
CuSO ₄	19	5

5.2.12 Extraction of Co(II) from CoCl₂ and Co(NO₃)₂ solutions

Extraction of Co(II) was also performed from CoCl₂ and Co(NO₃)₂ solutions using Htd, Hdbm, Ma, Ita, MaH and ItaH. Figure 5-11 below gives the levels of Co(II) extracted with these bioderived molecules from CoCl₂ and Co(NO₃)₂ solutions at pH of about 7. Such pH have been reported as appropriate for removal of Co(II) by Gerald *et al.*³¹¹ The removal of Co(II) was better from CoCl₂ solution than Co(NO₃)₂. The amount (mg/L) of the Co(II) removed from CoCl₂ solution were, 275 ±5, 251 ±10, 279 ±10, 223 ±10, 251 ±10, 181 ±10 with Htd, Hdbm, Ma, MaH, Ita and ItaH respectively. But with solution of Co(NO₃)₂, no Co(II) removal was detected with all these chelators for the method and condition used. The counter ions effect is also dominant in this case because the extraction of Co(II) from CoCl₂ and Co(NO₃)₂ solutions were carried out at comparable pH. This demonstrated that, removal of Co(II) in the pH range 5-7, is better in CoCl₂ solution with these bioderived compounds than from Co(NO₃)₂. Previous studies reported by Stary and Hladky³⁰⁹ have shown that Co(II) can also be extracted into organic phase with β-diketones (acetyl acetone, benzoylacetone and dibenzoylmethane). Solvent extraction of at least Cu(II), Co(II) and Ni(II) is commonly carried out in ammoniacal, Cl⁻ and SO₄²⁻

system.^{323,333,334} However, for this bioderived β -diketone and its derivatives, Cl^- solution are favourable for the removal Cu(II) and Co(II) than from SO_4^{2-} and NO_3^- solutions of these synthetic metal waste without pH adjustment. However Gerald *et al.*³¹¹ performed an extraction of Co(II) from aqueous solution of CoSO_4 using β -diketone (1-phenyl-3-methyl-4-(*p*-nitrobenzoyl)pyrazolone) and found that it was quantitative at pH 5.5- 7.0.³¹¹ The extraction of Cobalt(II) carried out by Sary showed that β -diketone extract cobalt (II) at pH of 7.5 – 10.¹⁵⁰

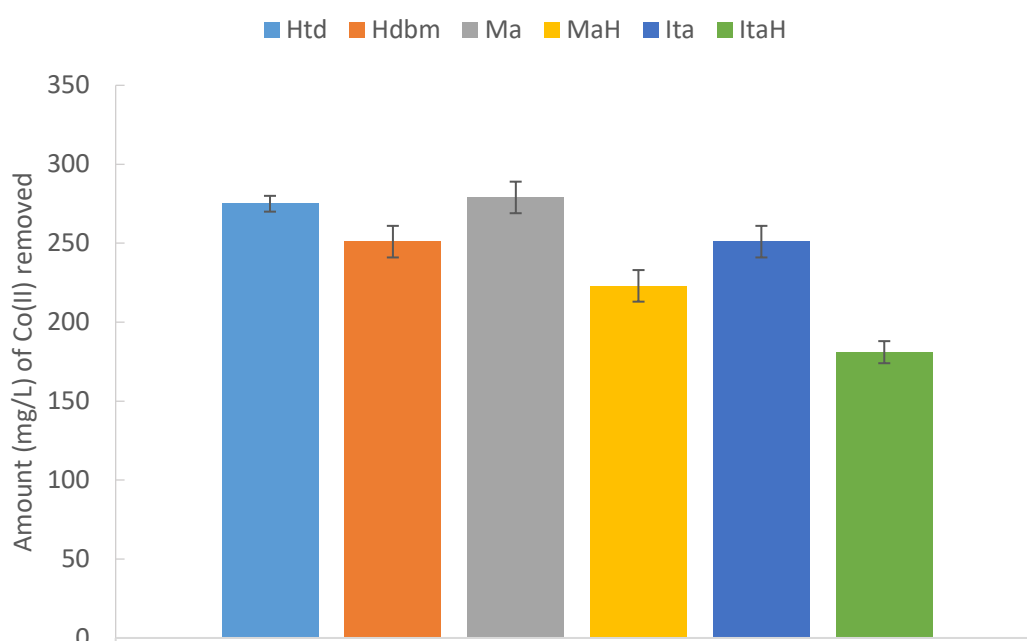
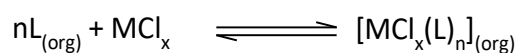


Figure 5-11: Removal of Co(II) from CoCl_2 solutions with the different biochelators

It is reported that, chloride is a good ligand to generate extractable and charge-neutral complexes, $[\text{MCl}_x(\text{L})_n]$ as given in Equation 5-3, hence it can act as ligand or counter ions pairs unlike NO_3^- and SO_4^{2-} .⁸⁹ This may have also accounted for the better extraction of Co(II) and Cu(II) from Cl^- solutions than SO_4^{2-} and NO_3^- .



Equation 5-3: Extraction equation with involvement of Cl⁻ counter ion

5.2.13 Removal of Ni(II) from NiCl₂ solution

The recovery of Ni(II) from NiCl₂ solution (at pH of 7.27) was also tested with these unmodified and modified Htd in comparison to Hdbm and the results are presented in Figure 5-12. The results showed that; 112 ±19, ND, 125 ±5, 80 ±5, ND, 140 ±5 mg/L Ni(II) were extracted into cyclohexane with the Htd, Hdbm, Ma, MaH, Ita and ItaH respectively. This implied that Hdbm and the Ita were not effective in extraction of the Ni(II) from NiCl₂ solution at this condition. Longer contact time of above 30 min may be required to effect the recovery of Ni(II) ion with dibenzoylmethane and dimethyl itaconate modified bioderived β-diketone. Separation of Ni(II) from say Co(II) from chloride solutions may be effected by carrying out the extraction with itaconate modified bioderived β-diketone and dibenzoylmethane using shorter contact time of 30 min.³³⁵ It has been reported that longer contact times of up to 3 days are required to extract nickel with dibenzoylmethane.^{153,309} This demonstrates that the Htd can chelate Ni(II) in shorter times than the Hdbm. Therefore, the extraction of nickel with the 14,16-hentriacontanedione is more efficient due to the faster nickel transfer into the organic phase.

More so, limonene was tested as a diluent in this case for the recovery of Ni(II) with Htd at same condition. 82 ±6 mg/L of the Ni(II) was extracted into to the limonene phase; while in the case of cyclohexane, 112 ±19 mg/L Ni(II) was extracted as earlier on highlighted. Both limonene and cyclohexane are non-polar thus their potential as diluent for Htd in the extraction of Ni(II) was comparable. The use of limonene as diluent in metal

extraction will be beneficial because it is substantially a biobased solvent unlike cyclohexane; it is a non-polar solvent hence can enhance intrasolute H-bonding essential for metals extraction; and the higher boiling point (449 K) of limonene above that of cyclohexane (349 K) would make it safe solvent in metals extraction.

Similarly, Wilson *et al.*⁸⁹ reported that an ideal chelator should readily facilitate metal loading into organic phase. Solvent extraction of nickel was reported to be optimum at pH range pH 8-10 with β -diketones.³¹⁷ Kumar *et al.*³¹⁰ reported removal of Ni(II) ions with β -diketone-functionalized styrene divinylbenzene resin at pH 6 from aqueous NiCl₂. Hence the equilibria for the extraction of Ni(II) and also Co(II) was attained at 100 min and 60 min respectively.³¹⁰ While Sekine *et al.*³²⁵ ascribed the poorer extraction of Ni(II) by Hacac to hydrophilic tendency of the Ni-complex formed.

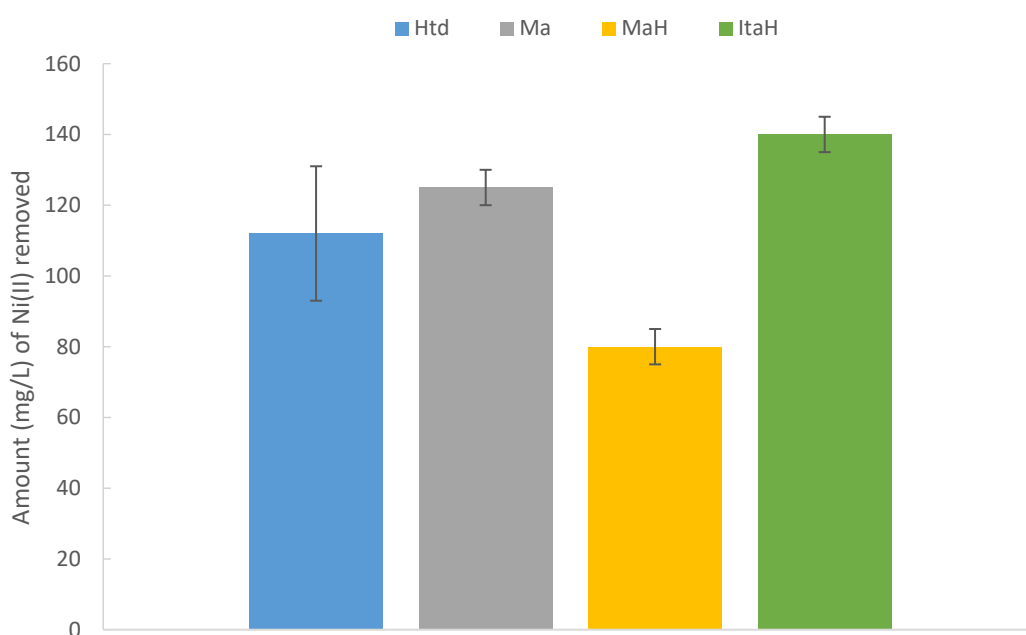


Figure 5-12: The extraction of Ni(II) from NiCl₂ solution

In addition, the contact time of extraction of Ni(II) with Htd, Hacac and Hdbm was varied between 1 min - 2 h. The results for this in Figure 5-13 indicated that no removal of Ni(II) was detected with Hdbm and Hacac even up to 2 h. This is due to longer contact time require for extraction of Ni(II) with Hdbm as earlier observed; and the hydrophilic tendency of Hacac-Ni chelate. But the extraction of the Ni(II) with Htd implied that the longer the contact time the more amount of the Ni(II) was removed from aqueous phase. At this condition of experiment increasing the contact time for the extraction of Ni(II) beyond 1 h did not make any difference in terms of the amount of Ni(II) extracted. Gupta and Singh reported that a minimum of 3 min and 4 min shaking time was found sufficient for attaining maximum extraction of Pt(IV) and Pd(II). And that excess shaking did not affect the results.³¹³

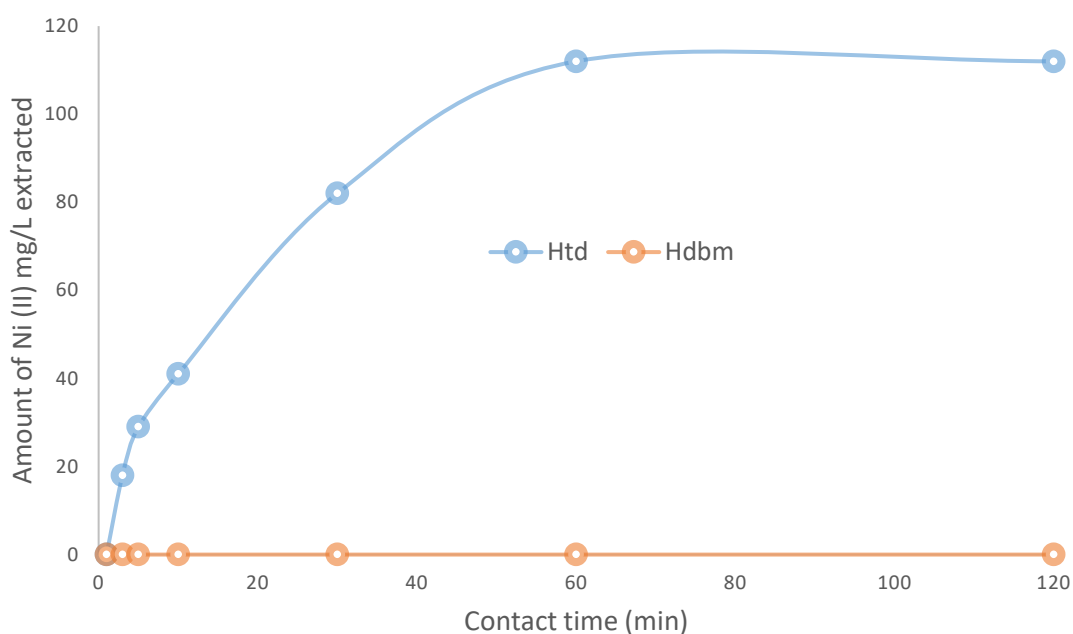
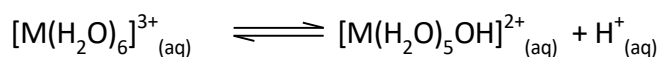


Figure 5-13: Extraction of Ni(II) with Htd and Hdbm as function of contact time

5.2.14 Removal of Fe(III) and Cr(III) from FeCl₃ and CrCl₃ solutions

From the literature it has been gathered that, β -diketones are versatile ligands;¹⁴² they are also used to extract trivalent ion such as Fe(III), Ga(III), In(III), Al(III).^{153,309} For the purpose of testing, an extraction of Fe(III) and Cr(III) from FeCl₃ and CrCl₃ solutions were performed using the Htd and Ma, MaH, Ita and ItaH. The results are displayed in Figure 5-14 below. Cr(III) at pH of 2.58 and Fe(III) at pH 1.59 were poorly extracted due to the low pH,¹⁵⁸ of their aqueous solutions; except that Htd and MaH extracted 81 \pm 30 mg/L and 167 \pm 25 mg/L Fe(III) respectively unlike Ma, Ita, Hdbm. The high charge density of Fe(III) and Cr(III) are able to polarise -O-H bonds of the water and liberates H⁺ as given in Equation 5-4. This makes the Cr(III) and Fe(III) solutions more acidic than that of the metals in +2 oxidation state. This phenomenon may have accounted for less extraction of FeCl₃ and CrCl₃ with these molecules as the pH were not adjusted. Use of MaH and ItaH for extraction of Cr(III) resulted into formation of emulsion and there was no phase separation likewise extraction Fe(III) with ItaH.



Equation 5-4: Liberation of H⁺ from water by high density +3 charge metal ions

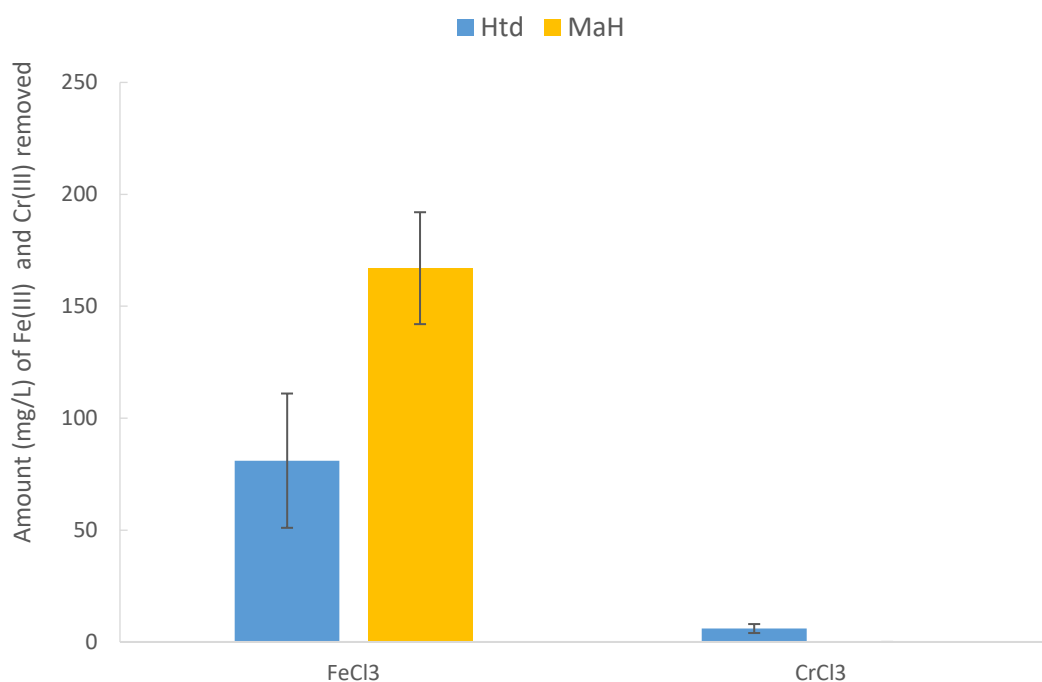


Figure 5-14: Removal of Fe(III) and Cr(III) from FeCl₃ and CrCl₃ solutions with Htd and Hdbm

The Htd also marginally removed Cr(III) while no extraction was detected using Hdbm at this low pH of 2.58. This is connected to the fact that, the establishment of the extraction equilibrium for most metals by dibenzoylmethane solution takes 4-5 h and above.³⁰⁹ Increasing pH of the CrCl₃ and FeCl₃ solution and also increasing concentration of Htd and Hdbm would enable the extraction of these metal ions. Previous reports have shown that, extraction of metals from acidic medium is better at higher concentration of acetyl acetone (and likely for other β-diketone).^{309,318,330} And equilibrium pH of 2.6,⁸⁸ 2 - 4¹⁵⁰ were reported for extraction of iron with acetyl acetone using a contact time of 30 min.⁸⁸ Extraction of iron at the pH 2-3 had also been previously reported using dibenzoylmethane.³¹⁷

It has been reported that the hydration energy of hydrated Cr(III) is high hence extraction of Cr(III) with acetyl acetone is slow because of the high energy barrier that must be

overcome for ligand substitution.⁸⁸ However, a test was carried out for extraction of Cr(III) by increasing pH from 2.58 to 4 – 5 and 5 – 6 with the Htd, Hdbm, Ma, Ita, MaH and ItaH. At the pH of 5- 6, there was reasonable extraction of Cr(III) than at pH of 4 – 5. Zoubi *et al.*³⁰⁴ also described an extraction of Cr(III) and Cu(II) from their metals chloride at pH range 5.5–8.2 in a less than 120 min contact time using Schiff base derived from terephthaldialdehyde and 5-amino-2-methoxy-phenol. The Htd, Hdbm, Ma and Ita extracted 238 ±6 mg/L, 32 ±4 mg/L, 255 ±17 mg/L and 305 ±12 mg/L Cr(III) respectively at the pH 5-6. The detail results are shown in Figure 5-15. The use of ItaH and MaH for the extraction of Cr(III) at pH of 5-6 resulted into emulsion and there was no phase separation.

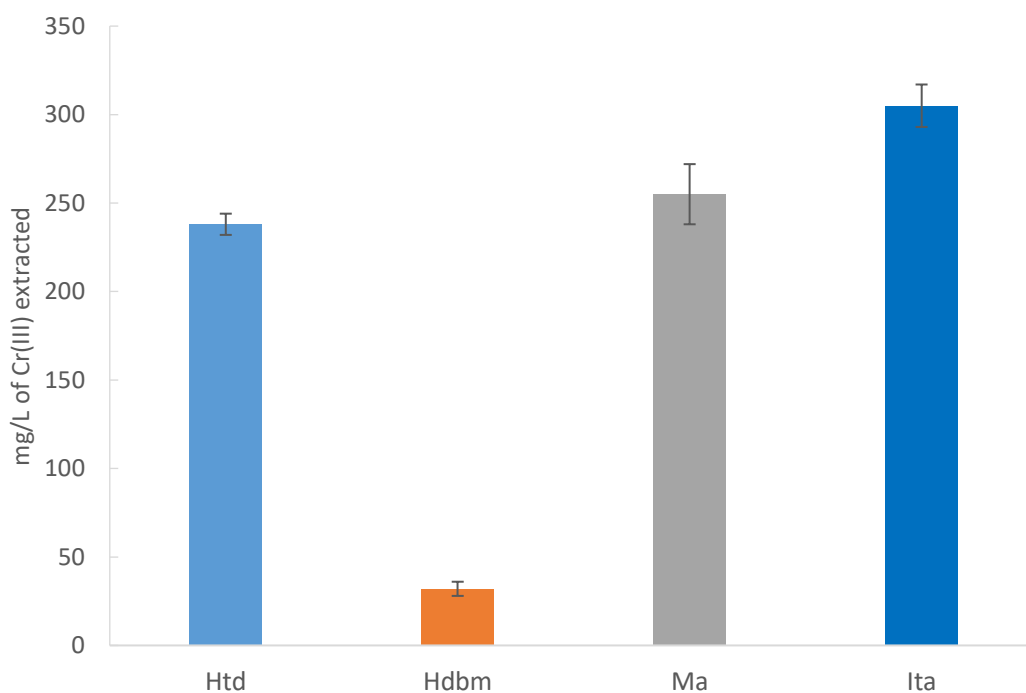


Figure 5-15: Cr(III) extraction from CrCl₃ solution with Htd, Hdbm, Ma and Ita at pH 5-6 using M: L of 10:1

5.2.15 Comparative summary of the extracted metal ions

Summary of the amount (mg/L) of Ni(II), Co(II), Cu(II), Fe(III) and Cr(III) extracted with these unmodified Htd and modified Htd in comparison to Hdbm are given in Table 5-9 as follows;

Table 5-9: Summary of metal ions extracted (mg/L) (10:1; M: L) with the unmodified and modified Htd at pH range 4 – 7 (Cu(II), Ni(II), Co(II)) and 1.5 – 2.6 (Fe(III) and Cr(III))

	Ni(II)	CuCl ₂	Cu(OAc) ₂	CoCl ₂	FeCl ₃	CrCl ₃	CuSO ₄	Cu(NO ₃) ₂
Htd	112 ±19	108 ±8	84 ±4	275 ±5	81 ±30	6 ±2	5 ±2	6 ±3
Hdbm	ND	120 ±8	118 ±2	251 ±10	ND	ND	5 ±3	6 ±2
Ma	125 ±5	107 ±19	16 ±3	279 ±10	ND	ND	ND	ND
MaH	80 ±5	88 ±13	232 ±3	223 ±10	167 ±25	ND*	15 ±3	28 ±4
Ita	ND	102 ±19	29 ±3	251 ±10	ND	ND	ND	ND
ItaH	140 ±5	86 ±6	226 ±15	181 ±10	ND*	ND*	16 ±3	78 ±5

ND= not detected and ND = there was no phase separation because of formation of emulsion*

It was found that the removal Co(II) from CoCl₂ solution was better than all of these other metal ions. This may be due to the higher solubility of the Co-chelate of these chelant in cyclohexane. However, Cu-chelates (from CuCl₂ and Cu(OAc)₂ solutions) and Ni-chelates (from NiCl₂) crashed out readily after letting their extracts with the Htd in cyclohexane to stand for 24 h. Sekine *et al.*³²⁵ reported low solubility of Ni-dbm complex than Co- and Cu-dbm complexes in carbon tetrachloride (10⁻⁶ M). Traditional solvents such as toluene, carbon tetrachloride, dichloromethane,²⁶³ chloroform and benzene³⁰⁹ are often used in solvent extraction of metals to enhance solubility of metal chelates because they can likely dissolve metal chelates better than cyclohexane. However, these solvents have highly negative environmental and safety considerations. Cyclohexane was selected because of its ability to enolise the Htd, and its improved safety credentials over the traditional solvents. In the literature, it is expected that complexes of β-diketones to be soluble in most organic solvents because they are charge neutral; which is why β-diketone are useful for macro extractions of metals.³³⁶

The crashing out of Cu- and Ni-extracts of the Htd (for 10:1, M: L) gives a third phase in which metal-Htd chelate accumulated at the interphase of the aqueous and organic layer.³³⁷ In the extraction of all these metals with the Ma and Ita, there was no such formation of third layer. In the case of the Hdbm, its metal extracts in the organic layer were yellow and cloudy; whereas the metal extracts of MaH and ItaH formed emulsion and separation became so difficult as similarly reported.¹⁵¹ Chloroform^{315,325} and toluene³³⁸ are said to be a preferred solvent to solve the issue of precipitation of chelate in solvent extraction of metals.³²⁵ Precipitation can also be overcome by using low amount of metal ions.³²⁵ Although the green credentials of these solvents is poor and further

work is needed to explore safer sustainable alternatives. Some of the benefits of these bioderived materials are highlighted as follows.

Re-use - it was possible to recover and reuse the Htd, Ma and Ita from the metal extracts in the organic layer by stripping with HCl as it has been similarly carried out.⁶⁸ But metal chelates of MaH and ItaH in cyclohexane was difficult to strip with HCl in order to get the original compounds. From literature it is understood that ideal chelator should readily release the metal ion under a changed conditions for it to be used again.³³⁹

A potential alternative to traditional chelating agent – These bioderived metals chelators have zero nitrogen and phosphorus content thus they will not release N or P (which are agents of eutrophication) into the environment like traditionally water soluble chelating agents (APCs and phosphonates).¹⁰⁴ The use of these bioderived chelators will reduce the consumption of phosphorus chelating agents as is currently desire. However, it will also be appropriate to fully understand the life cycle of these biobased chelators in the future and compare that to the traditional chelants. At least it has been shown in this work that these biobased chelators (especially Htd, Ma and Ita) are highly recyclable because they are essentially lipophilic.

Compatibility in solvent extraction technique- The fact that these chelants are hydrophobic make them suitable as metals chelator in solvent extraction processes. Solvent extraction technology itself is good for recovery of metals from secondary sources; low grade ores, mixed metals and can lead to excellent materials and energy balance.⁸⁹ Also the chelators are well dissolved in non-polar organic solvent which can promote enol formation that enables them to chelate metals. Previous reports have

observed also that, the metals chelating chelators should have low solubility in water and be highly soluble in nonpolar organic solvent to enable H-bonds which can enhance extraction.⁸⁹ This explains why a lot of metal extraction using lipophilic chelators have been reported in kerosene. Such H-bonding phenomenon was observed studying the keto-enol tauterism of the Htd in cyclohexane as is reported in chapter two.

Fast loading of metal into organic phase- The Htd in particular was able to bring about faster transfer of metal ions into organic phase than Hdbm. It is expected that chelator should have fast facilitation of metal transfer between the phases in loading or stripping and should be chemically stable under operation condition.⁸⁹ Being that the bio chelants exhibited metals extraction capabilities comparable to the Hdbm, these compounds can be used for recovery of metal ions and in other related applications.⁵¹ However, the binding capacities of the ligands could be enhanced by introducing amine groups.⁴⁸

5.2.16 Changes in pH during the extraction with these bioderived materials

The equilibrium pH in metal extractions is crucial to determining the nature of a chelator. Thus pH before and after extraction of some of the experiments were measured. The pH at equilibrium sometimes is either lower or higher than the initial pH of the aqueous metal solution depending on the nature of the chelator and the initial pH of the aqueous feed solution. These observations were similarly reported in the literature.³³¹ Table 5-10 and Table 5-11 below are showing the mean values of the pH of the metals solutions before and after metal extraction for these bioderived molecules in comparison to dibenzoylmethane. 0.03 M of each of the metals solutions were prepared and extracted with 3 mM of each of the chelating chelator without pH adjustment.

Table 5-10: pH variation following the removal of metal ions with the modified and unmodified Htd M: L (10:1)

	Htd		Hdbm		Ma		MaH		Ita		ItaH	
	I	F	I	F	I	F	I	F	I	F	I	F
CoCl ₂	7.29	6.98	7.29	7.2	7.29	7.38	7.29	6.52	7.29	7.38	6.60	5.5
NiCl ₂	7.27	6.82	7.27	6.90	7.27	7.29	7.27	5.5	ND	ND	7.3	6.73
FeCl ₃	1.59	1.52	ND	ND	ND	ND	1.44	1.42	ND	ND	Emulsion	Emulsion
CrCl ₃	2.58	2.57	ND	ND	ND	ND	ND	ND	ND	ND	Emulsion	Emulsion

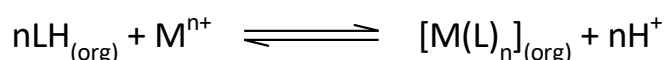
Note: I & F= Initial and final values of pH; ND= measurements were not taken because no extraction was observed

Table 5-11: pH variation following the extraction of Cu(II) in OAc⁻, Cl⁻, SO₄²⁻ and NO₃⁻ media with modified and unmodified Htd M: L (10:1)

	Htd		Hdbm		Ma		MaH		Ita		ItaH	
	I	F	I	F	I	F	I	F	I	F	I	F
Cu(OAc) ₂	6.13	5.84	6.13	5.85	6.13	5.96	6.13	5.48	6.13	5.95	6.11	5.73
CuCl ₂	4.17	3.72	4.17	2.48	4.17	4.61	4.17	3.37	4.17	4.59	4.17	3.05
Cu(NO ₃) ₂	5	3.95	5	2.93	ND	ND	5.34	4.22	ND	ND	5.34	3.75
CuSO ₄	4.84	4.19	4.84	3.04	ND	ND	4.89	3.89	ND	ND	5.43	3.91

Note: I & F= Initial and final values of pH; ND= measurements were not taken because no extraction was observed

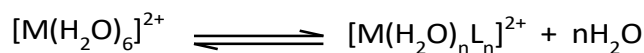
It may be deduced from results in Table 5-10 and Table 5-11 above that the pH of the raffinate were decreased after the extraction, with Htd, Hdbm, MaH and ItaH. This decrease in pH is an evidence of the deprotonation of the chelators during the metals extraction complying with metal extraction through chelating mechanism as depicted in Equation 5-5 below.^{90,331}



Equation 5-5: Release of H⁺ from the chelating chelators after extraction

While the removal of metals with Ma and Ita make the pH of the raffinate to increase in most cases. Thus, the increase in pH after extraction shows solvating mechanism of complexation for the extraction process as similarly reported in the past.³³¹ Wieszczycka *et al.*³³¹ studied extraction of Cu(II) ions from Cl⁻ and SO₄²⁻ solutions using hydrophobic pyridyl ketoximes found that at pH range of 1-3, after extraction the small increase of pH value was observed (ΔpH 0.05–0.1) which suggests a solvating mechanism of complexation, while for pH range of 3.8 – 5.3, the removal of Cu(II) resulted into decrease of pH value to approximately 2 units which suggests metal coordination through the chelating mechanism. First of all, in water the metal ions are hydrated,³⁴⁰ during the extraction, water is replaced from the aqua ions by the ligands as described by Equation 5-6 to form the chelator solvated ions. Carboxylates esters are known to remove metal ions as well.³⁴¹ Removal studies of mercury by monoesters of meso-2,3-dimercaptosuccinic acid (DMSA), monoisoamyl meso-2,3-dimercaptosuccinate (Mi-ADMS) and mono-n-hexyl meso-2,3-dimercaptosuccinate (Mn-HDMS) were compared to DMSA.³⁴² The monoesters were found to be more efficient than the acid analogue.³⁴² Solvating chelator are reported to be good for the extraction of Au as (AuCl₄)⁻.³⁴³

Therefore the Ma and Ita may also be tested for extraction of Au and other precious metals.



Equation 5-6: Replacement of water in the aqua ion by ligand

5.2.17 Competitive extraction of Cu(II) and Co(II) from mixture of CoCl₂ and CuCl₂ solution (0.015 M each)

Experiments to test the recovery of Cu(II) in the presence of Co(II) from their synthetic mixture was carried out. The removal of Cu(II) or Co(II) ions from the mixture of 0.015 M of CoCl₂ and CuCl₂ at pH 5 indicated that Htd, Ma and Ita removed more of Co(II) than Cu(II) just as it was the case when performing the extraction of Co(II) and Cu(II) from separate solutions of 0.03 M CoCl₂ and CuCl₂ each. Hdbm rather removed marginally higher amount of Cu(II) than Co(II) unlike the case when doing the extraction separately at pH 7.29 (for CoCl₂) and pH 4.17 (for CuCl₂). The data showing these observations are presented in Figure 5-16 (single metal extraction) and Figure 5-17 (competitive metal extraction). Although there was no strict selectivity (except with Ita), but there was reduced removal of Co(II) in the presence of Cu(II). This may be due to pH shift in favour of the Cu(II) that was found from the mixture of the two metals salts. Furthermore, only itaconate modified bioderived β -diketone (Ita) had selectivity for removal Co(II) in the presence of Cu(II). Most extraction of Co(II) with β -diketones like Hdbm and Hacac is optimally conducted at pH 7 and above. Kumar *et al.*³¹⁰ reported the removal of Co(II) at pH 5 with β -diketone-functionalized styrene divinylbenzene resin from aqueous CoCl₂ medium. Al Zoubi *et al.*³⁰⁴ reported selectivity for Cu(II) extraction from mixture Cu(II) and Cr(III) at pH 6.27 using [N,N'-p-phenylene bis (5-amino-2-methoxy-phenol)].

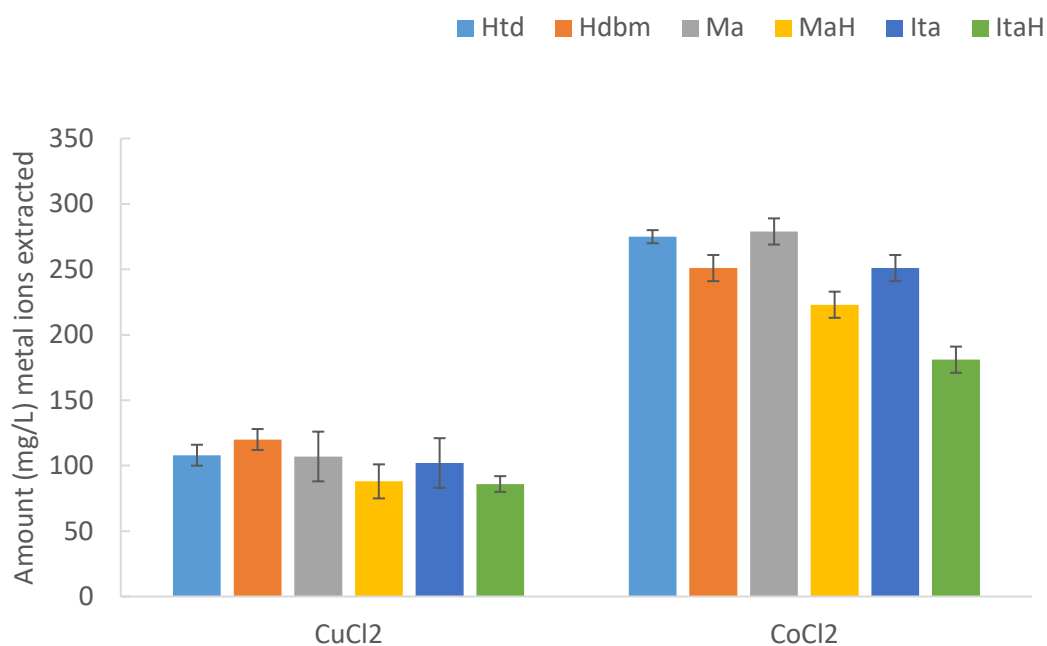


Figure 5-16: Single metal extraction of Co(II) and Cu(II) in Cl⁻ medium

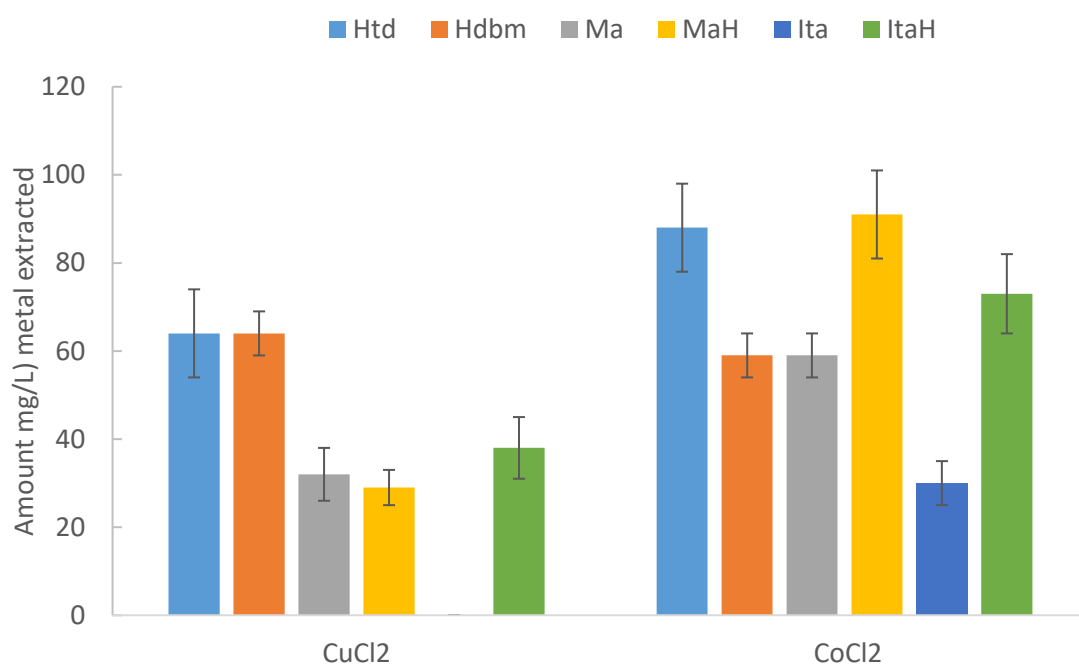


Figure 5-17: Competitive metal removal from mixture of Co(II) and Cu(II) in Cl⁻ medium

5.2.18 Effect of pH on extraction of Cu(II) from CuCl₂ solution with the bioderived materials and Hdbm

The pH of the CuCl₂ solution was adjusted from 5.56 to 6.18 and the extraction of Cu(II) performed with Htd, Hdbm, Ma, Ita and ItaH as given in Table 5-12. It was observed that

there was enhanced extraction of Cu(II) from CuCl₂ solution with all the chelators following this adjustment of the pH with NaOH similar to the reports in the literature.^{37,54,89,344} Extraction Studies of Cd(II), Cu(II), Mn(II), Ni(II) and Zn(II) using N,N',N,N'-Bis[(2-hydroxy-3,5-di-tert-butylbenzyl)(2-pyridylmethyl)]-ethylenediamine in the liquid-liquid (water- chloroform) extraction were also found to be pH dependent. In addition, maximum extraction of Cu(II) was obtained in the pH range of 4.5 - 6.0 as reported by Laus *et al.*⁵⁴ Kwon *et al.*³⁴⁴ found that the removal of Cu(II) from aqueous solutions by scoria (a vesicular pyroclastic rock with basaltic composition) was effective at solution pH of 5.0. previous studies reported that the presence of mineral acids can adversely reduce the effectiveness of complexation of chelators to metal ions.³³¹ The require pH for extraction of metal ions is also dependent on the chelator. Strong chelators remove metal cations at low pH values. Conversely, a weak chelator for metal cations is only capable of recovering metals at high pH.⁸⁹

Precipitation of the Cu(II) by the hydroxyl ions could have occurred resulting into these significantly higher levels of Cu(II) removed at the elevated pH of 6.18. Anyway, it is known that β -diketones extract better under basic conditions^{89,153} because the chelate are formed partially by replacement of hydrogen atoms in the β -diketone molecule.³³⁶ This could be the reason for extraction of copper with β -diketones from ammoniacal solutions.^{153,156,314,345} Again the higher enol content of Hdbm as discussed in chapter two is a likely factor that will make it chelate better than the Htd^{211,309} in some cases. From the literature the report of removal of Cu(II) using sterically hindered β -diketone showed that 95% Cu(II) was extracted at pH 8.43.⁵⁸ Solvent extraction copper at pH range 5- 9 have been reported using Hdbm.³¹⁷ Therefore increasing pH to basic condition enhances

Cu(II) recovery with β -diketones.^{159,336,346–350} Whereas acidic solutions hinder chelation with β -diketones by protonating the active site.^{37,344}

Table 5-12: Effect of pH on extraction of Cu(II) from CuCl₂ solution (M: L; 2:1)

Chelator	Amount Cu(II) extracted mg/L	
	(pH 5.56)	(pH 6.18)
Htd	19	529
Hdbm	25	224
Ma	6	412
Ita	9	519
MaH	6	489
ItaH	10	494

5.2.19 Determination of metal ions extracted with ICP-MS

ICP-MS was also applied to determine some extracted metal ions (Cu(II), Pb(II) and Mn(II)) by Htd from Cu(OAc)₂, Pb(OAc)₂ and MnCl₂ solutions using M: L of 1:1 and 3: L at pH 4.5 – 5.0. The % extraction of the metal ions for 1:1 (M: L) were in the range of 44 – 29; while for 3:1 (M: L), the % extraction were in the range of 27 – 22 as presented in Figure 5-18. Using higher concentration of Htd here also enhances the recovery of each of these metal ions as earlier explained. And the decreasing order of extraction is; Mn(II) > Pb(II) > Cu(II). Notwithstanding, according Laus *et al.*,⁵⁴ higher concentrations of chelating agent did not enhanced extraction of Cd(II), Cu(II), Mn(II), Ni(II) and Zn(II) using N,N',N,N'-Bis[(2-hydroxy-3,5-di-tert-butylbenzyl)(2-pyridylmethyl)]-ethylenediamine.

That is because, for most chelators, there is an optimal concentration beyond which any further increase in the amount of the chelator will not produce a directly proportional

amount of metals extracted. The percentage extraction (%E) of Mn(II) in this studies were more than Cu(II) and Pb(II) for the both M: L ratio of 1:1 and 3:1. This could be that the removal of Mn(II) from MnCl₂ solution was assisted by Cl⁻ counter ion more than the OAc⁻ in the case of Pb(II) and Cu(II).

Hence the effect of counter ion was once again tested for the extraction Cu(II) from CuCl₂, Cu(OAc)₂ and CuSO₄ solutions and the amount of metal ions extracted were measured with IC-PMS. The results for this in Figure 5-19 also indicated extraction of Cu(II) ions from Cl⁻ medium is better than from SO₄²⁻ and OAc⁻ at pH between 4.00- 4.50. This trend was re-established using spectrophotometric method of analysis as earlier explained. Although according to Wilson *et al.*,³¹⁶ majority of metal extraction system are carried out in SO₄²⁻ medium. But Cl⁻ system is better for extraction of most precious metals⁸⁹ because it's a strong inner sphere ligand. Conversely, SO₄²⁻ is weak inner sphere ligand.³¹⁶ That means sulphate acts as a weak counter ion thus do not enhance metals extraction like Cl⁻. Extraction of metals from OAc⁻ are not really common as from Cl⁻ and sulphate. Moreso, a real case studies carried out using Htd to extract Pd(II) from cyrene showed that 62% Pd(II) was recovered from the cyrene into cyclohexane phase. This shows that this Htd can also extract precious metals.

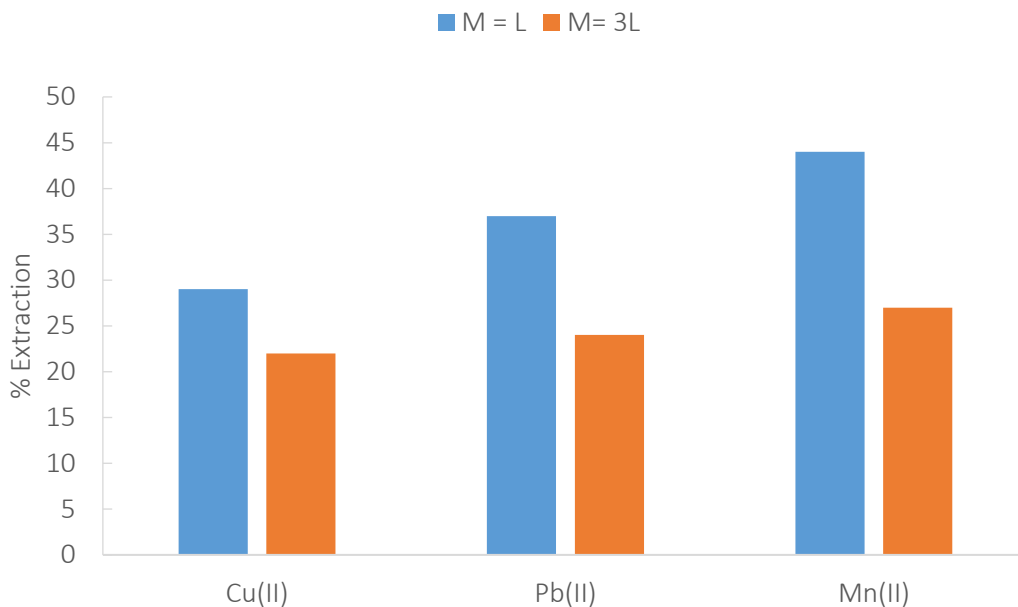


Figure 5-18: ICP-MS determination of extracted Cu(II), Pb(II) and Mn(II) using Htd

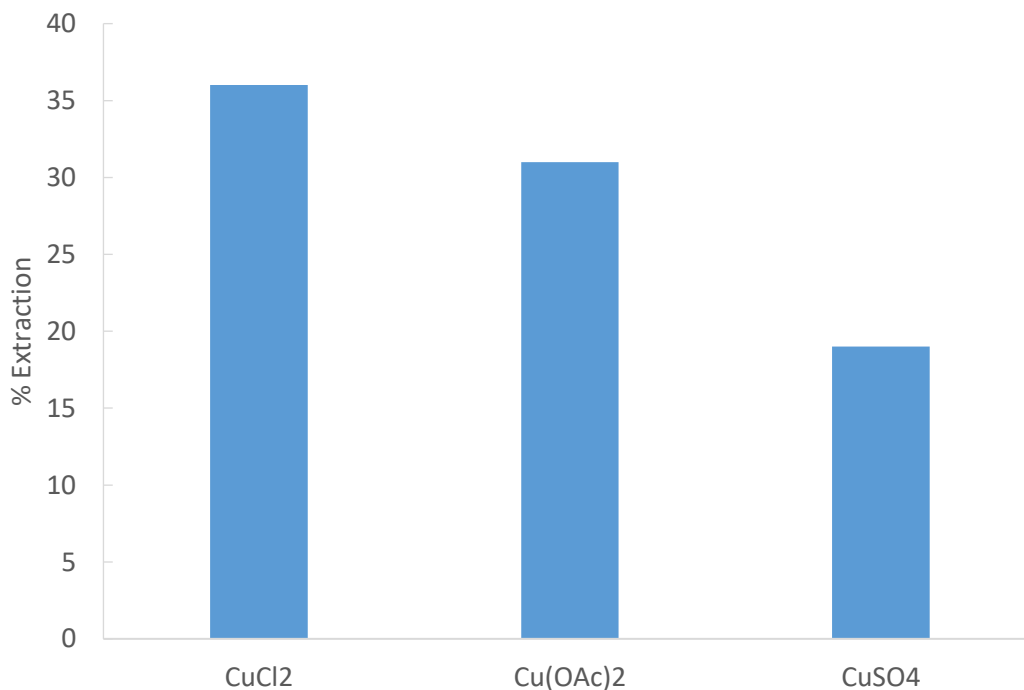


Figure 5-19: ICP-MS determination of extracted of Cu(II) from CuCl₂, Cu(OAc)₂ and CuSO₄ solutions with Htd (M: L, 1: 1)

5.2.20 ICP-MS determination of removed Pb(II) and Ga(III) with Htd and MaH

The removal of the Ga(III) and Pb(II) from Ga(NO₃)₃ and Pb(NO₃)₂ solutions were carried out with the Htd and MaH at pH range 2.83 – 3.41 and M: L ratio of 1:1 (1 mM for both

metal and ligand). The residual metal ions concentrations were measured with ICP-MS. From previous studies, pH of 4 was found to be an optimal for extraction of Pb(II) with β -diketone.²⁶³ The results presented in Figure 5-20 showed overall % E of Pb(II) > Ga(III). Extraction of gallium was better using the Htd, while MaH effectively removed Pb(II) (82%), more than the Htd which extracted 37% of Pb(II). This is an interesting case where the modified β -diketone is again better than the unmodified Htd.

Metals that have large ionic radius are often well extracted above those with low ionic radius.²⁶³ Particularly the ionic radius of Pb(II) is about 122 pm thus it was extracted higher with these molecules, whereas Ga(III) has ionic radius of 62 pm hence it was least extracted with Htd and MaH. Higher Pb(II) removal with gluconic than Cu(II), Cr(III), Ni(II) and Cd(II) has been reported by Fischer and Bipp.⁴⁷ An environmentally benign chelant ethylenediamine disuccinate (EDDS) was found to be an effective Pb(II) removal as compare to ethylenediamine tetraacetic acid (EDTA).¹²⁰ Also Xin *et al.*¹³⁵ observed better extraction of Pb(II) than Cu(II) and Zn(II) using tartaric acid. Better removal of Pb(II) was also observed against Cu(II), Zn(II), Cd(II) and As(III) from aqueous solutions by scoria (a vesicular pyroclastic rock with basaltic composition).³⁴⁴ It is then possible to apply these compounds in the extraction of Pb(II) as similarly reported.^{263,301,309,323} It was observed that there was decrease in pH after the extraction; from pH 2.83 to 2.30 – 2.56 for Ga(III) and from pH 3.41 to 2.81 – 3.01 for Pb(II). These are evidence for the removal of Ga(III) and Pb(II) with these acidic chelating chelators.

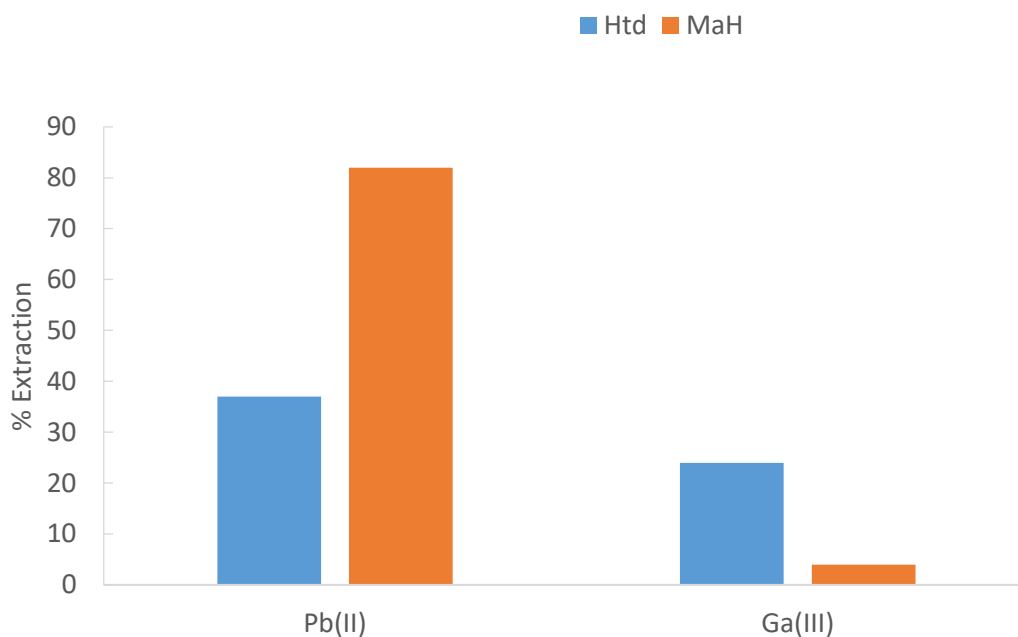


Figure 5-20: ICP-MS determination of recovered Ga(III) and Pb(II) with the Htd and MaH

5.2.21 UV/visible spectra of some of the metal extracts with Htd and Hdbm

UV/Visible spectroscopy is used to analyse ligand-metal chelate because free ligands produce different UV/Visible spectra to their ligand- metal chelates. Therefore, the UV/visible spectra of the Htd, Hdbm and their complexes (1.0×10^{-5} M) after metals extraction from NiCl_2 , CuCl_2 , CoCl_2 , and $\text{Cu}(\text{OAc})_2$ solutions were obtained in chloroform as presented in Figure 5-21 and Figure 5-22 in wavelength range of 249 – 349 nm. Such characterisation of ligand with carbonyl functional group has been described by Hamid.³⁵¹ The λ_{max} of the free Htd was found at 277 nm. The UV/Visible spectra of the Htd-metal extracts after extraction from NiCl_2 and CoCl_2 solutions were decayed; whereas in the Cu-Htd extracts, the λ_{max} shifted towards higher wavelength in the case of $\text{Cu}(\text{OAc})_2$ (λ_{max} 300 nm) and additional peak at about 300 nm in case of Htd- CuCl_2 chelate solution in chloroform. Previous works have also reported similar peaks.^{211,352} These differences (shift of λ_{max} or decaying of the UV/Visible spectra) of the free Htd after extraction is due to complexation of the Htd to these metal ions. Cakic *et al.*³⁵³ reported

280 nm as the λ_{\max} for Mn-acetyl acetone. The electronic absorption maxima of Hacac and Hdbm has been previously reported as 274 nm and 345 nm³⁵⁴ respectively. This absorption is for $n \rightarrow \pi^*$ transition due to C=O. Oladipo *et al.*¹⁴² also found a Uv/visible band of 349 nm for the Cu-dbm complex due to $n \rightarrow \pi^*$ transition.^{142,352}

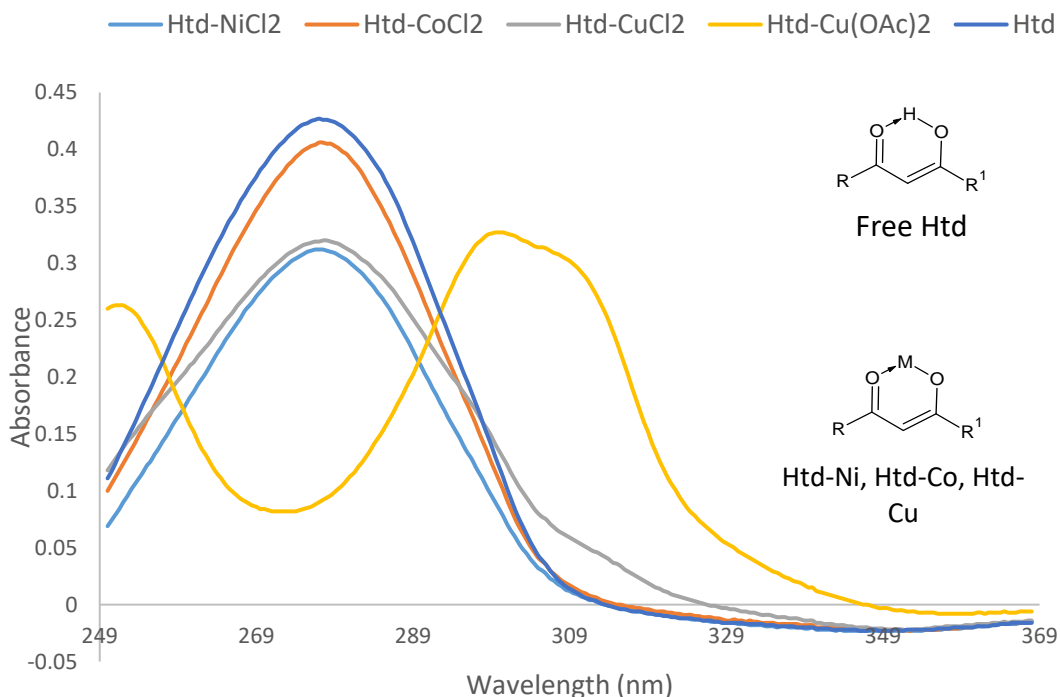


Figure 5-21: UV/visible spectra of the metal extracts with the Htd in chloroform (1.0×10^{-5} M)

In addition, the λ_{\max} of 343 nm found in the UV/Visible spectra of free Hdbm as previously reported¹⁴² slightly shifted to higher λ_{\max} and the intensity reduced in the UV/Visible spectra of the Hdbm-metal extracts after the extraction from CuCl₂, CoCl₂ and Cu(OAc)₂ solutions as presented in Table 5-13 and Figure 5-22. These also implied the metal ions were coordinated to the Hdbm during the extraction process. The intensity of absorption of curcumin at 427 nm was reduced due to coordination to Cu(II) as reported by Kanhathaisong *et al.*³⁵⁵ This evidence mean that the metal ions were removed from the aqueous phase with the Htd and Hdbm.

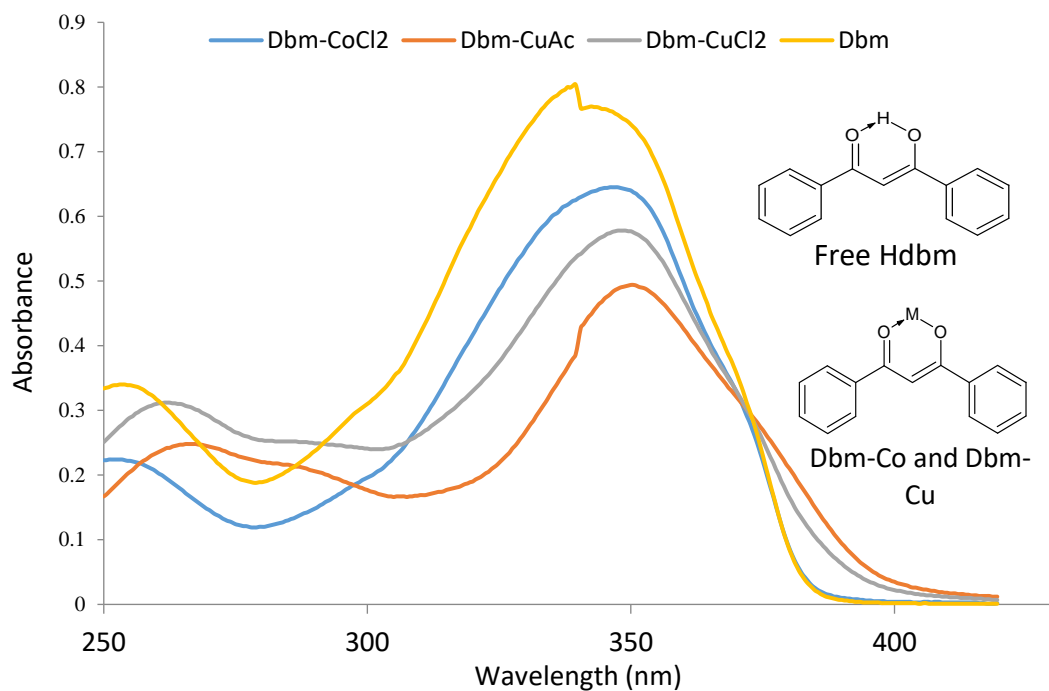


Figure 5-22: UV/visible- spectra of Hdbm and its metals complexes in chloroform- 1.0×10^{-5} M

Table 5-13: UV/visible spectra of Htd and Hdbm and their metal complexes in chloroform (1.0×10^{-5} M)

Samples	λ_{\max} (nm)	Samples	λ_{\max} (nm)
Hdbm	343, 254	Htd	277
Hdbm-CoCl ₂	347, 253	Htd-CoCl ₂	278
Hdbm-CuCl ₂	349, 261	Htd-CuCl ₂	277
-	-	Htd-NiCl ₂	278
Hdbm-Cu(OAc) ₂	351, 267	Htd-Cu(OAc) ₂	300

According to Urbaniak *et al.*,²¹¹ the UV/Vis spectra of the Cu- and Co-complexes with 3-allylacetylacetone showed a shift in λ_{\max} from 280 to 310 nm for Cu-complex and a slight shift in the λ_{\max} of the Co- complex from the free ligand at about 280 nm. These were taken as evidence for the coordination of the 3-allylacetylacetone to the metal ions, Cu(II) and Co(II).

5.2.22 $^1\text{H-NMR}$ spectrum of Co and Cu- extracts with Htd

When ligands coordinate metal ions, it makes their $^1\text{H-NMR}$ chemical shift to move to lower values.²²⁷ The $^1\text{H-NMR}$ spectrum of the Cu- and Co-Htd extract from extraction of 15 mM (Co(II) and Cu(II) each) with 3 mM Htd was obtained to see further evidence of coordination of the ligand to the metals as given in Figure 5-23 below. It is observed that the vinyl proton chemical shift of the Htd went down from 5.46 ppm to 4.68 and 3.93 ppm. This shift is most likely due to the shielding effect encounter by vinyl proton after the β -diketone formed covalent bond with metal ions as previously reported. This also show that there was an extraction of these metal ions. Carty *et al.*³⁵⁶ also reported a similar $^1\text{H-NMR}$ chemical shifts between 4.48 – 5.28 ppm for metal acetyl acetonates due to the covalent bonding between the metals and the Hacac.³⁵⁶

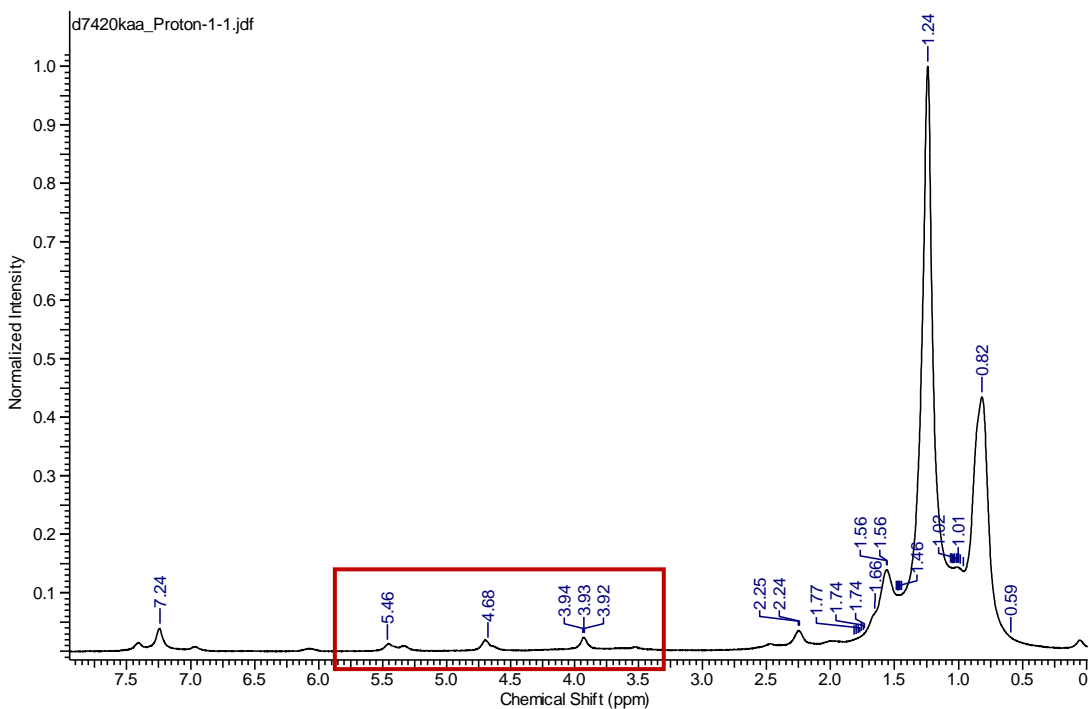


Figure 5-23: $^1\text{H-NMR}$ spectrum of Co and Cu- complexes after extraction with Htd

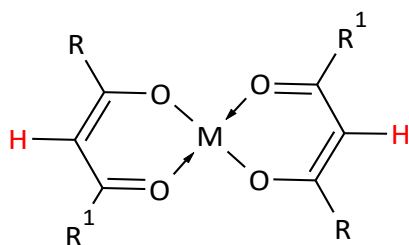


Figure 5-24: Co- and Cu- 14,16-hentriacontanedionate with the marked vinyl protons

5.2.23 FTIR evidence for the Co- and Cu-extracts with the Htd

In FTIR analysis, the free ligand and the metal-ligand complex display different absorptions.^{221,353,357} For ligands with carbonyl functionality, there is also decrease in its FTIR absorption frequency after coordination to metal ions.³⁵⁵ In this studies, the free bioderived β -diketone(Htd) has FTIR absorption (cm^{-1}) of 1639 and 1710 implying the presence of enol and the keto form C=O as given in the FTIR spectra in Figure 5-25. Complexation of the metal ions to the β -diketone for the extraction of the mixture of 15 mM Co(II) and Cu(II) with Htd (3 mM) shifted FTIR absorption of the Htd downward to 1523 cm^{-1} and 1563 cm^{-1} with a new band at 3300 cm^{-1} implying coordinated water molecules. Rajbhoj *et al.*²²³ reported that FTIR of $3185.17 - 3244.13 \text{ cm}^{-1}$ means -OH stretching of coordinated water molecule in Co-chelate of 1-(5-chloro,2-hydroxyphenyl)-3-(4-ethoxyphenyl)propane-1,3-dione.^{225,358} And in the FTIR of *tris*(3,5-heptanedionato)europium(III) ($\text{Eu}(\text{H}_5\text{H}_5)_3 \cdot 2\text{H}_2\text{O}$), the C=C and C=O FTIR absorption were assigned as 1511 cm^{-1} and 1587 cm^{-1} .²²¹ Others have reported that the coordinated β -diketones are under their enol form due to observed absence of keto carbonyl FTIR vibration band in the spectral range $1740 - 1780 \text{ cm}^{-1}$.²²¹ The FTIR spectrum of embelin with absorption at 1612 cm^{-1} (C=O) and 1326 cm^{-1} (C-O stretch) upon complexation with the Zn(II) to form the complex, $(\text{Emb})_2[\text{H}_2\text{O}_2]\text{H}_2\text{O}$, the carbonyl stretching frequency shifted to 1527 cm^{-1} .²²⁰ The complex exhibited two bands at 1372 and 1229 cm^{-1} due to

C–O stretch of enolic –OH groups.²²⁰ The C–O stretch shifted to 1110 cm⁻¹ in metal complex.²²⁰

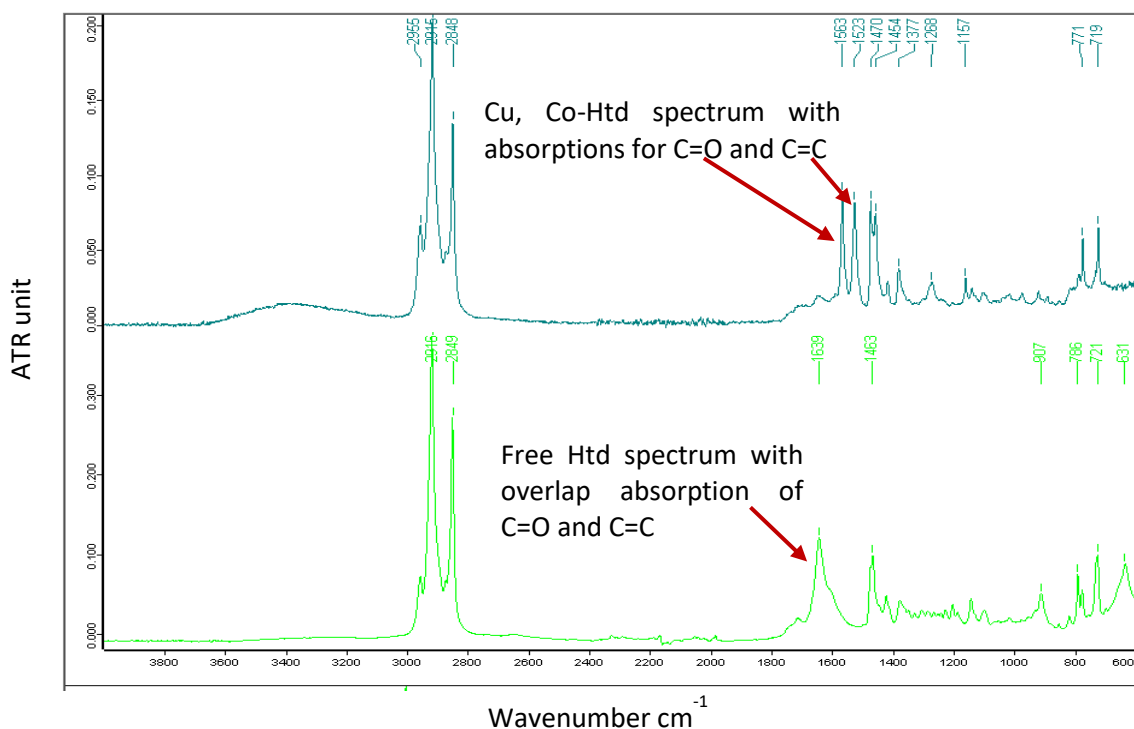


Figure 5-25: FTIR spectra of the free and metal-Htd chelate

The 1639 cm⁻¹ peak of the free β -diketone was reduced to a mere shoulder in the spectrum of metal-Htd complex. The shift is indication of coordination via donation of lone pair of electrons from the oxygen atom to the metal ions.²²² This provides further evidence of the removal of the metal ions from aqueous phase into organic layer. Some of these FTIR peaks of the free Htd and the metal-Htd chelate are succinctly interpreted as given in Table 5-14 as follows.

Table 5-14: FTIR (cm⁻¹) of the metal-Htd complexes and the free Htd

FTIR (cm ⁻¹)	Assignment	Ref.
3320 (broad)	-OH stretch or coordinated water	222,223,225
2990 - 2850	CH ₃ ; CH ₂ , (CH antisymmetric, and CH symmetric) stretch	11,222

1743	C=O	225
1547 -1570	Enolic stretch (C=C, lower and C=O, higher)	221,222,224
1268 - 1377	=C-O	221
1142	C-O	225
1400 - 3900	C- H bending vibrations, SP ³ (CH ₃)	222
1639	C=C-C=O	224,227

5.3 Conclusion

The unmodified and modified Htd were used for the extraction of some metal ions; Mn(II), Pb(II), Ni(II), Co(II), Cu(II), Ga(III), Fe(III) and Cr(III) in a liquid biphasic system from synthetic metal solutions. Influence of time, solvent, pH, ionic strength and temperature for the removal of Cu(II) with the Htd was first investigated. Follow by equilibrium slope analysis for stoichiometric determination of Cu(II) extraction with the Htd. In addition, UV/visible, FTIR and ¹H-NMR spectra evidence of some extracted metal ions with Htd were analysed. The extraction of metal ions (Cu(II), Ni(II), Co(II), Fe(III) and Cr(III)) using the Ma, Ita, MaH, and ItaH in comparison to the Htd and Hdbm were performed. Effect of pH and initial metal ion concentration on the extraction of Cu(II) with these modified biochelators were carried out in comparison to the Htd and Hdbm. MaH and ItaH were more effective in the extraction of Cu(II) and Pb(II) than the Htd and Ma, Ita and Hdbm. However, Ma, Ita and Htd were recovered and used for metal extractions. In general, these bioderived molecules will be useful for recovery of metals preferably in Cl⁻ and OAc⁻ media, but also can extract from SO₄²⁻ and NO₃⁻ solutions (in basic medium or using higher concentrations of the β-diketone). Therefore, extraction of metals (from Cl⁻, OAc⁻ and NO₃⁻ solutions) with these compounds will be quantitative and most effective at basic condition and by using higher concentrations of these chelators.

Chapter 6

Experimental

6 Chapter 6

6.1 Materials and reagents

Dichloromethane, heptane, cyclohexane, toluene, *tert*-butanol, ethanol, ethyl acetate, dimethyl sulfoxide (DMSO), methanol, 1-butanol, octanol, acetone, HCl (analytical and ICP-MS grade), petroleum ether (333 – 353 K), chloroform, methyl ethyl ketone, KOH, NaOH, sodium bicarbonate, brine solution and anhydrous magnesium sulphate were purchased from Fisher Scientific UK Limited. Acetyl acetone (Fluka), TLC plates (Merck), Ely Fly ash, wheat straw wax, distilled water, carbon dioxide of > 99.99% purity (purchased from BOC Group). While 2-methylTHF, cyclopentyl methyl ether, 2,2,5,5-tetramethylTHF, tetradecane, limonene, *p*-cymene, acetone-d₆, CDCl₃, toluene-d₈, cyclohexane-d₁₂, THF-d₈, methyl acrylate, dimethyl itaconate, methyl methacrylate, aconitic acid, KF, alumina, methyl trans cinnamate, KCl, methyl palmitate, acetic acid, potassium and sodium metals, lauric acid, dibenzoylmethane, acetic anhydride, DMAP (4-dimethylaminopyridine), CuSO₄·5H₂O, Cu(NO₃)₂·3H₂O, CrCl₃·6H₂O, Cu(OAc)₂, NiCl₂, CoCl₂, Co(NO₃)₂·6H₂O, FeCl₃ and CuCl₂ were purchased from Sigma- Aldrich, analytical grade > 99% purity. All chemicals were used without further purification.

6.2 Equipment

UV-1800 Shimadzu (UV/visible Spectrophotometer), GC-MS (Perkin Elmer Clarus 500 GC coupled with a Clarus 500 quadrupole mass spectrometer), GC-FID Agilent 7820A (Agilent 6890N, Hewlett Packard HP6890; column name, RXI-5HT; column diameter, 30 m x 0.25 mm x 0.25 μm and column maximum temperature of 673 K), FTIR Bruker Vertex 70, ¹H-NMR and ¹³C-NMR (JNM – ECS 400 of field strength, 400 MHz for ¹H and 100 MHz for ¹³C), MDSC Q 2000, scCO₂ extractor (SFE-500 extractor), CEM microwave, LC - Agilent

1260 Infinity and MS - Bruker micrOTOF time of flight MS, STA, UV lamp, Jenway 3505 pH meter, Biotage Isolera Four.

6.3 Experimental procedures

6.3.1 Purification of Htd using petroleum ether with cuprous acetate

The isolation of the Htd was carried out as previously reported by Horn *et al.*²¹⁶ with some slight modifications. A typical extraction procedure is as follows: 1 g of the wheat straw wax was thoroughly crushed with spatula in a 500 mL beaker and dissolved with 200 mL of petroleum ether (333 – 353 K) under magnetic stirring at room temperature. This mixture was filtered after standing for 30 min and the filtrate transferred to 500 mL separating flask, followed by addition of 100 mL hot excess saturated aqueous Cu(OAc)₂. The resulting mixture was shaken intermittently for 10 min and allowed to stand for 1 h. The organic phase (upper layer) became green, while the aqueous phase (lower layer) was light-bluish with a dark– bluish Cu-diketone in between the two phases. The system was heated with heat-gun to afford proper separation of the organic and aqueous phase. The aqueous layer was removed while the organic layer was collected and kept for 2 h for the complete crashing of the Cu-diketone. The precipitate was then filtered and the crude Cu-diketone washed with 5 mL petroleum ether. The copper salt was re- dissolved in about 100 mL of the hot petroleum ether, transferred into the 500 mL separating flask follow by addition of 2 mL concentrated hydrochloric acid. The separating flask and its contents was thoroughly shaken intermittently for 10 min to strip out the Cu(II) ions from the lipophilic β -diketone in the organic phase. The organic layer was washed with 100 mL deionised distilled water stepwise. The two layers were separated and the pale yellow product (Htd) was recovered from the organic layer by removing the petroleum ether under *in vacuo*. The excess aqueous cuprous acetate was recovered and re-used. ¹H-NMR

(400 MHz $CDCl_3$) δ ppm 0.79 – 0.92 (m, 9H), 1.24 (s, 60H), 1.41 (s, 3H), 1.37 (s, 4H), 1.49 – 1.75 (m, 16H), 2.22 – 2.31 (m, 5H), 2.48 (t, $j = 732$ Hz, 1H), 3.53 (s, 1H), 5.46 (s, 1H). ^{13}C -NMR (101 MHz, $CDCl_3$) δ ppm 14.19 (1 C, s), 22.77 (1 C, s), 25.83 (1 C, s), 29.32 (1 C, s), 29.44 (1 C, s), 29.55 (1 C, s), 29.69 (1 C, s), 29.73 (1 C, s), 29.76 (1 C, s), 32.00 (1 C, s), 38.50 (1 C, s), 99.13 (1 C, s), 123.71 (1 C, s), 193.28 (1 C, s), 194.66 (1 C, s). FTIR (cm^{-1}) - 2955, 2916, 2849, 1639, 1453, 1419, 1375, 1139, 907, 786, 722, 721, 631. GC-MS molecular ion; 464 m/z; Yield 18 ± 5 wt%. Melting point, 53.9 °C; r_f (80% cyclohexane and 20% ethyl acetate): 0.89 ± 0.03 , ESI-MS(+), 463.4506 m/z, 503.4437 m/z, 549.4853 m/z.

The Figure 6-1 below has itemized the stages involved in the isolation of the Htd.

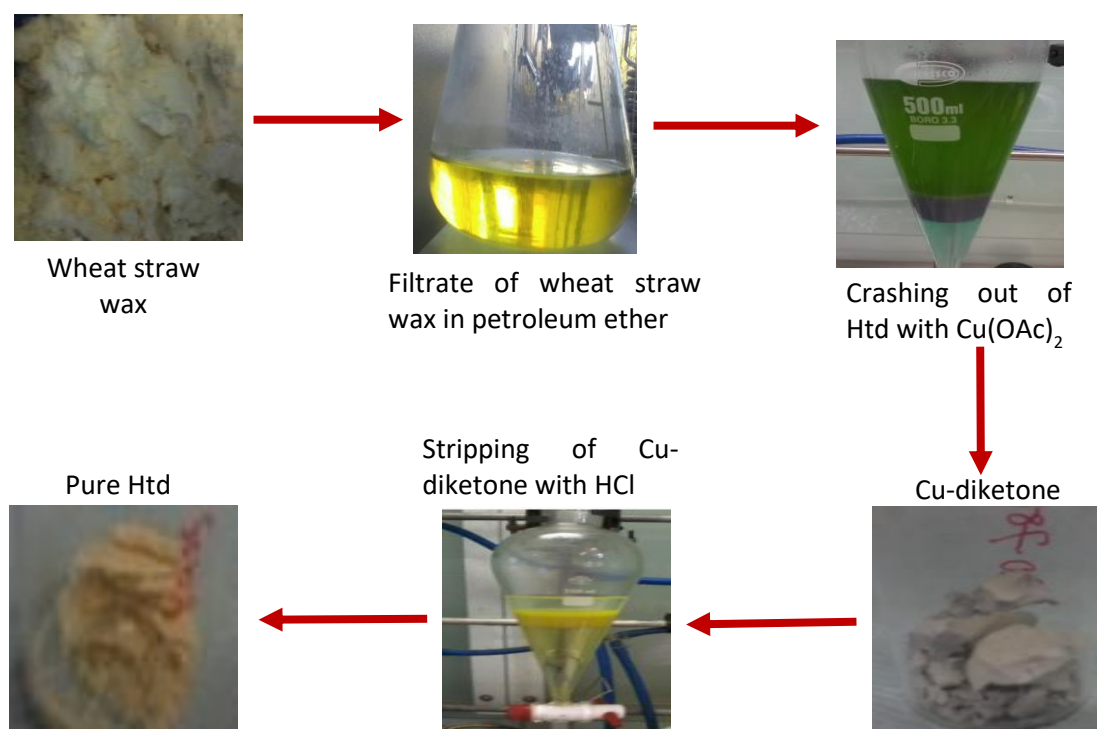


Figure 6-1: The stages for the isolation of the Htd from wheat straw wax using petroleum ether with $Cu(OAc)_2$

6.3.2 Solubility test of the Htd in different solvents

20 mg of the β -diketone was shaken in 1 mL of each of these selected solvents; heptane, cyclohexane, toluene, 2-methylTHF, cyclopentyl methyl ether (CPME), 2,2,5,5-tetramethylTHF (TMTHF), *tert*-butanol, methanol, ethanol, ethyl acetate, dimethyl

sulfoxide (DMSO), octanol, 1-butanol, limonene, *p*-cymene, acetone and water for 5 min and then the mixture allowed to stand for 30 min. The ability of these solvents to dissolve the sample were visually assessed based on complete or incomplete dissolution.

6.3.3 Keto-enol tautomeric studies of the Htd in comparison to Hdbm and Hacac

6.39 mg of Hdbm, 12.52 mg Htd and 2.77 mg Hacac were respectively dissolved with 0.7 mL of acetone- d_6 , $CDCl_3$, toluene- d_8 , cyclohexane- d_{12} and THF- d_8 forming approximately 0.04 M each. Thereafter, the 1H -NMR spectra of these solutions were measured at 296 K, from these the integral values of the keto- enol were determined.^{136,213,239} The integral value of the H^{keto} were divided by 2 to form 1: 1; H^{keto} : H^{enol} integral ratio. Then the % of keto- enol were determined from these 1: 1 integral values as previously evaluated.²³⁷

6.3.4 The scCO₂ fractionation of wheat straw wax for Htd

The scCO₂ fractionations of the wheat straw wax were carried out using Thar SFE-500 scCO₂ extractor with 99.99% pure CO₂. About 1 g or 10 g of wheat straw wax was crushed and dissolved with about 500 mL methylene chloride (DCM) in 1000 mL beaker, followed by addition of about 200 g of celite, silica or alumina adsorbent. The adsorbent was thoroughly mixed in the wax solution. Thereafter, the solvent was then completely removed in *vacuo* affording a dried uniform solid mixture of the wax- adsorbent. This solid mixture above was transferred into the 500 mL extracting vessel for the scCO₂ fractionation.

The fractionation of the wax was carried out sequentially or simultaneously by pre-setting the desired temperatures and pressures of the scCO₂ separators.^{162,174,244} An internal pump was used in order to obtain the required pressure. The system was run in dynamic mode, in which the scCO₂ via the wax lipids, was allowed to flow into the

collection vessel. A flow rate of 40 g/min of scCO₂ was applied and the extraction was carried out for at least 3 h simultaneously or sequentially. When the extraction was terminated, depressurisation of the system was carried out over a period of 4 h. The fractional lipids were collected by rinsing each separator vessel twice with approximately 100 mL of DCM. The solvent in the fractions collected was removed under vacuum and the mass of extract determined. The wax: adsorbent residue in the extractor was removed and a brush was used to clean the extraction vessel. The schematic major components and the scCO₂ extractor used in these fractionations of the wheat straw wax are described in Figure 6-2 and Figure 6-3.

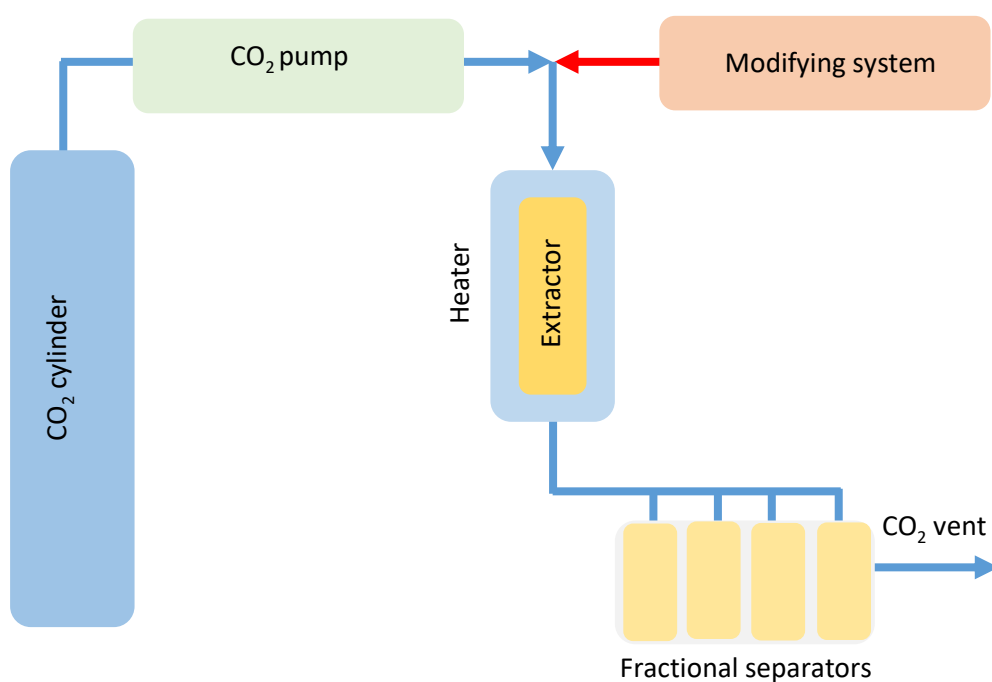


Figure 6-2: Schematic illustration of the scCO₂ extractor's basic components



Figure 6-3: The $scCO_2$ extractor used in the fractionation of the wax

6.3.5 Preparation of potassium *tert*-butoxide (*t*-BuOK)

Small pieces of potassium metal were dissolved with about 100 mL of dried hot *tert*-butanol in a 250 mL round bottom flask. The flask was covered with plastic cork fitted with syringe. The reaction was stirred for 1 h until all the potassium metal dissolve completely in the alcohol. Then the solvent was removed under vacuum to form white product of potassium *tert*-butoxide (*t*-BuOK).

6.3.6 Preparation of 2,4-hexanedione by Claisen condensation of methyl ethyl ketone (MEK) and ethyl acetate

To a 100 mL round bottom flask charged with magnetic stirrer, 1 mL of ethyl acetate was added. Then followed by 0.5 mL of methyl ethyl ketone and excess mole equivalent *t*-BuOK and the reaction was stirred for 30 min at 293 K. The reaction mixture was stopped and cooled in ice-cold water for 30 min. To this mixture, a pre-cooled concentrated acetic acid (0.3 mL) was added to neutralize the mixture as similarly performed.³⁵⁹ The product

was extracted with DCM and identified as 2,4-hexanedione by GC-MS with a retention time of about 4 min and the molecular ion, 114 m/z.

6.3.7 Preparation of methyl ketone using Dakin-West reaction

Into 30 mL vial, 0.2 g lauric acid, 2 mL of acetic anhydride, 0.2 g DMAP (4-dimethylaminopyridine), 0.05 g Ely Fly ash (EFA) were mixed. The mixture was heated using microwave CEM at 453 K, 200 W, 250 psi for 25 min. The retention time of the synthesized methyl ketone (2-tridecanone) as found by GC-MS chromatogram was about 14 min, and the molecular ion, 198 m/z.

6.3.8 Preparation of trimethyl aconitate

About 5 g aconitic acid and 33.3 mL (27 g) methanol (MeOH), in the mole ratio of 1: 30, and 3 drops of concentrated sulphuric acid were placed into 250 mL round bottom flask. The reaction mixture was refluxed overnight at 358 K with continuous agitation. The reaction was stopped after 18 h. Methanol was removed and fresh methanol and drops of sulfuric acid added and the system refluxed again for 18 h. That was repeated two times. In the end of the esterification process (after 3 days), the reaction mixture was poured into 75 mL distilled water in a separating funnel. The reaction vessel was rinsed with 35 mL petroleum ether (313 – 333 K) into the funnel. After shaking for equilibration, the organic layer was washed with 15 mL of distilled water followed by 25 mL of 5% sodium bicarbonate; 15 mL brine solution, and eventually dried with anhydrous magnesium sulphate and filtered. The solvent was removed under reduced pressure to give the product (light yellow oil). The yield obtained was 85%. ¹H-NMR (400 MHz, CDCl₃) δ ppm 3.62 (3 H, s), 3.70 (3 H, s), 3.75 (3 H, s), 3.89 (2 H, s), 6.78 - 6.96 (1 H, m) and ¹³C-NMR (100 MHz, CDCl₃) δ ppm 32.85 (1 C, s), 52.05 (1 C, s), 52.17 (1 C, s), 52.89 (1 C, s),

129.03 (1 C, s), 139.86 (1 C, s), 165.71 (1 C, s), 166.37 (1 C, s), 170.30 (1 C, s); molecular ion, 216 m/z.

6.3.9 Preparation of the KF/alumina catalyst

KF/alumina was prepared as previously reported by Clark *et al.*³⁶⁰ and Lenardão *et al.*²⁰⁵ Alumina was pre-treated by drying in oven at 423 K for 12 h. Then, 10 g alumina was mixed with 3 g KF and dissolved in 20 mL of methanol in 250 mL round bottom flask. This mixture was subjected to stirring for 30 min at 323 K. Thereafter, methanol was removed under vacuum with an intermittent mixing during solvent removal.³⁶⁰ The KF/alumina was dried in a vacuum oven for 14 h at 423 K. This mixture represents 5 mmol KF/g alumina.

6.3.10 Modification of Hacac with methyl acrylate by Michael addition

0.1 mL acetyl acetone, 5 mole equivalents methyl acrylate and 200 mg KF/alumina were put into a screw cap vial and reacted under stirring for 4h at 333 K under solvent free condition. The product was identified by GC-MS; molecular ion, 272 m/z (for double addition) and molecular ion, 186 m/z (for single addition).

6.3.11 Modification of the Htd using carboxylate esters by Michael addition

About 0.010 g of the 14,16-hentriacontanedione was weighed into the 15 mL microwave vial; follow by addition of 50 mg KF/alumina. The heterogeneous catalyst was well dispersed (suspension) with the Htd. Then 0.014 g (about 4 mole equivalents) dimethyl itaconate or 10 μ L (5 mole equivalents) methyl acrylate was added to the reaction mixture. The maximum pressure and the power in the CEM discover microwave were set at 300 psi and 300 watts respectively with a reaction time between 1- 15 min. 393 K was found to be appropriate for the modification of the bioderived β -diketone. See Figure 6-4 for the CEM microwave equipment used. These various reactions were also

conducted with traditional stirrer hot plate as a heat source using identical quantities of materials in 15 mL vial with screw cap. The reaction mixture was well stirred during the reaction time under solvent-less conditions.

The reactions were also scaled up using 0.2 g Htd, 1 g KF/alumina with 4 mole equivalents of the dimethyl itaconate or 5 mole equivalents of the methyl acrylate. Temperatures of 393 K, 2 h and 333 K, 4 h were used for the modification of the Htd with dimethyl itaconate and methyl acrylate respectively. At the end, the reaction mixtures were filtered to remove the catalyst using dichloromethane (DCM) and ethyl acetate. The products were purified using flash chromatography. In addition, short part distillation (Kugelrohr) was also applied to separate the excess dimethyl itaconate from the modified Htd. The $^1\text{H-NMR}$ of Ma: (400 MHz, CDCl_3) δ ppm 0.76 - 0.86 (6 H, m), 1.11 - 1.29 (41 H, m), 1.30 - 1.38 (3 H, m), 1.40 - 1.53 (5 H, m), 1.98 - 2.06 (3 H, m), 2.11 - 2.18 (4 H, m), 2.27 (4 H, t, $J=7.32$ Hz), 3.60 (6 H, s). $^{13}\text{C-NMR}$ (101 MHz, CDCl_3) δ ppm 14.21 (s, 1 C) 22.77 (s, 2 C) 23.67 (s, 1 C) 25.45 (s, 1 C) 28.79 (s, 1 C) 29.17 (s, 1 C) 29.37 - 29.61 (m, 4 C) 29.62 - 29.89 (m, 7 C) 31.55 (s, 1 C) 32.00 (s, 2 C) 39.29 (s, 1 C) 41.24 (s, 1 C) 42.27 (s, 1 C) 51.96 (s, 1 C) 68.77 (s, 1 C) 173.12 (s, 1 C) 193.09 (s, 1 C) 208.29 (s, 1 C). FTIR (cm^{-1}) 2915, 2849, 1723, 1689, 1475, 1462, 1438, 1408, 1375, 1258, 1234, 1200, 1175, 1133, 1110, 1067, 985, 823, 728, 718, 653, 627. ESI-MS peaks (m/z); 675.5 (Ma_d), 589.5 (Ma_s), r_f (80% cyclohexane and 20% ethyl acetate): 0.59 (Ma_s) and 0.41 (Ma_d). $^1\text{H-NMR}$ of Ita (400 MHz, CDCl_3) δ ppm 0.84 - 0.90 (5 H, m), 1.18 - 1.32 (42 H, m), 1.53 (7 H, s), 1.47 - 1.57 (3 H, m), 2.05 (2 H, s), 2.36 - 2.52 (4 H, m), 2.65 - 2.74 (2 H, m), 3.66 (2 H, s), 3.68 (2 H, s), 3.77 (1 H, dd, $J=8.70, 5.50$ Hz). $^{13}\text{C-NMR}$ (101 MHz, CDCl_3) δ ppm 14.21 (s, 1 C) 23.44 (s, 1 C) 29.10 (s, 1 C) 29.22 - 29.86 (m, 10 C) 32.01 (s, 3 C) 36.41 (s, 1 C) 39.45 (s, 1 C) 41.85 (s, 1 C) 42.67 (s, 1 C) 52.01 (s, 1 C) 52.19 (s, 1 C) 65.12 (s, 1 C) 171.80 (s, 1 C) 205.54 (s, 1 C). FTIR

(cm^{-1}) 2916, 2850, 1735, 1729, 1717, 1692, 1583, 1543, 1471, 1440, 1373, 1286, 1223, 1168, 1106, 1011, 967, 888, 844, 718, 630, 544, 537, 530, 521, 515, 503. ESI-MS; (m/z) 661.5, r_f (80% cyclohexane and 20% ethyl acetate): 0.51.



Figure 6-4: Traditional stirrer hot plate and SP discoverer microwave (CEM) heating sources used for the modification of the Htd

6.3.12 Preparation of cinnamic acid by hydrolysis of methyl cinnamate

The preparation of the cinnamic acid was performed following a similar procedure as described by Khurana *et al.*²⁶⁶ 0.208 g methyl *trans*-cinnamate and NaOH or KOH (about 3 mole equivalents) were put in 10 mL vial with a screw cap followed by mixture of 2 mL DCM/3 mL MeOH or 2 mL 2-methyl THF/3 mL MeOH. This was stirred at 303 K for 2 h 30 min. An intense white lump was formed with NaOH in the course of the reaction unlike with KOH. Thereafter, the reaction mixture was concentrated in 100 mL round bottom flask. Then 10 mL distilled water was added and the mixture acidified to pH of 2 with concentrated HCl. The product was filtered off using vacuum filtration. Then it was analysed with GC-FID and $^1\text{H-NMR}$ (400 MHz, CDCl_3) δ ppm 6.45 (d, $J=16.02$ Hz, 10 H) 7.36 - 7.45 (m, 28 H) 7.50 - 7.60 (m, 19 H) 7.79 (d, $J=16.02$ Hz, 9 H).

6.3.13 Preparation of palmitic acid by hydrolysis of methyl palmitate

0.2 g methyl palmitate and NaOH (about 3 mole equivalents; 0.100 g) were put into a mixture of 1.5 mL DCM/ 2 mL MeOH in a 10 mL screw cap vial, covered and stirred at 303 K for 2 h 30 min, 5 h and 24 h respectively. A white lump formed in the course of the reaction. The reaction was stopped at the appropriate time and concentrated under vacuum. Then 10 mL distilled water added and the mixture acidified to pH of 2 with concentrated HCl. The product was filtered and analysed with GC-FID.

6.3.14 Preparation of carboxylate acids of the Ma and Ita by hydrolysis

The hydrolysis of the carboxylate esters of the modified Htd were performed as similarly reported in the literature.²⁶⁷ 0.0479 g of the Ma was dissolve into 0.2 mL of dichloromethane (DCM) in a 5 mL vial, follow by 0.0175 g NaOH (5 mole equivalents) in 0.3 mL MeOH and this mixture stirred for 24 h at 303 K. The reaction mixture turned into a white lump at the end of the reaction implying sodium carboxylate of the modified β -diketone was formed. The reaction was stopped and the solvent removed under vacuum. 10 mL of distilled water was added to this sample and acidified with HCl to pH of 2. The product was then extracted with 10 mL DCM and concentrated. $^1\text{H-NMR}$ (400 MHz, CDCl_3) δ ppm 0.86 (7 H, s), 1.24 (47 H, s), 1.42 (3 H, br. s.), 1.54 (2 H, br. s.), 1.61 (2 H, br. s.), 1.88 (1 H, s), 2.33 (4 H, s), 2.48 (2 H, s). $^{13}\text{C-NMR}$ (101 MHz, CDCl_3) δ ppm 14.23 (s, 3 C) 22.79 (s, 3 C) 23.61 (s, 1 C) 24.77 (s, 1 C) 25.26 (s, 1 C) 29.46 (s, 2 C) 29.79 (br. s., 4 C) 32.02 (s, 2 C) 33.95 (s, 1 C) 42.69 (s, 1 C) 132.28 (s, 1 C) 165.90 (s, 1 C) 179.01 (s, 1 C) 207.62 (s, 1 C). FTIR (cm^{-1}); 3400 – 2400 (broad), 2916, 2849, 1700, 1472, 1464, 1431, 1291, 1250, 1228, 1210, 1198, 1094, 933 (–OH bend), 728, 720, 688, 544, 529, 518, 512. ESI (+)-MS; 647 m/z. The ItaH was prepared as earlier described using 0.0692 g of the Ita. The recovered yields of about 83% were found. $^1\text{H-NMR}$ (400 MHz, CDCl_3) δ ppm 0.77 -

0.90 (m, 9 H) 1.12 - 1.35 (m, 46 H) 1.62 (s, 3 H) 1.88 (s, 1 H) 2.29 - 2.43 (m, 4 H) 2.54 (d, $J=7.33$ Hz, 2 H) 2.76 (d, $J=16.49$ Hz, 1 H) 2.83 (br. s., 1 H). $^{13}\text{C-NMR}$ (101 MHz, CDCl_3) δ ppm 14.23 (s, 3 C) 22.79 (s, 4 C) 23.34 - 25.31 (m, 2 C) 28.48 - 29.94 (m, 8 C) 32.02 (s, 3 C) 34.04 (s, 1 C) 39.39 - 40.53 (m, 1 C) 43.09 (s, 1 C) 129.07 - 130.98 (m, 2 C) 166.30 (s, 1 C) 178.95 - 180.86 (m, 1 C) 210.18 (s, 1 C). FTIR (cm^{-1}); 3400- 2500, 2916, 2849, 1694, 1433, 1380, 1283, 1236, 942, 720. ESI(-)- MS, 383.2 m/z, 355.2 m/z.

6.3.15 UV/Visible spectrophotometric analysis of some of the metal-diketonates

These analyses were carried out with UV-1800 Shimadzu (UV Spectrophotometer). 1.0×10^{-5} M of the free Htd and Hdbm, metal chelates of the Htd and Hdbm were prepared in chloroform and their spectra measured between 249 – 400 nm with chloroform as a blank.

6.3.16 Calibration of some metals salts solutions by UV/Visible spectrophotometric technique

In order to investigate the metals extraction ability of Htd, calibration curves of some metal salts of Ni(II), Co(II), Cu(II), Fe(III) and Cr(III) were determined as described below using UV/Visible spectrophotometric method.

6.3.16.1 Calibration procedure of $\text{Cu}(\text{OAc})_2$

0.05 M of $\text{Cu}(\text{OAc})_2$ was prepared by dissolving 2.270 g of $\text{Cu}(\text{OAc})_2$ with 50 mL distilled water in 100 mL beaker, transferred into 250 mL volumetric flask and made up. Then 0.04 M, 0.03 M, 0.02 M, 0.01 M and 0.005 M standard solutions were obtained by diluting up 20 mL, 15 mL, 10 mL, 5 mL and 2.5 mL of 0.05 M in 25 mL volumetric flask respectively. The absorbance was measured at the $\text{Cu}(\text{OAc})_2$ λ_{max} , 766 nm using the distilled water as blank. The detail calibration curve is given in Figure 6-5.

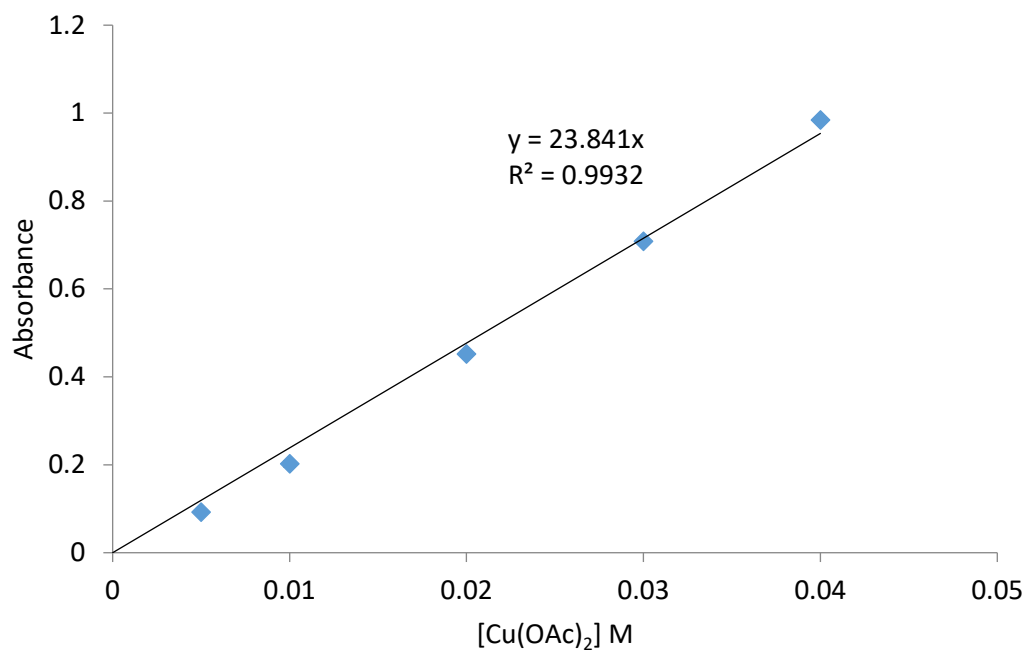


Figure 6-5 Calibration curve for Cu(OAc)₂

6.3.16.2 Calibration procedure for NiCl₂ and Co(NO₃)₂·6H₂O

0.320 g of NiCl₂ and 0.730 g Co(NO₃)₂·6H₂O were dissolved separately in 20 mL distilled water in 100 mL beaker, transferred into 50 mL volumetric flask and made up forming 0.05 M solutions respectively. Thereafter, 0.04 M, 0.03 M, 0.02 M, 0.01 M and 0.005 M solutions were prepared by diluting up 8 mL, 6 mL, 4 mL, 2 mL and 1 mL of 0.05 M NiCl₂ and Co(NO₃)₂·6H₂O in 10 mL volumetric flasks. The UV-Visible absorbance was measured at the predetermined wavelength of 394 nm (for NiCl₂) and 511 nm (for Co(NO₃)₂·6H₂O) with distilled water as blank. Then, the calibration curves were plotted as absorbance versus the concentration in each case as presented in Figure 6-6 and Figure 6-7.

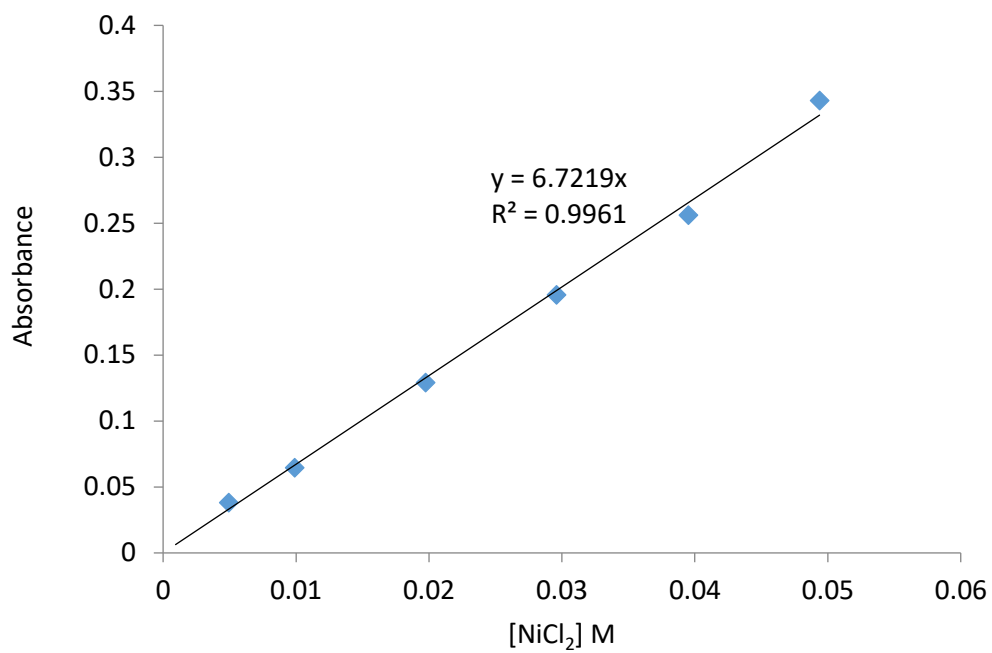


Figure 6-6: Calibration curve of NiCl₂

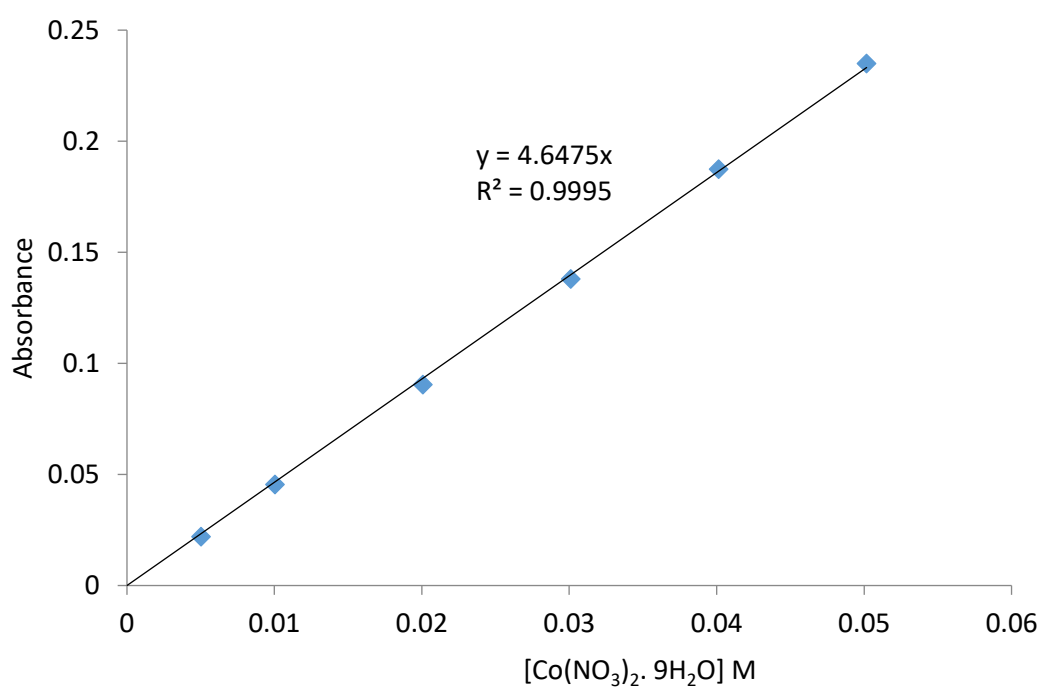


Figure 6-7: Calibration curve of Co(NO₃)₂·9H₂O

6.3.16.3 Calibration procedure for FeCl_3

0.065 M of FeCl_3 was prepared by dissolving 0.262 g in 10 mL of distilled water in 100 mL beaker, transferred into 25 mL volumetric flask and made up to the mark. Then 0.039 M, 0.026 M, 0.013 M and 0.007 M solutions of the FeCl_3 were prepared by diluting up into 10 mL volumetric flasks 6 mL, 4 mL, 2 mL and 1 mL of the 0.065 M FeCl_3 solution respectively. The absorbance measurements were made at 450 nm. Figure 6-8 is the calibration curve of the FeCl_3 found by plotting the absorbance against the concentrations.

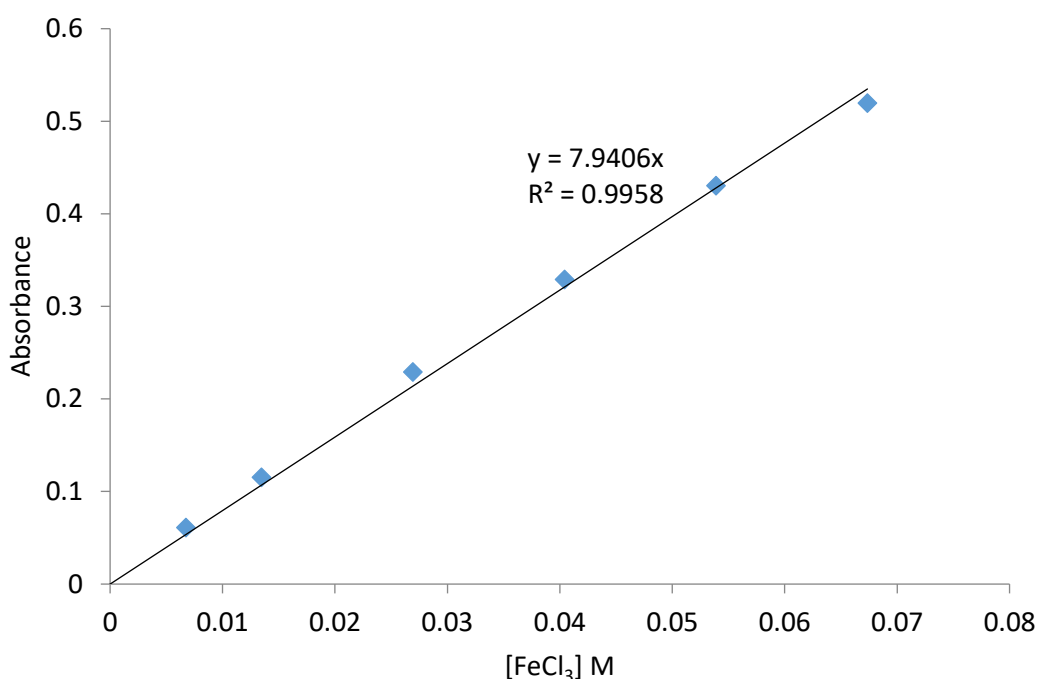


Figure 6-8: Calibration curve for FeCl_3

6.3.16.4 Calibration procedure for CuCl_2 , $\text{CrCl}_3 \cdot 6\text{H}_2\text{O}$ and CoCl_2

0.178 g (0.05 M) of CuCl_2 , 0.301 g (0.05 M) of $\text{CrCl}_3 \cdot 6\text{H}_2\text{O}$ and 0.196 g (0.06 M) of CoCl_2 were prepared by dissolving these salts separately with 10 mL distilled water in 100 mL beaker, transferred into 25 mL volumetric flask and made up. Thereafter 1 mL, 2 mL, 4 mL and 6 mL of each of these standards were diluted up into 10 mL volumetric flask to give 0.03 M, 0.02 M, 0.01 M and 0.005 M solutions (in the case of CuCl_2 and $\text{CrCl}_3 \cdot 6\text{H}_2\text{O}$)

and 0.045 M, 0.024 M, 0.012 M and 0.006 M solutions for CoCl_2 . Absorbances were measured at the λ_{max} of these salts solutions; 812 nm (CuCl_2), 578 nm ($\text{CrCl}_3 \cdot 6\text{H}_2\text{O}$)³⁶¹ and 511 nm (CoCl_2) against the distilled water as blank. The calibration curves are given in Figure 6-9, Figure 6-10 and Figure 6-11.

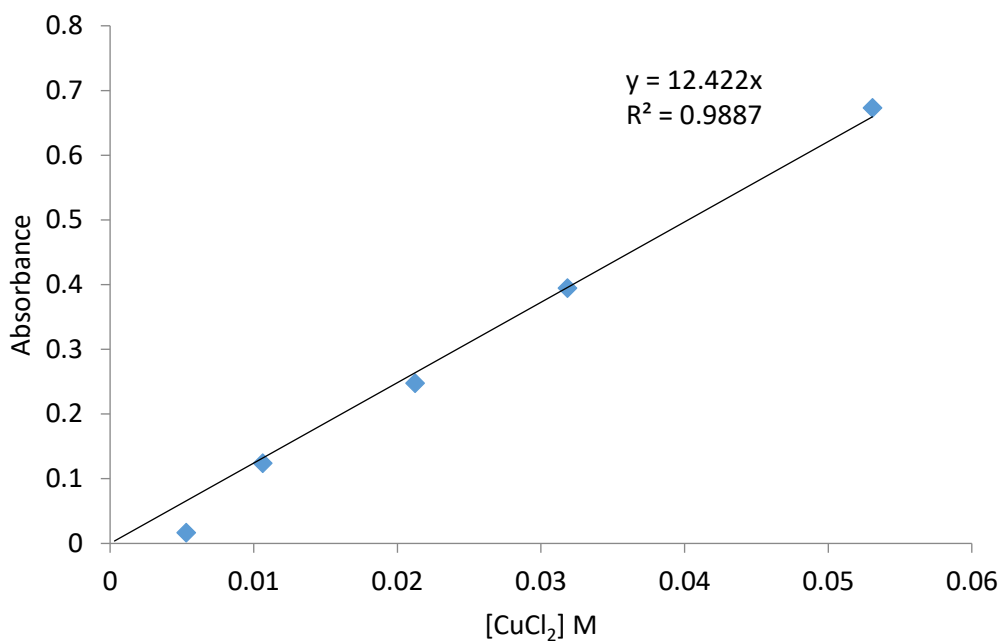


Figure 6-9: Calibration curve of CuCl_2 at 812 nm

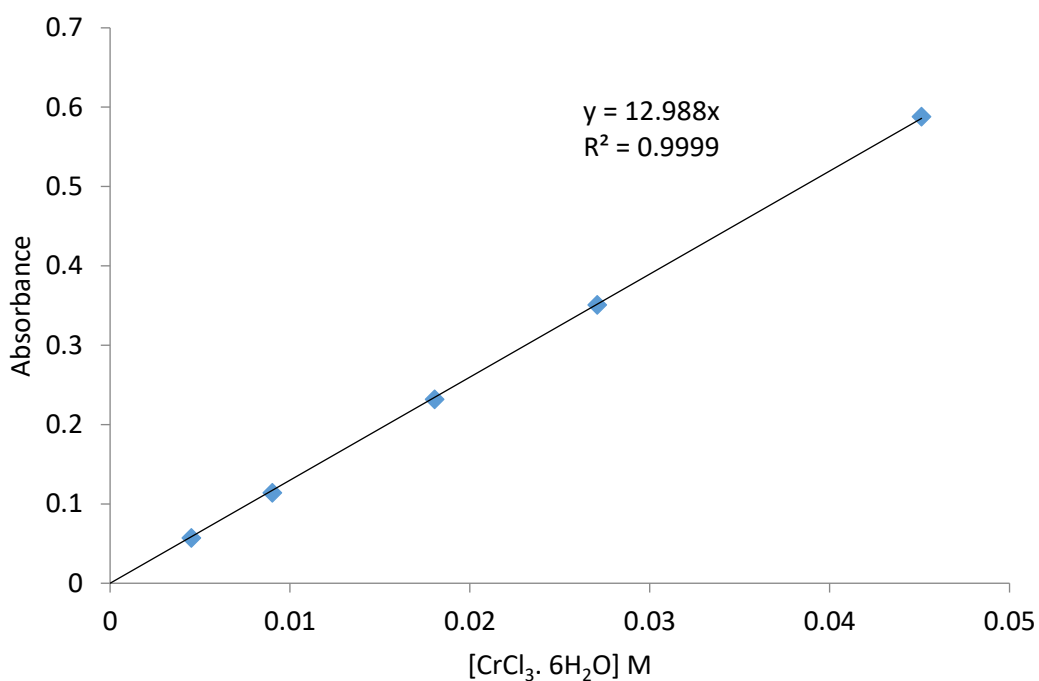


Figure 6-10: Calibration curve of $\text{CrCl}_3 \cdot 6\text{H}_2\text{O}$

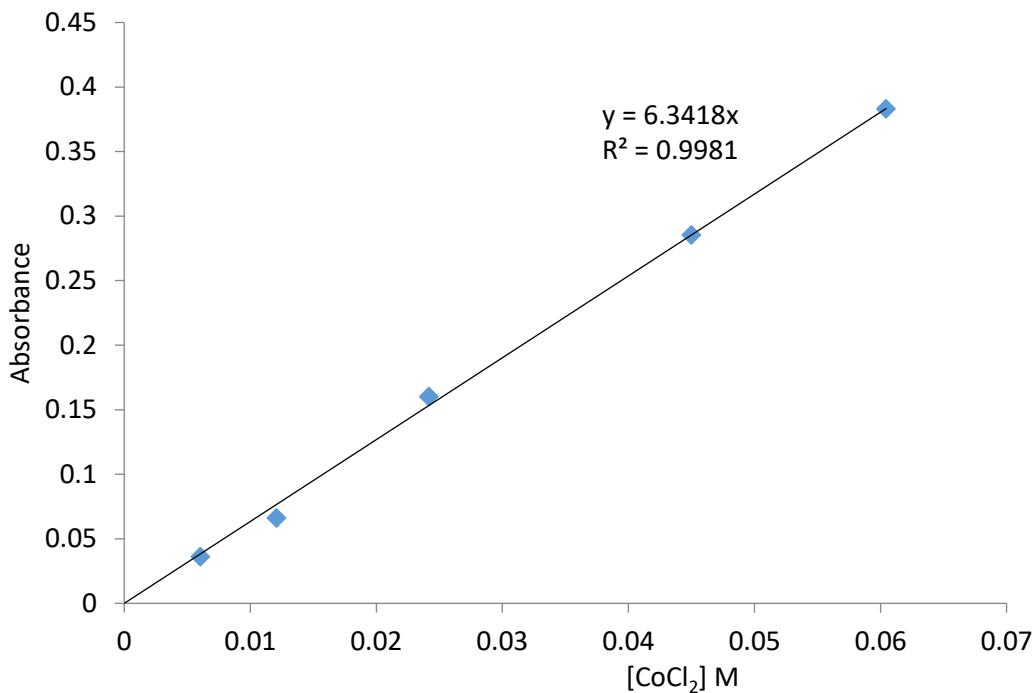


Figure 6-11: Calibration curve for CoCl₂ at 511 nm

6.3.16.5 Calibration procedure of CuSO₄.5H₂O

0.05 M CuSO₄.5H₂O was prepared by dissolving 0.636 g of the salt with about 20 mL of distilled water in 100 mL beaker, transferred into 50 mL volumetric flask and made up. 1 mL, 2 mL, 4 mL and 8 mL of the 0.05 M were further diluted and made up into 10 mL volumetric flasks representing 0.04 M, 0.02 M, 0.01 M and 0.005 M CuSO₄.5H₂O solutions respectively. Then the absorbances were measured at the λ_{max} of CuSO₄. 5H₂O, 809 nm. The calibration curve was obtained from plot of the absorbance against the concentration as given in Figure 6-12.

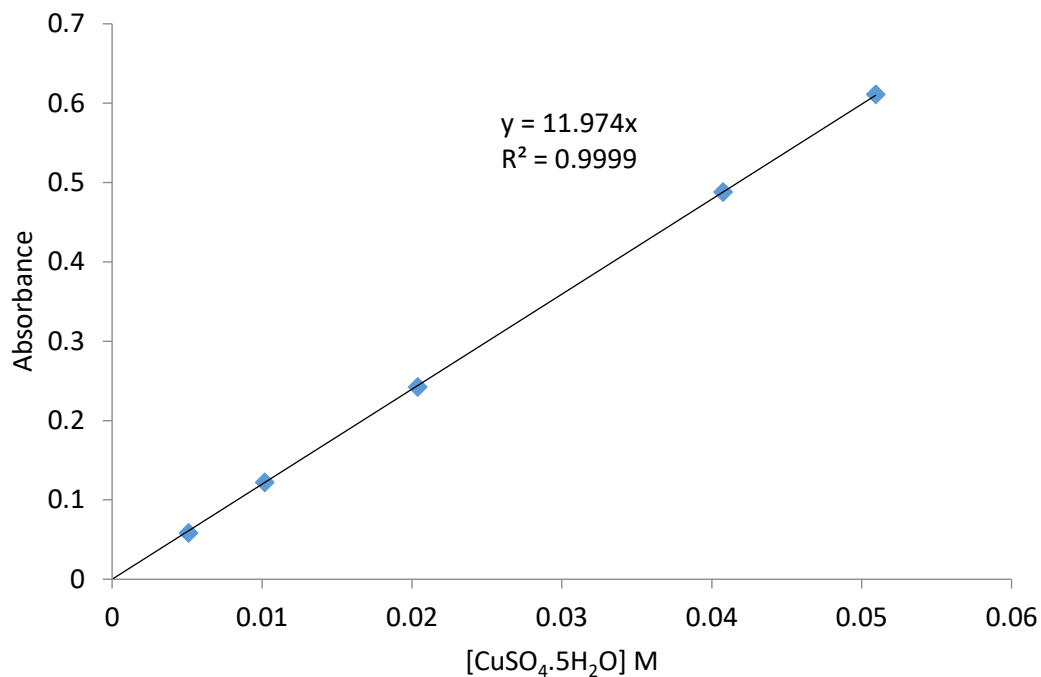


Figure 6-12: Calibration curve of CuSO₄·5H₂O

6.3.16.6 Calibration procedure of Cu(NO₃)₂·3H₂O

1.206 g (0.05 M) of Cu(NO₃)₂·3H₂O was dissolved with about 50 mL distilled water in 100 mL beaker, transferred into 100 mL volumetric flasks and made up. 1 mL, 2 mL, 4 mL and 8 mL of the 0.05 M were diluted into 10 mL volumetric flasks with water to form 0.005 M, 0.01 M, 0.002 M and 0.004 M solutions respectively. The absorbances were measured at the λ_{max} of Cu(NO₃)₂·3H₂O, 807 nm with distilled water as blank. The calibration curve obtained is as presented in Figure 6-13 as follows.

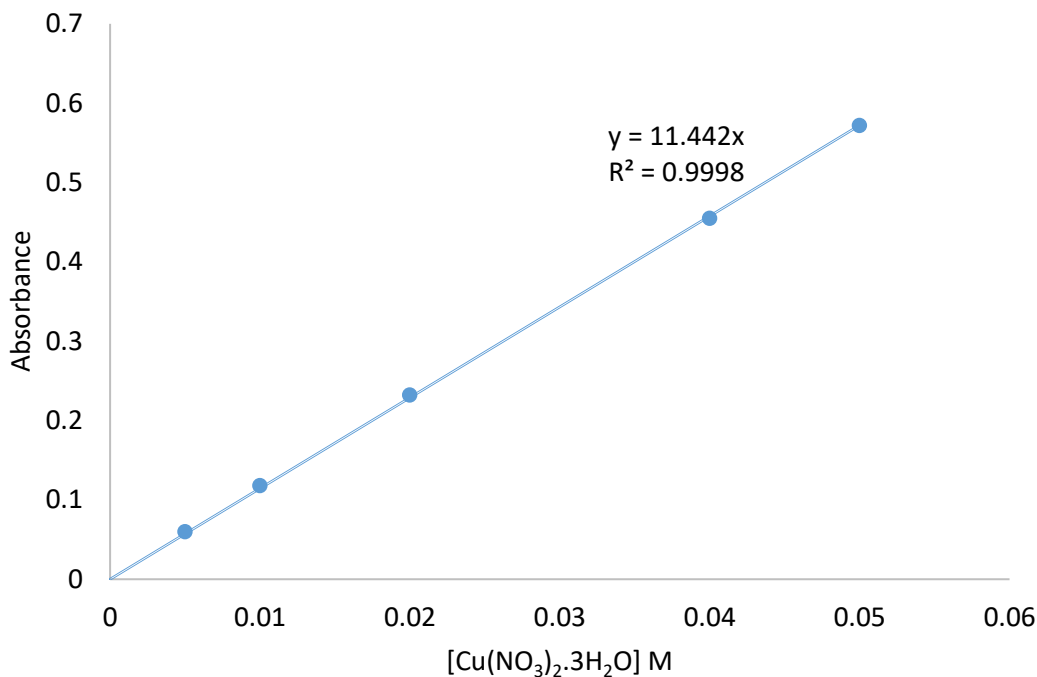


Figure 6-13: Calibration curve of $\text{Cu}(\text{NO}_3)_2 \cdot 3\text{H}_2\text{O}$

In order to find the λ_{max} for each of these salts solutions, the UV/visible spectrum of their solutions were determined by scanning for their UV/visible absorbance in wavelength range of 200-900 nm with deionised distilled water as the blank. The wavelength at which there was maximum absorbance for each salt solution was taken as it λ_{max} . The standards were prepared twice and the UV/visible absorbance measurements repeated. Thus the mean values were then used to prepare the calibration curves by plotting the absorbance against concentration. All the calibration curves obeyed beer-lambert law within the considered concentrations. Table 6-1 summarises the detail features of these calibration curves.

Table 6-1: The UV/visible spectrophotometric calibration curves' features of the metals solutions

Metal salt solution	Wavelength (nm)	Calibration range (M)	R ² obtained	Molar absorptivity (L Mol ⁻¹ cm ⁻¹)
Cu(OAc) ₂	766	0.005 – 0.04	0.99	23.841
CuCl ₂	812	0.005 – 0.05	0.99	12.422
Cu(NO ₃) ₂ ·3H ₂ O	807	0.005-0.05	0.99	11.442
CuSO ₄ ·5H ₂ O	809	0.005-0.05	0.99	11.974
CoCl ₂	511	0.005 – 0.06	0.99	6.342
Co(NO ₃) ₂ ·9H ₂ O	511	0.005 – 0.05	0.99	4.648
CrCl ₃ ·6H ₂ O	578	0.005-0.05	0.99	12.988
FeCl ₃	450	0.005-0.07	0.99	7.941
NiCl ₂	394	0.005 – 0.05	0.99	6.722

6.3.17 Preparation of the synthetic metal aqueous solutions (0.03 M each)

60 mL of 0.05 M Cu(NO₃)₂·3H₂O (as obtained in section 6.3.16.6) was diluted and made up in 100 mL volumetric flask to form 0.03 M solution. In addition, 0.496 g FeCl₃, 0.884 g Co(NO₃)₂·9H₂O, 0.406 g CuCl₂, 0.394 g NiCl₂, 0.389 g CoCl₂, 0.542 g Cu(OAc)₂, 0.399 g CrCl₃·6H₂O and 0.748 g CuSO₄·5H₂O were separately dissolved in about 40 mL of distilled water in a 100 mL beaker and transferred into 100 mL volumetric flask and made up to the mark forming 0.03 M standard solutions. These were then used as a synthetic aqueous waste for the extraction of these individual metals with the various chelators (M: L; 10: 1).

6.3.18 Preparation of the mixture of CuCl₂ and CoCl₂ (0.015 M each)

0.015 M CuCl₂ (0.190 g) and CoCl₂ (0.200 g) were put together and dissolved with 50 mL of distilled water in 100 mL beaker, transferred into 100 mL volumetric flask and made up to the mark. After the extraction of Co(II) and Cu(II) from this mixture as described in

the main procedure for the liquid extraction of metals, the amounts of the metal ions extracted were determined using the following Equation 6-1 based on Beer-Lambert law;

$$\lambda_1 \text{ (a): } A^1 = \epsilon_{\text{Co}}^1 LC_{\text{Co}} + \epsilon_{\text{Cu}}^1 LC_{\text{Cu}}$$

$$\lambda_2 \text{ (b): } A^2 = \epsilon_{\text{Co}}^2 LC_{\text{Co}} + \epsilon_{\text{Cu}}^2 LC_{\text{Cu}}$$

Equation 6-1 (a and b): Beer-Lambert equations for the mixture of CuCl₂ and CoCl₂ solution

Where; λ_1 and $\lambda_2 = \lambda_{\text{max}}$ of cobalt and copper, A^1 and A^2 = absorbances of copper and cobalt at the two wavelength, C_{Co} and C_{Cu} = concentration of Cu and Co, L = path length and ϵ = molar extinction coefficients. These equations denote that, total absorbance of a solution at a given wavelength is equal to the sum of the absorbance of the individual components. These were simultaneously solved to obtain the amount of each absorbing species; Co(II) and Cu(II) using their molar extinction coefficients determined at wavelength: λ_1 (812 nm); ϵ_{Co}^1 , 0.589 Lmol⁻¹cm⁻¹ and ϵ_{Cu}^1 , 12.422 Lmol⁻¹cm⁻¹ and λ_2 (511 nm); ϵ_{Co}^2 , 6.34 Lmol⁻¹cm⁻¹ and ϵ_{Cu}^2 , 0.811 Lmol⁻¹cm⁻¹. Each of the salts' solution (CoCl₂ and CuCl₂) was calibrated at 511 nm and 812 nm as described here.

0.015 M of CoCl₂ and CuCl₂ were further diluted by making up 1 mL, 2 mL, 4 mL and 8 mL into 10 mL volumetric flask to form 0.0015 M, 0.003 M, 0.006 M and 0.012 M solutions respectively. The absorbance of CoCl₂ and CuCl₂ were measured at each of the predetermined wavelength; 812 nm (CuCl₂ λ_{max}), 511 nm (CoCl₂ λ_{max}) with distilled water as the blank. The calibration curves are as found in Figure 6-14 and Figure 6-15.

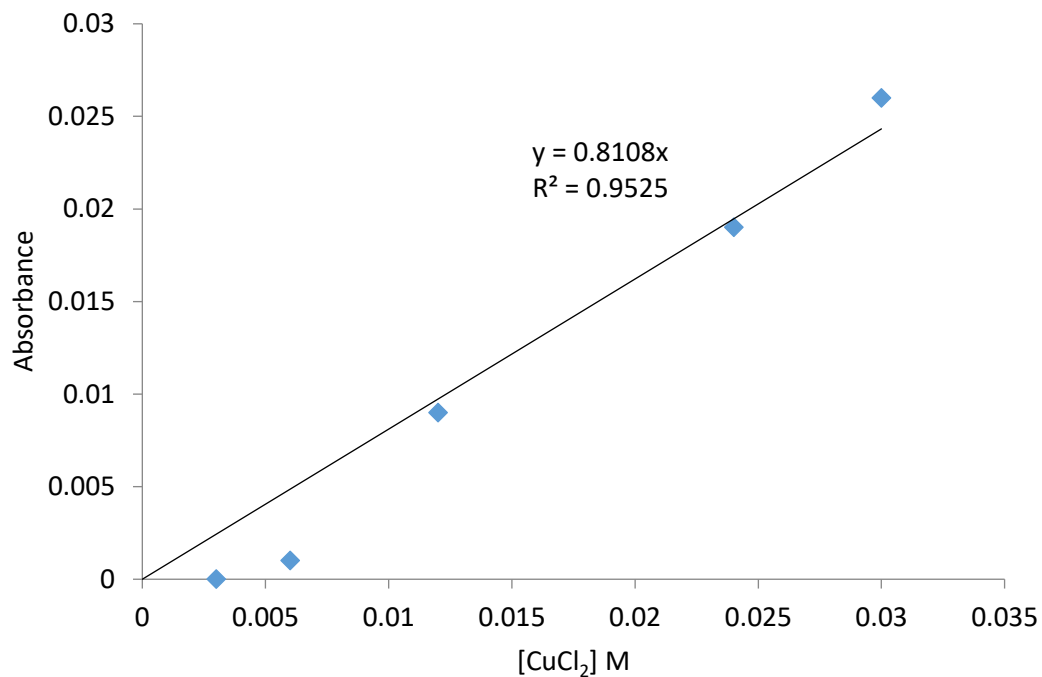


Figure 6-14: Calibration curve for CuCl₂ at 511 nm

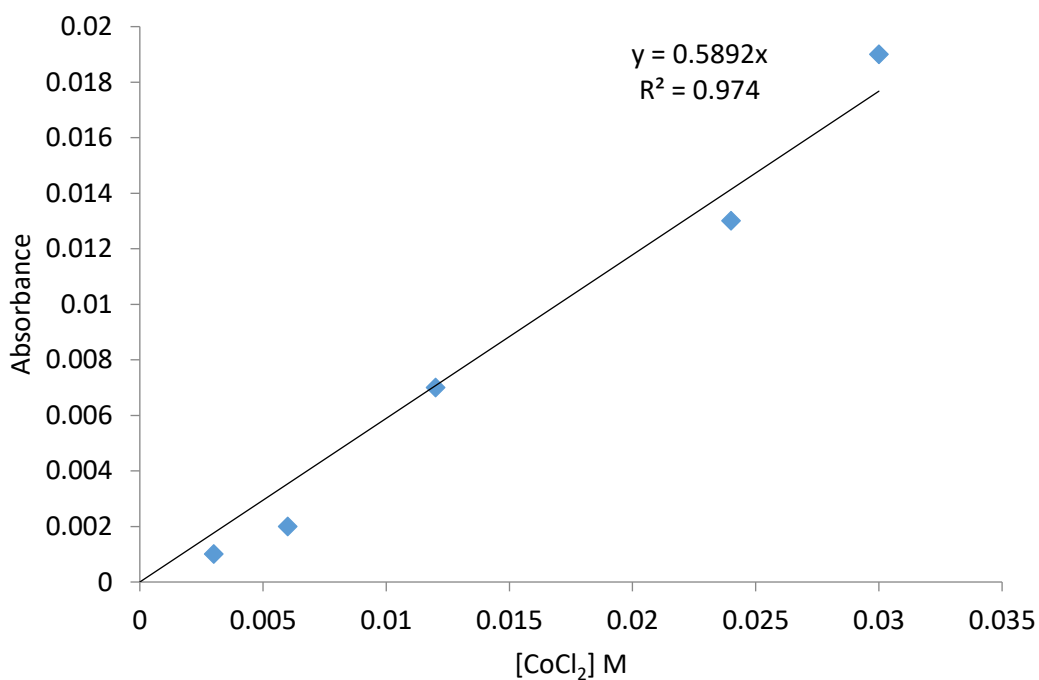


Figure 6-15: Calibration curve for CoCl₂ at 811.5 nm

6.3.19 Preparation of the chelators standard solutions (3 mM)

About 3 mM of each chelator were prepared as follows: Htd, 0.135 g; Hdbm, 0.067 g; Hacac, 0.03 g; Ma, 0.044 g; Ita, 0.048 g; MaH, 0.045 g; ItaH, 0.048 g were dissolved with about 20 mL of cyclohexane and transferred into 100 mL volumetric flask (Htd, Hacac

and Hdbm) or 25 mL volumetric flasks (for Ma, Ita, MaH and ItaH) respectively and made up with cyclohexane. These standard solutions were used as the metals extractants in most cases except where the concentration is specified otherwise.

6.3.20 Procedure of the solvent extraction of the metal ions

The extraction procedures were performed as previously reported.²⁶³ Equal volumes (5 mL) of aqueous metal solutions and each of the chelating extractants in cyclohexane (M: L, 10: 1) were mixed together in 50 mL vessel with screw cap and well agitated in order to bring the two phases into sufficient contact for the metal extraction at 293 K for 30 min as similarly reported in the literature.^{263,308,362} Thereafter the samples were allowed to stand for 24 h. The aqueous phase was carefully separated and the absorbance of the residual metal ions in the aqueous solution was measured with UV/Visible spectrophotometer. A blank (control) run with each metal solution and pure cyclohexane was treated as described above and the absorbance's of the aqueous phases collected from the blanks were also measured. The calibration curves of the metals solutions were used to determine the concentration of these raffinates and the blanks. Hence, the amounts of extracted metal ions were evaluated by difference.³⁰⁴ The distribution ratio, D was determined as the ratio of the concentration of the metal in the organic phase to its concentration in the aqueous phase.^{36,307} The pH of the aqueous phase after extraction was recorded as the equilibrium pH.³⁰⁴ The pH was adjusted with NaOH or HCl in some cases as specified. Figure 6-16 highlights the concept of isolation of the Htd from wheat straw wax; and the application of the unmodified and modified Htd in metals extraction. Pictures of the metals extraction samples are given in Figure 6-17 and Figure 6-18 below.

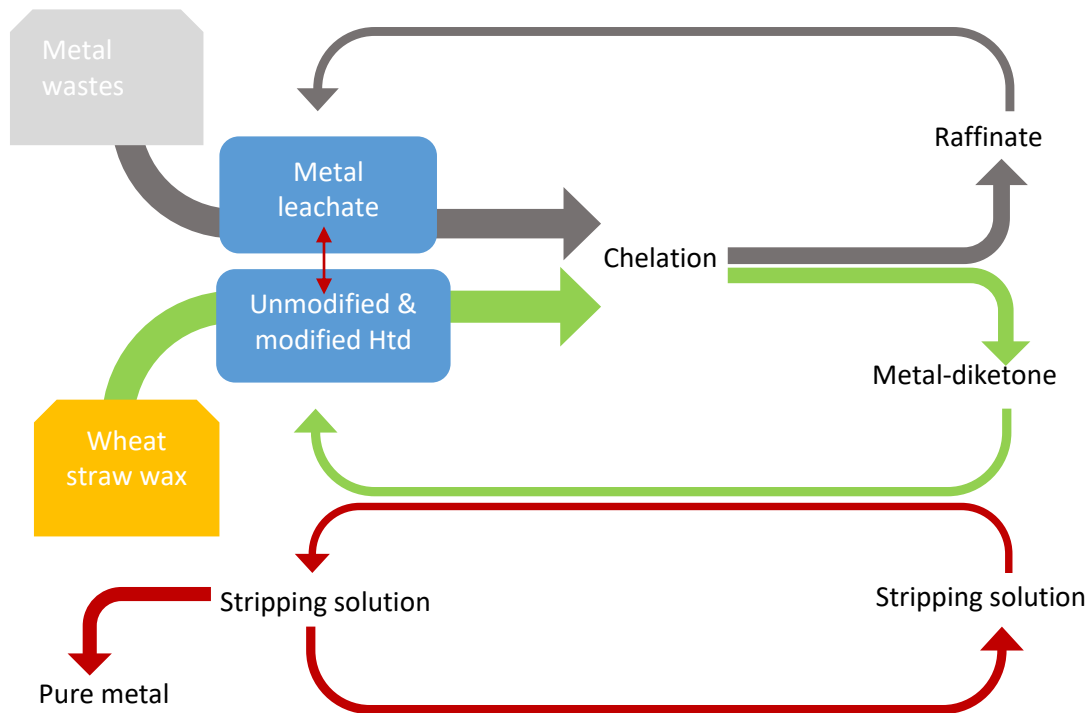
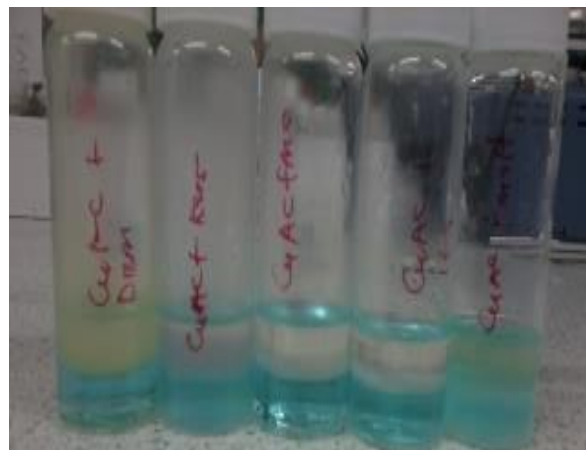


Figure 6-16: The Purification concept of the Htd from wheat straw and its application for metals recovery



Extraction of Ni(II) from NiCl₂ solution



Extraction of Cu(II) from Cu(OAc)₂ solution



Extraction of Co(II) from CoCl_2 solution



Extraction of Cu(II) from CuCl_2 solution



Extraction of Co(II) from $\text{Co}(\text{NO}_3)_2$ solution



Extraction of different metal ions with ItaH

Figure 6-17: Some samples during the biphasic extraction of the metal ions using the unmodified and modified Htd (0.03 M metals solution and 0.003 M chelants in each case)

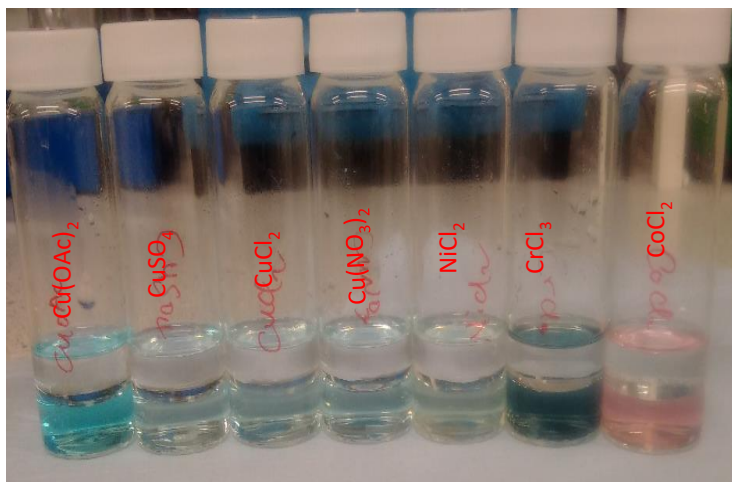


Figure 6-18: Some samples of the biphasic extraction of the metals with Hacac (M: L; 10: 1)

6.3.21 Determination of the metal ions extraction with ICP-MS

About 0.013 g $\text{Ga}(\text{NO}_3)_3$, 0.016 g $\text{Pb}(\text{NO}_3)_2$, 0.007 g CuCl_2 , 0.009 g $\text{Cu}(\text{OAc})_2$, 0.013 g $\text{CuSO}_4 \cdot 5\text{H}_2\text{O}$, 0.020 g $\text{Pb}(\text{OAc})_2 \cdot 3\text{H}_2\text{O}$, 0.012 g $\text{MnCl}_2 \cdot \text{H}_2\text{O}$ were dissolved with 20 mL of distilled water separately in 100 mL beaker, transferred into 50 mL standard volumetric flasks and made up to the mark forming 1 mM solutions respectively. Except were specified otherwise, the metals from these solutions were extracted with 1 mM Htd. The residual metal ions in the raffinate were measured with ICP-MS, hence the amount of extracted metal ions determined by difference.

6.4 Instrumental analyses

6.4.1 FTIR analysis

FTIR analysis of the samples was conducted with Bruker Vertex 70 FTIR spectrometer fitted with Specac Golden Gate ATR. The FTIR was equipped with a DigiTect™ DLATGS detector with integrated preamplifier scanning over a wavelength range of 4000 – 500 cm^{-1} at a resolution of 4 cm^{-1} . The spectra were collected using rapid scan software running under OPUS 5.5 and the spectrum of each sample was calculated from an average of 16 scans. About 30 mg of each sample were used for the analysis.

6.4.2 NMR analysis

^1H - and ^{13}C -NMR (JNM – ECS 400 of field strength, 400 MHz for ^1H , and 100 MHz for ^{13}C) spectra were used for the analysis of most reactions and extractions. 20 mg of the samples were dissolved in 1 mL CDCl_3 in most cases. The chemical shifts were recorded at 296 K. Spectra analysis was carried out with ChemSketch 1DNMR processor.

6.4.3 Thin layer chromatography (TLC) analysis

For each sample, about 20 mg was dissolved in DCM (1 mL) and an aliquot of these solutions were applied at the bottom of about 8 cm x 8 cm silica gel 60 F254 TLC plate (Merck) using a micropipette. The separation on the silica gel plate was obtained in about 15 minutes using 1: 4 (ethyl acetate: cyclohexane) mobile phase in vertical developing chamber. The components on the plates were revealed by staining with 10% w/w phosphomolybdic acid in ethanol or read with UV lamp.

For the stained plates, each plate was immediately dried at 373 K for around 1 min to reveal the position of the components. Hence the retention factors (r_f) were evaluated and compared to the starting materials. For the eluent that was obtained after flash chromatography (as described below), the fractions were identified on the TLC plate and then combined according to their r_f .

6.4.4 Purification of the Ita mixture by Kugelrohr distillation

About 3.5 g of the dimethyl itaconate modified Htd mixture was short part distilled by steadily increasing the temperature from 328 K- 393 K under 5.9- 9.2 x 10⁻¹ mbar for period of 3 h where the dimethyl itaconate was completely removed leaving behind the Htd and the itaconate modified Htd (70%).

6.4.5 Flash chromatographic separation of the Ma and Ita

Flash chromatographic separation was carried out using a Biotage Isolera Four. 0.5 g of sample was dissolved in 10 mL of DCM in a round bottom flask which contained a small amount of silica gel (high-purity grade). The solvent was removed *in vacuo* in order to coat the samples onto the silica gel. The mixture was then transferred to the top of a 50 g Biotage SNAP HP-Sil cartridge. The solvent system employed, cyclohexane (80%) and

ethyl acetate (20%) was run through the column at the flow rate of 50 mL/min under solvent gradient of 5 - 40%. UV active detection (254 – 280 nm) with start threshold of 20 mAU was used. 15 mL of eluent were collected into different test tubes. The products fractions were identified using TLC technique as previously described in section 6.4.3.

6.4.6 GC-FID analysis

GC analysis was performed using GC-FIDS Agilent 7820A (Agilent 6890N, Hewlett Packard HP6890) with RXI-5HT column, and column diameter of 30 m x 0.25 mm x 0.25 μ m nominal was fitted with constant pressure of 22.35 psi; column maximum temperature of 673 K. The carrier gas used was helium. The samples were injected by automated injection (1 μ L injection volume) with injection temperature, 563 K and a split ratio of 50:1. Oven condition; starts 323 K for 4 min, ramp at 283 K/min and finally reaches 563 K to hold for 10 min. The detector temperature was set to 613 K. The total time of the method was 38.0 min. 20 mg of each sample in 1 mL DCM or toluene were used in this analysis.

Another method was developed for GC-FID analysis of the Ma and Ita using a 15 m Zebron ZB-5HT column which has an inlet temperature of 623 K; split ratio, 50:1. Initial oven temperature, 323 K; the temperature was increased at ramp rate of 303 K/min until 498 K and second temperature ramp rate of 278 K /min up to 623 K and held for 8 min. The total time of the run was about 39 min.

6.4.7 GC-MS analysis

Mass spectra analysis was carried with 20 mg of each of the sample in 1 mL toluene on a Perkin Elmer Clarus 500 GC coupled with a Clarus 500 quadrupole mass spectrometer. The GC-MS was fitted with a DB5HT capillary column (30 m x 0.25 mm x 0.25 μ m nominal) with pressure of 22.35 psi carrier gas (helium). The temperature of the injector was 573

K and the flow rate was set to 1.2 mL/min. The initial oven temperature was maintained at 333 K for 1 min. The temperature was then ramped at a rate of 281 K/min until 633 K and held for 10 min. The Clarus 500 quadrupole mass spectrometer was operated in the electron ionisation mode (EI) at 70 eV, a source temperature of 573 K, quadrupole at in the scan range of 30 - 1200 amu/sec. The data was collected with the PerkinElmer enhanced TurboMass (Ver5.4.2) chemical software and compounds were identified by analysing the mass fragmentation patterns and comparison of mass fragmentation patterns with spectra contained in the NIST library (v. 2.2).

6.4.8 Differential scanning calorimetric (DSC) analysis

The melting points of the Htd and modified Htd were measured on a MDSC Q2000 modulated differential scanning calorimeter. 5 mg of each sample was weighed into an open aluminium DSC pan and analysed under nitrogen gas using a three-stage heating profile in order to remove any prior thermal character. The DSC measurements were recorded against an empty aluminium reference pan in the final heating cycle of analysis. In determining the melting point, the cell was purged with a flow of nitrogen gas (150 mL/min) and was cooled by nitrogen (150 mL/min) in a refrigerated cooling system. The sample was heated from 293 – 378 K at a rate of 283 K/min. It was held at 378 K for 1 min and cooled to 263 K at 283 K/min. The sample was held at 263 K for 1 min and then heated from 263 K to 378 K at 283 K/min and held for 1 min at 378 K. The melting point range was determined using the differential scanning calorimetry (DSC) curves of the second heating cycle.

6.4.9 ESI-MS analysis

20 mg of the Htd, Ma, MaH, Ita and ItaH samples were prepared in methanol: water (1:1). Their ESI-MS spectra were obtained using LC - Agilent 1260 Infinity with MS - Bruker

microTOF time of flight MS in mass range of m/z 200-900 positive ion mode, capillary voltage 4500V, nebuliser pressure 21.8 psi, dry gas flow 8 L/min and dry gas temp 433 K.

6.4.10 GC-FID calibration procedure for Htd quantification

Accurately weighed samples of 0.3 mg, 0.7 mg, 4.1 mg, 7.8 mg and 16.7 mg of Htd were each dissolved with 1 mL of cyclohexane. Then 10 µL, 2 µL, 2 µL, 2 µL and 2 µL of tetradecane (standard) was injected into the above Htd solutions respectively. GC-FID analysis of these samples was performed using GC-FIDS Agilent 7820A (Agilent 6890N, Hewlett Packard HP6890) whose other details have been earlier highlighted. The relative response of the Htd and tetradecane were obtained from their peak areas. Thereafter, the plot of relative response (peak area) against relative mass of Htd was made to obtain the response factor (R_f). The calibration for Htd with tetradecane as standard showed a linear response as described in Figure 6-19 below. The basis for this calibration is mathematically expressed in Equation 6-2. This response factor was used to determine the amount of the Htd in the wheat straw wax fractions collected from the scCO₂ fractionation as discussed in chapter three.

$$\frac{\text{Mass}_{\text{Htd}}}{\text{Mass}_{\text{Std}}} = R_f \times \frac{\text{Area}_{\text{Htd}}}{\text{Area}_{\text{Std}}}$$

Equation 6-2: Mass and Area response ratios for the GC-FID calibration

Note: R_f = Response factor, GC peaks areas of the Htd and tetradecane are; Area_{Htd} and Area_{Std} respectively; and Mass_{Htd} and Mass_{Std} = Mass of the Htd and tetradecane

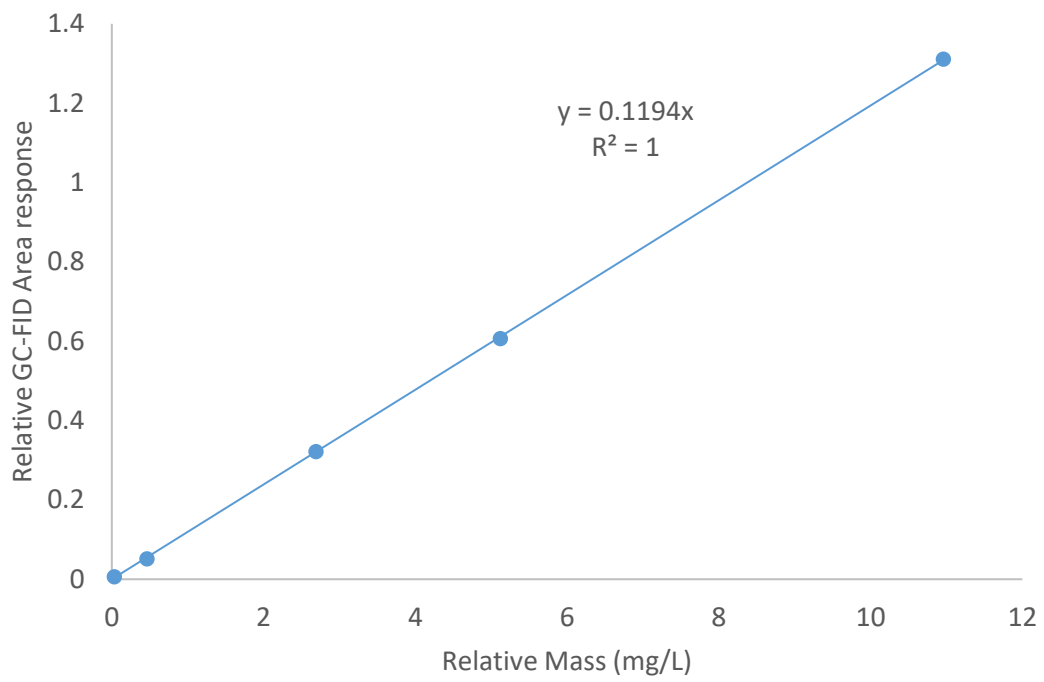


Figure 6-19: GC-FID calibration curve for Htd quantification using tetradecane standard

Chapter 7

Thesis conclusion and future work

7 Chapter 7

7.1 Concluding remarks

Lipophilic β -diketones have been reported as major components in waxes found in wheat straw, barley straw, oats, rye, eucalyptus, festuca, agropyron and vanilla bean. However, there are few reports on the purification and application of hydrophobic β -diketones from plant waxes. Therefore, an effective method for the isolation of Htd from wheat straw wax was developed with the use of $\text{Cu}(\text{OAc})_2$ chelation along petroleum ether. Petroleum ether is toxic nonbiobased solvent and replacement of this solvent had been recommended.³⁶³ Therefore, alternative solvents; cyclohexane, *p*-cymene, TMTHF and CPME were explored as greener alternatives for the purification of the Htd. It was observed that TMTHF, cyclohexane and CPME can be use in real life to replace the petroleum ether in the purification of the lipophilic β -diketone from wheat straw wax. Another alternative solvent used for the isolation of Htd was scCO_2 . However, the Htd obtained was less pure compare to those from the organic solvents above. Thus far, the purification of Htd from wheat straw wax can be effectively performed with the TMTHF, cyclohexane and CPME instead of petroleum ether. The keto-enol tautomerism studies of the Htd was investigated with different deuterated solvents; CDCl_3 , acetone- d_6 , cyclohexane- d_{12} , THF- d_8 and toluene- d_8 in comparison to Hacac and Hdbm. The % enol relative to % keto for the Htd at constant concentration in these solvents is in the order cyclohexane > toluene > CDCl_3 > acetone (i.e. Htd, gives highest % enol in cyclohexane). That is, the % enol of Htd was decreased with increase in polarisability, dipole moment and hydrogen bond acceptor of these solvents. The capacity for Htd to enolise in cyclohexane highlighted its potential suitability for metal ion chelation using a nonpolar diluent.

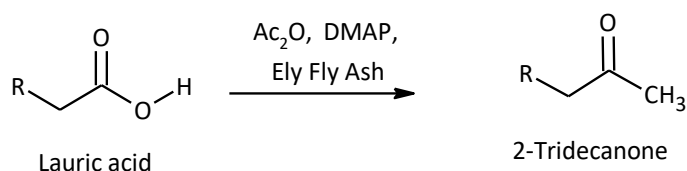
Htd was then modified under KF/alumina catalysed Michael addition reactions in solvent-free conditions using methyl acrylate, methylmethacrylate, dimethyl itaconate and trimethyl aconitate as Michael acceptors with microwave or traditional stirrer hot plate heating. Subsequently the recovered methyl acrylate and dimethyl itaconate modified bioderived lipophilic β -diketones were hydrolysed to form carboxylate acids of Htd and characterised with ESI-MS, FTIR and NMR spectroscopy techniques. Then, the unmodified and modified lipophilic Htd were tested for metal extraction in liquid biphasic system in comparison to Hdbm and Hacac. These biochelators extracted metal ions from Cl^- and OAc^- media better than from SO_4^{2-} and NO_3^- solutions. The modified acid carboxylate Htd were most effective for the extraction of Cu(II) and Pb(II). Also the unmodified Htd extracted Ni(II) more rapidly than Hdbm and Hacac. Htd, Ma and Ita were recycled and re-used for metal extraction. Thus, this research has effectively demonstrated the use of biobased chelators for recovery of metal ions from aqueous solution which can be apply in real life for recovery of metals for their sustainability.

7.2 Future work

7.2.1 Derivation of methyl ketone from lauric acid using Dakin-West reaction

A hypothesized synthetic route for obtaining lipophilic β -diketones from long chain bio-derived methyl ketones was initially examined here as an alternative green method for synthesising bio-derived hydrophobic β -diketones. Long chain methyl ketones can potentially be sourced from lauric acid *via* the Dakin-West reaction and used in Claisen condensation reactions along with ethyl acetate to form long chain β -diketones. According to Buchanan,³⁶⁴ the Dakin-West reaction refers to the direct conversion of carboxylic acids (aliphatic, aromatic and amino acids) into ketones in the presence of acetic anhydride (or other acetylating reagents) and strong base such as pyridine with

evolution of CO₂. A key reagent in the Dakin-west reaction is the acetylating agent which could be an acid chloride³⁶⁴ or acid anhydride.^{364,365} Acetic anhydride (Ac₂O) is preferred to other anhydrides with longer chains because it gives higher conversions of ketone, though by selecting other anhydrides it is possible for different substituents to be introduced next to the ketone; with Ac₂O only resulting in the formation of methyl ketones.³⁶⁴ Dakin-west reactions are usually performed at high temperatures (minimum 393 K),³⁶⁴ long reaction times, harsh conditions and often require tedious work-ups.³⁶⁶ However, in the presence of 4-dimethylaminopyridine (DMAP) as a base, the Dakin-West reaction proceeds faster even at room or near room temperature.³⁶⁴ In this work, a one pot synthesis of a methyl ketone from lauric acid and Ac₂O in the presence of a base using microwave heating was demonstrated. The reaction time was only 25 min and made use of DMAP and Ely Fly Ash. About 17% methyl ketone was formed, therefore making a longer reaction time (i.e. >5 h) under these conditions could improve the % formation of the methyl ketone. GC-MS of the synthesised methyl ketone is given in Figure A-11 under appendix 1 and the proposed fragmentation pattern in Scheme A-2 in appendix 2. The mechanism for the formation of this compound is described in Scheme A-1 in the appendices section; DMAP initiates the O-acetylation as previously reported³⁶⁴ and most likely the ash supports the rearrangement and second acetylation because of its basic nature. The conversion is represented in Equation 7-1.

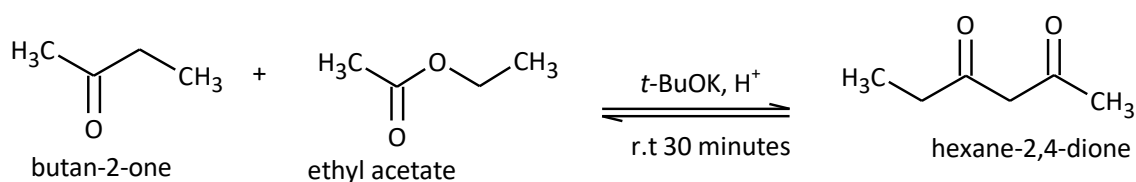


Equation 7-1: Dakin West conversion of lauric acid into methyl ketone

Fatty methyl ketones obtained above would then be subjected to Claisen condensation with an ester, under appropriate conditions, to produce lipophilic β -diketones. This could potentially be an alternative sustainable way for producing fatty β -diketones. However, a Claisen condensation of a low molecular weight methyl ketone has been demonstrated here in support of this concept.

7.2.2 Preparation of β -diketone using Claisen Condensation

Claisen condensation of corresponding esters or ketones with esters in the presence of sodium hydride (NaH), tetramethyl orthosilicate/ cesium fluoride, sodium ethoxide¹⁴⁷ or *n*-butyl lithium in dry xylene/dry ether or pyridine²²³ is a widely used method for the synthesis of β -diketones.^{202,268,367} According to Vibhute *et al.*,³⁵⁹ Claisen condensation reactions for the synthesis of β -diketones involves toxic reagents and special apparatus. In this this work a β -diketone (2,4-hexanedione) was made from butan-2-one and ethyl acetate with potassium *tert*-butoxide, *t*-BuOK, at room temperature in a simple vessel (screw cap vial) as described in Equation 7-2 below. This method is quick, simple and cost effective; with no need of toxic and hazardous reagents or special apparatus.



Equation 7-2: Claisen Condensation of ethyl acetate and butan-2-one to form 2, 4-hexanedione

The hydrogen(s) α to a ketone are weakly acidic and when treated with a strong base, the enolate of a ketone will react with the ester to produce a β -ketone. According to Esteb and Stockton,³⁶⁸ and Horta³⁶⁹, Claisen condensation reactions are typically performed at high temperatures.^{368,369} Erasmus and Swart³⁷⁰ performed Claisen

condensation reaction for the synthesis of ruthenocene-containing β -diketones using the appropriate methyl ester with acetyl ruthenocene. In addition, Esteb and Stockton³⁶⁸ explained that a Claisen condensation reaction is run in a solution where the ester, metal alkoxide and alcohol solvent should all be identical so as to prevent exchange of the alkoxy group among the substrate, reagent and solvent. Recently, in accordance with green chemistry principles, solvent-free Claisen Condensation reactions have been reported with excellent yields.^{368,369} Under solvent-free conditions it is possible to use an unmatched set of base and ester without resulting in the exchange of alkoxy groups.³⁶⁸ The synthesis of 2,4-diphenyl acetoacetate is produced by heating ethyl phenylacetate at 373 K for 30 min with *t*-BuOK under solventless conditions.³⁶⁸ The Claisen Condensation of diethyl succinate was carried out at 423 K for 20 min with microwaves (μw) under solvent free conditions.³⁶⁹

Meanwhile, the GC-MS of the hexane-2,4-dione synthesised here is found in Figure A-12, while the proposed mechanism is explained in Scheme A-3 as given in the appendix 2. Scheme A-4 also in the appendix 2 is the proposed fragmentation pattern for hexane-2,4-dione. Although only a 40% conversion was obtained, longer time of more than 30 min would likely improve the conversion. Similarly, Gouveia *et al.*¹⁴⁷ reported the synthesis of 2,4-decanedione using Claisen condensation reactions with ethyl acetate and *n*-hexyl methyl ketone in the presence of sodium ethoxide. Therefore, a sustainable approach for synthesising lipophilic β -diketones could be carried out using long chain bioderived methyl ketones and ethyl acetate.

7.2.3 Silica adsorbent support for the scCO_2 fractionation wheat straw wax for Htd

The qualitative analysis of the scCO_2 fractionation of the wheat straw wax for the Htd using 1 g wax: 200 g silica at different pressures thus far showed that 300 bar at 313 K

was somewhat better condition for the fractionation of the Htd from the wheat straw wax than 75 bar, 100 bar, 200 bar and 400 bar. Therefore, more studies would be needed using silica as an adsorbent for the scCO₂ fractionation of this wax for lipophilic β -diketones at different temperatures, pressures and wax: silica ratio.

7.2.4 Amine functionalisation of the Ma_d

Amine functional groups could be introduced on the product of double addition of the methyl acrylate modified bioderived lipophilic β -diketone (Ma_d). The metals chelation ability of such amine functionalised Ma_d could then be tested. EDTA is one such example of a chelant where amine groups are included to improve its efficacy in complexing with metals.

7.2.5 Preparation of polyfunctional molecules

Although the bio-derived lipophilic metals chelants were prepared and tested here for metals extraction, however the modified Htd could be polymerised to form a polyfunctional molecules. Application of these polyfunctional compounds could also be tested in metals extraction.

7.2.6 Preparation of the carboxylate acids of Ma and Ita by acid hydrolysis

The alkaline hydrolysis of the Ma and Ita was performed in this present study. Yet it could be good to hydrolyse these carboxylate esters of the modified Htd (Ma and Ita) with 50% trifluoroacetic acid in CH₂Cl₂ for 1 h at 273 K as similarly been reported²⁴⁰ and compare to the alkaline hydrolysis as described in this thesis in order to maximise this hydrolysis process in terms of time.

7.2.7 Precious metals extraction studies

Studies on precious metal (such as Pd, Pt, Au) extraction could be tested using these bio-derived unmodified and modified Htd. Low abundance of precious metals versus their importance in critical technologies means there is considerable value in looking at their recovery from waste streams using these bio-derived materials.

7.2.8 Competitive metals extraction studies

Selective extraction of metals in the presence of other metals could be investigated with our prepared lipophilic chelators. Chelating agents that bind metals selectively in the presence of other metals species are often preferred in metals extraction processes than nonselective metals extracting chelators. In this present studies selective extraction of Cu(II) in the presence of Co(II) was tested. The itaconate modified Htd (Ita) was found to extract only Co(II) in the presence of Cu(II). The other lipophilic chelators; Htd, Ma, MaH, ItaH and Hdbm extracted both Co(II) and Cu(II).

7.2.9 Use as surfactants

The carboxylate acids of the methyl acrylate and dimethyl itaconate modified Htd could be use as surfactants as they are similar to some reported in the literature.⁸⁹

Appendices

Appendix 1

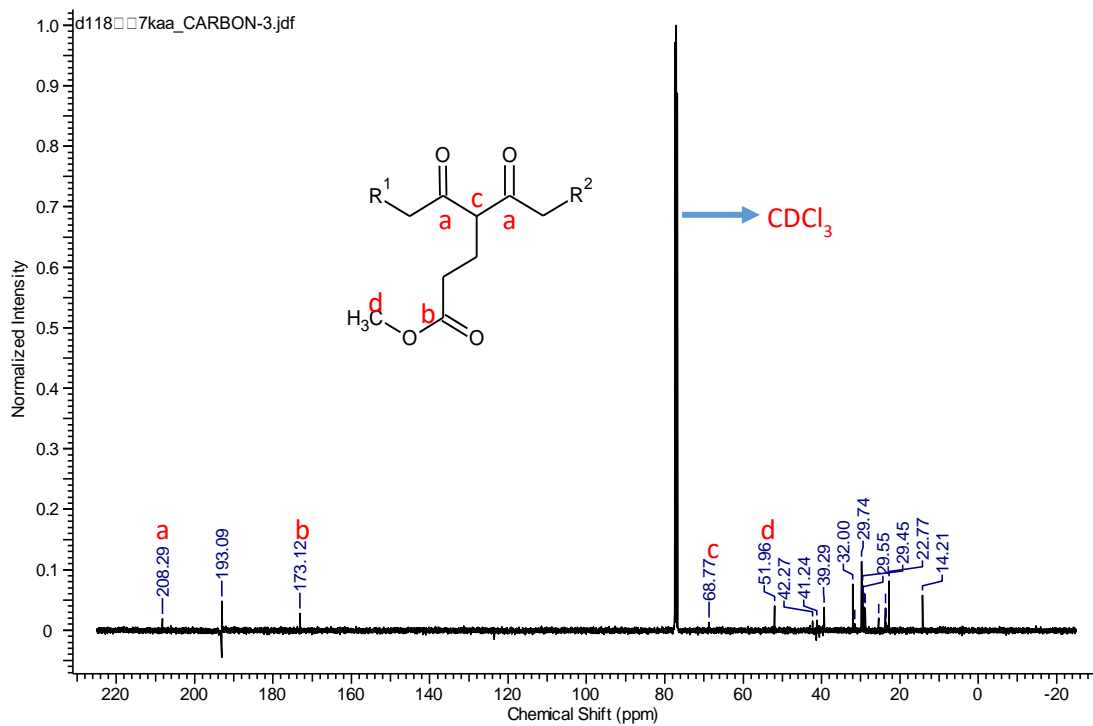


Figure A-1: ^{13}C -NMR spectrum of the Ma

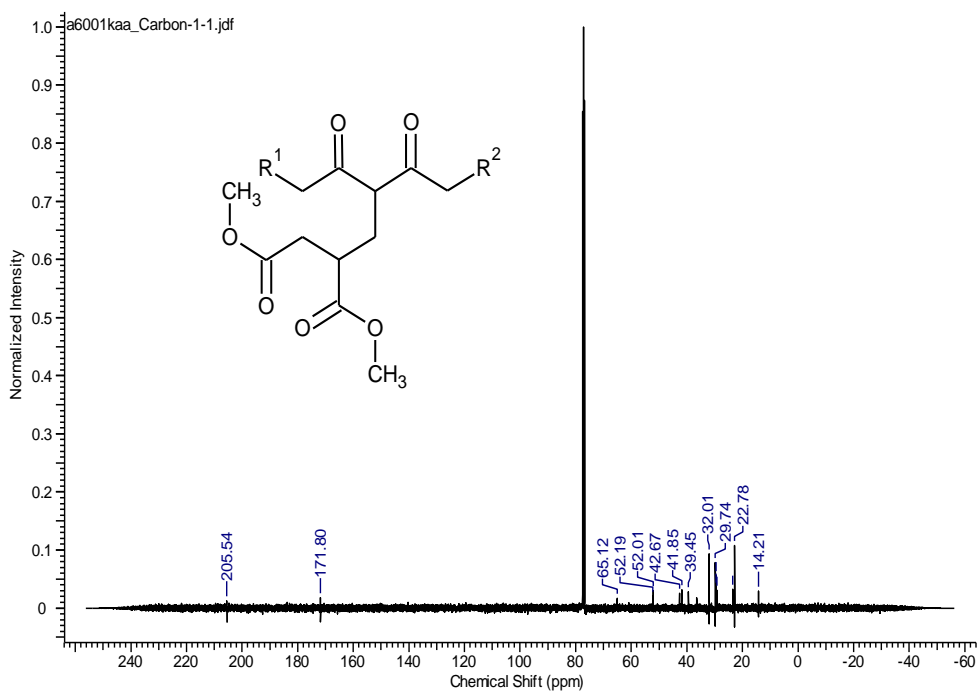


Figure A-2: ^{13}C -NMR spectrum of the Ita (similar assignment as in Fig. A-1)

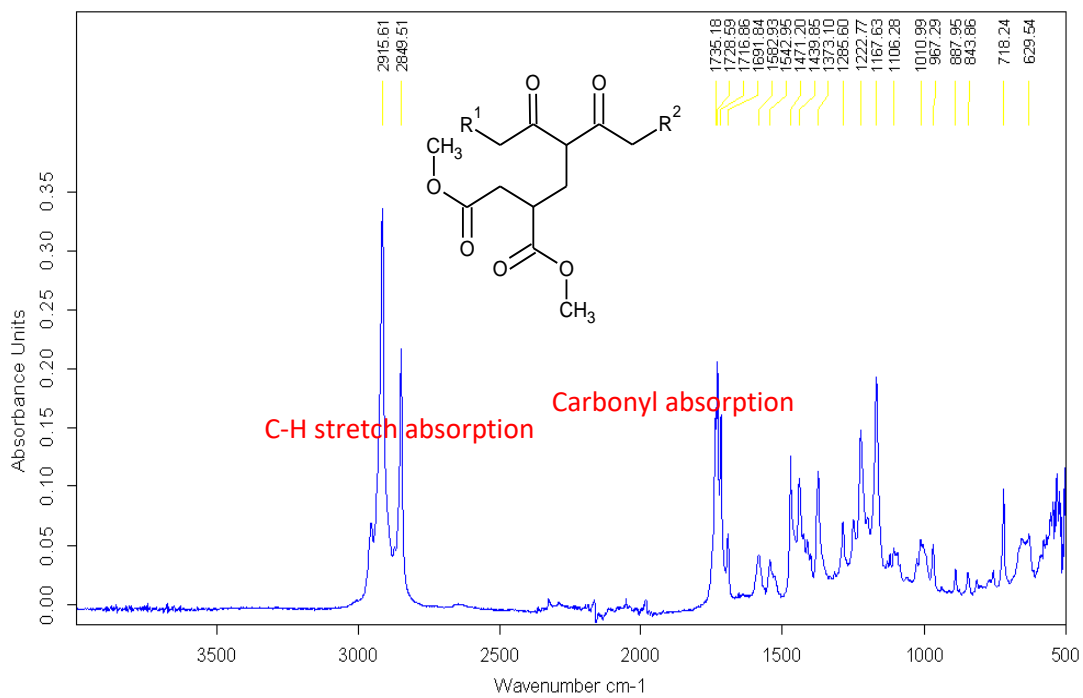


Figure A-3: FTIR spectrum of Ita

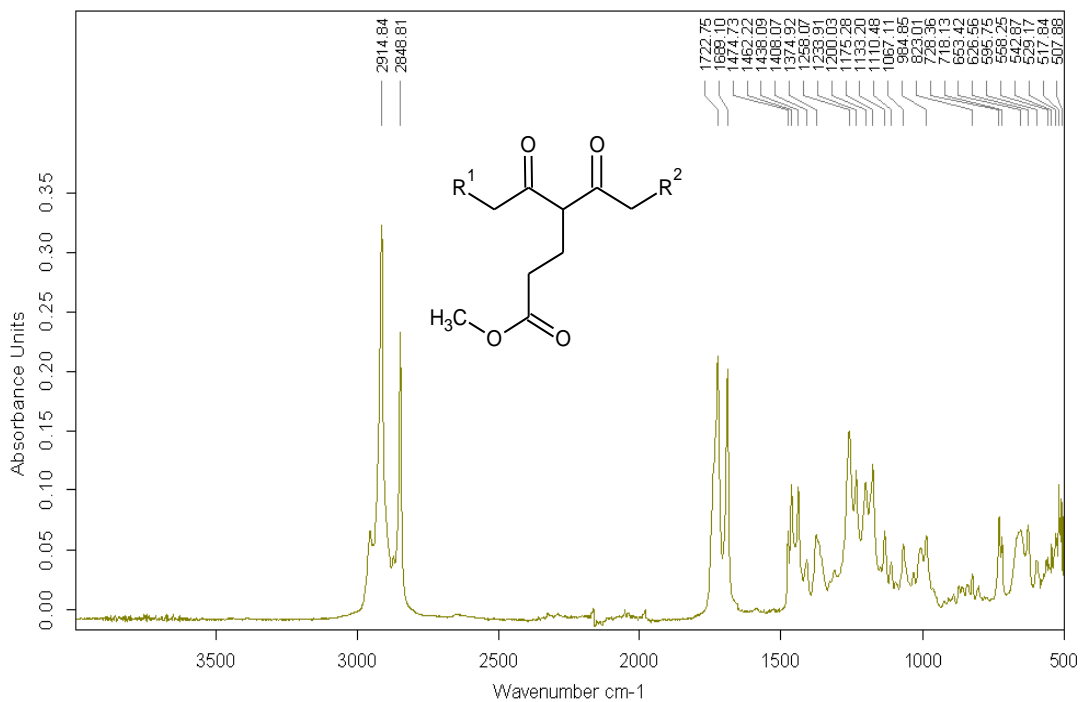


Figure A-4: FTIR spectrum of Ma (similar assignments as in Fig. A-3)

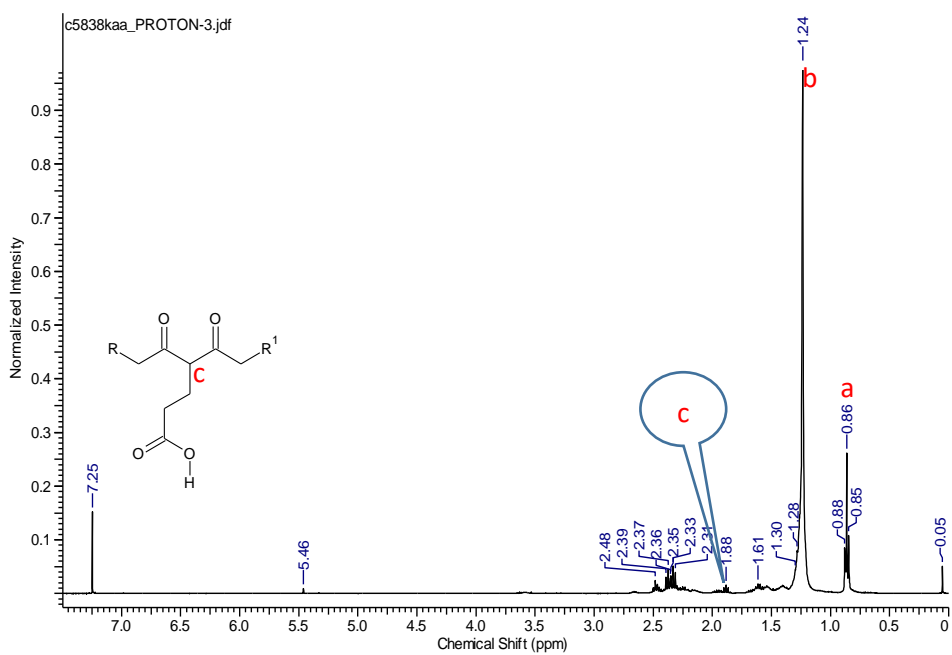


Figure A-5: $^1\text{H-NMR}$ spectrum of the MaH

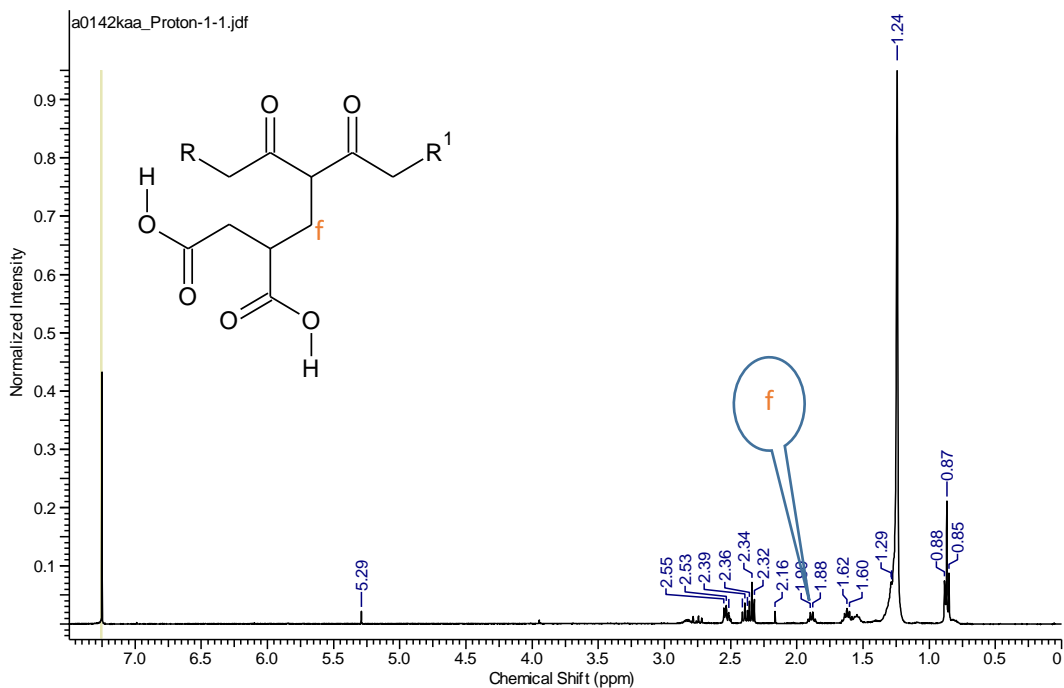


Figure A-6: $^1\text{H-NMR}$ spectrum of the ItaH

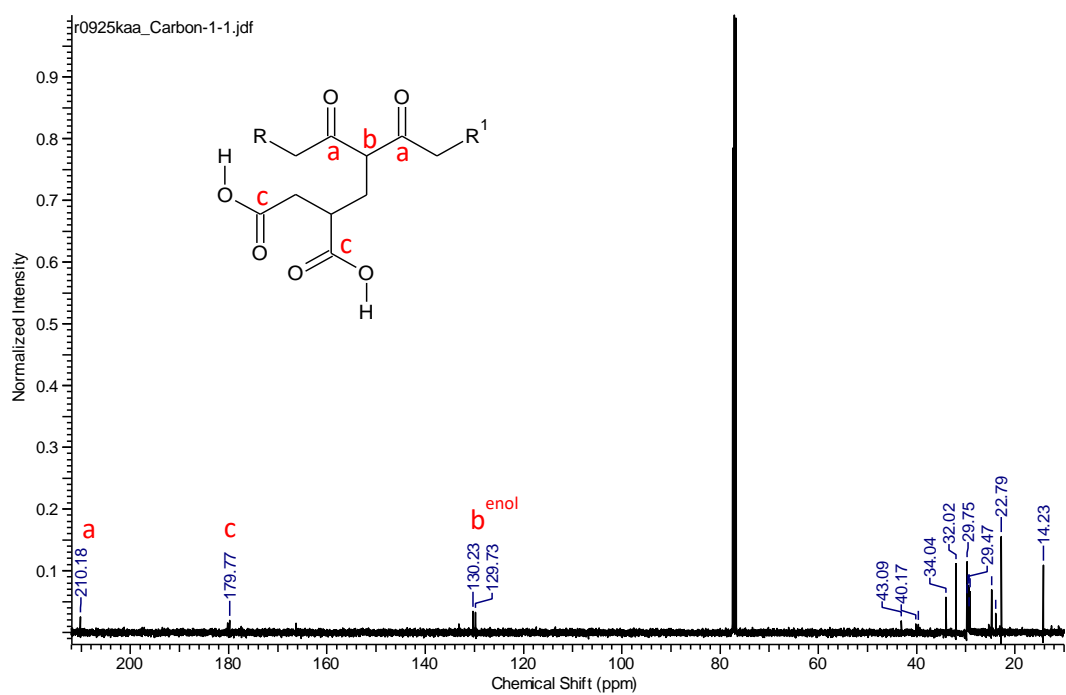


Figure A-7: ^{13}C -NMR spectrum of the ItaH

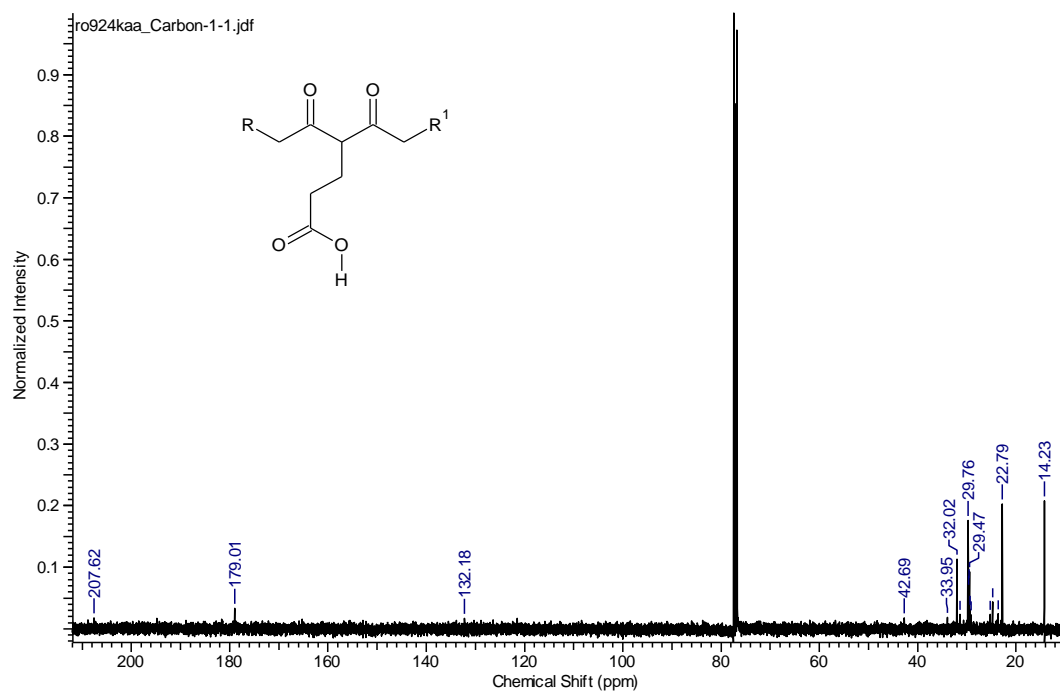


Figure A-8: ^{13}C -NMR spectrum of the MaH (similar assignment as in Fig. A-7)

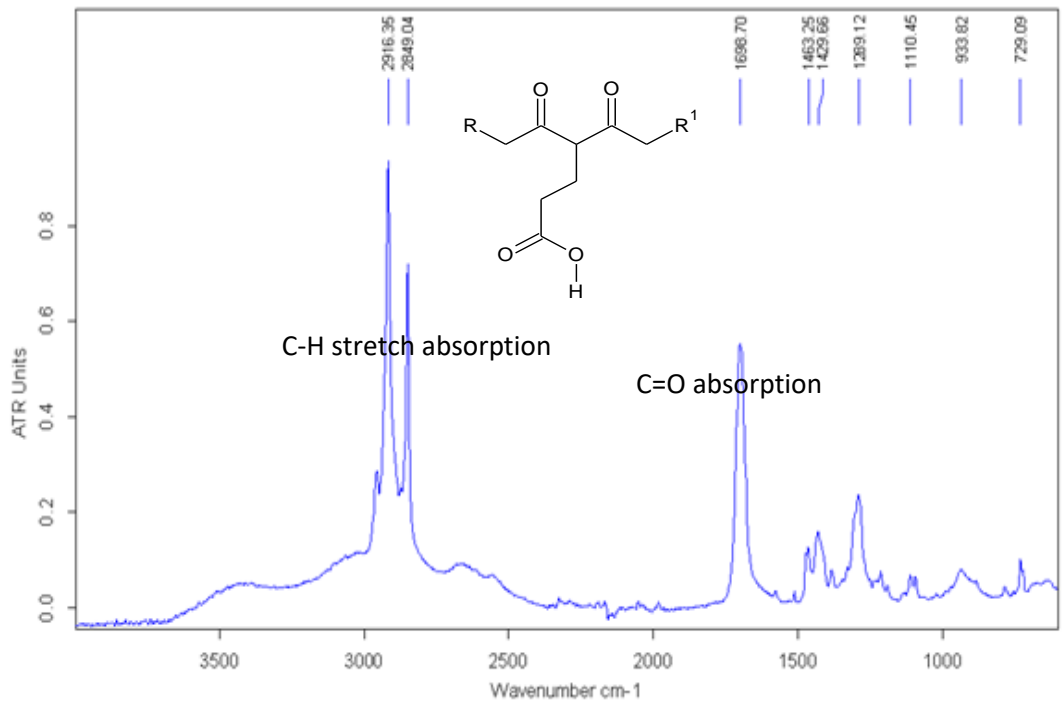


Figure A-9: FTIR spectrum of the MaH

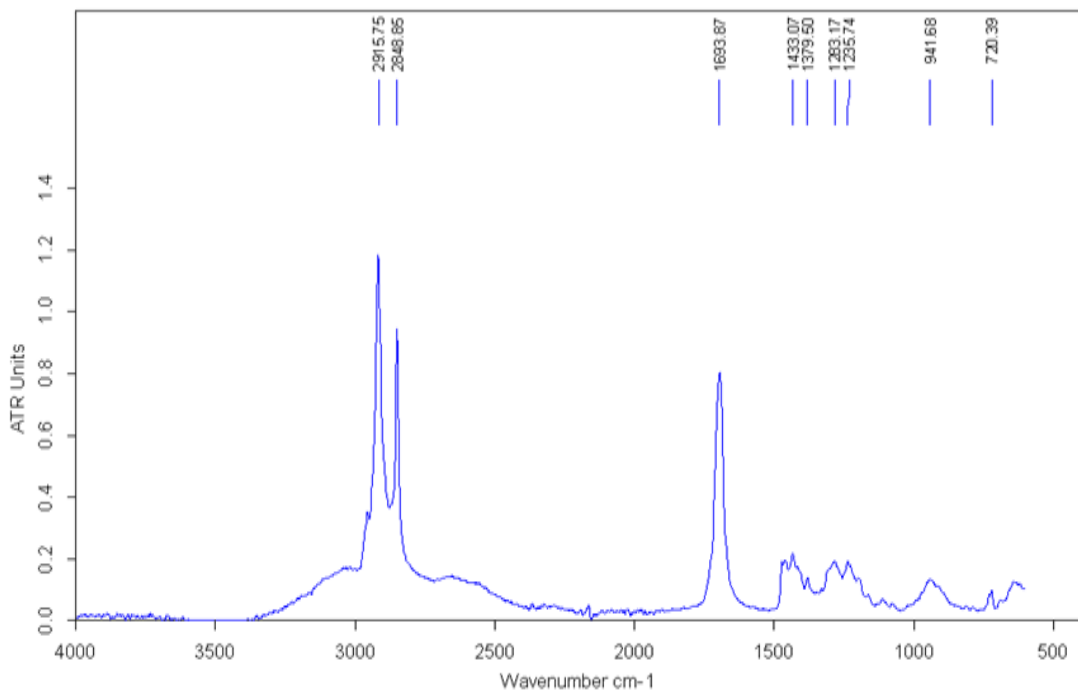


Figure A-10: FTIR spectrum of ItaH

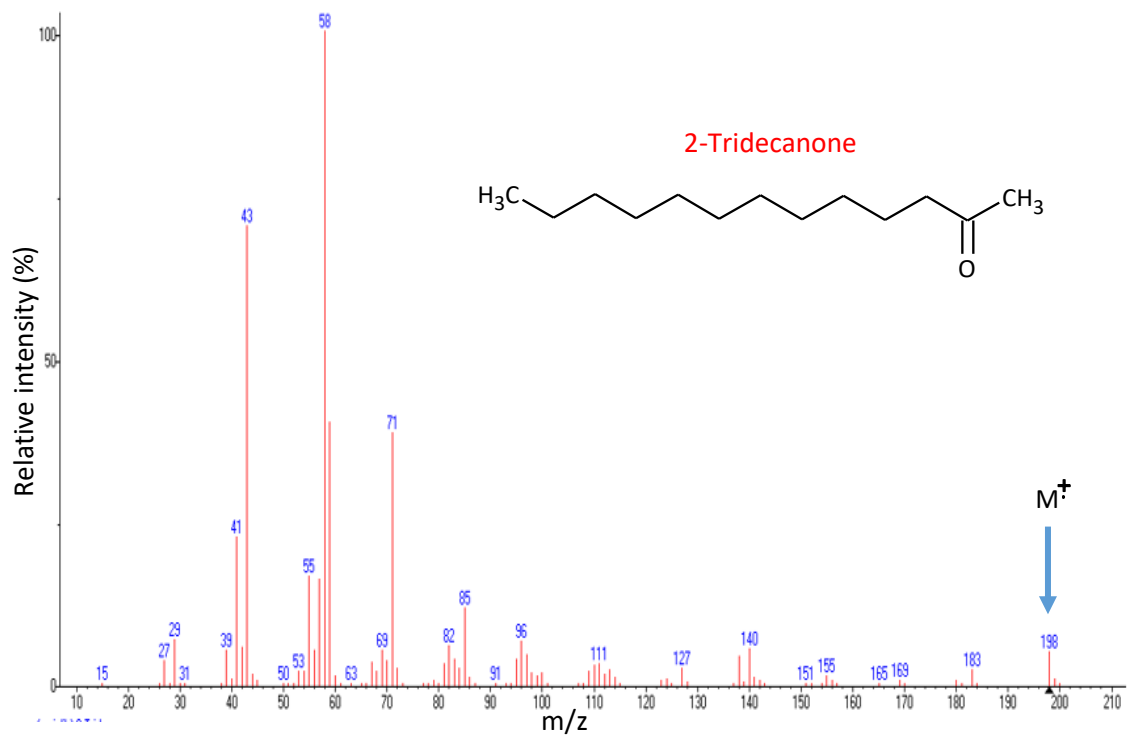


Figure A-11: MS of the 2-Tridecanone

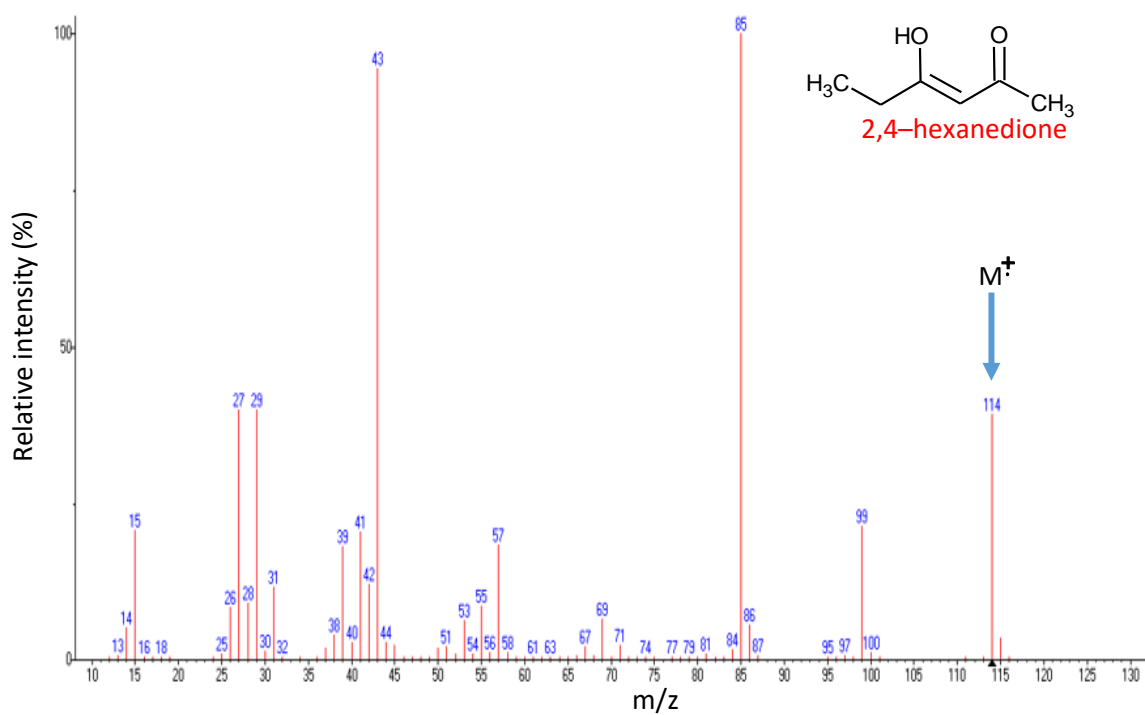
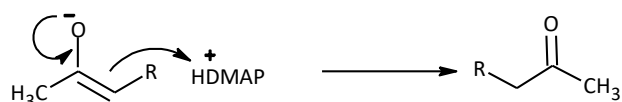
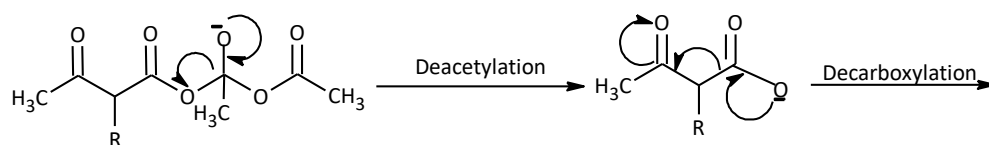
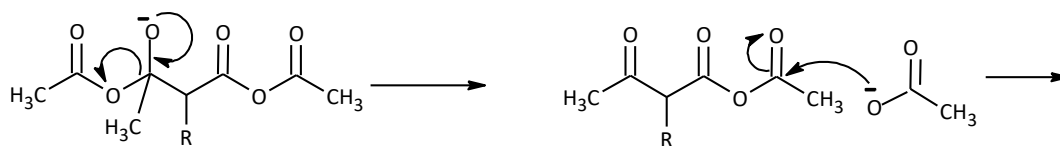
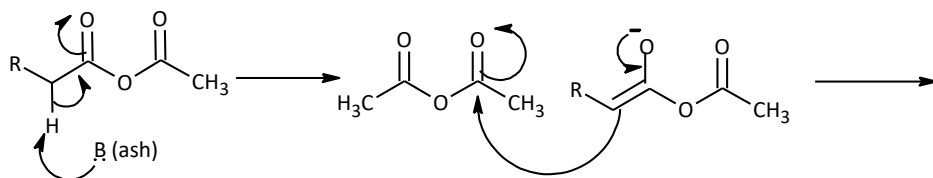
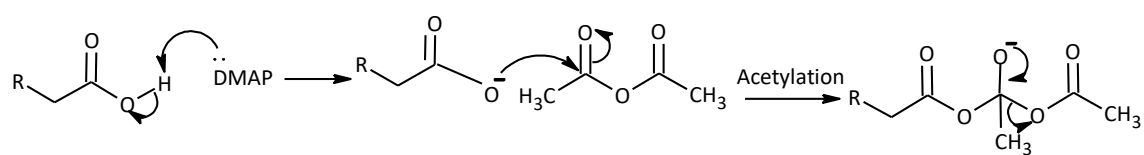
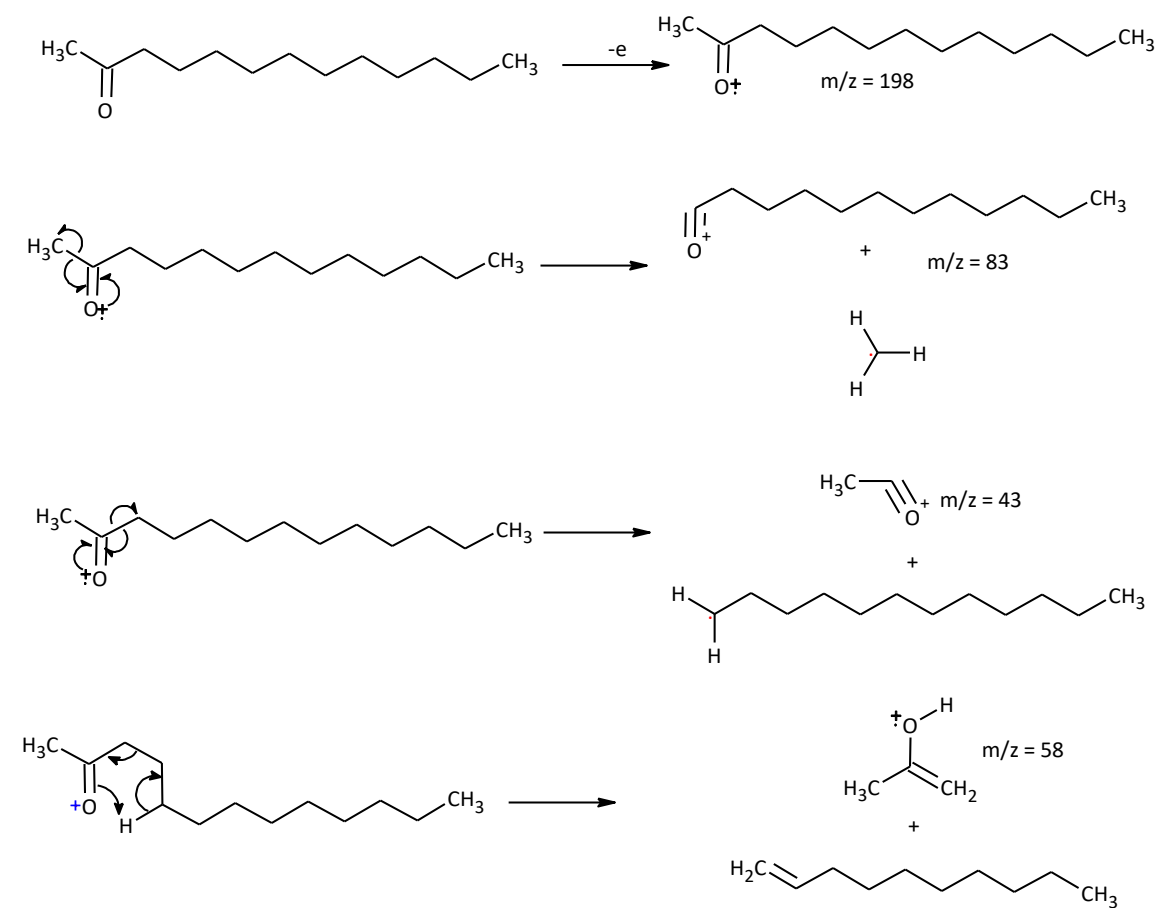


Figure A-12: GC-MS of 2,4-hexanedione

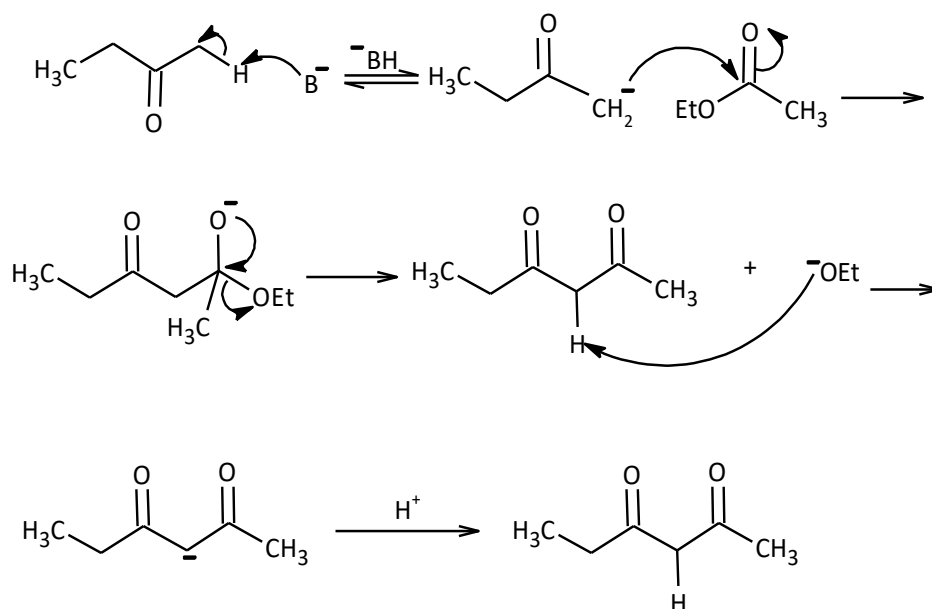
Appendix 2



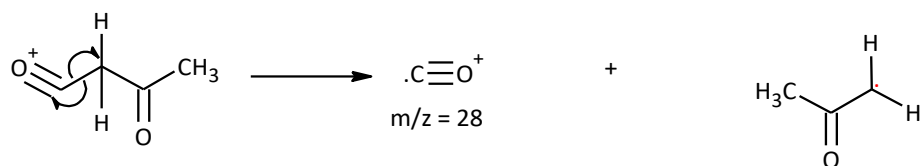
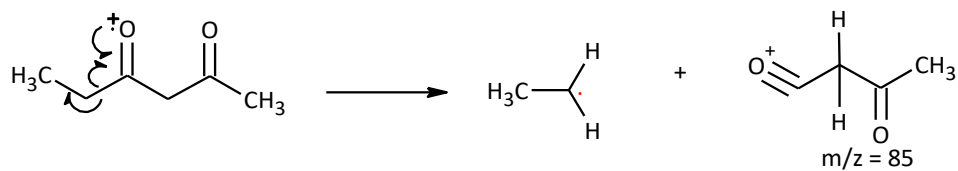
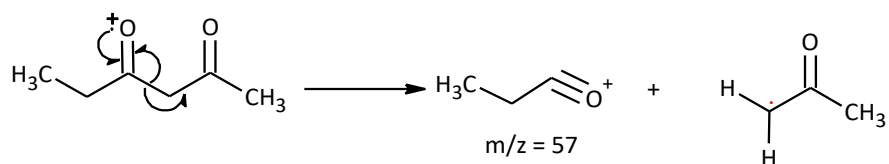
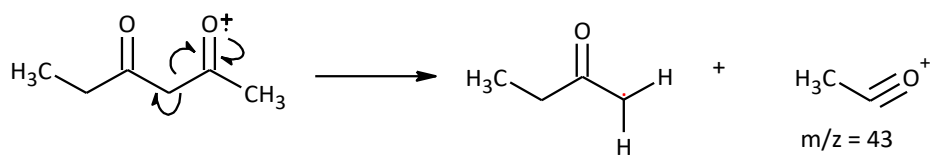
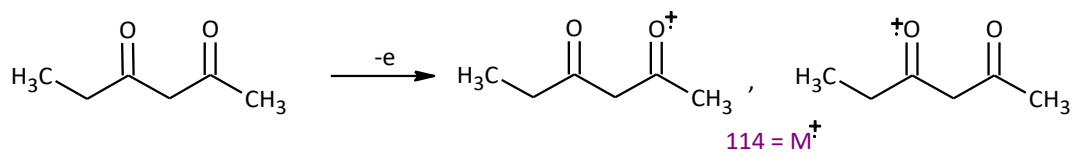
Scheme A-1: proposed mechanism for the Dakin-West formation of methyl ketone from lauric acid



Scheme A-2: Fragmentation pattern of the methyl ketone (2-Tridecanone)



Scheme A-3: Detail scheme for the formation of 2,4-hexanedione



Scheme A-4: Proposed fragmentation pattern of 2,4-hexanedione

List of abbreviations

Abbreviation	-	Definition
Abs	-	Absorbance
Ac ₂ O	-	acetic anhydride
APCs	-	aminopolycarboxylates
atm	-	atmospheric pressure
ATR	-	Attenuated total reflectance
C	-	Carbon
CCS	-	carbon capture and storage
¹³ C-NMR	-	carbon nuclear magnetic resonance spectroscopy
Co(II)	-	Cobalt (II)
Cr(III)	-	Chromium (III)
Cu(II)	-	Copper (II)
DCM	-	Dichloromethane
DMSO	-	Dimethyl sulphoxide
DSC	-	Differential scanning calorimetry
EDTA	-	Ethylenediaminetetraacetic acid
EWG	-	Electron withdrawing group
EI	-	Electron impact
EFA	-	Ely fly ash
ESI-MS	-	Electrospray ionization mass spectroscopy
Fe(III)	-	Iron (III)
FTIR	-	Fourier transforms infra-red
GC-MS	-	Gas chromatography coupled to mass spectrum
g	-	Grammes
Ga(III)	-	Gallium (III)
GC	-	Gas chromatography
GC-FID	-	Gas chromatography coupled to flame ionisation detector
Hacac	-	acetylacetone

Hbac	-	Benzoyl acetone
Hdbm	-	Dibenzoylmethane
¹ H-NMR	-	Proton nuclear magnetic resonance spectroscopy
h(s)	-	Hour(s)
Htd	-	14,16-hentriacontanedione
ICP-MS	-	Inductively coupled plasma mass spectrometry
i.e.	-	That is
Ita	-	Dimethyl itaconate modified bioderived β-diketone
ItaH	-	Carboxylate acid of dimethyl itaconate modified bioderived β-diketone
K	-	Kelvin
kJ	-	kilojoules
M	-	Molarity
M ⁺	-	Molecular ion
Ma _s	-	Single addition of methyl acrylate modified bioderived β-diketone
Ma _d	-	double addition of methyl acrylate modified bioderived β-diketone
MaH	-	Carboxylate acid of methyl acrylate modified bioderived β-diketone
Mn(II)	-	Manganese (II)
min	-	Minutes
mL	-	Millilitres
2-mTHF	-	2-Methyl Tetrahydrofuran
mg	-	milligrams
m/z	-	Mass-to-charge ratio
Ni(II)	-	Nickel (II)
NIST	-	National institute of standards and library
%	-	Percentage
Pb(II)	-	Lead (II)
pH	-	Potential of hydrogen

ppm	-	Parts Per Million
P_c	-	Critical Pressure
R^2	-	Correlation coefficient
r_f	-	Retention factor
R_f	-	Response factor
r.t	-	Room temperature
scCO ₂	-	Supercritical carbon dioxide
SFE	-	Supercritical fluid extraction
STA	-	Simultaneous Thermal Analysis
T_c	-	Critical temperature
TGA	-	Thermal Gravimetric Analysis
THF	-	Tetrahydrofuran
UK	-	United Kingdom
UV	-	Ultraviolet
α	-	Alpha
β	-	Beta
λ	-	Wavelength
λ_{max}	-	Wavelength for maximum absorbance
π	-	Pi
δ	-	Delta
ϵ	-	Molar extinction coefficient
μ	-	Micro
\$		Dollar

Reference

8 Reference

1. J. R. Dodson, A. J. Hunt, H. L. Parker, Y. Yang, and J. H. Clark, *Chem. Eng. Process. Process Intensif.*, 2012, **51**, 69–78.
2. C. P. Baldé, F. Wang, R. Kuehr, and J. Huisman, *The global e-waste monitor – 2014*, Bonn, Germany, 2015.
3. H. Shen and E. Forsberg, *Waste Manag.*, 2003, **23**, 933–949.
4. X. W. X. Wen, Y. Z. Y. Zhao, C. D. C. Duan, X. Z. X. Zhou, H. J. H. Jiao, and S. S. S. Song, in *Proceedings of the 2005 IEEE International Symposium*, 2005, 121–128.
5. S. I. Amer, *Met. Finish.*, 2004, **102**, 1–5.
6. K. Narasimhulu and P. S. Rao, *J. Eng. Appl. Sci.*, 2009, **4**, 58–63.
7. S. Şenel, B. Elmas, T. Çamlı, M. Andaç, and A. Denizli, *Sep. Sci. Technol.*, 2004, **39**, 3783–3795.
8. D. Kołodyńska, in *Expanding Issues in Desalination*, DOI: 10.5772/21180, 2011, 339–370.
9. T. Knepper, *Trends Anal. Chem.*, 2003, **22**, 708–724.
10. H. Hyvönen, University of Helsinki, Finland, 2008.
11. P. Theptat, S. Chavadej, and J. F. Scamehorn, *World Acad. Sci. Eng. Technol.*, 2013, **76**, 806–809.
12. B. Nowack, S. Federal, and T. Zu, *Environ. Sci. Technol.*, 2002, **36**, 4009–4016.
13. M. Sillanpää, *Rev. Environ. Contam. Toxicol.*, 1997, **132**, 85–111.
14. C. Oviedo and J. Rodríguez, *Quim. Nova*, 2003, 26, 901–905.
15. IHS Chemical, <https://www.ihs.com/products/chelating-agents-chemical-economics-handbook.html>. Accessed on 2/4/2016, 2013, 1–2.
16. J. H. Clark and F. E. I. Deswarte, in *Introduction to Chemicals from Biomass*, eds. J. H. Clark and F. E. I. Deswarte, John Wiley & Sons, Ltd, 2008, 1–20.
17. S. Ravichandran, *Int. J. ChemTech Res.*, 2011, **3**, 1511–1513.
18. S. D. Dhage and K. K. Shisodiya, *Int. Res. J. Pharm.*, 2013, **4**, 1–4.
19. P. T. Anastas, J. C. Warner, and J. Warner, *Green Chemistry: Theory and Practice*, Oxford University Press, Oxford, 2000.
20. P. T. Anastas and J. C. Warner, *Green Chemistry: Theory and Practice*, Oxford

University Press: Oxford, New York, 1st edn., 1998.

21. R. L. Moss, E. Tzimas, H. Kara, P. Willis, J. Kooroshy, R.L.Moss, E.Tzimas, H.Kara, P.Willis, J.Kooroshy, R. L. Moss, E. Tzimas, H. Kara, P. Willis, and J. Kooroshy, *Critical Metals in Strategic Energy Technologies: Assessing Rare Metals as Supply-Chain Bottlenecks in Low-Carbon Energy Technologies*, 2011, 1-164.
22. K. Nansai, K. Nakajima, S. Kagawa, Y. Kondo, S. Suh, Y. Shigetomi, and Y. Oshita, *Environ. Sci. Technol.*, 2014, **48**, 1391–400.
23. A. J. Hunt, T. J. Farmer, and J. H. Clark, in *RSC Green Chemistry Series*, ed. A. J. Hunt, RSC publishing, London, 2013, 1–28.
24. A. J. Hunt, A. S. Matharu, A. H. King, and J. H. Clark, *Green Chem. (RSC)*, 2015, **17**, 1949–1950.
25. *U.S Department of Energy*, 2010.
26. C. Voica, M. H. Kovacs, A. Dehelwan, D. Ristoiu, and A. Iordache, *Environ. Phys.*, 2012, **57**, 1184–1193.
27. S. R. Vaidya, V. A. Shelke, S. M. Jadhav, S. G. Shankarwar, and T. K. Chondhekar, *Arch. Appl. Sci. Res.*, 2012, **4**, 1839–1843.
28. L. S. Morf, R. Gloor, O. Haag, M. Haupt, S. Skutan, F. Di Lorenzo, and D. Böni, *Waste Manag.*, 2013, **33**, 634–44.
29. U. Jadhav and H. Hocheng, *J. Achiev. Mater.*, 2012, **54**, 159–167.
30. O. Osibanjo, in *R'09 World Congress*, 2009, 1–7.
31. I. K. Wernick and N. J. N. J. Themelis, *Annu. Rev. Energy Environ.*, 1998, **23**, 465–97.
32. M. Buchert, D. Schuler, and D. Bleher, *Sustainable innovation and technology transfer industrial sector studies: Critical metals for future sustainable technologies and their recycling potential*, 2009, 1-112.
33. *USGS, Minerals Commodity Summaries*, 2010.
34. S. Hongbo, C. Liye, X. Gang, Y. Kun, Z. Lihua, and S. Junna, *Significance*, 2011, **30**, 143–167.
35. P. C. Nagajyoti, K. D. Lee, and T. V. M. Sreekanth, *Environ. Chem. Lett.*, 2010, **8**, 199–216.
36. S. I. El Dessouky, Y. A. El-Nadi, I. M. Ahmed, E. A. Saad, and J. A. Daoud, *Chem. Eng. Process.*, 2008, **47**, 177–183.
37. E. MacIngvova and A. Luptakova, *Chem. Eng. Trans.*, 2012, **28**, 109–114.

38. A. J. Hunt, C. W. N. Anderson, N. Bruce, A. M. García, T. E. Graedel, M. Hodson, J. A. Meech, N. T. Nassar, H. L. Parker, E. L. Rylott, K. Sotiriou, Q. Zhang, and J. H. Clark, *Green Process Synth*, 2014, **3**, 3–22.
39. J. R. Dodson, H. L. Parker, A. M. García, A. Hicken, K. Asemave, T. J. Farmer, H. He, J. H. Clark, and A. J. Hunt, *Green Chem. (RSC)*, 2015, 1–15.
40. J. Hein, T. Conrad, and H. Staudigel, *Oceanography*, 2010, **23**, 184–189.
41. I. S. S. Pinto, I. F. F. Neto, and H. M. V. M. Soares, *Env. Sci Pollut Res*, 2014, **21**, 11893–11906.
42. H. Hasegawa, I. M. M. Rahman, Y. Egawa, H. Sawai, Z. A. Begum, T. Maki, and S. Mizutani, *Microchem. J.*, 2013, **106**, 289–294.
43. P. Selvi, M. Ramasami, M. H. P. Samuel, P. Adaikkalam, and G. N. Srinivasan, *Ind. Eng. Chem. Res.*, 2004, **43**, 2216–2221.
44. T. K. Chikako Nakayama, Shigeyuki Uemiya, *J. Alloys Compd.*, 1995, **225**, 288–290.
45. J. Roosen and K. Binnemans, *J. Mater. Chem. A*, 2014, **2**, 15–30.
46. S. Tandy, K. Bossart, R. Mueller, J. Ritschel, L. Hauser, R. Schulin, and B. Nowack, *Environ. Sci. Technol.*, 2004, **38**, 937–944.
47. K. Fischer and H. P. Bipp, *Water. Air. Soil Pollut.*, 2002, **138**, 271–288.
48. C. De Stefano, G. Lando, A. Pettignano, and S. Sammartano, *J. Chem. Eng. Data; Am. Chem. Soc.*, 2014, **59**, 1970–1983.
49. J. Rämö, University of Oulu, Finland, 2003.
50. S. Ravichandran, *Asian J. Biochem. Pharm. Res.*, 2011, **1**, 129–135.
51. N. J. 2012. Dixon, in *Handbook of green chemistry volume 9: Designing safer chemicals*, eds. R. Boethling and A. Voutchkova, Wiley-VCH verlag GmGH & Co. KGaA, First., 2012, 9:281–307.
52. D. Kolodynska, *Env. Sci Pollut Res*, 2013, **20**, 5939–5949.
53. K. R. Vuyyuru, K. K. Pant, V. V. Krishnan, and K. D. P. Nigam, *Ind. Eng. Chem. Res.*, 2010, **49**, 2014–2024.
54. R. Laus, A. DosAnjos, R. E. H. M. B. Osorio, A. Neves, M. C. M. Laranjeira, and V. T. De Favere, *Pak. J. Anal. Environ. Chem.*, 2008, **9**, 58–63.
55. F. Asrafi, A. Feyzbakhsh, and N. E. Heravi, *Int. J. ChemTech Res.*, 2009, **1**, 420–425.
56. M. Ak, D. Taban, and H. Deligöz, *J. Hazard. Mater.*, 2008, **154**, 51–4.

57. K. Chung, C. Chu, and M. Chang, *Bull. Korean Chem. Soc.*, 2004, **25**, 417–419.
58. H. Hu, C. Liu, X. Han, Q. Liang, and Q. Chen, *Trans. Nonferrous Met. Soc. China*, 2010, **20**, 2026–2031.
59. F. Kubota, M. Goto, and F. Nakashio, *Solvent Extr. Ion Exch.*, 1993, **11**, 437–453.
60. H. Karimi and M. Gheadi, *Asian J. Chem.*, 2007, **19**, 4173–4176.
61. C. L. Edwards, Blacksburg, Virginia, 2013.
62. M. Bucheli-Witschel and T. Egli, *Fems Microbiol. Rev.*, 2001, **25**, 69–106.
63. W. Z. Kocialkowski, J. B. Diatta, and W. Grzebisz, *Polish J. Environ. Stud.*, 1999, **8**, 149–154.
64. F. B. Stifel and R. L. Vetter, *J Anim Sci*, 1967, **26**, 129–135.
65. A. Wallace and G. A. Wallace, *J. Plant Nutr.*, 1992, **15**, 1487–1508.
66. S. Okano, K. Ishida, and S. Kuse, *Konica Tech. Rep.*, 2003, **16**, 13–18.
67. B. Nowack and J. M. VanBriesen, in *Biogeochemistry of Chelating Agents*, eds. B. Nowack and J. M. VanBriesen, ACS, 2005, 910, 1–18.
68. D. E. Douglas, *J. Lipid Res.*, 1991, **32**, 553 – 558.
69. Z. Kun and C. Hui, *J. Environ. Sci.*, 1994, **6**, 99–106.
70. A. Cao, A. Carucci, T. Lai, G. Bacchetta, and M. Casti, *J. Chem. Technol. Biotechnol.*, 2009, **84**, 884–889.
71. D. Lestan, C. Luo, and X. Li, *Environ. Pollut.*, 2008, **153**, 3–13.
72. Y. Sun, M. Fenster, A. Yu, R. M. Berry, and D. S. Argyropoulos, *Can. J. Chem.*, 1999, **77**, 667–675.
73. A. Álvarez-Fernández, S. García-Marco, and J. J. Lucena, *Eur. J. Agron.*, 2005, **22**, 119–130.
74. I. Levitin, M. Tsikalova, N. Sazikova, V. Bakhmutov, Z. Starikova, A. Yanovsky, and Y. Struchkov, *Inorganica Chim. Acta*, 1998, **270**, 169–176.
75. M. Pyun, K. Choi, Y. Hong, and S. Choi, *Bull Korean Chem. Soc.*, 2009, **30**, 1187–1189.
76. M. K. Moi, S. J. DeNardo, and C. F. Meares, *Cancer Res.*, 1990, **50**, 789–793.
77. S. Tandy, A. Ammann, R. Schulin, and B. Nowack, *Environ. Pollut.*, 2006, **142**, 191–9.

78. W. Jiang, T. Tao, and Z. Liao, *Open J. Soil Sci.*, 2011, **1**, 70–76.
79. I. Alkorta, J. Hernández-Allica, J. M. Becerril, I. Amezaga, I. Albizu, M. Onaindia, and C. Garbisu, *Rev. Environ. Sci. Biotechnol.*, 2004, **3**, 55–70.
80. S. D. Ingale and R. Kankariya, *Int. Res. J. Pharm.*, 2013, **4**, 131–132.
81. M. C. Brasil, E. V. Benvenutti, J. R. Gregório, and A. E. Gerbase, *React. Funct. Polym.*, 2005, **63**, 135–141.
82. A. L. Willis, Z. Chen, J. He, Y. Zhu, N. J. Turro, and S. O'Brien, *J. Nanomater.*, 2007, **2007**, 1–7.
83. J. Shen, Z. Song, X. Qian, and W. Liu, *BioResources*, 2009, **4**, 1190–1209.
84. A. T. Ruley, N. C. Sharma, S. V Sahi, S. R. Singh, and K. S. Sajwan, *Environ. Pollut.*, 2006, **144**, 11–8.
85. B. Singh, *J. Hazard. Mater.*, 2009, **167**, 24–37.
86. G. Chauhan, K. K. Pant, and K. D. P. Nigam, *Environ. Sci. Process. Impacts*, 2015, **17**, 12–40.
87. B. Nowack, *Water Res.*, 2003, **37**, 2533–46.
88. P. A. Clarke, Durham University, 1991.
89. A. M. Wilson, P. J. Bailey, P. A. Tasker, J. R. Turkington, R. A. Grant, and J. B. Love, *Chem. Soc. Rev.*, 2014, **43**, 123–134.
90. J. Saji, Cochin University of science and technology, 2002.
91. C. W. A. do Nascimento, D. Amarasiriwardena, and B. Xing, *Environ. Pollut.*, 2006, **140**, 114–23.
92. T. T. Teng, Y. Yusup, and L. W. Low, in *Heavy Metal Ion Extraction Using Organic Solvents*, ed. A. Innocenti, 2012, 121–132.
93. Presidential Green Chemistry Challenge: 2001 Greener Synthetic Pathways Award, <https://www.epa.gov/greenchemistry/presidential-green-chemistry-challenge-2001-greener-synthetic-pathways-award>. Accessed on 2/4/2016, 2001.
94. S. Mudgal, S. Pahal, and L. Petersen, *Evaluation of the use of phosphates in Consumer Automatic Dishwasher Detergents (CADD)*, 2014, 1-84.
95. HERA, *Human & Environmental Risk Assessment on ingredients of European household cleaning products*, 2004, 1-114.
96. J. Jaworska, H. Van Genderen-Takken, A. Hanstveit, E. van de Plassche, and T. Feijtel, *Chemosphere*, 2002, **47**, 655–65.

97. J. H. Clark, *Green Chem.*, 2006, **8**, 17.
98. P. J. A. Withers, J. J. Elser, J. Hilton, H. Ohtake, W. J. Schipper, and K. C. Van Dijk, in *Green Chemistry; Elemental recovery and sustainability*, eds. A. J. Hunt, A. S. Matharu, A. H. King, and J. H. Clark, Royal Society of Chemistry, 2105, 1229–2588.
99. H. Ohara, *Appl. Microbiol. Biotechnol.*, 2003, **62**, 474–477.
100. F. Cherubini, *Energy Convers. Manag.*, 2010, **51**, 1412–1421.
101. J. seetz and G. P. Stafford, *soap, Perfum. comestics*, 2007, 75–76.
102. T. P. Knepper, A. Werner, and G. Bogenschütz, *J. Chromatogr. A*, 2005, **1085**, 240–246.
103. D. C. W. Tsang, I. M.-C. Lo, and R. Y. Surampalli, *ASCE Publ.*, 2012, 1-284.
104. H. Hyvönen and R. Aksela, *J. Coord. Chem.*, 2007, **60**, 901–910.
105. N. Dixon and S. Norden, *Chelants in detergents*, 2009.
106. P. Saling, A. Grosse-sommer, M. Pierobon, and D. Kolsch, in *RSC Speciality Chemicals Symposium-'The Sustainability Challenge'*, 2008, 1–38.
107. J. Jefferis and K. Zack, [https://patentscope.wipo.int/search/en/detail.jsf?docId=WO2011100344&recNum=164&docAn=US2011024217&queryString=\(catalyst\)%2520AND%2520\(PA/basf\)%2520&maxRec=2779](https://patentscope.wipo.int/search/en/detail.jsf?docId=WO2011100344&recNum=164&docAn=US2011024217&queryString=(catalyst)%2520AND%2520(PA/basf)%2520&maxRec=2779), 2011. Accessed on 23/6/2016.
108. C. A. De Wolf, H. Nasr-El-Din, M. M. A. Nasr-El-Din, J. N. Lepage, J. H. Bemelaar, A. J. M. Bouwman, and G. Wang, <http://www.google.nl/patents/WO2012080463A1?cl=en>, 2012. Accessed on 23/6/2016.
109. T. Kakhia, <http://tarek.kakhia.org>, 1–99. Accessed on 23/6/2016.
110. B. Sims, <http://biomassmagazine.com/articles/7500/canadian-co-seeks-to-penetrate-biobased-aspartic-acid-market>, 2011. Accessed on 3/10/14.
111. Guido Lingua, M. G. Valeria Todeschini, A. P. Daniela Baldantoni, A. Cikatelli, S. Biondi, and S. C. Patrizia Torrigiani, *J. Environ. Manage.*, 2014, **132**, 9–15.
112. F. Pavelcik and J. Majer, *Chem. zvesti*, 1978, **32**, 37–41.
113. L. R. Schowanek D, Feijtel TC, Perkins CM, Hartman FA, Federle TW, *Chemosphere*, 1997, **34**, 2375–91.
114. T. C. Ho, A. R. Katritzky, and S. J. Cato, *Ind. Eng. Chem. Res.*, 1992, **31**, 1589–1597.
115. M. W. H. Evangelou, M. Ebel, and A. Schaeffer, *Chemosphere*, 2007, **68**, 989–1003.

116. H. Grčman, D. Vodnik, Š. Velikonja-Bolta, and D. Leštan, *J. Environ. Qual.*, 2003, **32**, 500–506.
117. L. Di Palma, O. Gonzini, and R. Mecozzi, *Chem. Ecol.*, 2011, **27**, 97–106.
118. R. Yang, C. Luo, G. Zhang, X. Li, and Z. Shen, *J. Env. Sci (China)*., 2012, **24**, 1985–94.
119. A. Ullmann, N. Brauner, S. Vazana, Z. Katz, R. Goikhman, B. Seemann, H. Marom, and M. Gozin, *J Hazard Mater*, 2013, **260**, 676–88.
120. M. Niinae, K. Nishigaki, and K. Aoki, *Mater. Trans.*, 2008, **49**, 2377–2382.
121. C. R. Soccol, L. P. S. Vandenberghe, C. Rodrigues, and A. Pandey, *Citric Acid Prod. Food Technol. Biotechnol.*, 2006, **44**, 141–149.
122. S. Ramachandran, P. Fontanille, A. Pandey, and C. Larroche, *Food Technol. Biotechnol.*, 2006, **44**, 185–195.
123. D. del M. Dacera and S. Babel, *Water Sci Technol.*, 2006, **54**, 129–135.
124. L. Huang, Q. Zhou, and Q. Zhang, *Ying Yong Sheng Tai Xue Bao*, 2008, **19**, 641–6.
125. F. R. Xiu and F. S. Zhang, *J. Hazard. Mater.*, 2009, **170**, 191–196.
126. H. Kiel, R. Guvrin, and Y. Henis, *Appl Env. Microbiol.*, 1981, **42**, 1–4.
127. A. Bera, S. Verma, and V. Suneetha, *Der Pharm. Lett.*, 2013, **5**, 58–64.
128. Khadijah-Al-Khadir, *Int. J. Eng. Sci. Technol.*, 2011, **3**, 4849–4856.
129. S. E. Gaber, M. S. Rizk, and M. M. Yehia, *Biokemistri*, 2011, **23**, 41–48.
130. L. Hauser, S. Tandy, R. Schulin, and B. Nowack, *Env. Sci Technol.*, 2005, **39**, 6819–24.
131. S. Ramachandran, P. Fontanille, A. Pandey, and C. Larroche, *Food Technol. Biotechnol.*, 2006, **44**, 185–195.
132. N. Finzgar, B. Kos, and D. Lestan, *Chemosphere*, 2004, **57**, 655–61.
133. Z. A. Begum, Y. T. Ismail M. M. Rahman, H. Sawai, T. Maki, and H. Hasegawa, *Chemosphere*, 2012, **87**, 1161–1170.
134. R. A. Wuana, F. E. Okieimen, and J. A. Imborvungu, *Int. J. Environ. Sci. Tech.*, 2010, **7**, 485–496.
135. K. Xin, L. Pei-jun, Z. Qi-xing, Z. Yun, and S. Tie-heng, *J. Environ. Sci.*, 2006, **18**, 727–733.
136. N. A. Abood and A. F. Ajam, *J. Chem. Soc. Pak.*, 1985, **7**, 1–6.

137. Nguyen Thanh Cuong, L. K. Long, and D. U. Van, *J. Chem.*, 2006, **44**, 249–254.
138. M. T. Rogers and J. L. Burdett, *Can. J. Chem.*, 1965, **43**, 1516–1526.
139. J. A. Kenar, *JAOCs*, 2003, **80**, 1027–1032.
140. J. Zhang, N. Yang, and L. Yang, *Molecules*, 2012, **17**, 6415–6423.
141. P. N. Verma, J. I. Sheikh, and H. D. Juneja, *World Appl. Sci. J.*, 2011, **14**, 1154–1157.
142. M. Oladipo, O. S. Bello, and A. Adeagbo, *African J. Pure Appl. Chem.*, 2012, **6**, 35–41.
143. S. T. Heller and S. R. Natarajan, *Org. Lett. (American Chem. Soc.)*, 2006, **8**, 2675–2678.
144. A. G. Netting and P. Von Wettstein-Knowles, *Arch. Biochem. Biophys.*, 1976, **174**, 613–621.
145. J. D. Mikkelsen and P. Von Wettstein-Knowles, *Arch. Biochem. Biophys.*, 1978, **188**, 172–181.
146. G. Bianchi and M. De Amici, *J.C.S. Chem. Comm.*, 1978, 962–963.
147. M. A. Gouveia, M. D. J. Tavares, and R. G. De Carvalho, *J. inorg. nucl. Chem.*, 1971, **33**, 817–822.
148. C. M. Wai and S. Wang, *J. Chromatogr. A*, 1997, **785**, 369–383.
149. H. Koshimura and T. Okubo, *Anal. Chim. Acta*, 1970, **49**, 67–75.
150. J. Stary, *Solvent extraction of metal chelate*, Elsevier, 2013.
151. M. Svärd, *KTH R. Inst. Technol. Sweden*, 2013.
152. M. Cerna, *Environ. Monit. Assess.*, 1995, **34**, 151–162.
153. S. S. Przeszlakowski and H. Wydra, *Hydrometallurgy*, 1982, **8**, 49–64.
154. L. He, Q. Jiang, Y. Jia, Y. Fang, S. Zou, Y. Yang, J. Liao, N. Liu, W. Feng, S. Luo, Y. Yang, L. Yang, and L. Yuan, *J Chem Technol Biotechnol*, 2013, **88**, 1930–1936.
155. M. S. Beltran, Chalmers University of Technology, 2009.
156. M. Mackenzie, *The solvent extraction of some major metals: An overview*, <http://storage.globalcitizen.net/data/topic/knowledge/uploads/20111102114038533.pdf>, 1957, 1-37. Accessed on 23/6/2016.
157. W. S. Wang, X. Q. Shan, B. Wen, and S. Z. Zhang, *Chemosphere*, 2003, **53**, 523–530.

158. T. Abushi and M. Asayuki, *Bull. Inst. Chem. Res. Kyoto Univ.*, 1959, **37**, 232–236.
159. J. S. Preston and A. C. du Preez, *Hydrometallurgy*, 2000, 58, 239–250.
160. F. S. Nworie and F. I. Nwabue, *Nat. Sci.*, 2014, **12**, 87–96.
161. J. W. Mitchell, Iowa State University, 1970.
162. F. E. I. Deswarte, J. H. Clark, J. J. E. Hardy, and P. M. Rose, *Green Chem.*, 2006, **8**, 39–42.
163. J. Copeland and D. Turley, *National and regional supply/demand balance for agricultural straw in Great Britain*, York, UK, 2008.
164. F. Deswarte, *Towards a wheat straw based biorefinery*, University of York, 2008, 1-26.
165. J. C. del Río, P. Prinsen, and A. Gutiérrez, *J. Agric. Food Chem.*, 2013, **61**, 1904–1913.
166. E. H. K. Sin, University of York, 2012.
167. K. Koch and W. Barthlott, *Phil. Trans. R. Soc. A*, 2009, 1487–1509.
168. A. P. P. Tulloch, in *Chemistry and Biochemistry of Natural Waxes*, ed. P. E. Kolattukkudy, Elsevier, Amsterdam, 1976, 235–287.
169. P. Prinsen, A. Gutiérrez, and J. C. del Río, *J. Agric. Food Chem.*, 2012, **60**, 6408–6417.
170. M. A. Jenks, C. H. Gaston, M. S. Goodwin, J. A. Keith, and R. S. Teusink, *Hortscience*, 2012, **37**, 673–677.
171. M. Dvoyashkin, http://www.uni-leipzig.de/~pore/files/3rd_irtg_workshop/dvoyashkin.pdf, 1–8. Accessed on 2/4/2016.
172. M. M. V. Krukoniš, *Supercritical Fluid Extraction*, Butterworth-Heinemann, 2nd edn., 1994.
173. X. Zhang, S. Heinonen, and E. Levänen, *RSC Adv.*, 2014, **4**, 61137–61152.
174. A. Demirbas, *Energy Convers. Manag.*, 2001, **42**, 279–296.
175. S. M. Pourmortazavi and S. S. Hajimirsadeghi, *J. Chromatogr. A*, 2007, 1163, 2–24.
176. A. Capuzzo, M. E. Maffei, and A. Occhipinti, *Molecules*, 2013, **18**, 7194–7238.
177. V. Mičić, D. Novaković, Ž. Lepojević, M. Jotanović, B. Pejović, P. Dugić, and Z. Petrović, *Contemp. Mater.*, 2011, **2**, 84–87.

178. W. Tumas and J. M. DeSimone, Eds., *Green Chemistry Using Liquid and Supercritical carbon dioxide*, Oxford University press, 2003.
179. E. J. Beckman, *J. Supercrit. Fluids*, 2004, **28**, 121–191.
180. P. G. Jessop, Y. Hsiao, T. Ikariya, and R. J. Noyori, *Am. Chem. Soc.*, 1996, **118**, 344–355.
181. J. M. del Valle, C. Mena, and M. Budinich, *Brazilian J. Chem. Eng.*, 2008, **25**, 532–542.
182. S. Mayadevi, *Indian J. Chem.*, 2012, **51A**, 1298–1305.
183. Y. Athukorala and G. Mazza, *Ind. Crop. Prod.*, 2010, **31**, 550–556.
184. C. M. Wai, *Anal. Sci.*, 1995, **11**, 165–167.
185. Z. Li, Humboldt-Universität zu Berlin, 2005.
186. B. Basu, P. Das, and S. Das, *Curr. Org. Chem.*, 2008, **12**, 141–158.
187. L. M. Weinstock, J. M. Stevenson, S. A. Tomellin, and S. H. P. Dordrecht, 1994, 403.
188. L. M. Weinstock, J. M. Stevenson, S. A. Tomellini, S.-H. Pan, T. Utne, R. B. Jobson, and D. F. Reinhold, *Tetrahedron Lett.*, 1986, **27**, 3845–3848.
189. T. Ando, J. H. Clark, D. G. Cork, T. Hanafusa, J. Ichihara, and T. Kimura, *Tetrahedron Lett.*, 1987, **128**, 1421–1424.
190. T. Ando, *Stud. Surf. Sci. Catal.*, 1994, **90**, 9.
191. K. Girling, University of Glasgow, 2011.
192. R. L. Augustine, *CRC Press*, 1996, 241.
193. J. H. Clark, A. P. Kybett, and D. J. Macquarrie, *J. Chem. Educ.*, 1993, **70**, A251.
194. B. L. Hayes, in *Microwave synthesis: Chemistry at the speed of Light*, 2002, 1–291.
195. E. A. Schmittling and J. S. Sawyer, *Tetrahedron Lett.*, 1991, **32**, 7207–7210.
196. H. Hattori, *Chem. Rev.*, 1995, **95**, 537–558.
197. F. Bernhardt, R. Trotzki, T. Szuppa, A. Stolle, and B. Ondruschka, *Beilstein J. Org. Chem.*, 2010, **6**, 1–9.
198. I. Kharbanga, R. Rohman, H. Mecadon, and B. Myrboh, *Int. J. Org. Chem.*, 2012, **2**, 282–286.
199. B. Basu and S. Paul, *J. Catal.*, 2013, 1–21.

200. R. Chowdhury, Homi Bhabha National Institute, 2011.
201. B. D. Mather, K. Viswanathan, K. M. Miller, and T. E. Long, *Prog. Polym. Sci.*, 2006, **31**, 487–531.
202. J. Clayden, N. Greevs, S. Warren, and P. Wothers, *Organic chemistry*, Oxford University press Inc., New York, 2nd edn., 2012.
203. Y. Ono and T. Baba, *Catal. Today*, 1997, **38**, 321–337.
204. C. Garima and K. P. Rama, *Green Chem.*, 2011, **13**, 276–282.
205. E. J. Lenardão, D. O. Trecha, P. da C. Ferreira, R. G. Jacob, and G. Perin, *J. Braz. Chem. Soc.*, 2009, **20**, 93–99.
206. J. Escalante, M. Carrillo-Morales, and I. Linzaga, *Molecules*, 2008, **13**, 340–347.
207. J. Neilan, [http://www2.volstate.edu/chem/2020/Labs/Solventless Claisen.pdf](http://www2.volstate.edu/chem/2020/Labs/Solventless%20Claisen.pdf), 2004, 1-4. Accessed on 23/6/2016.
208. C. Oliver Kappe, *Chem. Soc. Rev.*, 2008, **37**, 1127–1139.
209. C. O. Kappe and D. Dallinger, *Mol. Divers.*, 2009, **13**, 71–193.
210. S. Ravichandran and E. Karthikeyan, *Int. J. ChemTech Res.*, 2011, **3**, 466–470.
211. W. Urbaniak, K. Jurek, K. Witt, and A. Gorączko, *Chemik*, 2011, **65**, 273–282.
212. G. Schweitzer and E. Benson, *J. Chem. Eng. Data*, 1968, **13**, 452–453.
213. L. W. Reeves, *Can. J. Chem.*, 1957, **35**, 1351–1365.
214. B. Ramarosan-Raonizafinimanana, E. M. Gaydou, and I. Bombarda, *J. Agric. Food Chem.*, 2000, **48**, 4739–4743.
215. A. P. Tulloch and L. L. Hoffman, *Phytochemistry*, 1971, **10**, 871–876.
216. D. H. S. Horn, Z. H. Kranz, and J. A. Lambertson, *Australian J. Chem.*, 1964, **17**, 464–476.
217. R. K. Henderson, C. Jimenez-González, D. J. C. Constable, S. R. Alston, G. G. A. Inglis, G. Fisher, J. Sherwood, S. P. Binks, and A. D. Curzons, *Green Chem. (RSC)*, 2011, **13**, 854–862.
218. J. M. DeSimone, *Science*, 2002, **297**, 799–803.
219. S. A. V. Colnaghi, D. S. da Silva, M. R. Lambais, and E. Carrilho, *J. Mass Spectrom.*, 2007, **42**, 490–496.
220. R. Aravindhan, T. Sreelatha, P. T. Perumal, and A. Gnanamani, *Complex met.*

(*Taylor's Fr.*), 2014, 7–79.

221. A. S. Chauvin, F. Gumy, I. Matsubayashi, Y. Hasegawa, and J. C. G. Bünzli, *Eur. J. Inorg. Chem.*, 2006, 473–480.
222. O. S. Bull and C. C. Obunwo, *Chem. Mater. Res.*, 2014, **6**, 69–75.
223. A. S. Rajbhoj, N. S. Korde, S. T. Gaikwada, and S. S. Korde, *Der Pharma Chem.*, 2012, **4**, 1868–1872.
224. J. R. Sohn and S. I. Lee, *J. Ind. Eng. Chem.*, 1997, **3**, 198–202.
225. J. Sheikh, H. Juneja, V. Ingle, P. Ali, and T. Ben Hadda, *J. Saudi Chem. Soc.*, 2013, **17**, 269–276.
226. D. H. W. I. Fleming, *Spectroscopic Methods in Organic Chemistry*, McGraw – Hill Book Company (UK) Limited, 3rd editio., 1980.
227. E. A. A. Al-Alawi, Kingdom of Saudi Arabia King Saud University, 2007.
228. M. A. Kassim, K. Kirtania, D. D. La Cruz, N. Cura, S. C. Srivatsa, and S. Bhattacharya, *Algal Res.*, 2014, **6**, 39–45.
229. R. T. Nassu and L. A. G. Gonçalves, *Grasas y Aceites*, 1999, **50**, 16–22.
230. A. A. S. Araújo, M. dos S. Bezerra, S. Storpirtis, and J. do R. Matos, *Brazilian J. Pharm. Sci.*, 2010, **46**, 37–43.
231. Z. Rugu, Z. Hua, Z. Hong, F. Ying, L. Kun, and Z. Wenwen, *Procedia Eng.*, 2011, **18**, 101–106.
232. P. G. Jessop, D. A. Jessop, D. Fu, and L. Phan, *Green Chem.*, 2012, **14**, 1245–1259.
233. K. Hofmann, K. Schreiter, A. Seifert, T. Rüffer, H. Lang, and S. Spange, *Suppl. Mater. New J. Chem.*, 2008, 1–8.
234. J. H. Clark, D. J. Macquarrie, and J. Sherwood, *Green Chem.*, 2012, **14**, 90–93.
235. A. Barik, N. K. Goel, K. I. Priyadarsini, and H. Mohana, *J. Photoscience*, 2004, **11**, 95–99.
236. K. Binnemans, in *Handbook on the Physics and Chemistry of Rare Earths*, eds. K. A. Gschneidner, J.-C. G. Bünzli, and V. K. Pecharsky, Elsevier, Belgium, 2005, 107–272.
237. G. Allen and R. A. Dwek, *Phys. Org.*, 1965, 161–163.
238. R. M. Claramunt, C. López, M. D. S. María, D. Sanz, and J. Elguero, *Prog. Nucl. Magn. Reson. Spectrosc.*, 2006, **49**, 169–206.
239. S. L. Laurella, M. G. Sierra, J. J. P. Furlong, and P. E. Allegretti, *Open J. Phys. Chem.*,

2013, **3**, 138–149.

240. E. Ferrari, M. Saladini, F. Pignedoli, F. Spagnolo, and R. Benassi, *New J. Chem.*, 2011, **35**, 2840–2847.
241. J. H. Clark, D. J. Macquarrie, and J. Sherwood, *Chem. Eur. J.*, 2013, **19**, 5174–5182.
242. N. Cyr and L. W. Reeves, *Can. J. Chem.*, 1965, **43**, 3057–3062.
243. P. O. Sandusky, *J. Chem. Educ.*, 2014, **91**, 739–742.
244. F. M. Kerton, *Alternative Solvents for Green Chemistry*, The Royal Society of Chemistry, 2009.
245. T. Ishida, F. Hirata, and S. Kato, *J. Chem. Phys.*, 1999, **110**, 3938–3945.
246. H. H. Schaumburg and P. S. Spencer, *Brain*, 1976, **99**, 183–192.
247. A. J. Hunt, E. H. Sin, R. Marriot, and J. H. Clark, *ChemSusChem.*, 2010, **3**, 306–328.
248. T. Attard, University of York, 2015.
249. P. G. Jessop, *Green Chem.*, 2011, **13**, 1391–1398.
250. C. M. Alder, J. D. Hayler, R. K. Henderson, A. M. Redman, L. Shukla, L. E. Shuster, and H. F. Sneddon, *Green Chem.*, 2016, 1–12.
251. B. Tirillini, G. Verdelli, F. Paolocci, P. Ciccioli, and M. Frattoni, *Phytochemistry*, 2000, **55**, 983–985.
252. G. Yanlong, *Bio-based chemicals: a sustainable candidate for new generation of green solvents*, 2013.
253. K. Watanabe, N. Yamagiwa, and Y. Torisawa, *Org. Process Res. Dev.*, 2007, **11**, 251–258.
254. A. J. Hunt and T. Attard, *Optimisation of supercritical extractions of C4 biomasses and Fractionation of sugarcane*, 2013.
255. M. Matricardi, R. Hesketh, and S. Farrell, *Effect of Operating Conditions on Static/Dynamic Extraction of Peanut Oil Using Supercritical Carbon Dioxide*, 2015.
256. J. M. Dobbs and K. P. Johnston, *Ind. Eng. Chem. Res.*, 1987, **26**, 1476–1482.
257. P. C. K. Cheung, *Food Chem.*, 1999, **65**, 399–403.
258. A. K. Gupta, K. M. Agrawal, and D. Severin, *Pet. Sci. Technol.*, 2006, **24**, 1–6.
259. B. Staniszewski and W. W. Urbaniak, *Chem. Pap.*, 2009, **63**, 212–216.

260. P. Tundo, P. Venturello, and E. Angeletti, *J. Chem. Soc. Perkin Trans*, 1987, **1**, 2159–2162.
261. N. Kalyanam, J. W. Karban, and J. L. M. Jr, *Org. Prep. Proced. Int. New J. Org. Synth.*, 1979, **11**, 100.
262. T. C. Rimmin and C. Hauser, *J. Org. Chem.*, 1967, **32**, 2615–2616.
263. D. Fanou, B. Yao, S. Siaka, and G. Ado, *Jour. Appl. Sci.*, 2007, **7**, 310–313.
264. J. Salimon, B. M. Abdullah, and N. Salih, *Chem. Cent. J.* 2011, 567, 2011, **5**, 1–9.
265. V. Das Gupta and H. W. Ho, *Am J Hosp Pharm.*, 1977, **34**, 653–4.
266. J. M. Khurana, S. Chauhan, and G. Bansal, *Monatshefte fur Chemie*, 2004, **135**, 83–87.
267. V. Theodorou, K. Skobridis, A. G. Tzakos, and V. Ragoussis, *Tetrahedron Lett.*, 2007, **48**, 8230–8233.
268. A. F. Parsons, *Keynotes in organic chemistry*, Blackwell publishing, 2003.
269. N. D. Bhatt and K. Nimavat, *Int. J. Pharm. Res. Sch.*, 2013, **2**, 51–53.
270. G.-Z. Li, R. K. Randev, A. H. Soeriyadi, G. Rees, C. Boyer, Z. Tong, T. P. Davis, C. R. Becera, and D. M. Haddleton, *Polym. Chem. (RSC)*, 2010, **1**, 1196–1204.
271. K. Tanaka, *Solvent-free Organic Synthesis*, WILEY-VCH Verlag GmbH & Co. KGaA, Weinheim, 2003.
272. R. S. Varma, *Green Chem.*, 1999, **1**, 43–55.
273. H. S. P. Rao and S. Jothilingam, *J. Chem. Sci.*, 2005, **117**, 323–328.
274. T. X. T. Luu, T. T. Lam, T. N. Le, and F. Duus, *Molecules*, 2009, **14**, 3411–3424.
275. A. J. J. Straathof, S. Sie, T. T. Franco, and L. A. M. van der Wielen, *Appl. Microbiol. Biotechnol.*, 2005, **67**, 727–734.
276. T. Werpy, G. Petersen, J. Holladay, J. White, A. Manheim, D. Elliot, L. Lasure, S. Jones, M. Gerber, K. Ibsen, L. Lumberg, and S. Kelley, *Top Value Added Chemicals from Biomass*, 2004, **1**, 1-76.
277. J. Van Haveren, E. L. Scott, and J. Sanders, *Biofuels, Bioprod. Biorefining*, 2008, **2**, 41–57.
278. H. Danner, M. Urmös, M. Gartner, and R. Braun, *Appl. Biochem. Biotechnol.*, 1998, **70–72**, 887–894.
279. X. U. Xiaobo, L. I. N. Jianping, and C. E. N. Peilin, *Chinese J. Chem. Eng.*, 2006, **14**,

419–427.

280. R. Chandragiri and R. C. Sastry, *Can. J. Chem. Eng. Technol.*, 2011, **2**, 128–135.
281. C. Sudarkodi, K. Subha, K. Kanimozhi, and A. Panneerselvam, *Adv. Appl. Sci. Res.*, 2012, **3**, 1126–1131.
282. H. Kautola, *Appl. Microbiol. Biotechnol.*, 1990, **33**, 7-11.
283. L. Dwiarti, M. Otsuka, S. Miura, M. Yaguchi, and M. Okabe, *Bioresour. Technol.*, 2007, **98**, 3329–3337.
284. A. Li, N. Pfelzer, R. Zuijderwijk, and P. Punt, *BMC Biotechnol.*, 2012, **12**, 57.
285. M. Okabe, D. Lies, S. Kanamasa, and E. Y. Park, *Appl. Microbiol. Biotechnol.*, 2009, **84**, 597–606.
286. M. Fernández-García, E. L. Madruga, and R. Cuervo-Rodriguez, *Polymer (Guildf.)*, 1996, **37**, 263–268.
287. L. C. Brent, J. L. Reiner, R. R. Dickerson, and L. C. Sander, *Anal. Chem (American Chem. Soc.)*, 2014, 1–9.
288. M. Yuan, M. Namikoshi, and A. Otsuki, *J Am Soc Mass Spectrom*, 1999, **10**, 1138–1151.
289. O. J. Pozo, P. Van Ennoo, K. Deventer, and F. T. Delbeke, *Journa Mass Spectrom.*, 2007, **42**, 497 – 516.
290. W. Buchmann, R. Spezia, G. Tournois, T. Cartailier, and J. Tortajada, *J. Mass Spectrom.*, 2007, **42**, 517 – 526.
291. U. S. Orlando, A. U. Baes, W. Nishijima, and M. Okada, *Green Chem.*, 2002, **4**, 555–557.
292. V. Theodorou, K. Skobridis, A. G. Tzacos, and V. Ragoussis, *Tetrahedron Lett.*, 2007, **48**, 8230–8233.
293. S. Laughlin and W. D. Wilson, *Int. J. Mol. Sci.*, 2015, **16**, 24506–24531.
294. J. A. Leenheer, C. E. Rostad, P. M. Gates, E. T. Furlong, and I. Ferrer, *Anal. Chem.*, 2001, **73**, 1461–1471.
295. K. P. C. Vollhardt and N. E. Schore, *Organic Chemistry; Palgrave version: Structure and Function*, W. H. Freeman, 2014.
296. J.-J. Max and C. Chapados, *J. Phys. Chem.*, 2004, **A**, 3324–3337.
297. D. Villemin and M. A. Didi, *Orient. J. Chem.*, 2013, **29**, 1267–1284.

298. T. Rubcumintara, *Int. J. Chem. Eng. Appl.*, 2015, **6**, 95–100.
299. C. Tasdelen, S. Aktas, E. Acma, and Y. A. Guvenilir, *Hydrometallurgy*, 2009, **96**, 253–257.
300. A. Demirbas, *J. Hazard. Mater.*, 2008, **157**, 220–229.
301. G. H. Jeffery, J. Bassett, J. Mendham, and R. C. Denney, *Vogel's textbook of quantitative chemical analysis*, Longman Scientific and Technical, 5th edn., 1989.
302. S. Tandy, K. Bossart, R. Mueller, J. Ritschel, L. Hauser, R. Schulin, and B. Nowack, *Environ. Sci. Technol.*, 2004, **38**, 937–944.
303. D. D. Pereira, S. D. F. Rocha, and M. B. Mansur, *Sep. Purif. Technol.*, 2007, **53**, 89–96.
304. W. Al Zoubi, F. Kandil, and M. K. Chebani, *Arab. J. Chem.*, 2011, 1–6.
305. S. S. Lutfullah, N. Rahman, S. N. H. Azmi, and B. Iqbal, *J. Chinese Chem. Soc.*, 2010, **57**, 622–631.
306. M. Elizalde, A. Ocio, F. Andrade, and B. Menoyo, *Solvent Extr. Ion Exch.*, 2013, **31**, 269–280.
307. R. Lertlapwasin, N. Bhawawet, A. Imyim, and S. Fuangswasdi, *Sep. Purif. Technol.*, 2010, **72**, 70–76.
308. A. Nezhadali, A. Sadeghi, and M. Roigar, *Arab. J. Chem.*, 2015, **8**, 164–167.
309. J. Stary and E. Hladky, *Anal. Chim. Acta*, 1963, **28**, 227–235.
310. R. Kumar, S. K. Jain, R. K. Misra, M. Kachchwaha, and P. K. Khatri, *Int. J. Environ. Sci. Technol.*, 2012, **9**, 79–84.
311. O. Gerald, A. Judith, and O. Martin, *J. Miner. Mater. Charact. Eng.*, 2013, **1**, 90–94.
312. N. Begum, F. Bari, S. B. Jamaludin, and K. Hussin, *Int. J. Phys. Sci.*, 2012, **7**, 2905–2910.
313. B. Gupta and I. Singh, *Hydrometallurgy*, 2013, **134–135**, 11–18.
314. B. Sengupta, M. S. Bhakhar, and R. Sengupta, *Hydrometall.*, 2007, **89**, 311–318.
315. U. J. Chukwu and J. Godwin, *Am. Chem. Sci. J.*, 2013, **3**, 479–488.
316. R. Sepulveda, J. Romero, and J. Sanchez, *J Chem Technol Biotechnol*, 2013, **89**, 899–908.
317. T. Shigematsu, M. Tabushi, and T. Tarumoto, *Bull. Inst. Chem. Res. Kyoto Univ.*, 1963, **40**, 388–399.

318. K. Burger, *Organic Reagents in Metal Analysis: International Series of Monographs in Analytical Chemistry*, Elsevier, 2013.
319. T. Oshima, I. Fujiwara, and Y. Baba, *Solvent Extr. Res. Dev. Japan*, 2015, **22**, 119–125.
320. E. Löfström-Engdahl, E. Aneheim, C. Ekberg, M. Foreman, and G. Skarnemark, in *ACSEPT (Actinide reCycling by SEParation and Transmutation)*, Libson, Portugal, 2010, 1–9.
321. M. D. Al-Sabti, *Eng. & Tech.*, 2008, **26**, 496–500.
322. Y. Pranolo, W. Zhang, and C. Y. Cheng, *Hydrometallurgy*, 2010, 102, 37–42.
323. D. Barkat, Z. Derriche, and A. Tayeb, *Turk J Chem*, 2001, **25**, 381–389.
324. M. K. Nazal, M. A. Albayyari, and F. I. Khalili, *J. Saudi Chem. Soc.*, 2014, **18**, 59–67.
325. T. Sekine, M. Katori, R. Murai, and T. Saitou, *Bunseki Kagaku (The Japan Soc. Anal. Chem.)*, 1984, **33**, E351–E358.
326. J. Stary and J. O. Liljenzin, *Pure Appl. Chem.*, 1982, **54**, 2557–2592.
327. G. Chauhan, K. K. Pant, and K. D. P. Nigam, *Ind. Eng. Chem. Res.*, 2012, **51**, 10354–10363.
328. L. Hauser, Institute of Terrestrial Ecology, ETH Zurich., 2003.
329. G. O. El-Sayed, H. A. Dessouki, and S. S. Ibrahim, *Malaysian J. Anal. Sci.*, 2011, **15**, 8–21.
330. H. Koshimura and T. Okubo, *Anal. Chim. Acta*, 1970, **49**, 67–75.
331. K. Wieszczycka, M. Krupaa, and A. Olszanowska, *Sep. Sci. Technol.*, 2012, **47**, 1278–1284.
332. Y. Dai, *J. Chem. Eng. Data*, 2007, **52**, 438–441.
333. V. Kumar, S. K. Sahu, and B. D. Pandey, *Hydrometallurgy*, 2010, **103**, 45–53.
334. E. Dziwiński and J. Szymanowski, *Solvent Extr. Ion Exch.*, 1996, **14**, 219–226.
335. J. J. Jacobs, M. Allard, S. Behmo, and J. Moreau, *Nickel & Cobalt Extraction Using Organic Compounds*, Elsevier, 2013.
336. J. R. Beevers, *Solvent Extraction and Atomic Absorption Spectrophotometry Applied to Rock Analysis*, 1967.
337. K. Sarangi, P. K. Parhi, E. Padhan, A. K. Palai, K. C. Nathsarma, and K. H. Park, *Sep. Purif. Technol.*, 2007, **55**, 44–49.

338. D. V. Koladkar and P. M. Dhadke, *J.Serb.Chem.Soc.*, 2002, **67**, 265–272.
339. D. M. Roundhill, I. B. Solangi, S. Memon, M. I. Bhangar, and M. Yilmaz, *Pak. J. Anal. Environ. Chem.*, 2009, **10**, 1–13.
340. J. D. Lee, *Concise Inorganic Chemistry*, Blackwell Science Ltd., 5th edition., 1996.
341. G. Saxena, U. Pathak, and S. J. S. Flora, *Toxicology*, 2005, **214**, 39–56.
342. K. Kostial, M. Blanusa, M. Piasek, M. M. Jones, and P. K. Singh, *Pharmacol. Toxicol.*, 1995, **77**, 216–218.
343. B. P. Charlesworth, *Platin. Met. Rev.*, 1981, **25**, 106–112.
344. J.-S. Kwon, S.-T. Yun, J.-H. Lee, S.-O. Kim, and H. Y. Jo, *J. Hazard. Mater.*, 2010, **174**, 307–313.
345. Q. Liang, H. Hu, W. Fu, T. Ye, and Q. Chen, *Trans. Nonferrous Met. Soc. China*, 2011, **21**, 1840–1846.
346. R. M. Alghanmi, *E-Journal Chem.*, 2012, **9**, 1007–1016.
347. Y. Renxiu, L. Chunling, Z. Gan, L. Xiangdong, and S. Zhenguo, *J. Environ. Sci.*, 2012, **24**, 1985–1994.
348. T. Suzuki, M. Niinae, T. Koga, T. Akita, M. Ohta, and T. Choso, *Colloids Surfaces A Physicochem. Eng. Asp.*, 2014, **440**, 145–150.
349. K. R. Reddy and S. Chinthamreddy, *Soil Sediments Contam.*, 2000, **9**, 449–462.
350. K. Kidani, N. Hirayama, and H. Imura, *Anal. Sci.*, 2008, **24**, 1251–4.
351. H. Hamid, *Pharmaceutical analysis: Ultraviolet and Visible Spectrophotometry*, 2007.
352. U. Mariana, Babes-Bolyai University, Cluj - Napoca, 2012.
353. S. Cakic, C. Lacnjevac, G. Nikolic, J. Stamenkovic, M. B. Rajkovic, M. Gligoric, and M. Barac, *Sensors*, 2006, **6**, 1708–1720.
354. V. I. Avdeev, E. A. Shugman, and S.D.Nasirdinov, *Teor. i Eksp. naya Khimiya*, 1970, **5**, 600–606.
355. S. Kanhathaisong, S. Rattanaphani, V. Rattanaphani, and T. Manyum, *Suranaree J. Sci. Technol.*, 2011, **18**, 159–165.
356. A. J. Carty, D. G. Tuck, and E. Bullock, *Can. J. Chem.*, 1965, **43**, 2559–2565.
357. T. O. Aiyelabola, I. A. Ojo, A. C. Adebajo, G. O. Ogunlusi, O. Oyetunji, E. O. Akinkunmi, and A. O. Adeoye, *Adv. Biol. Chem.*, 2012, **2**, 268–273.

358. J. I. S. and H. D. J. Pooja N. Verma, *World Appl. Sci. J.*, 2011, **14**, 1154–1157.
359. A. Y. Vibhute, S. B. Zangade, V. M. Gurav, and Y. B. Vibhute, *Orbital Elec. J. Chem.*, 2012, **4**, 1–6.
360. J. H. Clark, T. J. Farmer, and D. J. Macquarrie, *ChemSusChem*, 2007, **2**, 1025–1027.
361. D. L. Maples, R. D. Maples, W. A. Hoffert, T. H. Parsell, A. van Asselt, J. D. Silversides, S. J. Archibald, and T. J. Hubina, *Inorganica Chim Acta*, 2009, **362**, 2084–2088.
362. A. Ohashi, N. Kawashima, M. Kosugi, and H.-B. Kim, *Solvent Extr. Res. Dev. Japan*, 2015, **22**, 201–207.
363. F. P. Byrne, S. Jin, G. Paggiola, T. H. M. Petchey, J. H. Clark, T. J. Farmer, A. J. Hunt, C. R. McElroy, and J. Sherwood, *Sustain Chem Process*, 2016, **4**, 1–24.
364. G. L. Buchanan, *Chem. Soc. Rev.*, 1988, **17**, 91-109.
365. M. Nasr-Esfahani, M. Montazerozohori, and T. Gholampour, *Bull. Korean Chem. Soc.* 2010, 2010, **31**, 3653–3657.
366. R. Tayebee and S. Tizabi, *Chinese J. Catal.*, 2012, **33**, 923–932.
367. J. Pradhan and A. Goyal, *Int. J. Pharm. Res. Allied Sci.*, 2015, **4**, 1–18.
368. J. J. Esteb and M. B. Stockton, *J. Chem. Educ.*, 2003, **80**, 1446–1447.
369. J. E. Horta, *J. Chem. Educ.*, 2011, **88**, 1014–1015.
370. E. Erasmus and J. Swarts, *New J. Chem.*, 2013, **37**, 2862-2873.